CONTENTS

ADSORPTION AND HEAT OF WETTING STUDIES OF TEFLON[1]

BY J. J. CHESSICK, F. H. HEALEY AND A. C. ZETTLEMOYER

Contribution from the Surface Chemistry Laboratory, Lehigh University, Bethlehem, Penna.

Received August 29, 1955

Adsorption and heat of wetting measurements were used to study the surface properties of Teflon and the results were compared with those previously found with the graphitized carbon black, Graphon. Both solids are hydrophobic. From water adsorption and related isosteric heat data it was determined that Teflon has more hydrophilic surface sites per unit area and that these sites are of higher adsorption energy than those present on the surface of Graphon. Nevertheless, Teflon is the more hydrophobic of the two solids over-all since it has a much lower heat of wetting and a much larger contact angle with water. These values are −6 ergs/cm.² and 108°, respectively, compared to −32 ergs/cm.² and 82° for Graphon. It was concluded that the greater hydrophobicity of Teflon was due primarily to a different nature of non-polar sites rather than to the distribution of hydrophilic sites on these surfaces.

The purpose of this paper is to compare the surface properties of two hydrophobic solids, Graphon and Teflon. Graphon was investigated previously[2] by water adsorption and heat of wetting measurements. While generally considered homogeneous, Graphon was shown to possess a small fraction of heterogeneous sites considered to be primarily responsible for the adsorption of water. To determine the role of such limited number of hydrophilic sites on other surface properties such as contact angle and heat of wetting, a more hydrophobic solid Teflon, already studied extensively by other methods,[3] also was investigated.

Experimental

Water vapor adsorption isotherms were determined at temperatures of 15, 20 and 25° for Teflon-6. This tetrafluoroethylene polymer (TE3086, Coded B-3933) was supplied in powder form by E. I. du Pont de Nemours and Co., Wilmington, Delaware, and had a nitrogen area of 9.0 m.²/g. This sample was washed with hexane, absolute alcohol, alcohol–water and finally distilled water, dried at 50° for 48 hr., then degassed at 25° for 48 hr. at 10⁻⁵ mm., before adsorption or heat of wetting measurements were started. At least two adsorption runs were made at each temperature.

The amount of water absorbed was determined volumetrically using a modified Orr apparatus previously described.[4] Equilibrium pressures were read after one hour on a manometer filled with Apiezon B oil. Water absorption by the

oil was shown previously to be negligible,[4] but because of the very small amounts of water vapor adsorbed it was necessary to apply corrections for adsorption on the walls of the apparatus.

The calorimeter used in the heat of wetting studies and the treatments of the organic wetting liquids have been described.[4,5] Two different calorimeter units were used. The one in which the wetting liquid was water utilized a thermistor coated with picein and required 250 ml. of water. The second calorimeter, with an uncoated thermistor, required only 200 ml. of organic liquid. Because of this smaller volume, the smaller heat capacity of the organic liquid, and the greater interaction, considerably more accuracy was possible in the determination of the heats of wetting of Teflon in the organic liquids than in water.

The calculated maximum deviation in heats of immersion due to errors inherent in the calorimetric technique was about ±10% for this low area Teflon in the organic liquids. On the other hand, the maximum deviations for the immersion of evacuated Teflon and Teflon exposed to water vapor at 80% R. H. before immersion were calculated to be ±90 and ±34%, respectively. The experimental deviations from mean values were also found to be within these orders of magnitude.

The isosteric heat values were calculated from the integrated form of the Clausius–Clapeyron equation

$$\ln p = -q_{st}/RT + C$$

using equilibrium pressure data obtained at three temperatures.

Results and Discussion

The isotherms for the adsorption of water on Teflon and Graphon shown in Fig. 1 are similar and have predominant Type III character despite the slight rise in the curve at low pressures. The adsorption of water on the hydrophobic solid Graphon

(1) Presented before the ACS Colloid Division, Minneapolis, Minnesota, September, 1955.

(2) G. J. Young, J. J. Chessick, F. H. Healey and A. C. Zettlemoyer, THIS JOURNAL, **58**, 313 (1954).

(3) A. H. Ellison and W. A. Zisman, *ibid.*, **58**, 260 (1954).

(4) A. C. Zettlemoyer, G. J. Young, J. J. Chessick and F. H. Healey, *ibid.*, **57**, 649 (1953).

(5) F. H. Healey, J. J. Chessick, A. C. Zettlemoyer and G. J. Young, *ibid.*, **58**, 887 (1954).

has already been explained on the basis of at least two types of adsorption sites on the surface of this material. The vast majority of sites are hydrophobic and apparently correspond to a graphite-like array of carbon atoms. These sites show no tendency to adsorb water at least up to pressures close to saturation. The hydrophilic sites are few in number and probably arise from traces of surface oxide such as might be expected at edge atoms of graphite planes. These sites account for the initial Type II character of the water adsorption isotherms. After adsorption of the first layer of water molecules on these sites, the molecules build up additional layers on and around these sites rather than adsorb on the adjacent hydrophobic area. The mechanism for the adsorption of water on Teflon would be expected to be the same.
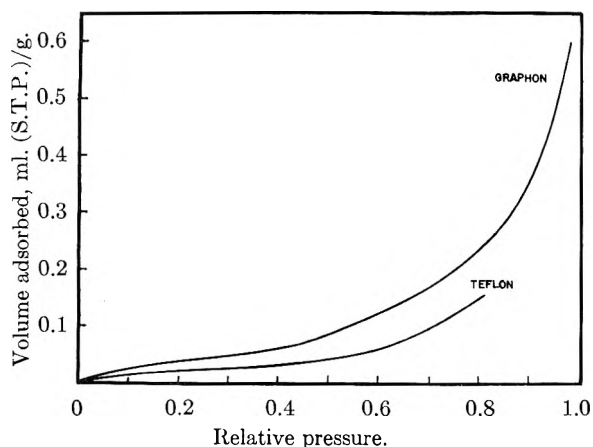
Fig. 1.—Adsorption isotherms for water–Graphon at 18°; water–Teflon at 20°.

The calculated areas obtained from nitrogen and water V_m values are listed in Table I for both Graphon and Teflon. The water areas of the two are small and not vastly different; the specific areas calculated from nitrogen adsorption data are much larger. Furthermore, Graphon has a specific area nearly ten times that of the Teflon powder. If the water area represents adsorption on the hydrophilic sites only, then the ratio of the water area to the nitrogen area times 100 gives the per cent. surface hydrophilicity for a given sample. On this basis, Teflon has a surface hydrophilicity of 0.75% compared to 0.15% for Graphon.

TABLE I

HEATS OF IMMERSIONAL WETTING AND OTHER SURFACE
PROPERTIES FOR TEFLON-6 AND GRAPHON

Liquid	Teflon $h_e(sl)$, ergs/cm.²	Graphon
Butyl alcohol	−56	−114
Nitropropane	−54	...
Butyl chloride	−56	−106
n-Heptane	−58	−112
Water	− 6	− 32
ΣN₂, m.²/g.	9.0	85.0
ΣH₂O, m.²/g.	0.07	0.13
(ΣH₂O/ΣN₂) 100	0.75	0.15
Equilibrium contact angle with water	108°³	82°²

Isosteric heat values for the Graphon–water system were calculated from heat of immersion measurements as a function of the amount of water preadsorbed on the Graphon surface and from adsorption data at one temperature.[2] These heat values fall mostly below the heat of liquefaction of water and have a minimum value of 5.5 kcal./mole near the calculated BET V_m value. The isosteric heats then increase slowly toward the heat of liquefaction. An approximate estimate of the isosteric heat values for water adsorption on Teflon from three temperature adsorption values agreed with the results based on one isotherm and heat of immersion data.

The shape of the heat curve was somewhat similar to that obtained for water adsorption on Graphon, i.e., a minimum near the BET V_m followed by an increase in heat values with increasing coverage. However, the minimum isosteric heat value was only slightly below the heat of liquefaction and the heat values increased rapidly to about 12 kcal./mole then slowly fell toward the heat of liquefaction. The small adsorption on Teflon as well as its low area and correspondingly small heat of immersion values preclude accurate determinations of isosteric heats. It can be stated, however, that heat values for the Teflon–water system are not far from the heat of liquefaction near the BET monolayer region and, further, these values are significantly higher than found for the adsorption of water on Graphon.

On the basis of the water adsorption data and the related isosteric heat values, Teflon is more hydrophilic than Graphon. On the other hand, the heat of immersion of Teflon in water, while small and difficult to measure accurately, was definitely lower than that for Graphon. The values of the heats of immersion of Teflon samples in the organic liquids were large enough to be measured with considerably more accuracy and were found, as with Graphon, to remain the same as the functionality of the wetting liquid was varied. Furthermore, the heats of wetting were about one-half the magnitude found for the immersion of Graphon in these same organic liquids. The low heat of wetting of Teflon in water is in accord with the high contact angle of 108°; whereas the contact angle measured for water on a pelletized button of Graphon was 82°. The contact angle for water on a chip of Teflon pressed from the powder used in the adsorption measurements was found to be 110 ± 2°. Teflon unlike Graphon is also not wet by many organic liquids. For example, the equilibrium contact angle measured for n-decane on Teflon was 35°.[3] These data reveal Teflon to be more hydrophobic than Graphon.

Most probably both the polar and non-polar portions of a surface influence the contact angle and heat of wetting values for a hydrophobic solid. Certainly the heat of wetting of Graphon in water was shown to increase as the number of hydrophilic heterogeneities on the surface was increased by controlled oxidation[6]; the contact angle changes with oxidation were not followed. With Teflon the influence of the non-polar surface must pre-

(6) F. Healey, Y. Yu and J. Chessick, THIS JOURNAL, 59, 399 (1955).

dominate in producing a greater hydrophobicity (a lower energy surface) compared to Graphon, although the number of polar sites per unit area and the adsorption energy of these sites are greater for Teflon. The limited polarizability of the surface fluorine atoms would account for the small interaction energy between water and Teflon. The higher polarizability of the surface atoms of Graphon, due to some double bond character of the C–C bonds, leads to a greater contribution to the total adsorption energy by non-polar van der Waals forces. This difference in polarizability is evident too from the much lower heat of wetting of Teflon in the organic liquids when the only important interaction is the non-polar van der Waals type. In addition, the contribution resulting from the interaction of a water dipole and its image force accounts for the higher heat of wetting of Graphon in water compared to Teflon.

It is interesting to speculate on the nature of the hydrophilic heterogeneities present on the surface of Teflon. This material was coagulated from an aqueous suspension and possible surface impurities are surface active agents and fluoride salts. A calculation of the coulomb interaction of a water dipole oriented parallel to an isolated KF ion pair impurity leads to a heat of adsorption of 10.2 kcal./mole if a distance of separation of the water dipole

charge is taken as 0.38 Å. This heat value should not be far from the actual value if the situation proposed exists; the contribution to the total adsorption energy from the non-polar van der Waals forces would be small. Lower values would of course result if impurity centers are pregrouped rather than isolated as ion pairs in the surface. Nevertheless, heats of adsorption near the heat of liquefaction, as found for the adsorption of water on Teflon, can be explained adequately by this type of impurity.

An additional experiment was carried out to determine whether heat treatment would affect the nature of the surface. After activation at 280° for 20 hr., the nitrogen area decreased only from 9.0 to 7.5 m²./g. but the water vapor adsorption was reduced to about one-third its former value. Pellets heated under the same conditions showed no change in the contact angle with water. The volatility of the hydrophilic sites points toward strongly adsorbed surfactants as the principal active centers. The lack of change in the contact angle supports the view that the angle is determined primarily by the nature of the non-polar surface.

THE ENERGETICS AND STATISTICAL MECHANICS OF THE KINETICS OF SOLID → SOLID REACTIONS

BY R. S. BRADLEY

Department of Inorganic and Structural Chemistry, University of Leeds, England

The kinetics of reconstructive solid → solid transformations are developed in terms of a vapor transition state. The application to experimental data, especially those observed near the transition temperature, is discussed in the light of current theories of crystal growth. A critical discussion is given of the difficulties in interpreting the temperature independent factor of solid → solid reactions in terms of transition state theory and also those theories which rely on crystal imperfections.

I. Energetics

The simplest way of leading up to the complexities of solid → solid reactions is to imagine that the conversion is brought about *via* the vapor phase in an enclosure which contains the two separate solids, so that the rate depends on the "affinity."[1]

If α_α and α_β are the evaporation coefficients, and p_α and p_β the saturation vapor pressures of the two solids α and β, of which the latter is unstable at temperature T, then for equality of loss and gain of vapor

$$(\alpha_\alpha p_\alpha + \alpha_\beta p_\beta)/(2\pi m k T)^{1/2} = (\alpha_\alpha p + \alpha_\beta p)/(2\pi m k T)^{1/2} \quad (1)$$

where p is the vapor pressure in the vessel, k is the Boltzmann constant, m the molecular mass, and it is assumed that the solids have equal surface area exposed to the vapor. It follows that

$$p = (\alpha_\alpha p_\alpha + \alpha_\beta p_\beta)/(\alpha_\alpha + \alpha_\beta) \quad (2)$$

(1) De Donder and Van Rysselberghe. "Thermodynamic Theory of Affinity," Stanford University, Stanford, Cal., 1936.

The rate of the solid → solid reaction in molecules cm.$^{-2}$ sec.$^{-1}$ is therefore

$$v = \alpha_\alpha(p - p_\alpha)/(2\pi m k T)^{1/2} = \alpha_\alpha \alpha_\beta(p_\beta - p_\alpha)/[(\alpha_\alpha + \alpha_\beta)(2\pi m k T)^{1/2}] \quad (3)$$

If d is the density of the α phase the linear rate for this phase is vm/d cm.sec.$^{-1}$.

To a first, and often very good, approximation

$$p_\beta = B_\beta e^{-E_\beta/(RT)}, \text{ and } p_\alpha = B_\alpha e^{-E_\alpha/(RT)} \quad (4)$$

where the B's are so-called temperature independent factors (and are related to entropies of vaporization) and the E's are latent heats of sublimation.

Hence the rate of the solid → solid reaction is given by

$$v = \frac{\alpha_\alpha \alpha_\beta}{(\alpha_\alpha + \alpha_\beta)} \frac{B_\beta}{(2\pi m k T)^{1/2}} e^{-E_\beta/RT}(1 - e^{\Delta G/RT}) \quad (5)$$

since

$$-\Delta G = RT \ln(p_\beta/p_\alpha) \quad (6)$$

assuming that the vapors are perfect gases.

Equation 5 holds whether or not there is a transi-

tion point. For enantiotropes $\Delta G = 0$ at the transition temperature T_0, in agreement with equation 5. If this equation is rewritten in the form

$$v = \frac{\alpha_\alpha \alpha_\beta}{(\alpha_\alpha + \alpha_\beta)} \frac{1}{(2\pi mkT)^{1/2}} (\beta_\beta e^{-E_\beta/RT} - B_\alpha e^{-E_\alpha/RT}) \quad (7)$$

the condition at the transition point

$$B_\beta e^{-E_\beta/(RT_0)} = B_\alpha e^{-E_\alpha/(RT_0)} \quad (8)$$

gives

$$v = \frac{\alpha_\alpha \alpha_\beta}{(\alpha_\alpha + \alpha_\beta)} \frac{B_\beta}{(2\pi mkT)^{1/2}} e^{-E_\beta/RT}$$
$$[1 - e^{(q/R)(1/T_0 - 1/T)}] \quad (9)$$

where q, the reaction heat per mole, is given by $q = E_\alpha - E_\beta$.

An equation of a form similar to 9 was first given by Hartshorne,[2] who put $\alpha_\alpha \alpha_\beta/(\alpha_\alpha + \alpha_\beta) = 1/2$ (10) and this equation has the merit of explaining the maximum in v below the transition point. If we neglect the effect of the factor $T^{1/2}$ and the possible temperature variation in α_α and α_β,

$$1/T_{max} = 1/T_0 + R [\ln (1 + q/E_\beta)]/q \quad (11)$$

Since $q << E_\beta$

$$1/T_{max} = 1/T_0 + R/E_\beta \text{ (app.)} \quad (12)$$

The inclusion of the $T^{1/2}$ factor gives

$$1/T_{max} = 1/T_0 + 2R/(2E_\beta - RT_0) \text{ (app.)} \quad (13)$$

The variation of v with T is sketched in Fig. 1. The mathematical curve has dv/dT continuous through T_0, where v becomes negative. Physically this corresponds to the reaction solid$_\alpha \to$ solid$_\beta$, for which the curve is the mirror image of the dotted
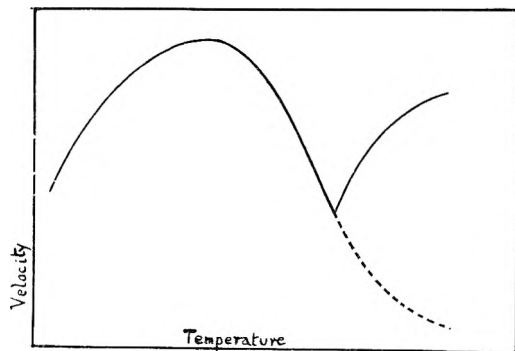
Fig. 1.

negative portion. If the effect of the $T^{1/2}$ factor is neglected, v rises to an asymptote (the $T^{1/2}$ factor will have a noticeable effect only at temperatures above which the solid phases disappear). There is a point of inflection in the mathematical curve (dotted) which point is in general not at T_0.

It should be noted that at low temperatures

$$v = \frac{\alpha_\alpha \alpha_\beta}{(\alpha_\alpha + \alpha_\beta)} \frac{B_\beta}{(2\pi mkT)^{1/2}} e^{-E_\beta/RT}$$
$$(1 - e^{-q/RT}) \text{ app.}$$

because $1/T_0 << 1/T$. This gives

$$d \ln v/d (1/T) = -E_\beta/R \text{ (app.)} \quad (14)$$

and hence at sufficiently low temperatures we obtain the usual rate law. Conversely the tempera-

(2) N. H. Hartshorne, *Disc. Faraday Soc.*, **5**, 149 (1949).

ture coefficient of v is very large near to T_0 since then

$$v = \frac{\alpha_\alpha \alpha_\beta}{(\alpha_\alpha + \alpha_\beta)} \frac{B_\beta}{(2\pi mkT)^{1/2}} e^{-E_\beta/RT} \left(\frac{T_0 - T}{T T_0}\right) \frac{q}{R} \quad (15)$$

since $T_0 - T << T_0$. It follows that

$$d \ln v/d(1/T) = -E_\beta/R + T/2 + T T_0/(T_0 - T) \quad (16)$$

For small enough values of $T_0 - T$ the temperature coefficient of $\ln v$ is independent of E_β and will in fact be the same for all solid reactions which obey the same general formula 9, which gives $dv/dT =$ constant, if $T_0 - T << T_0$.[3]

It is remarkable how closely the simple considerations above apply to a solid reaction in which the two solids are "in contact." Many solids with two polymorphic forms give velocity curves showing a maximum, and the apparent activation energy at low temperatures is near to the heat of sublimation of the unstable form. Examples are best chosen from experiments in which the linear motion of the interface has been observed, rather than some bulk property such as dilatation, in order to avoid difficulties associated with random nucleation.

These results suggest that such solid → solid reactions are examples of crystal growth from the vapor supplied by the unstable form. At first sight, however, it seems unlikely that the gap between the two solids, which cannot be resolved by the optical microscope can act as a gas reservoir which provides supersaturated vapor. It is much more likely that "molecular streaming" occurs across the gap, and that molecules jump across and are either caught by the second surface or are reflected, without building up anything like a bulk vapor region. We may apply directly transition state theory for the transmission coefficient,[4] so that on the first reflection of N molecules coming from β, $N(1 - \alpha_\alpha)$ recoil, of which $N\alpha_\beta(1 - \alpha_\alpha)$ are taken up by solid β and $N(1 - \alpha_\alpha)(1 - \alpha_\beta)$ recoil, and so on. This gives for the net flux in molecules cm.$^{-2}$sec.$^{-1}$ from solid $\beta \to$ solid α

$$v = \frac{\alpha_\alpha \alpha_\beta}{1 - (1 - \alpha_\alpha)(1 - \alpha_\beta)} \frac{(p_\beta - p_\alpha)}{(2\pi mkT)^{1/2}} \quad (17)$$

If $\alpha_\alpha = \alpha_\beta = 1$ equation 17 differs from equation 3 only by a factor $1/2$ in the latter, which is a difference small compared with uncertainties in kinetic studies of this kind. The evaporation coefficient is often near to unity for solids, e.g., the writer's experiments[5] and those of Rideal[6] and Wiggins suggest that α_α is of the order 0.7 for rhombic sulfur (S_α). It follows that the discussion on the temperature coefficient of v may be taken over in its entirety to equation 17, which is based on a physical picture of the solid → solid reaction which is much more likely to apply than that given in the Introduction.

As an example of a reaction which to a first approximation follows equation 17 we may take

(3) *Cf.* F. S. Dainton and K. J. Ivin, *Trans. Faraday Soc.*, **46**, 331 (1950), for a similar treatment applied to polymerization.
(4) J. O. Hirschfelder and K. Wigner, *J. Chem. Phys.*, **7**, 616 (1939).
(5) R. S. Bradley, *Proc. Roy. Soc. (London)*, **A205**, 553 (1951).
(6) Sir Eric K. Rideal and P. M. Wiggins, *ibid.*, **A210**, 291 (1951).

the transition of monoclinic to rhombic sulfur, i.e., $S_\beta \to S_\alpha$ as studied by Hartshorne[7] and co-workers. The energy of activation well below the transition point was 22,000–23,000 cal. against 23,240 cal. at 96–115° for the latent heat of vaporization of S_β as given by Neumann.[8] However, the maximum in the velocity and temperature curve occurred at 65° instead of at 84°, the value calculated from equation 12; moreover the curve obtained by plotting $\ln v - \ln [1 - e^{(q/R)(1/T_0 - 1/T)}]$ against $1/T$ is not truly straight, especially at temperatures near to the transition temperature T_c. In this latter region the experimental results depart considerably from equation 9, as will be discussed more fully later. It should, however, be remembered that q is not a constant, but changes from 616 to 840 cal. from 0 to 96° and that the vapor pressure equations are approximations. There is also the point common to all experiments on solid reaction kinetics, that results are not strictly reproducible but show a coefficient of variance of 10–25%, indicating that all factors which affect the rate are not under control. It is possible that with these thin films between glass plates there is some strain set up: the nature of the gap is obscure, since the difference in densities should cause a progressive widening of the gap as the reaction progresses.

In spite of the uncertainties, the approximate equality of the heat of sublimation of the unstable phase and the activation energy at low temperatures in a number of solid → solid reactions is very striking. Some examples are given in Table I, together with solid reactions in which this equality is not observed: it is noticeable that the first group are all molecular solids.

<div align="center">

TABLE I

</div>

Ref.	Substance	Phases reacting	Low temp. actn. energy (cal.)	Heat of subn. of unstable form (cal.)
7	Sulfur	$\beta \to \alpha$	22,000–23,000	23,240
9	o-Nitroaniline	$\alpha \to \beta$	17,000–18,000	19,000
10	Azoxybenzene	II → I	22,500	23,000
11	Carbon tetrabromide	cubic → monoclinic	?	
12	Mercuric iodide	Yellow → red	10,000–11,000	19,000
13	Tin	White → grey	~6,000	78,000

Further support for the concept of the vapor gap is provided by the observation for $\beta \to \alpha$ sulfur and II → I azoxybenzene that the stable phase grows without change of orientation when it crosses crystal boundaries in the β phase, i.e., the orientation

(7) N. H. Hartshorne and M. H. Roberts, J. Chem. Soc., 1097 (1951).

(8) Neumann, Z. physik. Chem., 171, 416 (1934).

(9) N. H. Hartshorne, G. S. Walters and W. O. M. Williams, J. Chem. Soc., 1860 (1935).

(10) A. Hodkin and D. Taylor, ibid., 489 (1955).

(11) N. H. Hartshorne and P. McL. Swift, ibid., 3705 (1955).

(12) D. G. Eade and N. H. Hartshorne, ibid., 636 (1948). C. S. Smith, "Imperfections in Nearly Perfect Crystals," John Wiley and Sons, New York, N. Y., 1952, p. 400.

(13) G. Tammann and K. L. Dreyer, Z. anorg. Chem., 199, 97 (1931).

of the stable phase bears no relation to that of the unstable.

Since the simple theory is only obeyed very approximately it is relevant to inquire whether the treatment can be improved in the light of recent studies on the growth of crystals from the vapor. The first attempt in this direction was made by Dunning,[14,15] who suggested that the temperature coefficient of a solid → solid reaction could be explained by means of a nucleation hypothesis. This is applicable only in the unlikely event of perfection in the crystal and gives an equation

$$\ln v = \text{const.} - E_\beta/(RT) - \text{const.}/[T(T_0 - T)] \quad (18)$$

Although this equation fits the sulfur data quite well up to 80° it is unlikely that nucleation is indeed a controlling process in this type of crystal growth. In fact the values of $(p_\beta - p_\alpha)/p_\alpha$, i.e., the supersaturation, are much smaller than would be expected for two-dimensional nucleation, for which a supersaturation of 50% is usually expected.

It is in fact unlikely that the crystals used are perfect since they are grown in thin films from the melt under conditions far from ideal. It is probable that growth from the vapor occurs on the steps provided by screw dislocations, as first suggested by Frank.[16] At low supersaturations, i.e., at low values of $(p_\beta - p_\alpha)/p_\alpha$ the rate of growth is proportional to $(p_\beta - p_\alpha)^2/p^2_\alpha$, the mechanism of growth being the collision of vapor molecules with the "horizontal" portion of the steps, followed by diffusion on the surface to the vertical portions. At high supersaturations the effective width x_s of the diffusion zone on either side of the vertical step, such that molecules in this zone will reach the top of the step before evaporating, is greater than half the distance between the vertical steps, and the rate of growth is proportional to $(p_\beta - p_\alpha)/p_\alpha$. In fact the rate of growth is then as for a plane surface in the absence of nucleation. In general we may write as an approximation

$$v = \text{const.} \frac{e^{-E_\alpha/(RT)}}{T^{1/2}} \left(\frac{(p_\beta - p_\alpha)}{p_\alpha}\right)^n \quad (19)$$

where n takes the limiting values 1 and 2 for high and low supersaturation. A more complex function is given by Frank, Burton and Cabrera,[17] which gives these limiting forms, namely

$$v = (\text{rate at high supersatn.}) \left(\frac{p_\beta - p_\alpha}{p_\beta' - p_\alpha}\right) \tanh\left(\frac{p_\beta' - p_\alpha}{p_\beta - p_\alpha}\right) \quad (20)$$

where p_β' is a value of the vapor pressure of β such that below p_β' the rate is approximately parabolic in $p_\beta - p_\alpha$ and above it is approximately linear in $p_\beta - p_\alpha$. If we use equation 3 we therefore have

$$v = \frac{m}{d} \frac{\alpha_\alpha \alpha_\beta}{\alpha_\alpha + \alpha_\beta} \frac{(p_\beta - p_\alpha)^2}{(2\pi mkT)^{1/2}} \frac{1}{(p_\beta' - p_\alpha)} \tanh\left(\frac{p_\beta' - p_\alpha}{p_\beta - p_\alpha}\right) \quad (21)$$

(14) M. Volmer, "Kinetic der phasenbildung," Steinkopff, 1939.

(15) W. T. Dunning, Disc. Faraday Soc., 5, 194 (1949).

(16) F. C. Frank, ibid., 5, 48 (1949); Phil. Mag., 1, 91 (1952).

(17) W. K. Burton, N. Cabrera and F. C. Frank, Phil. Mag. Roy. Soc., A243, 299 (1951).

for the linear rate of growth of phase α.

It follows that when $n = 1$ (equation 19) the discussion is as before, but when $n = 2$, *i.e.*, at low supersaturation

$$\ln v = 2 \ln [e^{-\Delta G/(RT)} - 1] - E_\alpha/(RT) \quad (22)$$

if we neglect the effect of $T^{1/2}$ on the temperature coefficient. This equation at low supersaturation may well explain the failure of equations 9 or 17 to account for the behavior of sulfur near the transition point, indeed there is some indication that the experimental results do fit equation 22 over a limited region near T_0. (Hartshorne and Thackray private communication.) It may be noted that the experimental curve of v *versus* T near to T_0 is quite different from that predicted by equations 9 or 17, since dv/dT is zero at T_0, whereas equation 9 or 17 predict that the $v - T$ curve cuts the axis at an angle, as in Fig. 1. When $n = 2$ equation 19 may be rewritten in the form

$$p_\alpha v = \text{const.} (p_\beta - p_\alpha)^2/T^{1/2}$$

and hence $d(p_\alpha v)/dT = 0$ when $p_\beta = p_\alpha$; moreover

$$d(p_\alpha v)/dT = v \, dp_\alpha/dT + p_\alpha dv/dT = p_\alpha dv/dT$$

when $v = 0$. It follows that equation 19, with $n = 2$, gives the experimental value $dv/dT = 0$ at $T = T_0$.

However, the picture is spoiled somewhat by the fact that the experimental results appear to fit a curve with $n = 4$–5 (eq. 19) between the regions to which $n = 2$ and $n = 1$ apply.

In addition to these studies on the reaction between two solid forms it is occasionally possible to make measurements on systems in which three forms are known and the thermodynamics and kinetics of the three solid–solid transformations are interwoven in a fascinating way. Sulfur provides a suitable example,[18] since S_γ sulfur is frequently obtained when a film of sulfur is melted between coverslips and allowed to cool. In addition to the transformation $S_\beta \rightarrow S_\alpha$ already discussed it is therefore possible to study the changes $S_\gamma \rightarrow S_\alpha$ and $S_\gamma \rightarrow S_\beta$, by making use of the different appearance of α-, β- and γ-sulfur when viewed by the polarizing microscope. Results are given in Fig. 2, in which, in contrast to Fig. 1, log v and not v is plotted against T. The sharp drop in the $S_\gamma \rightarrow S_\beta$ curve suggests that there is a transition temperature near to $40°$, since log v would become $-\infty$ at T_0. The apparent activation energy, 150,000 cal. per mole, does not correspond to any physical process likely to occur, since it implies the breaking of S_8 bonds.

From equation 16, $-150,000/R = -23,000/R - 313 \, T_0/(313 - T_0)$ for $T_0 = 40°$, and hence T_0 should be near to $40°$, as suggested by the dotted curve. However, as discussed above, Hartshorne's equation does not represent the facts near to T_0, and it is very likely that the curve of v *versus* T has a rounded minimum at T_0, in which least T_0 could be considerably less than $40°$.

It is not possible to follow this dotted curve directly, since the rates are too low to measure, and Hartshorne and Thackray therefore tried the expedient of adding CS_2, which is known to accelerate

(18) R. S. Bradley, N. H. Hartshorne and M. Thackray, *Nature*, **173**, 400 (1954).

the rate of phase change in $\beta \rightarrow \alpha$ sulfur. Provided that a saturated phase of CS_2 solution is present no change in transition temperature will occur. In accordance with expectation, the rate of transformation $\gamma \rightarrow \beta$ sulfur was greatly increased by CS_2. Contrary to what was expected, however, no reversal of the rate occurred down to $-18°$, so that there remains an unexplained anomaly in this work.

It is interesting to observe that all the theoretical formulas above may be expressed in the forms

$$v_{\beta\alpha} = F (\Delta G_{\beta\alpha}, T, p_\alpha) \quad (23)$$

or

$$\Delta G_{\beta\alpha} = H (v_{\beta\alpha}, T, p_\alpha) \quad (24)$$

and

$$\Delta G_{\gamma\alpha} = H (v_{\gamma\alpha}, T, p_\alpha) \quad (25)$$

where F and H mean "some function of." The two H functions in equations 24 and 25 have the same form and the same constants (since the growing phase is the same in each, namely α) as will be seen by inspection of the equations given above. The vapor pressure of the unstable phase may always be eliminated by the use of equations such as $- \Delta G_{\beta\alpha} = RT \ln(p_\beta/p_\alpha)$.

Now

$$\Delta G_{\gamma\beta} = \Delta G_{\gamma\alpha} - \Delta G_{\beta\alpha} \quad (26)$$

Hence if $v_{\beta\alpha} = v_{\gamma\alpha}$

$$\Delta G_{\beta\alpha} = \Delta G_{\gamma\alpha} \text{ (by 24 and 25)}$$
$$\Delta G_{\gamma\beta} = 0 \text{ (by 26)}$$

It follows that the transition point for $\gamma \rightleftarrows \beta$ sulfur corresponds to the point $v_{\beta\alpha} = v_{\gamma\alpha}$, which, from Fig. 2, is well above $0°$. This result is therefore not in agreement with the work on CS_2 catalysis. It may also be noted that the data in Fig. 2 do not stand up to detailed analysis in the light of a vapor-gap reaction, since this would imply that $v_{\gamma\beta} = v_{\gamma\alpha} - v_{\beta\alpha}$, which is not obeyed. It is possible that these thermodynamic requirements apply only to perfect phases, and that the actual crystal is imperfect and will give a kinetic behavior depending on the presence of imperfections in a matter discussed later. The final test of the $\beta - \gamma$ transition point will await a determination of the vapor pressure of γ-sulfur.

Something must now be said of the reactions which do not appear to proceed by a vapor phase intermediate. It may be noted that the discussion on the temperature of maximum velocity proceeds much as before, even although the transition state may be ill-defined. Consider, for example, the reaction Sn(white) $\rightarrow$ Sn(grey). The rate may be expressed in general terms in the form

$$v = A_w e^{-E_w/(RT)} - A_g e^{-E_g/(RT)} \quad (27)$$

where the suffixes refer to white and grey tin and the energies E_w and E_g to transformation to the transition state. As will be clear from Fig. 3

$$p_w/p_g = B_w e^{-(E_w + E_t)/RT}/[B_g e^{-(E_g + E_t)/RT}] = B_w e^{-(E_w + E_g)/RT}/B_g \quad (28)$$

where E_t is the energy required to pass from the transition to the vapor phase.

Hence

$$v = A_w e^{-E_w/(RT)} [1 - A_g B_w e^{\Delta G/(RT)}/(A_w B_g)] \quad (29)$$

From equation 27, it follows that at the transition point

$$A_w e^{-E_w/(RT_0)} = A_g e^{-E_g/(RT_0)}$$

and from equation 28

$$B_g e^{-E_g/(RT_0)} = B_w e^{-E_w/(RT_0)}$$

Hence

$$A_w B_g = A_g B_w \qquad (30)$$

and hence

$$v = A_w e^{-E_w/(RT)} [1 - e^{\Delta G/(RT)}] \qquad (31)$$

This equation is of the same form as before, and will give a maximum in the velocity curve.

The reaction velocity for the transformation white → grey tin passes through a maximum at −30° according to the work of Tammann[13] and his co-workers, but this is probably in error since a dilatometric method was used to study velocities, and the results are therefore obscured by random nucleation. On the other hand this method is best for the determination of the transition temperature, since a large expansion occurs during the reaction, and since the rate of nucleation and the rate of motion of the interface are both zero at T_0, which Cohen[19] gives at 13.2°. Unfortunately the rate is very dependent on impurities and is greatly accelerated by cold working, but it appears from the somewhat meager data of Tammann that the energy of activation at low temperatures is of the order 6,000 cal. per g. atom. The results of Tammann and Dreyer can be roughly represented (present writer) by the equation for the linear velocity

$$v = 0.1065 \, e^{-6000/RT} [1 - e^{-(526/R)(1/T - 1/286)}] \text{ cm. sec.}^{-1}$$

where the mean heat of transformation has been taken as 526 cal. per g. atom. This equation gives $T_{max} = 258°K.$, in rough agreement with the observed value, 243°K.

It is difficult to see what is the structure of the transition phase, since the energy of activation considerably exceeds the latent heat of melting, 1700 cal. Possibly we are concerned here with some kind of surface migration in grain boundaries. There is also the point that a profound electronic rearrangement must occur from the metallic tin to the semi-conductor diamond-like grey tin. The vapor pressure of tin at room temperature is extremely small, and it is not surprising that the reaction does not go by a vapor-phase transition. It is possible that for any given reaction there are a number of simultaneous mechanisms operating, one of which may predominate.

Another example of a solid → solid reaction which does not appear to proceed via the vapor is provided by yellow → red mercuric iodide at 0–40°.[12] This reaction is complicated by the slowing up of the transformation at constant temperature, perhaps because the gap between the solids widens, but the activation energy remains the same as the reaction proceeds. The whole curve has not been studied. There is evidence that the orientation of the parent phase persists in the product, i.e., that some type of martensitic transformation occurs with single microscopic crystals. The two forms of HgI_2 differ in coördination number, and it is interesting

(19) E. Cohen and A. K. W. A. van Lieshout, Z. physik. Chem., **A173**, 23 (1935); L. J. Green, Nature **174**, 836 (1954).
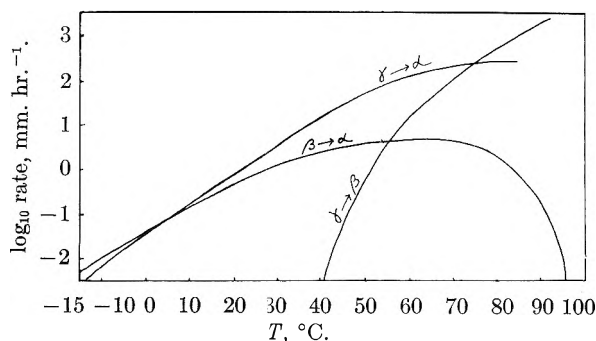
Fig. 2.—Sulfur transformation.
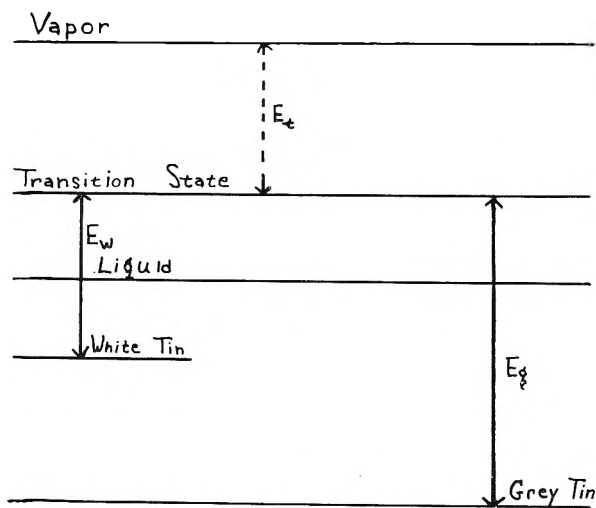
Fig. 3.

to note that according to C. S. Smith a coherent interface is possible with such differences. He writes "the prediction is hazarded that no rapid transformation will be found that does not involve a change in lattice coördination."

II. The Statistical Mechanics: The Temperature Independent Factor

Although the quasi thermodynamic approach is helpful and gives a certain amount of information about the mechanism of solid → solid reactions, a complete theory should enable us to calculate the actual value of velocities of transformation. It is important not to overlook the relative weight of the two factors (activation energy and temperature independent factor).

On the simplest view of the vapor gap theory the temperature independent factor would be

$$\frac{\alpha_\alpha \alpha_\beta}{\alpha_\alpha + \alpha_\beta} \frac{1}{(2\pi mkT)^{1/2}} B_\beta \frac{m}{d} \text{ cm. sec.}^{-1}$$

for the transformation solid β → solid α, where d is the density of the α-form and taking the rate of movement of the face of the α-form to be the rate of advance of the interface. Little change would result if equation 17 were used. Putting $\alpha_\alpha = \alpha_\beta$ for simplicity, for sulfur at 30° this gives a theoretical factor which is $\sim 10^{-3}$ times the experimental factor.

The experimental factor is surprisingly high, in fact it is much greater than the speed of a shock wave, which can hardly move faster than say

10^{-8} cm. in $10^{-12} - 10^{-13}$ sec., giving a velocity of $10^4 - 10^5$ cm.sec.$^{-1}$. It is worth noting, however, that the temperature independent factor for evaporation is itself very large. However, the solid reaction proceeds much faster even than would be expected on a simple evaporation theory.

We have therefore the impasse—the activation energy for a reaction such as $\beta \rightarrow \alpha$ sulfur suggests a vapor transition layer, but the experimental rates are too fast for such a mechanism. This state of affairs is not improved if an attempt is made to replace the evaporation formula by one based on the Polanyi–Wigner[20] theory. These authors consider a monatomic solid and calculate the possibility of a favorable phase relation in the three-dimensional atomic vibrations such that the surface atoms may move away from the surface and dissociate from the latter. They quote without proof

$$\text{linear rate} = 2\,\nu\,\delta\,(E/RT)\,e^{-E/RT} \text{ cm. sec.}^{-1} \quad (32)$$

where ν is the vibration frequency and δ the molecular diameter. More recently a proof is given by Pelzer.[21] Equation 32 gives far too small a value for the temperature independent factor of the reaction $\beta \rightarrow \alpha$ sulfur, since it also gives too small a value for the rate of evaporation of rhombic sulphur: ν may be taken to be $10^{12} - 10^{13}$ sec.$^{-1}$ and δ to be 6×10^{-8} cm. The discrepancy can be reduced somewhat if an analysis of the vibrations of the sulfur lattice be made in terms of linear and torsional oscillations by the application of Debye's theory,[22] but there still remains a large discrepancy for the solid reaction.

It may be noted in passing that the Polanyi–Wigner theory, which has been a kind of corner stone of solid reaction kinetic theory, is itself very imperfect. No allowance is made in this theory for the presence of internal modes of oscillation and for energy exchange between intermolecular and intramolecular vibrations. In Pelzer's derivation the use of a harmonic potential well is unsatisfactory for a dissociation process, and the molecule has to be assumed to be dissociated when removed from the surface by an arbitrary amount r_0. Nevertheless an analogous theory due to Slater[23] for gaseous unimolecular reactions seems to work well. It would be of some interest to examine the dissociation according to Slater's theory of a gaseous molecule which has grown to an infinite size, i.e., has become a solid surface.

A similar large discrepancy in the temperature independent factor occurs in the transformation of azoxybenzene studied by Dr. D. Taylor[10] and has also been noted in many solid reactions of the type solid $\rightarrow$ solid + gas.[24] Similar large discrepancies are observed in the grain growth of metals, and prompt the question, to what extent is the secondary structure of solids of importance in solid $\rightarrow$ solid reaction kinetics. Some indication of this is provided by the fact that there is always a spread in the results, the coefficient of variance being often

of the order 10%, and that a statistical study is necessary. In this way it is possible to overcome to some extent the heart-breaking lack of reproducibility in this field, but it must be admitted that the scatter of result indicates factors not under control.

Burgers and Mott[25,26] first suggested that the "abnormal" factors may be explained on the assumption of a rapid movement through a mosaic block, due to a kind of "falling over" of molecules into new lattice positions, followed by a delay consequent upon the arrival of the reaction interfacial zone at a grain boundary, which had to be bridged, possibly by some kind of reorganization of the dislocation group constituting the grain boundary. On this interpretation the reaction inside the block is "displacive" and that between blocks "reconstructive."[27] The transformation within the block may, under favorable circumstances, require small lattice molecular movements as perhaps in the martensitic transformation in alloys (e.g., Au–Cd). It is even possible that minute embryos of the stable phase are present in the unstable phase. With phases such as white and grey tin the atomic arrangement would not be favorable to this kind of transformation.

The application of these ideas to the type of solid reaction studied by chemists was first made by Garner.[28] Two activation energies are postulated, one for transformation inside the block (E_{block}), usually considerably smaller than the latent heat of sublimation, another for the process, which may be evaporative, of bridging the gaps (E_{gap}). If we consider a reaction at temperatures well below the transition point, we can formulate the reaction rate by adding the time for the interface to cross the gaps to that to cross the mosaic blocks in 1 cm. The former is $Ke^{E_{\text{gap}}/(RT)}/(w + c)$ sec., where K is some unspecified constant, w the mean width of the blocks and c of the gaps, so that there are $1/(w + c)$ gaps per cm. The time to cross the blocks may be written in the form

$$\frac{w}{w + c}\frac{e^{E_{\text{block}}/(RT)}}{\nu\delta}$$

since there are $1/(w + c)$ blocks per cm. Hence the reaction velocity is

$$\frac{1}{K\dfrac{e^{E_{\text{gap}}/(RT)}}{w + c} + \dfrac{w}{w + c}\dfrac{e^{E_{\text{block}}/(RT)}}{\nu\delta}}$$
$$= \nu\delta/[we^{E_{\text{block}}/(RT)}/(w + c) + K\nu\delta e^{E_{\text{gap}}/(RT)}/(w + c)]$$
$$\text{cm. sec.}^{-1} \quad (33)$$

Now if the activation in the block is sufficiently small, the net rate will be

$$\frac{w + c}{K}e^{-E_{\text{gap}}/(RT)}$$

Putting $c \sim 0$, $w \sim 10^{-5}$ we find for K a value 10^{-17} sec. or $1/K = 10^{17}$ sec.$^{-1}$. This is a very high frequency, which does not seem to correspond to anything physical and could only be reduced by making the blocks much wider, in fact of visible size.

(20) M. Polanyi and E. Wigner, Z. physik. Chem., **A139**, 439 (1928).

(21) Pelzer, cf. ref. 14.

(22) R. S. Bradley, Trans. Faraday Soc., **50**, 1182 (1954).

(23) N. B. Slater, Phil. Trans. Roy. Soc., **246**, 57 (1953).

(24) R. S. Bradley, M. M. T. Anous and J. Colvin, J. Chem. Soc., 3348 (1951).

(25) K. Burgers, Ned. Akad. Wet., **50**, 726 (1947).

(26) N. F. Mott, Proc. Phys. Soc., **60**, 391 (1948).

(27) M. S. Buerger, "Phase Transformations in Solids," John Wiley and Sons, New York, N. Y., 1951, p. 183.

(28) W. E. Garner, Disc. Faraday Soc., **5**, 194 (1949).

As criticism of the gap-block theory we have therefore the following points:

(i) The frequency factor in the gap bridging process is quite mysterious and physically unreal.

(ii) The gaps have to slow up the reaction so that (for sulfur) vapor transfer may occur, and hence must completely isolate regions of the unstable form. This does not at first sight seem to fit the motion of crystal lineages put forward by Buerger, according to which there would be nothing to prevent the reaction proceeding throughout the mass, which is made up of dendritic branches with small orientation differences. However, the motion of an interface up a dendritic branch may cause a gap to form between the two phases, and hence the reaction would be held up. If shrinkage occurs away from the glass this is not necessarily true.

It is worth noting that a small mosaic block of width 10^{-5} cm. would not cause much separation between the phases owing to density difference, and any bulk changes in volume could be taken up by major cracks. These often form behind the interface and if present ahead of the interface do not seem to cause much hindrance as the reaction rapidly flows round the end of a crack.

(iii) It is difficult to see how the gap is bridged by the growth from the vapor. Some local difference must arise, either in temperature or due to curvature, which results in a bridge. Simple distillation between two flat faces will never cause a bridge since the gap will in fact widen in the case of sulfur.

(iv) This theory would predict that "perfect" crystals would react as regards motion of the interface much faster than those containing a high concentration of mosaics or other imperfections in contrast to what would be expected for nucleation kinetics.

(v) It is curious that the Burgers–Mott factor does not apply to transformations such as those undergone by nitroaniline or tin. However, the arrangement of lattice sites may not be favorable to a displacive transformation in the block.

(vi) The data for sulfur would require a block width which decreases as T increases (Dr. N. H. Hartshorne, private communication).

Shortly after the original formulation of the crack-block theory Mott published a slightly different version in which grain growth was interpreted as a melting phenomena in which the abnormal temperature independent factor was regarded as an entropy contribution and the activation energy could be much greater than the latent heat of melting owing to the simultaneous melting of a group of atoms or molecules; this group was equal in number to the energy of activation divided by the latent heat of melting, i.e., it was much less than the number of molecules in a mosaic block of dimension 10^{-5}cm. To the writer this formulation seems somewhat artificial, and its application to solid $\rightarrow$ solid reactions would not account for the remarkable coincidence between the energy of activation and the latent heat of sublimation of the unstable form, as discussed above.

We are here beginning to use the language of the transition state theory, and this is a suitable point at which to consider the application of this theory to solid reactions. It is always possible to interpret a factor in the temperature independent term as a contribution from standard entropy of activation, but it is not always clear whether anything is gained by this procedure. According to this theory we should expect the frequency with which molecules leave the two phases to be $kT/he^{-\Delta G_\alpha*/RT}$ and $(kT/h)e^{-\Delta G*_\beta/RT}$ where the $\Delta G*$'s are the standard free energies of activation to the transition state. If δ is the width of a molecule, this will give a linear rate[29]

$$v = \frac{kT}{h}\,\delta\,e^{-\Delta G_\beta*/RT}(1 - e^{\Delta G/RT}) =$$
$$\frac{kT}{h}\,\delta\,e^{\Delta S_\beta*/R}\,e^{-E_\beta/RT}\,(1 - e^{\Delta G/RT}) \quad (33)$$

where $E_\beta*$ refers to the enthalpy change to the transition state. A small point concerns the use of the universal frequency factor kT/h: it seems to the writer that it is much more likely that this should be an actual frequency of the molecules in the surface, which frequency would not change with temperature. This, however, would not greatly affect the results at room temperature.

On this theory the sulfur results could be accounted for by a standard entropy of activation of 32 cal. per degree per mole. While it is tempting to regard an entropy contribution of this kind as arising from the change in disorder consequent upon the nature of the transition state, it must be remembered that the solid reaction shows a greater discrepancy than the evaporation process. The latter can be formulated as

$$v = \frac{kT}{h}\,\delta e^{\Delta S*_{vap}/R}\,e^{-E*_{vap}/RT} \text{ cm. sec.}^{-1} \quad (34)$$

and $\Delta S*$ will be 23 cal. per degree per mole. This is strange in so far as the vapor state would be regarded as having the maximum degree of disorder.

In Mott's analysis, which he applied to the velocity of recrystallization of metals, $\Delta S = E_{vap}/T_m$ where T_m is the melting point of the unstable phase. For sulfur this gives a value of ΔS which is about twice that quoted as the experimental value for the change $\beta \rightarrow \alpha$ sulfur (32 cal. per degree per mole of S_8) and the writer considers that the melting hypothesis is unlikely for this type of solid.

Cagle and Eyring[30] have formulated the transition state theory in a slightly different fashion, using partition functions instead of entropies and introducing a term for the mole fractions of the two forms at the interface which are so located that they can react. It is curious that these authors find for the reaction white $\rightarrow$ grey tin values of the mole fractions which are extremely small, of the order $10^{-10} - 10^{-13}$, i.e., very few atoms are located such that reaction can proceed. They interpret this in terms of cross lines on the two surfaces. However, the treatment mentioned above by the writer gives a temperature independent factor which is too small in comparison with theory by a much smaller factor 10^5, i.e., experimental rate = $10^{-5} \times$ rate calculated.

(29) J. H. Burke, and D. Turnbull, *Progr. Metal Phys.*, 220 (1952).
(30) F. N. Cagle and H. Eyring, THIS JOURNAL, **57**, 942 (1953).

An alternative explanation of some of these discrepancies has been offered by Turnbull[31] for the case of grain growth, namely the presence of impurities, which may lower the free energy difference between the phases. If this lowering is temperature dependent, then the apparent values of the energy and entropy of activation are increased. Although it is quite possible that inclusions are present, these are not in a sufficient concentration in the solid reactions studied to give a variation in transition temperature between the different samples, and it seems unlikely that this effect could be large. The influence of inclusions and of strain on the free energy will be most noticed near to the transition temperature and may give rise to an "indeterminacy thickening" of the type discussed by Ubbelohde.

Summing up, although the application of transition state theory is suggestive it does not seem to take the subject of solid–solid reactions much fur-

(31) D. Turnbull, *J. Metals Trans.*, **191**, 3 (1951).

ther, since the difficulties are thrown back on to the properties of an unknown transition phase, but neither are the other attempts at a solution free from criticism. It appears that most progress could be made by studies on single crystals. It would also be interesting to test the vapor transport theory on a system such as claudetite-arsenolith (As_2O_3), for which the phase with the higher vapor pressure evaporates slower than the other phase, owing to the anomalous nature of the evaporation coefficients. The writer would like to put in a plea for the determination of activation energies wherever possible and believes that chemists and metallurgists would profit greatly by pooling their ideas. However, it should be remembered that metals have high surface energies, are often alloyed, and are often studied at temperatures at which diffusion readily occurs.

It is a pleasure to acknowledge my indebtedness to Dr. N. H. Hartshorne of the University of Leeds for valuable discussions and permission to refer to some of his work prior to publication.

MICROWAVE ABSORPTION AND MOLECULAR STRUCTURE IN LIQUIDS. XVI. DIPOLE DIRECTION AND RELAXATION TIME IN PYRIDINE, TRIOXANE AND THEIR SYMMETRICAL TRIMETHYL DERIVATIVES[1]

By Robert C. Miller[2] and Charles P. Smyth

Contribution from the Frick Chemical Laboratory; Princeton University, Princeton, N. J.

Measurements of dielectric constant and loss have been carried out at wave lengths of 1.24, 3.22 and 10.4 cm. and 300 m. and temperatures from 20 to 80° upon collidine, or 2,4,6-trimethylpyridine, *sym*-trioxane and paraldehyde. The viscosities and densities have also been measured. The results are combined with those previously published for pyridine to investigate the effect of dipole orientation in the molecule upon dielectric relaxation. 2,4,6-Trimethylpyridine and paraldehyde, in spite of much larger molecular size, have virtually the same viscosity as pyridine. However, the critical wave length, at which the dielectric loss is a maximum, has a value for 2,4,6-trimethylpyridine approximately 4 times that for pyridine, probably because of close-packing of the triangular 2,4,6-trimethylpyridine molecules in the liquid and, also, because of their larger size. Paraldehyde, which has a molecule similar in size and shape to that of 2,4,6-trimethylpyridine, has a critical wave length about twice as large, presumably, because the dipole is perpendicular to the molecular triangle instead of parallel to it as in 2,4,6-trimethylpyridine, thus requiring the triangular slabs to turn over instead of rotating in their plane when orientation occurs in the applied field.

An earlier paper[3] of this series has discussed ten flat, rigid molecules such as those of pyridine and quinoline, which have the permanent dipole in the plane of the ring. It is the purpose of this paper to compare the dielectric relaxation times of two such molecules with those of two similarly shaped molecules in which the dipole axes are perpendicular to the planes of the rings. The previously studied pyridine[3] and the newly investigated 2,4,6-trimethylpyridine, or collidine, $2,4,6\text{-}(CH_3)_3C_5H_2N$, will be compared with *sym*-trioxane, $(CH_2O)_3$, and paraldehyde, $(CH_3CHO)_3$.

Experimental Methods and Results

Trioxane from Brothers Chemical Company was fractionally distilled; m.p. 60.5°; lit.[4] 61–62°. U.S.P. paraldehyde was washed with water and fractionally distilled; m.p. 12.3°; lit.[5] 12.5°; b.p. 123.8°; lit.[5] 124°. Collidine from the Brothers Chemical Company was dried over barium oxide and fractionally distilled; b.p. 170.0–170.2°, lit.[6] 172°.

Dielectric constants ϵ' and losses ϵ'' at wave lengths of 1.24, 3.22 and 10.4 cm., and the so-called static dielectric constant ϵ_0 at a wave length of 300 meters were measured by methods described or referred to in earlier papers of this series.[3] The values obtained at each temperature of measurement are given in Table I. The values of the critical wave length λ_m, at which the loss is a maximum, and of the empirical constant α for the distribution of the relaxation

(4) J. F. Walker, "Formaldehyde," Reinhold Publ. Corp., New York, N. Y., 1953, p. 146.

(5) J. Timmermans, "Physico-Chemical Constants of Pure Organic Compounds," Elsevier Publishing Co., New York, N. Y., 1950, p. 500.

(6) "International Critical Tables," McGraw–Hill Book Co., New York, N. Y.

times calculated by the usual methods[7] are given in Table II. Although the collidine and paraldehyde dielectric constant and loss values fitted the Cole and Cole arc plots, the critical wave length values calculated at different frequencies did not agree with one another. The critical wave lengths were, therefore, taken from the values measured at the nearest wave length. The slightly revised values included in Table II for pyridine differ from those previously published by no more than the probable error. Table II also gives the values measured for the viscosities of the liquids and the molar volumes calculated from the measured densities.

TABLE I

DIELECTRIC CONSTANTS AND LOSSES

t, °C.	1.24 cm. ϵ'	ϵ''	3.22 cm. ϵ'	ϵ''	10.4 cm. ϵ'	ϵ''	ϵ_0
			Collidine, $2,4,6\text{-}(CH_3)C_5H_2N$				
20	2.71	0.77	3.37	1.67	6.15	2.07	8.00
40	2.75	.95	3.75	1.80	6.06	1.71	7.46
60	2.85	1.03	4.09	1.90	5.95	1.40	6.94
			sym-Trioxane, $(CH_2O)_3$				
65	8.51	6.80	13.11	5.27	15.75	2.16	15.55
80	8.00	5.97	12.29	4.36	15.04	1.62	14.20
			Paraldehyde, $(CH_3CHO)_3$				
20	2.43	1.00	2.87	2.08	5.14	4.78	14.70
40	2.42	1.09	3.21	2.26	6.54	4.24	12.25
60	2.53	1.15	3.74	2.56	7.26	3.36	10.30
80							8.70
100							7.46
120							6.42

TABLE II

CRITICAL WAVE LENGTHS, DISTRIBUTION COEFFICIENTS, VISCOSITIES AND MOLAR VOLUMES

t, °C.	λ_m (cm.)	α	η (cps.)	V (cc.)
		Pyridine		
1	1.74	0.04	1.31	79.5
20	1.40	0.02	0.95	80.6
40	1.09	0	.72	82.2
60	0.91	0	.58	84.0
		Collidine		
20	7.6	0.08	0.98	131.9
40	6.2	.09	.73	134.6
60	4.4	.10	.58	137.0
		sym-Trioxane		
60[a]	1.55	0	0.94	76.9
80	1.36	0	0.73	78.5
		Paraldehyde		
20	20	0.05	1.18[5]	133.6[5]
40	12.6	.07	0.81[5]	136.5[5]
60	8.2	.10	0.60[5]	139.7[5]

[a] Extrapolated from values at 65°.

Discussion of Results

The dielectric or macroscopic relaxation time, $\tau = \lambda_m/6\pi \times 10^{10}$, differs from the molecular relaxation time because of the effect of the internal field of the liquid. It is greater than the molecular or microscopic relaxation time because, when a given molecule in a polar liquid turns, its neighbors must assume new orientations, thus increasing the macroscopic relaxation time. In terms of the very approximate internal field factor derived by

(7) C. P. Smyth, "Dielectric Behavior and Structure," McGraw-Hill Book Co., New York, N. Y., 1955, pp. 69–70.

O'Dwyer and Sack[8] and Powles,[9] the molecular relaxation times for these four liquids are 0.70 to 0.75 of the macroscopic relaxation times[3] τ. It is evident, therefore, that the critical wave length values provide a means of comparing the relative behaviors of the molecules.

Examination of Stuart–Briegleb models for the four molecules under consideration shows that the shape of the pyridine molecule is approximately that of an oblate spheroid, that of the collidine and paraldehyde molecules a triangular slab with flattened corners and slightly indented sides, and that of the trioxane intermediate between the other two forms. The dipoles of the pyridine and collidine molecules lie in the planes of the rings. The dipole moment of sym-trioxane indicates that the molecules are largely in a chair form and the same is probably true of the paraldehyde molecules.[10,11] In this form the molecular dipole moment is perpendicular to the ring. In the paraldehyde molecule, steric repulsion makes the three equatorial positions appear to be the most probable locations for the three methyl groups and the closeness of the molar volumes of paraldehyde and collidine in Table II supports this supposition.[11] The previously described models for these two molecules have been constructed on the basis of these considerations. The approximate dimensions of the molecules (Table III) obtained by measuring these models may be expressed in terms of the thickness of the spheroidal or triangular slab, the length of the side of the triangle, and the diameter of the circle described when the slab is rotated about the axis of symmetry perpendicular to it.

TABLE III

APPROXIMATE MOLECULAR DIMENSIONS (Å.) AND DIPOLE MOMENTS ($\times 10^{18}$)

	Thickness	Side	Diameter	Moment (in soln.)
Pyridine	3.2	...	6.7	2.23[12]
Collidine	3.6	8.3	8.6	1.93[13]
sym-Trioxane	3.6	5.9	6.6	2.18[12]
Paraldehyde	3.9	8.0	8.6	2.03[12]

When the viscosities of these four liquids at 60° are compared, it is evident that collidine and paraldehyde, in spite of their much larger molecular sizes, have virtually the same viscosity as pyridine. This suggests the possibility that viscous flow in these liquids may involve primarily the slipping of molecular layers over one another with little rotation of the individual molecules. The higher viscosity of trioxane as compared to pyridine is consistent with the closer packing of the molecules indicated by the smaller molar volume and the larger dielectric constant. The critical wave length of trioxane at 60° is 1.70 times that of pyridine as compared to a viscosity ratio 1.62 for

(8) J. J. O'Dwyer and R. A. Sack, *Australian J. Sci. Research*, **A5**, 647 (1952).

(9) J. G. Powles, *J. Chem. Phys.*, **21**, 633 (1953).

(10) A. A. Maryott and S. F. Acree, *J. Research Natl. Bur. Standards* **33**, 71 (1944).

(11) See also R. J. W. Le Fèvre, J. W. Mulley and B. M. Smythe, *J. Chem. Soc.*, 290 (1950).

(12) C. P. Smyth, ref. 7, pp. 299, 343.

(13) M. A. G. Rau and B. N. Narayanaswamy, *Z. physik. Chem.*, **B26**, 23 (1934).

the two liquids. There is no proportionality between critical wave length and viscosity for the other two liquids which have practically the same viscosity as pyridine at 60°, paraldehyde increasing more rapidly with decreasing temperature than collidine and pyridine. The critical wave length of collidine is approximately 4 times that of pyridine, although its greater diameter should make it only 1.6 times as large. Probably, the additional difference may be attributed to close packing of the triangular collidine molecules in the liquid, which necessitates a considerable amount of displacement of the neighboring molecules when rotational orientation occurs, while the pyridine molecules can orient by rotation in the plane of the ring with very little displacement of neighboring molecules. The critical wave length of paraldehyde is 2.6 times that of collidine at 20° and 1.9 times it at 60°, although the viscosities and the molecular sizes and shapes of the two are very nearly the same. In paraldehyde, however, the axis of the molecular dipole is perpendicular to the triangular slab instead of parallel to it as in collidine. Con-

sequently, dipole orientation involves the turning of the triangular slabs out of their planes with consequent greater displacement of neighboring molecules than is required for rotation in the plane of the slab and resultant longer relaxation time and critical wave length. In other words, the collidine critical wave length is lower because its molecules can orient by rotating in the plane of the triangular slab, although they may do so by turning out of the plane as well, while the paraldehyde molecules have to orient by turning out of this plane. The paraldehyde critical wave length at 60° is about 5 times that of trioxane at the same temperature, just as that of collidine is about 5 times that of pyridine, and for similar reasons.

The approximately zero values of α, the coefficient of distribution of relaxation times, for pyridine and trioxane are consistent with their molecular symmetries, while the small but appreciable values for the other two molecules are about what is often found for molecules of this somewhat lower symmetry.

THE CRYOSCOPIC HEAT OF FUSION OF AMMONIUM NITRATE[1]

BY A. G. KEENAN

Department of Chemistry, Illinois Institute of Technology, Chicago 16, Illinois

Received February 16, 1956

Freezing point depression data have been measured for fused salt systems with Li, Na, K, Rb, Cs, Tl and Ag nitrates as solutes and NH_4NO_3 as solvent, in the concentration range 0.5–4.0 mole % and temperature range 160–170°. The reproducibility of the data is within ±0.02°. The results show interesting correlation with ionic radii and structure. The data are interpreted to indicate that there is no solid solution formation in the case of the Li, Na and Ag nitrates, without recourse to actual analysis of the solid phase. These solutions are, in fact, very close to ideal and the data yield a value of 1.53 kcal. mole^{-1} for the latent heat of fusion of ammonium nitrate.

In preparation for other work, the freezing-point depressions for a number of solutions of alkali nitrates in fused ammonium nitrate as solvent were determined in an apparatus developed for this purpose. The results proved to be of sufficient interest to warrant a more systematic study. A series of cryoscopic measurements was, therefore, carried out using the nitrates of Li, Na, K, Rb, Cs, Ag and Tl as solutes in the concentration range of 0.5 to 4.0 mole %. Most of these systems have been covered in the extensive phase-rule studies of the past,[2] but neither the accuracy nor the range of concentrations have, in general, been comparable with the present work.

The interpretation of cryoscopic data at elevated temperatures is seriously complicated by the prevalent occurrence of solid solutions under these conditions. Precision in the direct analysis of the

solid phase is usually very difficult experimentally.[3] The extensive phase-rule studies, in which no solid solution formation is reported, are usually of limited accuracy so that the existence of such solutions to the extent of several per cent. concentration is not precluded by the data. It is believed that the present results can be interpreted in such a way as to exclude the possibility of solid solutions in certain systems without recourse to a direct experimental analysis of the solid phase. It has, therefore, been possible to calculate unequivocally a value for the heat of fusion of ammonium nitrate from the data for these systems. The apparatus and technique are relatively simple and give freezing points which are reproducible to a few hundredths of a degree within the temperature range studied so far, namely, 160 to 170°.

Experimental

A diagram of the freezing point cell is shown in Fig. 1. The inner tube containing the sample was made of 20 mm. Pyrex tubing, and the outer wall of the vacuum jacket was of 40 mm. tubing. The complete assembly shown in the diagram was 45 cm. high. The jacket was evacuated to the ultimate vacuum of a conventional two-stage mercury

(1) This research was supported by the United States Air Force through the Office of Scientific Research of the Air Research and Development Command under contract No. AF 18(600)-1148.

(2) Some of the more recent and pertinent references are: E. O. Holmes, E. O'Connell and F. Hankard, *J. Am. Chem. Soc.*, **73**, 2885 (1951); E. O. Holmes and D. Revinson, *ibid.*, **66**, 453 (1944); J. Whetstone, *Can. J. Res.*, **B26**, 499 (1948); H. M. Glass, K. Laybourn and W. M. Madgin, *J. Chem. Soc.*, 199 (1933); R. G. Early and T. M. Lowry, *ibid.*, **121**, 963 (1922); E. P. Perman and W. J. Howells, *ibid.*, **123**, 2128 (1923).

(3) H. Flood, T. Forland and A. Nesland, *Acta Chem. Scand.*, **5**, 1193 (1951); E. P. Perman and D. R. Dawkins, *J. Chem. Soc.*, **125**, 1239 (1924).

Fig. 1.—Freezing point cell.

Fig. 2.—Representative cooling curves.
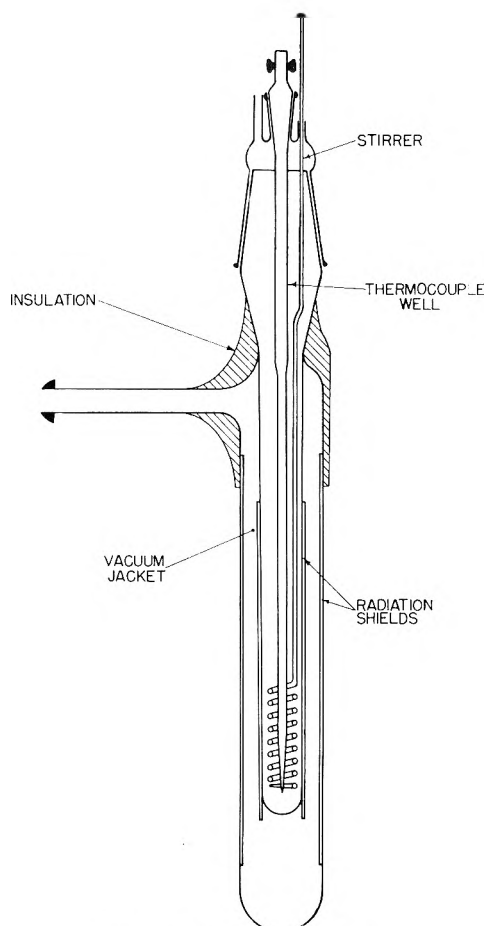
diffusion pump. The top of the glass stirrer shaft was attached to the soft-iron armature of an electromagnet which had a solenoid of 3800 ampere turns, made of B. and S. No. 28 copper wire. The current in the solenoid was interrupted with a commutator made from a discarded one-tenth H.P., d.c. motor. The frequency of the stirrer could be varied from about 400 to 700 strokes per minute and the length of the stroke from 0.5 to 2.5 cm.

The freezing point cell was inserted as far as the bottom of the asbestos-insulation collar into a closely-fitting vertical tube-furnace. The furnace had extra windings at each end to compensate for heat loss and a uniform full-length winding. The voltage of the former was set by trial with a Variac while the latter was regulated by a Brown Type 152 preset-program temperature controller, operating a proportioning motor and Variac.[4] The sensing element of the controller was a single-junction iron–constantan thermocouple clamped to the inner wall of the furnace tube at the approximate elevation of the mid-point of the sample. The regulation at this point was constant to about 0.5°, and this was found to be sufficient to give perfectly smooth cooling curves for the samples.

The temperature within the sample was measured with a single-junction copper–constantan thermocouple made of No. 30 B. and S. gauge glass-insulated duplex wire. The lower 3 cm. of the thermocouple well was pulled out to a thin wall and filled with a silicone liquid. The cold junction of the thermocouple was inserted into a glass tube containing mineral oil which in turn was in a 9 × 35 cm. vacuum flask filled with crushed ice. The temperature of the cold junction was monitored with a calibrated platinum resistance thermometer and a Leeds and Northrup Type G-2 Mueller Bridge. The temperature of this junction was found to be constant and reproducible at 0.000° within a few thousandths, provided the (commercial) ice was first washed several times with tap water, and then kept constantly drained free of the water produced by gradual melting.

The larger part of the e.m.f. of the thermocouple was bucked out with a Leeds and Northrup Type K-2 potentiometer. The remainder was amplified with a Leeds and Northrup Stabilized D-C Microvolt Indicating Amplifier, the output of which was recorded on one pen of a Leeds and Northrup Model S Speedomax Type G two-pen strip-chart X_1–X_2 millivolt recorder. Tracings of representative cooling curves are shown in Fig. 2. The copper–constantan thermocouple was calibrated with the platinum resistance thermometer in the range 150–175°. Thermo-regulation for this purpose was achieved by means of a 4 × 15 cm. copper cylinder inserted into a regulated and stirred fused-salt bath of $NaNO_3$–KNO_3–$NaNO_2$ eutectic.[5]

The ammonium nitrate used in this work was Merck Reagent Grade chemical which has been shown by others[6] to have an ammonia content of 21.28% (calcd. 21.28%). It was dried by storing in a 115° oven and grinding daily until no further caking occurred overnight, after which it was simply stirred daily.[7] The absence of water in this material has been confirmed by specific heat measurements.[6] The lithium nitrate was Eimer and Amend C.P. chemical. It was recrystallized once from hot water which had been acidified with HNO_3, filtered hot, and the crystals dried in an oven at 170°. The temperature was not allowed to fall below 70° at any stage to prevent the formation of hydrate.[8] The silver nitrate was Merck Primary Standard Reagent, and was dried as described by Kolthoff and Sandell.[9] Both the lithium and silver nitrates were ground and transferred to weighing bottles, in a dry-box. The purity of the remaining nitrates was not critical for the present

(4) A. G. Keenan, J. Am. Chem. Soc., **77**, 1379 (1955).

(5) W. E. Kirst, W. M. Nagle and J. B. Castner, Chem. Met. Eng., **47**, 472 (1940).

(6) C. C. Stephenson, D. R. Bentz and D. A. Stevenson, J. Am. Chem. Soc., **77**, 2161 (1955).

(7) R. G. Early and T. M. Lowry, J. Chem. Soc., **115**, 1387 (1919).

(8) E. H. Archibald, "The Preparation of Pure Inorganic Substances," John Wiley and Sons, New York, N. Y., 1932, p. 32.

(9) I. M. Kolthoff and E. B. Sandell, "Quantitative Inorganic Analysis," 3rd Ed., The Macmillan Co., New York, N. Y., 1952, p. 541.

work. The best grades available commercially were used after drying at 110°.

To make a run, the furnace and cell were brought to approximately 200°, a weighed amount (20–30 g.) of ammonium nitrate and solute introduced from weighing bottles, and the system allowed to stand for about 50 min. An atmosphere of dry nitrogen, introduced through the inlet in the cell cap shown in Fig. 1, was used as much as possible during the transferring operations to prevent entry of water vapor from the air. The nitrogen was allowed to flow slowly during the rest of the run. After about 50 min. the ammonium nitrate usually had melted partially allowing the stirrer and thermocouple well to be inserted. The stirrer was started as soon as possible and the furnace temperature adjusted downward gradually until the temperature in the melt rose to a maximum of 4–5° above the expected freezing point. The jacket was then evacuated, the furnace set at its final value of about 3–5° below the freezing point, and the cooling curve recorded. Only a short range of the cooling curves, prior to melting, is shown in Fig. 2.

The freezing point was determined from the cooling curves by the method of simple graphical extrapolation, since this was found to give results well within the reproducibility of the over-all procedure. The range of extrapolation both in time and in temperature in the present instance is sufficiently small that elaborate analytical procedures were not required. The curves in Fig. 2 pertain to solutions of different concentrations and are located arbitrarily on a relative temperature scale. The results were independent of variations in sample size, stirrer speed, degree of supercooling and cooling rate (0.1 to 0.28 deg./min.) within the limits tried. This indicates adequate stirring efficiency and thermal equilibrium.

Discussion

The thermal decomposition of ammonium nitrate has been the subject of much study,[4,10–12] and in fact, the present work was initially undertaken for this purpose. It seems to be generally agreed that the rate of thermal decomposition at the melting point is extremely slow, but a quantitative estimate of the rate is more difficult because of the discordant data available and because of the continuous variation of temperature with time during the actual freezing point measurements. Calculations based on the rate equations and activation energies available,[11–13] indicate that at the freezing point, the rate constant for the decomposition reaction

$$NH_4NO_3 \longrightarrow N_2O + 2H_2O$$
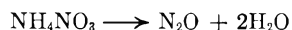
is of the order of magnitude of 1×10^{-7} sec.$^{-1}$. Using reasonable estimates for the reaction time during a freezing point run, it was calculated that the depression of freezing point due to accumulation of products of decomposition was less than experimental error. Possible errors in the concentration values due to loss of ammonium nitrate, either by decomposition or volatilization, were also negligible because of the large excess of solvent in the dilute solutions used. The present series of measurements was undertaken when it became evident that the freezing points of the various solutions were reproducible within a few hundredths of a degree despite reasonable variations in experimental procedure. This fact and the general consistency of the data presented below are perhaps the best arguments to show that thermal decomposition of solvent has not introduced any serious error into the measurements.

(10) R. J. Wood and H. Wise, *J. Chem. Phys.*, **23**, 693 (1955).
(11) G. Feick, *J. Am. Chem. Soc.*, **76**, 5858 (1954).
(12) G. Feick and R. M. Hainer, *ibid.*, **76**, 5860 (1954).
(13) A. J. B. Robertson, *J. Soc. Chem. Ind.*, **67**, 221 (1948).

The results are shown in Fig. 3, plotted as T (freezing point) against concentration in mole fractions. It is evident that the data fall into two distinct groups. Systems with lithium, sodium and silver nitrates as solutes have freezing points which lie close together and tend to a common limiting slope with increasing dilution. The interpretation is suggested, therefore, that these three nitrates are insoluble in the ammonium nitrate solid phase while the widely varying freezing point curves obtained with the other nitrates are due to solid solution formation. This interpretation is consistent with the fragmentary phase-rule data available,[2] but the present data, in addition to being more complete and systematic, also delimit the solid solubility with a much higher precision. Calculations based on standard thermodynamic equations show, for example, that when the solute concentration in the liquid phase is of the order of 1.5 mole % a solute concentration of only 0.04 mole % in the solid phase would raise the freezing point by 0.1° and would be clearly detectable by the present apparatus. Large changes of solid solubility with change in ionic radius are observed in the case of larger ions. It is unlikely that the solid solubility would be the same for all three of the smaller ions since these vary over a twofold range in ionic radius among themselves (Table I).[14] It can, therefore, be concluded that the solid solubility is inappreciable in these three cases. The remaining small differences in these freezing point curves, which are of a different order of magnitude, are discussed later. Deductions based on ionic radii cannot be pressed too far, since the radii themselves are semi-empirical and variable. Nevertheless, the freezing point data are completely consistent with the usual crystal radii given in Table I. The solid solubility is essentially zero for the three ions which are appreciably smaller than ammonium; it increases, beginning with potassium, as the radii approach that of ammonium; then decreases again with cesium where the radius now appreciably exceeds that of ammonium. The occurrence of eutectics very close to the pure-solvent axis in the rubidium, thallium and cesium systems seems unlikely in view of the low concentrations and the shapes of the curves, but is not entirely precluded by the present data. A more detailed investigation was not considered pertinent. Continuously rising curves have been found in the ammonium sulfate–ammonium nitrate system.[15]

TABLE I

Ion	Li	Na	Ag	K	Tl	Rb	NH₄	Cs
Radius (Å.)	0.60	0.95	1.26	1.33	1.44	1.48	1.48	1.69

The most interesting deductions result, however, from a further consideration of the data for the lithium, sodium and silver nitrates. The heat of fusion of the ammonium nitrate is not known with any accuracy so that it is not possible to calculate the ideal cryoscopic curve. However, the argument can be reversed in the present case. The factors which contribute to non-ideal cryoscopic

(14) A. F. Wells, "Structural Inorganic Chemistry," Oxford, 1950, p. 70.
(15) N. L. Bowen, THIS JOURNAL, **30**, 736 (1926).
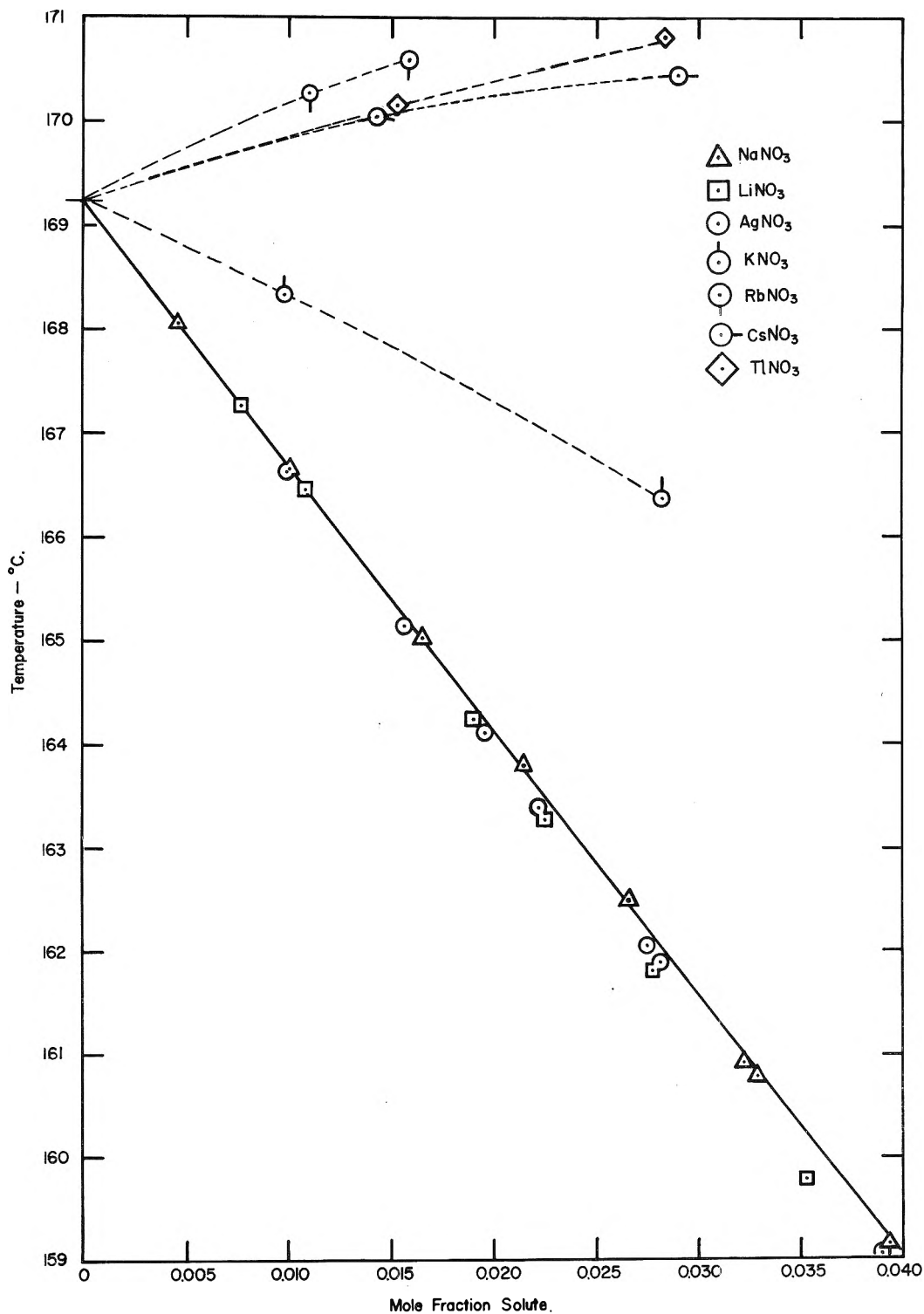
Fig. 3.—Freezing point data.

behavior may be listed as: (1) solid solution formation between solvent and solute; (2) anomalous molecular species in solution due to complex ion formation or irregular dissociation; and (3) various secondary interactions and polarization effects which are usually grouped under an activity coefficient. It is quite unlikely that these factors would all either be equal or cancel out in their effect for all three of the systems under consideration.

As is well known,[16,17] only the foreign ion is effective in depressing the freezing point in fused salts, so that the Van't Hoff "i-factor" has a value of 1 in the ideal case despite the dissociation of solute into two species. The experimental limiting cryoscopic curve may, therefore, be taken to represent ideal behavior and the data plotted according to

(16) H. M. Goodwin and H. T. Kalmus, Phys. Rev., 28, 1 (1909).
(17) E. R. Van Artsdalen, J. Tennessee Acad. Sci., 29, 122 (1954).
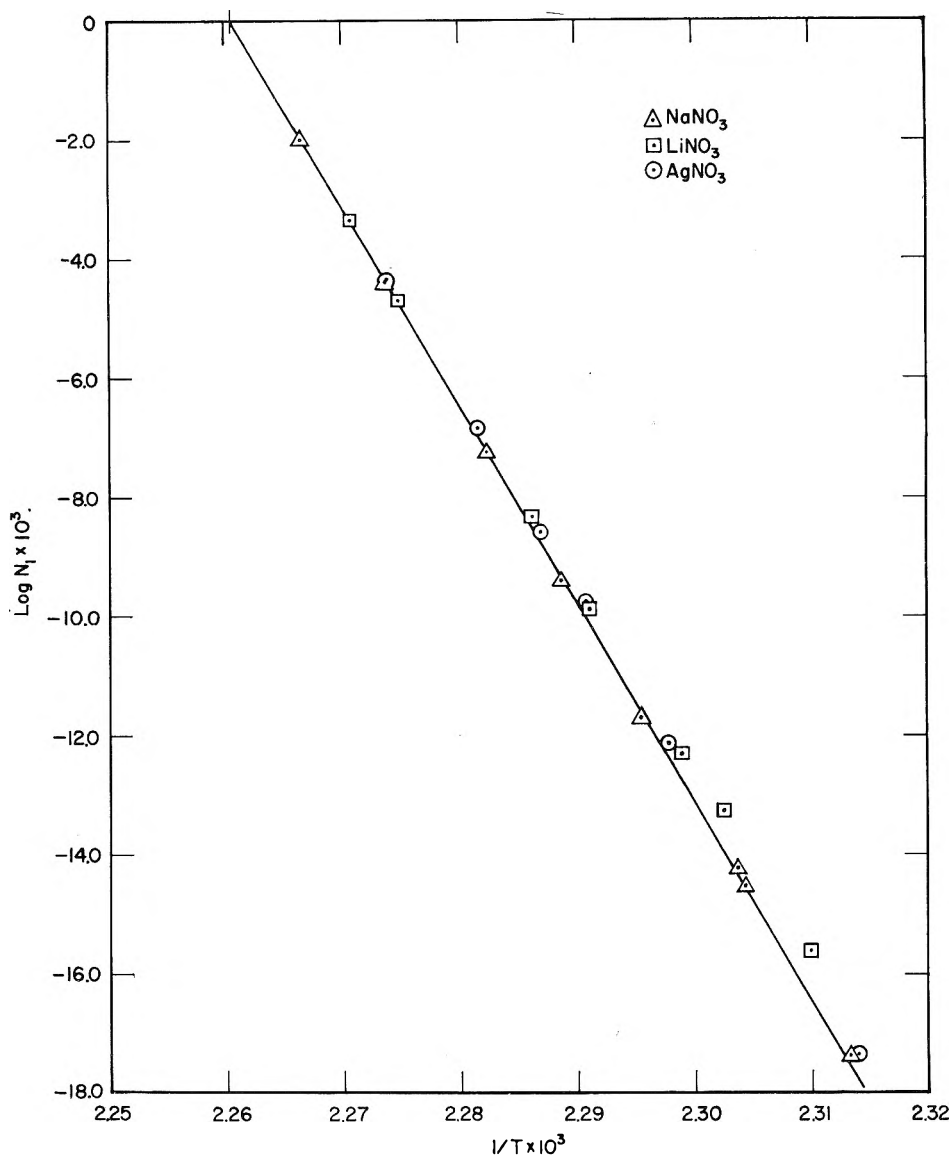
Fig. 4.—Data plotted according to equation 1 of text.

the thermodynamic equation

$$\log N_1 = \frac{\Delta H_f}{2.303R}\left[\frac{1}{T_0} - \frac{1}{T}\right]$$ (1)

where N_1 is the solvent mole fraction, ΔH_f the heat of fusion of the solvent, T_0 the freezing point of the pure solvent, and T, that of the solution. This plot is shown in Fig. 4. The mean deviation from the least-squares line for the five lowest sodium nitrate points is $\pm0.008°$. Equation 1 is derived on the assumption that ΔH_f does not vary with temperature, namely, that ΔC_p (fusion) is zero. The slight deviation of the higher sodium nitrate points may be accounted for by a small positive value of ΔC_p (fusion). For example, it can be shown by calculation that the deviation of the highest sodium nitrate point from the ideal line, which amounts to about $0.1°$, corresponds to ΔC_p (fusion) $= 1.6$ cal. mole^{-1} deg.$^{-1}$ for ammonium nitrate. This is consistent with the values ranging from 0–4.2 cal. mole^{-1} deg.$^{-1}$ for the alkali ni-

trates.[18] The somewhat greater deviations (amounting to a maximum of $0.4°$) in the case of lithium and silver are reasonably attributable to polarization of anions by the lithium ion due to its small radius, and to the pseudo-inert gas electronic structure and the complexing tendency of silver ion. The deviation of the highest concentration point for lithium nitrate corresponds to an activity coefficient of 0.998 for the solvent, calculated according to the equation of Flood, Forland and Nesland.[3] Numerous statements have appeared in recent literature to the effect that fused salt solutions are surprisingly ideal, but the qualitative statement conveys little information.

Using the sodium nitrate data, for the reasons given above and because it is the most stable salt, the limiting slope of Fig. 4 leads to a value of 1.53_0 kcal. mole^{-1} for the latent heat of fusion of ammonium nitrate. Values in the literature, based

(18) G. N. Lewis and M. Randall, "Thermodynamics," 1st Ed., McGraw-Hill Book Co., Inc., New York, N. Y., 1923, p. 78.

on phase studies and on high-pressure compressibilities, range from 1.3 to about 2.0 kcal. mole^{-1}, with 1.46[19] and 1.3[20] being given in recent compilations.

Feick[11] has calculated a value of 45.6 cal. mole^{-1} deg.$^{-1}$ for the specific heat of crystal modification

(19) K. K. Kelley, *Bull. U.S. Bur. Mines*, **393**, 82 (1936).

(20) Nat. Bur. Standards, (U.S.), Cir., **500**, 564 (1952).

I (442.8–398°K.) of ammonium nitrate, using his measured value of the enthalpy of the liquid, and other necessary data from the literature. The present value of 1.53 kcal. mole^{-1} for the heat of fusion, when used in these calculations, gives a specific heat of 40.6 cal. mole^{-1} deg.$^{-1}$ for C,I. The value for the absolute entropy of ammonium nitrate calculated by Feick is not, however, affected appreciably.

THERMAL DISSOCIATION PRESSURE OF CALCIUM CARBONATE

By K. J. Hill and E. R. S. Winter

John & E. Sturge Limited, Birmingham, England

Received February 28, 1956

The thermal dissociation pressure of calcium carbonate has been measured over the temperature range 449–904°. The results fit the equation $\log_{10} p_{(mm.)} = -8792.3/T + 10.4022$, and are compared with those of other authors.

The thermal dissociation of calcium carbonate has long been the subject of investigation. Most workers have confined their study of the variation of the thermal dissociation pressure with temperature to the range of temperature in which the pressure can be measured by a simple mercury manometer. An investigation of the behavior at higher temperatures and pressures, up to and beyond the eutectic point, was reported three decades ago by Smyth and Adams,[1] but no dissociation pressures have been reported at temperatures below about 600° when the pressure is of the order of 1 mm. It has been the object in the present work to extend the range to as low temperatures as possible.

Experimental

The calcium carbonate contained in a platinum boat inside a silica tube was heated in a tubular furnace 1.5 inches in diameter and 14 inches long, which had a central constant-temperature zone of some three inches, in which was placed the sample. During the major part of the work the furnace tube was wound with three separate windings insulated from each other with asbestos paper; first a platinum resistance thermometer was wound non-inductively onto the tube using 0.1 mm. platinum wire, the other two windings were of 25 S.W.G. nichrome wire. The resistances of these windings at room temperature were about 18, 60 and 60 ohms, respectively. In operation an a.c. voltage of up to 250 volts was applied to the inner of the two nichrome windings from a Variac variable transformer. The voltage was adjusted to supply the majority of the heat required to maintain the furnace at the desired temperature. The resistance thermometer was then used in an a.c. Wheatstone bridge circuit to control the supply to the second nichrome winding by means of an electronic controller of the on-off type. This method of control was used at temperatures up to just over 800° and it was possible to maintain the temperature constant to within ±0.5° for periods of up to three weeks or more. At higher temperatures the tube was run with a single winding, the energy supplied being controlled by a Sunvic Simmerstat energy controller, which maintained the selected temperature constant to within ±1° over periods of up to 12 hours.

The temperature of the furnace was measured by means of a platinum/platinum–13% rhodium thermocouple using a commercial pyrometer, which could be read to 1°. The thermocouple used was standardized at the sulfur point at intervals throughout the work. A small platinum resistance thermometer was used to check the constancy of the temperature of the furnace over long periods. This was placed

(1) F. H. Smyth and L. H. Adams, *J. Am. Chem. Soc.*, **45**, 1167 (1923).

with its sensitive tip just outside the silica tube alongside the platinum boat and beside the thermocouple; it was used in a Wheatstone bridge network supplied by a single accumulator. The bridge was balanced at the approximate temperature of the furnace and the out of balance current was then supplied to a recording galvanometer of high resistance and sensitivity. In this way a continuous record of the variation of the temperature was obtained and drifts and temperature changes of the order of 0.25° or less could be detected.

The silica tube containing the platinum boat and sample was connected by a graded seal to the remainder of the vacuum system which was of Pyrex glass and contained no stopcocks or ground joints, being isolated from the pumps, etc., by a mercury cut-off. Thermal dissociation pressures over 1 mm. were measured by a mercury U-manometer with arms of about 1 cm. diameter, one of which was evacuated continuously; a cathetometer was used for pressures below ~10 cm. Pressures below 3 mm. and above 0.04 mm. were measured by a McLeod gage, and a more sensitive McLeod gage was employed for pressures below 0.04 mm. Satisfactory cross-calibration was achieved in the pressure regions where the gage and the manometer overlapped. A thermostated Pirani gage protected from mercury vapor by a trap at −78°, and which had been calibrated against a McLeod gage using carbon dioxide, was also used to check pressures where the ranges of the two McLeod gages met.

The calcium carbonate used throughout these experiments was Grade 80 Pure Precipitated Calcium Carbonate (manufactured by John & E. Sturge Ltd.). It consisted of irregular calcitic rhombs about 40 μ in diameter and had the analysis

Chloride (Cl)	<0.02%
Sulfate (SO$_4$)	0.13%
Iron (Fe)	<5 p.p.m.
Lead (Pb)	<5 p.p.m.
Copper (Cu)	<4 p.p.m.
Nickel (Ni)	<3 p.p.m.
Phosphate (PO$_4$)	0.002%
Silica (SiO$_2$)	0.02%
Alkali metals (Na)	0.015%
Magnesium (Mg)	<0.03%
Ammonia (NH$_3$)	<0.05%
Water (H$_2$O) (after drying in air at 105°)	0.35%

Water is the chief impurity and proved rather troublesome as it began to be evolved as soon as thermal dissociation commenced. In order to obtain consistent and reproducible results it was found necessary to completely decompose the sample by heating *in vacuo* at about 650° and then to recarbonate at the same temperature with carbon dioxide admitted through a trap cooled to −78°; the sample was then cooled over a period of 100 min. to about 400° and evacuated overnight. After this treatment no further troublesome evolution of water was observed.

A series of observations of the thermal dissociation pressure was obtained by heating the sample at a constant temperature and allowing the pressure to become constant. At temperatures of 800° or so, equilibrium was established rapidly (in a few hours) but at lower temperatures the time required became progressively longer until at 449° about three weeks were required to attain a steady pressure. Points were obtained by the evolution and by the absorption of carbon dioxide over the whole of the temperature range studied and both sets of points fell on the same smooth curve.

Results and Discussion

The equilibrium dissociation pressures are given in Table I.

TABLE I

Temp., °C.	Pressure, mm.	Temp., °C.	Pressure, mm.	Temp., °C.	Pressure, mm.
449	0.0170	615	3.15	785	117.5
465	.0330	632	5.26	803	168.4
466	.0334	640	6.75	816	219.0
480	.0483	656	9.47	822	220.0
493	.0806	662	10.22	832	271.2
508	.128	673	13.46	850	365.6
528	.262	686	16.95	853	372.0
540	.360	698	23.10	864	457.0
540	.432	706	29.04	870	495.0
554	.579	719	37.85	876	518.8
556	.598	737	53.80	886	584.0
564	.801	747	65.19	898	692.5
579	1.120	767	90.94	904	813.0
596	2.025	767	95.94		
607	2.46	784	132.7		

Our values are in good general agreement with the results of other workers and lie, at higher pressures, between the extreme results already published. At temperatures between 600 and 700°, where the only values are due to Johnston,[2] agreement is reasonable and the scatter of results less than in the earlier work. No results for comparison are available below about 600°.

It should be possible to express the variation of dissociation pressure with temperature by an equation of the form

$$\log p = \frac{A}{T} + B \log T + CT + DT^2 + E \quad (1)$$

Equations 2, 3, 4 and 5 were put forward by Smyth and Adams,[1] Johnston,[2] Southard and Royster,[3] and Forland,[4] respectively, on the basis of their measured pressures, whilst an equation equivalent to eq. 6 has been derived by Kelley and Anderson[5] from the variation of specific heats of the three phases of the system and an average value of the chemical constant (calculated from the thermal dissociation results of various authors).

(2) J. Johnston, J. Am. Chem. Soc., **32**, 938 (1910).
(3) J. C. Southard and P. H. Royster, THIS JOURNAL, **40**, 435 (1936).
(4) T. Forland, ibid., **59**, 154 (1955).
(5) K. K. Kelley and C. T. Anderson, Bur. Mines Bull., No. 384, 1935.

$$\log_{10} p_{(mm.)} = \frac{-11355}{T} - 5.388 \log_{10} T + 29.119 \quad (2)$$

$$\log_{10} p_{(mm.)} = \frac{-9340}{T} + 1.1 \log_{10} T - 0.0012T + 8.882 \quad (3)$$

$$\log_{10} p_{(mm.)} = \frac{-9140}{T} + 0.382 \log_{10} T - 0.000668 T + 8.3171 \quad (4)$$

$$\log_{10} p_{(atm.)} = \frac{-9678}{T} - 1.389 \log T + 2.842 \times 10^4 T^{-2} - 2.186 \times 10^{-4} T + 12.780 \quad (5)$$

$$\log_{10} p_{(atm.)} = \frac{-9290}{T} + 0.332 \log_{10} T - 0.000471 T + 448 T^{-2} + 7.558 \quad (6)$$

The plot of log p against $1/T$ for the results presented here is a good straight line, which by the method of least squares has been found to fit eq. 7 over the whole range

$$\log_{10} p_{(mm.)} = \frac{-8792.3}{T} + 10.4022 \quad (7)$$

Least squares calculations using equations with more terms in T gave meaningless results owing to the small values of the coefficients of these other terms. The lack of terms in T and log T is at first sight surprising but this is due to the relatively limited temperature range in which we have worked. Thus over the range 700–1000°K., in which most of our experimental results lie the numerical value of $0.332 \log_{10} T$ from Kelley and Anderson's equation for example is approximately proportional to $1/T$ and hence within experimental error the lack of these terms can be compensated for by a change in the coefficient of $1/T$.

Individual determinations of the dissociation pressure give results which differ from those calculated from equation 7 by not more than ±10% on the pressure measured, and in most cases less than 5%, which represent in the particular temperature ranges used, temperature errors of at most ±2° and usually < ±1°. In particular the calculated pressures are too high at temperatures above 800°, where it may be noted our method of temperature control was less precise (cf. Experimental).

Pressures calculated from eq. 7 fall between those calculated from the equation of Smyth and Adams, which are too low, and those calculated from Johnston's equation, which gives values close to that of Southard and Royster. Our equation predicts a dissociation pressure of 760 mm. of carbon dioxide at 896°, which may be compared with 894.4° by Southard and Royster,[3] 882° by Andrussov[6] and also by Tamaru, Siomi and Adati,[7] 897° by Smyth and Adams[1] and 898° by Johnston.[2]

(6) L. Andrussov, Z. physik. Chem., **116**, 81 (1925).
(7) S. Tamaru, K. Siomi and M. Adati, ibid., **157**, 447 (1931).

THE PARTITION OF ELECTROLYTES BETWEEN AQUEOUS AND ORGANIC PHASES. II. FREE ENERGY OF TRANSFER FROM PURE WATER TO WATER SATURATED WITH NITROMETHANE[1]

BY G. R. HAUGEN AND HAROLD L. FRIEDMAN

Contribution from the Department of Chemistry, University of Southern California, Los Angeles, Calif.

Received March 5, 1956

Measurements have been made of the solubility at 25° of $KClO_4$, $KReO_4$, $RbClO_4$, $CsClO_4$ and $CsReO_4$ in aqueous nitromethane solutions as a function of nitromethane concentration and of the solubility of nitromethane in aqueous solutions of $HClO_4$, $LiCl$, $LiClO_4$, $NaCl$, $NaClO_4$, KCl and $CsCl$ as a function of electrolyte concentration. The data are used to calculate the following molar free energies of transfer of ions from pure water to water saturated with nitromethane (1.99 molal) at 25°: Li^+, 0.21; Na^+, 0.19; K^+, 0.07; H^+, 0 (Reference); Rb^+, −0.01; Cs^+, −0.03; Cl^-, −0.05; ClO_4^-, −0.40; ReO_4^-, −0.49 kcal., with uncertainties mostly about ±0.03 kcal.

In the first paper of this series[2] it was pointed out that partition measurements combined with suitable measurements of salting-out constants could lead to values for the free energy of transfer of electrolytes from pure water to pure organic solvent and thus to standard free energies of formation of ions in organic solvents. More explicitly, measurements of the partition of an electrolyte (MA) between aqueous and organic phases, extending over a suitable range of electrolyte concentration, lead to the increase in standard free energy (ΔF_1^0) for the process[3]

$$MA(AQ') \longrightarrow MA(ORG') \qquad (1)$$
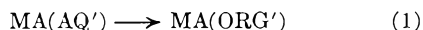
In reference 2, ΔF_1^0 was reported for the alkali perrhenates and reineckates $[Cr(NH_3)_2(SCN)_4^-]$ in the solvent system, water–nitromethane at 25°.

In this paper results are reported which lead to the free energy change $[\Delta F_2^0]$ for the process

$$MA(AQ) \longrightarrow MA(AQ') \qquad (2)$$
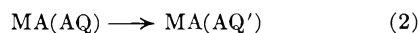
for several alkali metal salts in water–nitromethane at 25°. It is hoped that similar methods can be applied to obtain ΔF_3^0 for

$$MA(ORG') \longrightarrow MA(ORG) \qquad (3)$$

because the sum of these reactions gives

$$MA(AQ) \longrightarrow MA(ORG) \qquad (4)$$
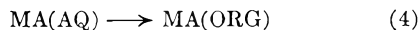
The complete set of values of ΔF_4^0 allows the calculation of the standard free energies of formation of the alkali metal ions in nitromethane. Although the procedure outlined here may appear to be unnecessarily complicated, the more direct methods for obtaining the standard free energies of a series of ions in a solvent such as nitromethane seem to offer greater experimental difficulties.

The results reported in this paper are of interest, both as a step in obtaining ionic free energies in nitromethane and as an experimental analysis of salting-out relationships in the nitromethane–

water system which is in some ways more complete than has been obtained for any other system.

Solute–Solute Interaction Coefficients.—The present method of determining ΔF_2^0 depends upon the relation

$$\Delta F_2^0 = \int_{m_{00}}^{m_{0s}} (\partial \mu_e / \partial m_0)_{m_{e0}} \, dm_0 \qquad (5)$$

where m_0 is, in this system, the molality of nitromethane and μ_e is the chemical potential of the electrolyte. The integration is from pure water, m_{00}, to water saturated with nitromethane, m_{0s}, and $(\partial \mu_e / \partial m_0)_{m_{e0}}$ applies for infinitesimal elec-
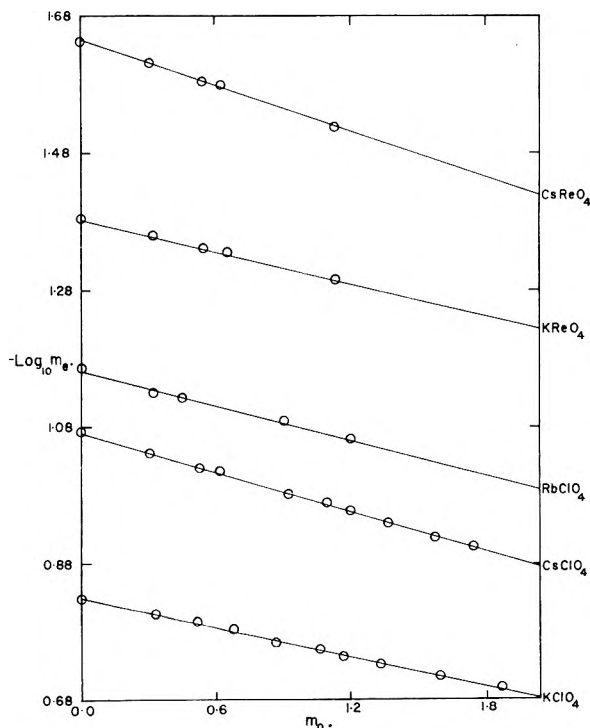
Fig. 1.—Solubility of the electrolytes as a function of nitromethane concentration at 25° m_e is the solubility of the electrolyte in the ternary solution. m_0 is the concentration of the nitromethane in the ternary solution.

trolyte concentration. This derivative is related[4] to two solubility interaction coefficients which are experimentally accessible

$$k_e = -(\partial \ln m_e / \partial m_0)_{\mu_e} \qquad (6)$$

$$k_0 = -(\partial \ln m_0 / \partial m_e)_{\mu_0} \qquad (6')$$

(1) This work was supported by the U. S. Atomic Energy Commission.

(2) H. L. Friedman and G. R. Haugen, *J. Am. Chem. Soc.*, **76**, 2060 (1954).

(3) In this paper (AQ) indicates solution in pure water, (ORG) in pure organic solvent. (AQ') and (ORG') refer to solution in solvents of the composition of the aqueous and organic phases, respectively, formed when water and organic solvent are equilibrated. In the standard state the electrolyte is completely ionized. In the partition experiments the standard states were taken as Hyp. 1 molar solution of the electrolyte in the different solvents (AQ' and ORG'), but in the present work the standard states are Hyp. 1 molal solution of the electrolyte in the different solvents (AQ and AQ').

(4) H. L. Friedman, THIS JOURNAL, **59**, 161 (1955).
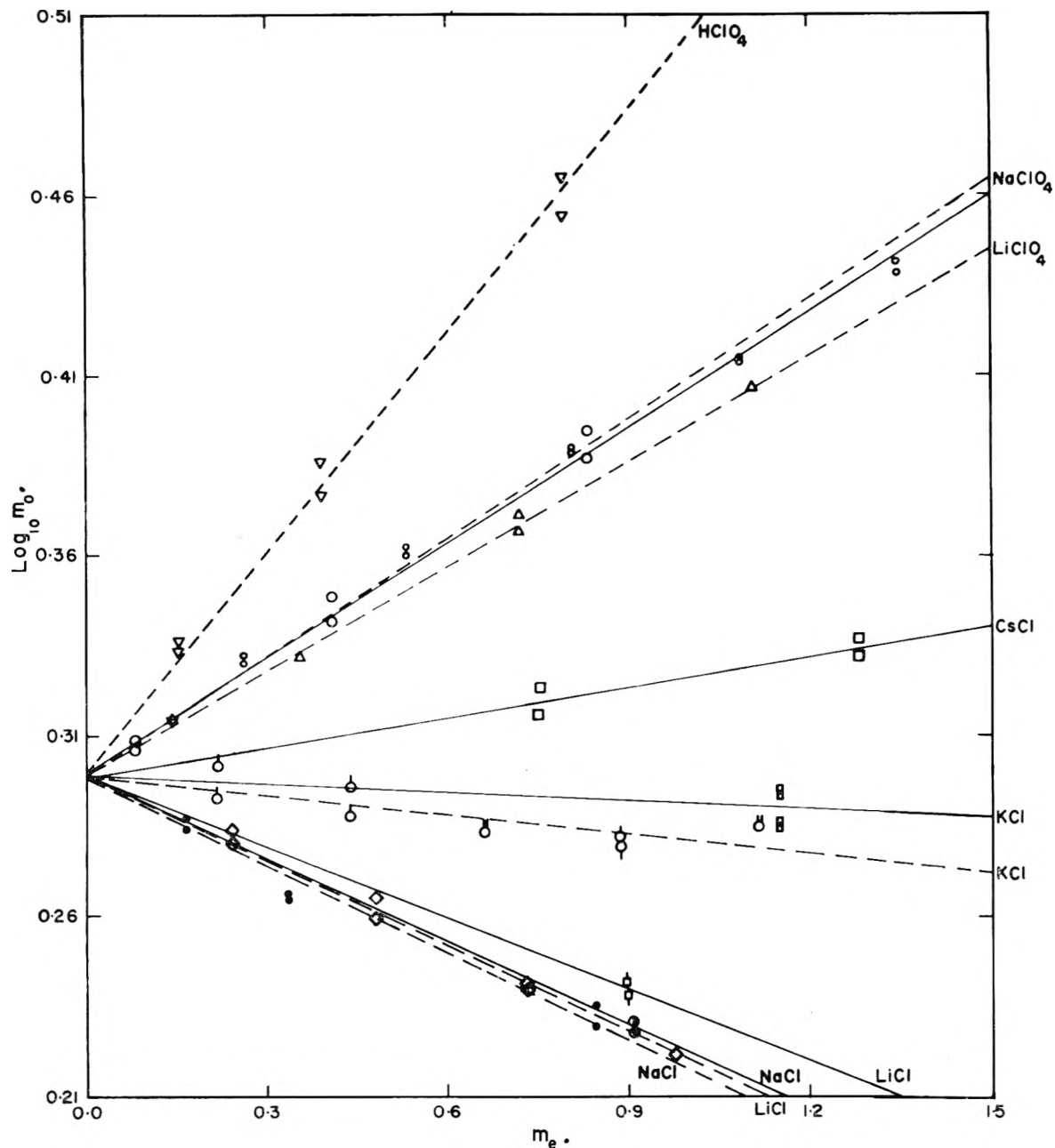
Fig. 2.—Solubility of nitromethane as a function of electrolyte concentration at 25°. m_0 is the solubility of nitromethane, in the ternary solution. m_e is the concentration of the electrolyte in the ternary solution.   The dotted lines correspond to experimental values obtained by equilibrium volume method and the solid lines correspond to experimental values obtained by O. D. method: ▽, $HClO_4$ (equilibrium volume method);   ◯, $NaClO_4$ (equilibrium volume method);   ○, $NaClO_4$ (O.D. method);   △, $LiClO_4$ (equilibrium volume method);   ☐, $CsCl$ (O.D. method);   ♂, KC (equilibrium volume method);   ☐, KCl (O.D. method);   ⌂, $LiCl$ (O.D. method);   ◇, $LiCl$ (equilibrium volume method) ◑, $NaCl$ (O.D. method);   ●, $NaCl$; (equilibrium volume method).

The solubilities of several electrolytes in water–nitromethane mixtures are shown in Fig. 1. Since all of the solutions which are represented by the points on a given curve have the same chemical potential of electrolyte, namely, that of the solid phase, the slope at each point is $k_s/2.303$ for a solution of that composition. It is important to note that k_e is found to be independent of m_0: the lines are straight. A more complete analysis of the k_e data is given in Table I.

The solubility of nitromethane in several water–electrolyte mixtures is shown in Fig. 2. In this case the solutions along a given line do not have exactly the same chemical potential of nitromethane, because both water and electrolyte dissolve to some extent in the nitromethane phase, and the composition of the nitromethane phase depends upon the activities of these components in the aqueous phase. However, it can be shown[5] that the corrections for these effects are negligible for the systems investigated here and that the slope of each line in Fig. 2 is therefore $k_0/2303$. It is found that k_0 (Table I) is independent of m_e for a given

(5) Ref. 4, eq. 21.

Table I

Slope and Intercept of Setschenow Equation Calculated by Method of Least Squares at 24.9°

Salt	$k_e \pm \sigma^d$		Intercept[c] $\log_{10} m_{es}$
KClO$_4$	−0.162	±0.006	−0.828
KReO$_4$	− .181	.003	−1.385
RbClO$_4$	− .192	.019	−1.162
CsClO$_4$	− .221	.007	−1.073
CsReO$_4$	− .252	.008	−1.645

Salt	$k_0 \pm \sigma^d$		Intercept[c] $\log_{10} m_{0s}$
LiClO$_4$[a]	−0.224	±0.017	0.299
LiCl[a]	+ .181	.017	.299
LiCl[b]	+ .150	.007	.299
NaClO$_4$[a]	− .256	.032	.299
NaClO$_4$[b]	− .246	.017	.300
NaCl[a]	+ .185	.031	.298
NaCl[b]	+ .176	.005	.299
KCl[a]	+ .039	.027	.299
KCl[b]	+ .017	.010	.299
CsCl[b]	− .064	.009	.299
HClO$_4$[a]	− .472	.005	.299

[a] Data obtained by equilibrium volume method. [b] Data obtained by O.D. method. [c] m_{es} = solubility of salt in pure water and m_{0s} = solubility of nitromethane in pure water. The standard deviation of these values ranges from 0.001 to 0.004. [d] Standard deviation.

electrolyte, corresponding to the Setschenow law.[6] Thus it is found by experiment that k_e is independent of m_0 and k_0 is independent of m_e in the experimental concentration range.

Returning to eq. 5, we have as results of earlier work[4,7]

$$(\partial \mu_e / \partial m_0)_{m_e} = (\partial \mu_0 / \partial m_e)_{m_0} \quad (7)$$

$$(\partial \mu_e / \partial m_0)_{m_e} / 2RT = k_e (1 + m_e (\partial \ln \gamma_e / \partial m_e)_{m_0}) \quad (8)$$

$$(\partial \mu_0 / \partial m_e)_{m_0} / RT = k_0 (1 + m_0 (\partial \ln \gamma_0 / \partial m_0)_{m_e}) \quad (8')$$

property of the saturated solution of electrolyte in pure water. We evaluate it from the Guntelberg formula[8]

$$\ln \gamma_e = -1.17 \sqrt{m_e} / (1 + \sqrt{m_e}) \quad (9)$$

because experimental data for the activity coefficients of these electrolytes at 25° are lacking and because this semi-empirical formula is moderately accurate at the low electrolyte concentration encountered in the measurement of k_e. The quantity obtained from eq. 8 in this way is $(\partial \mu_e / \partial m_0)_{m_e}$ for m_e fixed at the solubility of the electrolyte in water, and for vanishingly small m_0. This will be abbreviated $(\partial \mu_e / \partial m_0)_{m_{es}}^{m_{00}}$.[9] The calculations are summarized in Table II.

In a similar way, using the measured k_0's and eq. 8', we obtain $(\partial \mu_0 / \partial m_e)_{m_{0s}}^{m_{e0}}$ (Table III). For this purpose $(\partial \ln \gamma_0 / \partial m_0)_{m_{e0}}$ was determined by measurement of the vapor pressure of nitromethane over its aqueous solutions. The value of this derivative at the saturation concentration of nitromethane in water is −0.144 molal^{-1} and the solubility of nitromethane in water is 1.989 molal.

The derivative $(\partial \mu_0 / \partial m_e)_{m_{0s}}^{m_{e0}}$ must be composed of additive contributions of the ions of the electrolyte, like all other properties of the electrolyte at infinite dilution. A check upon the data is afforded by the comparison of the difference of $(\partial \mu_0 / \partial m_e)_{m_{0s}}^{m_{e0}}$ for the following points

LiCl–LiClO$_4$ = 0.165 ± 0.025 kcal. mole^{-1} molal^{-1}
NaCl–NaClO$_4$ = 0.182 ± 0.032 kcal. mole^{-1} molal^{-1}

The additivity property may then be used to calculate the values of $(\partial \mu_0 / \partial m_e)_{m_{0s}}^{m_{e0}}$ for HCl, KClO$_4$ and CsClO$_4$ which are, respectively: −0.026 ± 0.060, −0.162 ± 0.020, −0.201 ± 0.035 kcal.

Table II

Calculations on Data of Table I According to Equation 3

Electrolyte	m_{es}[a] (pure water)	$\left(\dfrac{\partial \ln \gamma_e}{\partial m_e}\right)_{m_{00}}$	$\left(\dfrac{\partial \mu_e}{\partial m_0}\right)_{m_{es}}^{m_{00}}$ kcal. mole^{-1} molal^{-1}	$m_{es}^{b,c}$ (pure water)
KClO$_4$	0.148 ± 0.0007%	−0.787	−0.169 ± 0.011	0.149[e]
KReO$_4$	.0412 ± .0001	−2.00	− .196 ± .007	.042 ± 0.008[d]%
RbClO$_4$	.0688 ± .0006	−1.41	− .206 ± .024	.065 ± .003[e]
CsClO$_4$	.0846 ± .0005	−1.22	− .236 ± .012	.088 ± .002[e]
CsReO$_4$	.0226 ± .0002	−2.91	− .278 ± .013	.024 ± .001[d]

[a] The uncertainties were estimated from the standard deviation of the intercepts. [b] The uncertainties were estimated from the standard deviation of k_e, and from the assumption of a 20% uncertainty in $m_{es}(\partial \ln \gamma_e / \partial m_e)_{m_{00}}$ in each case. [c] Literature values for the solubility of the salts in pure water. [d] W. T. Smith and S. H. Long, J. Am. Chem. Soc., 70, 354 (1948); E. W. Dorfurt and T. Gunzert, Z. anorg. Chem., 215, 369 (1933). [e] "International Critical Tables," McGraw–Hill Book Co., Inc., New York, N. Y., 1930.

It is important to note that all of the quantities in any one of these equations must be properties of the same solution. Thus in applying eq. 8 one obtains from one of the lines of Fig. 1 a value of k_e characteristic of a series of solution. Using m_e and $(\partial \ln \gamma_e / \partial m_e)_{m_0}$ for any one of these solutions, one may then calculate $(\partial \mu_e / \partial m_0)_{m_e}$ for *that* solution.

For each electrolyte in Fig. 1, we note that k_e is determined at $m_0 = 0$ as well as at higher m_0. At $m_0 = 0$, the derivative $(\partial \ln \gamma_e / \partial m_e)_{m_0}$ is a

mole^{-1} molal^{-1}. A comparison of the values of $(\partial \mu_0 / \partial m_e)_{m_{0s}}^{m_{e0}}$ and $(\partial \mu_e / \partial m_0)_{m_{es}}^{m_{00}}$ for KClO$_4$ and CsClO$_4$ shows that at least for these salts

$$(\partial \mu_0 / \partial m_e)_{m_{0s}}^{m_{e0}} = (\partial \mu_e / \partial m_0)_{m_{es}}^{m_{00}} \quad (10)$$

Since at any one composition eq. 7 is valid, the simplest deduction from eq. 10 is that $(\partial \mu_e / \partial m_0)_{m_e} = (\partial \mu_0 / \partial m_e)_{m_0}$ does not vary appreciably from $m_e = 0 = m_0$ up to electrolyte concentrations of the

(6) F. A. Long and W. F. McDevit, Chem. Revs., 51, 119 (1952).

(7) H. A. C. McKay, Trans. Faraday Soc., 49, 237 (1953).

(8) E. A. Guggenheim, "Thermodynamics," Interscience Publishers, Inc., New York, N. Y., 1950.

(9) $(\partial \mu_e / \partial m_0)_{m_{es}}^{m_{00}}$ is an abbreviation for $\lim\limits_{m_0 \to 0} (\partial \mu_e / \partial m_0)_{m_{es}}$

TABLE III

CALCULATED FROM DATA OF TABLE I ACCORDING TO EQUATION 8'

Electrolyte	$(\partial\mu_0/\partial m_0)^{me0,\,a}_{m_{0s}'}$ kcal. mole^{-1} molal^{-1}
LiClO$_4$	-0.095 ± 0.015
NaClO$_4$	$-0.106 \pm .019$
HClO$_4$	$-0.199 \pm .035$
LiCl	$+0.070 \pm .011$
NaCl	$+0.076 \pm .014$
KCl	$+0.012 \pm .009$
CsCl	$-0.027 \pm .006$

^{a} The uncertainties were estimated from the standard deviation of k_0 and from the assumption that m_{0s} ($\partial \ln \gamma_0/\partial m_0)_{m_{eo}}$ was subject to 20% uncertainty.

order of 0.1 M and nitromethane concentration of the order of 2 M, and therefore the coefficients calculated by (8) and (8') are the limiting interaction coefficients. The other possibility would be a special configuration of the $(\partial\mu_e/\partial m_0)_{m_e}$ vs. m_e and m_0 surface to make (10) valid for each of the cases for which it was checked. The simpler hypothesis will be adopted here, and assumed to apply to all of the systems dealt with in this paper, although this cannot be verified without measurements other than solubility measurements on the ternary systems[4] (i.e., vapor pressure measurements or some other direct measurements of activity are required).

nitromethane concentration. Thus equation 5 reduces to

$$\Delta F_2^0 = (\partial\mu_e/\partial m_0)^{m_{00}}_{m_{e0}} \int_{m_{00}}^{m_{0s}} dm_0 = (\partial\mu_e/\partial m_0)^{m_{00}}_{m_{e0}} \times m_{0s}$$

ΔF_2^0 is given in Table IV for the various electrolytes. The results can be expressed most concisely by calculating the standard free energies of transfer of the various ions involved (Table IV). The standard free energy of transfer of H$^+$ is defined as zero.

The comparison of ΔF_2^0 with ΔF_1^{02} shows smaller magnitudes by a factor of 10, for the former, but similar trends with size for the alkali metal ions, even to the close similarity of Li$^+$ and Na$^+$ compared to the larger ions. It is planned to discuss the present results more completely in a later paper together with the data for reaction (3) when these become available.

Experimental

Materials.—The preparation and purification of most of the materials have already been described.[2] RbCl was purified by conversion to chloroiodide and repeated crystallization before conversion to RbClO$_4$. RbClO$_4$ and CsClO$_4$ were recrystallized twice from water. Nitromethane was dried by filtering at $-25°$.

Measurement of k_e.—The solubility of the salt in aqueous nitromethane solutions was studied by equilibrating an excess of the solid anhydrous salt with an aqueous solution of known nitromethane concentration at 24.8° for 2–3 hours in a screw cap vial, which had a film of Teflon placed under the cap to keep the solution from coming into contact with

TABLE IV

FREE ENERGY OF TRANSFER FROM PURE WATER TO WATER SATURATED WITH NITROMETHANE

Electrolyte	$(\partial\mu_e/m_0)^{m_{00}}_{m_{e0}}$ ^{b}, kcal. mole^{-1} molal^{-1}	ΔF_2^0 (25°),^{a} kcal. mole^{-1}	Ion	Ionic standard free energy ΔF_2^0 (25°), kcal. mole^{-1}
LiClO$_4$	-0.095 ± 0.015	-0.19 ± 0.03	H$^+$	0.00 (ref.)
NaClO$_4$	$-.106 \pm .019$	$-.21 \pm .04$	Li$^+$	$+.21$
KClO$_4$	$-.166 \pm .016$	$-.33 \pm .03$	Na$^+$	$+.19$
RbClO$_4$	$-.206 \pm .024$	$-.41 \pm .05$	K$^+$	$+.07$
CsClO$_4$	$-.218 \pm .024$	$-.43 \pm .05$	Rb$^+$	$-.01$
LiCl	$+.070 \pm .011$	$+.14 \pm .02$	Cs$^+$	$-.03$
NaCl	$+.076 \pm .014$	$+.15 \pm .03$	ClO$_4^-$	$-.40$
KCl	$+.012 \pm .009$	$+.02 \pm .02$	ReO$_4^-$	$-.49$
CsCl	$-.027 \pm .006$	$-.05 \pm .01$	Cl$^-$	$-.05$
KReO$_4$	$-.196 \pm .007$	$-.39 \pm .02$		
CsReO$_4$	$-.278 \pm .013$	$-.55 \pm .03$		
HClO$_4$	$-.199 \pm .035$	$-.40 \pm .07$		

^{a} The uncertainties in ΔF_2^0 were estimated from the uncertainties listed in Table II and III for $(\partial\mu_e/\partial m_e)^{m_{00}}_{m_{es}}$ and $(\partial\mu_0/\partial m_e)^{m_{e0}}_{m_{0s}}$ and from the 0.5% uncertainty in m_{0s}. ^{b} $(\partial\mu_e/\partial m_0)^{m_{00}}_{m_{e0}}$ was obtained from Table II or III, except for the entries of KClO$_4$ and CsClO$_4$ which are best values based upon both tables.

The derivative $(\partial\mu_e/\partial m_0)^{m_{00}}_{m_{es}}$ is also found to be composed of additive contributions from the ions of the electrolyte, although this is not necessarily to be expected except as a consequence of eq. 10. A check upon the additivity property is afforded by the comparison of the difference of $(\partial\mu_e/\partial m_0)^{m_{00}}_{m_{es}}$ for the pairs of salts with common ions

KClO$_4$–CsClO$_4$ = 0.067 ± 0.023 kcal. mole^{-1} molal^{-1}
KReO$_4$–CsReO$_4$ = 0.082 ± 0.024 kcal. mole^{-1} molal^{-1}

Standard Free Energies of Transfer.—ΔF_2 is obtained from the present experimental results by applying eq. 5. Now in order to be consistent with equations 10 and 7 and the assumption that $(\partial\mu_e/\partial m_0)^{m_{00}}_{m_e}$ is equal to the limiting interaction coefficients, $(\partial\mu_e/\partial m_0)_{m_{e0}}$ must be independent of

the wax liner of the cap. A weighed sample of the solution phase was evaporated to dryness, first with an infrared lamp and then in an oven at 100° to constant weight. It was established that no decomposition of the salt accompanied the recovery method employed here. The values for the solubilities of the salts in pure water (Table II) agree with the values found in the literature.

Measurement of k_0.—The solubility of nitromethane was measured by two methods. In the first method the solubility of nitromethane was measured by mixing a known volume of water-saturated nitromethane with an aqueous electrolyte solution of known concentration. After equilibration for 2–3 hours at 24.8° the mixture was centrifuged and the volume of the nitromethane phase was determined. The solubility of the nitromethane in the solution was determined from the difference in the original volume and the final volume. Since the nitromethane phase is more dense than the aqueous phase, a vial with a calibrated pipet attached to the bottom was used in these experiments. The second method was similar except that a sample of the

equilibrium aqueous phase was taken, diluted so that the concentration of nitromethane was in the range of 0.025 to 0.075 M (with an electrolyte concentration in the range 0.02 to 0.06 M) and was analyzed by measuring the optical density at 270 mμ. The extinction coefficient for nitromethane in aqueous solution was found to equal 14.7 at 270 mμ and 9.51 at 246 mμ. The extinction coefficient of nitromethane was found to be unaffected by electrolyte concentration up to 0.2 M.

The Activity Coefficient of Aqueous Nitromethane.— The vapor pressure of nitromethane above the binary solution was determined by spectrophotometry of the saturated vapor, using a simple apparatus consisting of a silica spectrophotometer cell connected to a Pyrex solution bulb by a graded seal. An aqueous nitromethane solution of known concentration was introduced into the solution bulb, which was then frozen with liquid nitrogen to prevent the concentration of the solution from changing while the air was pumped out of the apparatus. After evacuation the solution bulb was placed in a constant temperature bath (24.8°), and after equilibration the optical density of the vapor in the silica cell (at room temp.) was measured at 220 mμ and a slit width of 0.3 mm. The optical density of the vapor over pure nitromethane at different constant temperatures was measured and it was found that nitromethane obeys Beer's law in the vapor phase from zero pressure to 39 mm. pressure: optical density = 0.0385P (mm.). The

$$\log_{10} P = -2423.7/T - (3.3821) \log_{10} T + 18.0571$$

equation[10] was used to compute the vapor pressure of pure

nitromethane at the different temperatures. The activity coefficient of nitromethane in the solution is obtained from the equation

$$\log_{10} \gamma_0 = \log_{10} P_v/m - \log_{10} h$$

where P_v = partial pressure of nitromethane in the vapor, γ_0 = activity coefficient of nitromethane in solution, m = molal concentration of nitromethane in solution, and h is the Henry's law constant ($\lim_{m \to 0} (P_v/m)$). It is assumed here that the fugacity of nitromethane equals its partial pressure. This assumption can be justified for idealized gaseous mixtures in which the fugacity, f_v, is given by the equation

$$\ln(f_v/P_v) = (P_t/RT)B$$

where P_t is the total pressure of the mixture and B is the second virial coefficient for nitromethane vapor. B has been determined[11] as

$$-300 - 12.97e^{1700/T}(\text{cc./mole})$$

Then in the present experiments, $0.987 \leq f_v/P_v \leq 1$.

The partial pressure of nitromethane above the liquid solution from $m = 0.2$ to $m = 2.0$ is well represented by the equation

$$\log_{10} P/m = -(0.063 \pm 0.13)m + 1.362 \pm 0.009$$

Again, P is the pressure in mm. and the uncertainties are standard deviations. The slope is evidently independent of m_1 and therefore is equal to $(\partial \ln \gamma_0/\partial m_0)_{m_{os}}/2.303$.

(10) C. A., **34**, 4316⁸ (1940); E. B. Hodge, *Ind. Eng. Chem.*, **32**, 748 (1940).

(11) J. P. McCullough, D. W. Scott, R. E. Pennington, I. A. Hossenlopp and Guy Waddington, *J. Am. Chem. Soc.*, **76**, 4791 (1954).

THE REACTIONS OF CHLORINE ATOMS—A TEST OF THE TRANSITION STATE THEORY

By J. H. KNOX AND A. F. TROTMAN-DICKENSON

Chemistry Department, The University, Edinburgh

The relative A factors for reactions of the type Cl + RH = HCl + R have been calculated on the assumptions of the transition state theory. A comparison of these values with the accurate experimental data reveals considerable discrepancies.

The transition state theory of chemical kinetics has been applied with fair success to the calculation of the order of magnitude of the Arrhenius A factors of bimolecular reactions.[1] Little more can however be claimed for two reasons: firstly, doubtful assumptions as to the configurations of the activated complexes had to be made which led to considerable uncertainty in the calculated values, and secondly, experimental results of sufficient accuracy to sustain an unambiguous test were not available. The usual errors in the measurement of activation energies of these reactions were, under the most favorable conditions, of the order of ± 300 cal./mole. The corresponding error in the A factor is then $10^{\pm 0.2}$ (about ± 60%).

In the present paper, relative A factors calculated from transition state theory are compared with those determined experimentally by us[2,3] for the competitive reactions of chlorine atoms with several hydrocarbons. Calculated A factor ratios are also given for a number of reactions which have

not yet been studied but which we hope to investigate in due course. These reactions of chlorine atoms offer a number of advantages for such a study. In the first place there is much less doubt about the configuration of the activated complexes in reactions of atoms than in the corresponding reactions of free radicals, there being no uncertainty about the free rotation of the radical in the former case. Secondly, the activation energies of the reactions are low and may therefore be measured with very small absolute errors (although the percentage error will be of the usual magnitude). It may furthermore be assumed that in such cases the bond lengths C–H–Cl will vary little from complex to complex and that the C–H and C–Cl bond lengths will be only slightly longer than those in normal molecules. Thirdly, by employing a competitive technique, relative A factors can be determined with unusual precision. In the most favorable cases relative activation energies have been measured to within 30 cal./mole giving relative A factors to within 5%.

These relative A factors can therefore provide a stringent test of the transition state theory since not only can they be measured experimentally with

(1) A. F. Trotman-Dickenson, "Gas Kinetics," Academic Press, Inc., New York, N. Y., 1955.

(2) H. O. Pritchard, J. B. Pyke and A. F. Trotman-Dickenson, *J. Am. Chem. Soc.*, **77**, 2629 (1955).

(3) J. H. Knox, *Chem. and Ind.*, 1631 (1955).

high precision but they may also be calculated with high accuracy making use of fewer assumptions than are required in the calculation of absolute values.

According to transition state theory the relative A factors for the competitive reaction of chlorine atoms with methane and ethane are given by the equation

$$\frac{A_{CH_4}}{A_{C_2H_6}} = \frac{[\phi^{tr}_{CH_4Cl} \, \phi^{rot}_{CH_4Cl} \phi^{vib}_{CH_4Cl}]/[\phi^{tr}_{CH_4} \, \phi^{rot}_{CH_4} \, \phi^{vib}_{CH_4}]}{[\phi^{tr}_{C_2H_6Cl} \, \phi^{rot}_{C_2H_6Cl} \, \phi^{vib}_{C_2H_6Cl}]/[\phi^{tr}_{C_2H_6} \, \phi^{rot}_{C_2H_6} \, \phi^{vib}_{C_2H_6}]}$$

$$= \exp\left[\frac{1}{R}(\Delta S^{tr}_{CH_4} - \Delta S^{tr}_{C_2H_6} + \Delta S^{rot}_{CH_4} - \Delta S^{rot}_{C_2H_6} + \Delta S^{vib}_{CH_4} - \Delta S^{vib}_{C_2H_6})\right]$$

where the partition functions, denoted by ϕ's, are measured from the ground state of the parent molecule and of the complex, respectively. The activation energy appropriate to these theoretical A factors is therefore the activation energy at absolute zero which may be denoted ΔE_0°. The ΔS values are the entropies of activation appropriate to the translational, rotational and vibrational degrees of freedom. In the above expression for the A factors the transmission coefficients have been omitted, and the symmetry numbers are taken to be included in the rotational partition functions. If the partition functions are evaluated without the symmetry numbers the values for the A factors are those for individual hydrogen atoms. Denoting such factors by A' the above equation can be written

$$\frac{A'_{CH_4}}{A'_{C_2H_6}} = \left\{\frac{M_{CH_4Cl}/M_{CH_4}}{M_{C_2H_6Cl}/M_{C_2H_6}}\right\}^{1/2} \times$$

$$\left\{\frac{(ABC)_{CH_4Cl}/(ABC)_{CH_4}}{(ABC)_{C_2H_6Cl}/(ABC)_{C_2H_6}}\right\}^{1/2} \times \exp\left[\frac{1}{R}(\Delta S^{vib}_{CH_4} - \Delta S^{vib}_{C_2H_6})\right]$$

where M's are the molecular weights of the various substances and the product (ABC) is the product of the moments of inertia about the three principal axes of the molecules. While the masses are known exactly, the values of (ABC) are not known with the same precision because of the slight uncertainty (probably less than 0.2 Å.) as to the C–H–Cl distances. Values of (ABC) can however be calculated to any degree of accuracy once a configuration has been accepted. Since any error in the C–H–Cl distances will affect the (ABC)'s of all complexes in the same sense and roughly in the same proportion, any error of choice will largely cancel out. There are three likely sources of error in comparing the calculated values with the experimental ones The calculation of the vibrational entropy term is not possible with any certainty. It will however almost certainly be small. The vibrational entropies of methane and ethane are both less than 1.e.u. and the vibrational entropies of activation will therefore be much smaller than 1 e.u. Differences in vibrational entropies of activation as between say methane and ethane will be even smaller and probably not greater than ±0.1 e.u. The vibrational term which might at first sight appear to result in large uncertainty in the calculation of the theoretical A factor should not therefore contribute more than about exp $0.1/R$, that is, about 5% uncertainty.

In these calculations the contributions from internal rotations in the parent molecules and the

complexes have been neglected. The appropriate allowance may readily be made only in the simplest cases where the rotators are symmetrical tops. In the case of ethane, for example, the contribution to the entropies of the parent and the complex due to free internal rotation are, ignoring the symmetry factor, 5.06 and 5.66 e.u., respectively. An error of about 30% may therefore be introduced in the particular case of ethane/methane by ignoring internal rotation. For higher homologs the contributions due to changes in internal rotation will be smaller than this. In the cases considered we are moreover concerned with restricted rotation rather than free rotation, and the effect of neglecting rotations is thus further reduced.

Lastly, there is likely to be a discrepancy between the theoretical and experimental A factors resulting from the fact that the experimental activation energy and the theoretical activation energy differ according to the equation

$$\Delta E_{exp} = \Delta E_0^\circ + \int_0^T \Delta C_v \, dT$$

giving
$$A_{exp} = A_{calc} \exp[(\int \Delta C_v/dT)/RT]$$

The difference in ΔC_v for two similar reactions will however be very small since the translational and rotational specific heat changes will be identical for the two reactions and only the changes in vibrational specific heats will be important. As with the vibrational entropy contributions, these will be very small indeed.

We therefore conclude that the major factors influencing the relative A factors for two similar reactions are the changes in the translational and rotational entropies. Errors of up to some 5% are introduced by ignoring the vibrational contributions, and rather more by ignoring internal rotation. The latter is however never likely to be more than about 20%, even in an extreme case such as the comparison of the chlorinations of methane and ethane.

The details of the calculations are given below and a summary of the results appears in Table I. It already has been shown[2] that A factors of the right order of magnitude may be calculated for these chlorination reactions so that considerable interest attaches to the much more accurate values found for the relative A factors. These are given in Table II where they are compared with the experimentally determined values. Examination of the table reveals that the simple transition state theory predicts only approximately the relative A factors and that the discrepancy between the calculated and the experimental values is in the sense that too large an A factor is predicted for the lighter relative to the heavier molecules except in the indirect comparison of neopentane with isobutane where the mass difference is relatively small. These discrepancies (factors of up to ten) are well without both experimental error and any reasonable estimate of the theoretical error in our calculations. They may possibly be resolved in terms of transmission coefficients which we have neglected, but as yet no general method has been suggested by which such allowance might be made. The calculations show clearly the limits of the application of the simple transition state theory, and

TABLE I
TRANSLATIONAL AND ROTATIONAL ENTROPIES

Compound	S_{trans}	Log_{10} ABC^a	σ	S_{rot}
Cl	36.6	0	..	0
H_2	28.1	$\bar{1}.68^b$	2	4.1
H_2-Cl	36.8	0.89^b	1	11.0
CH_4	34.3	1.56	12	10.3
CH_4-Cl	37.8	4.29	3	19.3
C_2H_6	36.1	3.62	18	14.2
C_2H_6-Cl	38.9	5.78	3	22.7
C_3H_8	37.2	4.84	18	17.0
C_3H_8 cond.^{c}	37.2	4.65	18	16.5
p-C_3H_8-Cl (a)	39.0	6.36	3	24.0
p-C_3H_8-Cl (a) cond.	39.0	6.26	3	23.8
p-C_3H_8-Cl (b)	39.0	6.35	3	24.0
p-C_3H_8-Cl (b) cond.	39.0	6.31	3	23.9
s-C_3H_8-Cl	39.0	6.47	9	22.1
s-C_3H_8-Cl cond.	39.0	6.43	9	22.0
iso-C_4H_{10}	38.1	5.76	81	16.1
iso-C_4H_{10} cond.	38.1	5.46	81	15.4
p-iso-C_4H_{10}-Cl (a) cond.	39.5	6.91	9	23.1
p-iso-C_4H_{10}-Cl (b) cond.	39.5	6.75	9	22.7
t-iso-C_4H_{10}-Cl	39.5	6.93	81	18.7
t-iso-C_4H_{10}-Cl cond.	39.5	6.79	81	18.4
$C(CH_3)_4{}^d$	38.8	6.18	324	14.3
$C(CH_3)_4$-Cl^d	40.1	7.33	27	21.9
CF_3H	38.7	5.11	3	21.2
CF_3H-Cl	40.0	6.86	3	26.2
CCl_3H	40.1	6.88	3	26.2
CCl_3H-Cl	41.1	7.73	3	28.2

^{a} Units of ABC are [molecular weight $\times$ Å.^{2}]^3. ^{b} These values are $\log_{10} A$ where A is the moment of inertia. ^{c} "cond." stands for the condensed CH_3 approximation. ^{d} The molecule was treated as a series of spherical shells.

TABLE II
RELATIVE A FACTORS FOR CHLORINE ATOM REACTIONS
$Cl + RH = HCl + R$

Compounds		Relative A factors/H atom A'_X/A'_Y	
X	Y	Calcd.	Exptl.
Hydrogen/methane		9.8	6.3 ± 2
Methane/ethane		3.58	0.39 ± 0.03
Ethane/neopentane		5.43	2.0 ± 0.1
Ethane/chloroform		9.46	.....
Ethane/fluoroform		2.08	.....
p-Propane/sec-propane (a)		0.89^a; 0.82^b	0.61 ± 0.05
p-Propane/sec-propane (b)		0.87^a; 0.87^b	
p-isobutane/t-isobutane (a)		1.14^c	0.75 ± 0.1
p-isobutane/t-isobutane (b)		0.95^c	

	Relative A factors per molecule,^{c} A_X/A_Y	
Ethane/propane^c	1.9^a ; 1.6^b	0.68 ± 0.04
Ethane/isobutane^c	2.8^b	0.61 ± 0.04

^{a} Calculated for the complete molecule. ^{b} Calculated using the condensed approximation. ^{c} These results are given in terms of the molecule as a whole because no experimental distinction was made between the different types of hydrogen atoms.

invite further work on other series of reactions which might likewise be compared with theoretical predictions.

The Calculations.—Values for the translational and rotational entropies have been calculated for each of the reactants and complexes studied. The translational entropies were calculated from the Sackur–Tetrode equation; the values are given in Table I. The values obtained for the rotational entropies depend upon the precise configurations assumed for the molecules (see below). These calculations of the moments of inertia can be considerably simplified if the hydrogen atoms of the methyl groups are "condensed" into the appropriate carbon atom; each methyl group is then treated as a mass of 15 located at the center of gravity of the original methyl group. Some examples of such condensations are given in Table I, and it can be seen from Table II that this simplification yields values of the relative A factors which are only slightly different from those obtained by more laborious means.

The Configurations.—It was assumed throughout that the carbon valency angles were all equal to 109.5°. In the linear C–H–Cl groups of the activated complexes the C–H distance was taken as 1.15 Å. and the H–Cl as 1.45 Å.; other bond lengths assumed were C–C 1.54 Å., C–H 0.98 Å., C–F 1.36 Å. and C–Cl 1.76 Å. The following points may be mentioned in connection with the configurations of individual reactants and complexes.

Propane.—Calculations were made for two different configurations of the complex obtained by attack of the chlorine atom at the primary position: (a) in which the chlorine atom in the complex is at the greatest possible distance from the third carbon atom (i.e., with the C–H–Cl bond parallel to the opposite C–C bond) (b) in which the chlorine atom is as close as possible to the third carbon atom.

Isobutane.—Calculations were again made for two configurations of the complex: (a) in which the chlorine atom was at the greatest possible distance from the tertiary hydrogen atom (i.e., the C–H–Cl bond parallel to the tertiary C–H bond); (b) in which the chlorine atom is as close as possible to the tertiary hydrogen atom.

Neopentane.—This molecule was treated as a central atom of mass 12 surrounded by two spherical shells one of mass 48 and radius 1.54 Å. and the other of mass 12 and radius 2.20 Å.; the chlorine atom in the complex was taken to be a distance of 3.65 Å. from the central carbon atom.

APPLICATION OF THE PLATE THEORY TO THE ANION-EXCHANGE CHROMATOGRAPHY OF GLYCOLS

By Roger Sargent and William Rieman III

Ralph G. Wright Chemical Laboratory, Rutgers University, New Brunswick, New Jersey

Received March 19, 1956

The plate theory of ion-exchange chromatography has been applied to the separation of the complex anions formed between vicinal glycols and the borate ion. A theoretical elution equation giving the elution behavior of the glycols has been derived and tested. As the result of this investigation, equilibrium constants for the complexation reactions have been determined. One may then, with the use of the elution equation and the equilibrium constants, predict the position of the peak of an eluted glycol for any concentration of sodium borate eluent or find the conditions that will lead to the separation of a mixture of glycols.

The analysis of a mixture of glycols is greatly simplified by their separation prior to determination. Since vicinal hydroxy compounds are known to complex with the borate ion to form anions,[1] a method of separation of the glycols by the anion-exchange chromatography of their borate complexes was investigated. A theoretical approach is desirable so that a maximum amount of information may be obtained from a small number of preliminary elutions. The plate theory of ion-exchange chromatography, developed by Martin and Synge[2] and Mayer and Tompkins[3] has been extended, tested, and shown to be very helpful in developing a method of separation of the condensed phosphates by Beukenkamp, Rieman and Lindenbaum,[4] whose notation will be employed throughout this paper. The purpose of this paper is to show the applicability of the plate theory to the study of the elution of glycol–borate complexes.

Derivation of the Elution Equation

A solution of sodium borate, used as the complexing agent as well as the eluent, was prepared by the addition of slightly more than two moles of sodium hydroxide to one mole of borax to ensure complete neutralization of all boric acid. In solutions of borax or boric acid, the boric acid undergoes polymerization with the borate ion to form an undetermined number of polymeric anionic species. The number of equilibria involved under these conditions is so large that a detailed mathematical treatment is impracticable. However, with solutions of sodium borate, the formation of the glycol–borate complex ion may be represented as
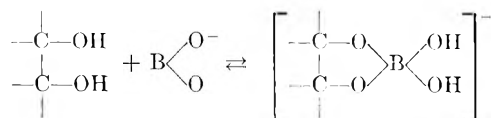
The slight excess of hydroxide ion in the eluent solution results in the conversion of a small amount of resin to the hydroxide form which remains inactive. The effective exchange capacity of the resin is therefore taken as the milliequivalents of resin in the borate form, RBO_2.

The reactions which take place in an elution of a glycol, G, on a column of anion exchanger in the borate form may be represented by the equilibria

$$G + BO_2^- \rightleftharpoons GBO_2^- \qquad K_1 = \frac{[GBO_2^-]}{[G][BO_2^-]} \qquad (1)$$

$$G + RBO_2 \rightleftharpoons RBO_2G \qquad K_2 = \frac{[RBO_2G]}{[G][RBO_2]} \qquad (2)$$
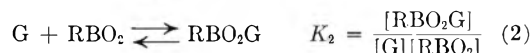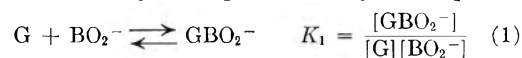
According to the plate theory of ion-exchange chromatography, the distribution ratio, C—i.e., the total quantity of a glycol in the resinous phase divided by the total quantity of the glycol in the solution phase—is given by

$$C = \frac{WQ}{V} \frac{[RBO_2G]}{[G] + [GBO_2^-]} = \frac{WQ}{V} \frac{K_2[G][RBO_2]}{[G] + K_1[G][BO_2^-]}$$

$$\frac{CV}{WQ} = \frac{K_2[RBO_2]}{1 + K_1[BO_2^-]}$$

Here W is the weight of resin in the column; Q is the capacity of the resin in milliequivalents per gram; and V is the interstitial volume of the column. Rearrangement of the foregoing equation gives an equation which describes the elution behavior of a glycol.

$$\frac{WQ[RBO_2]}{CV} = \frac{K_1}{K_2}[BO_2^-] + \frac{1}{K_2} \qquad (3)$$

Thus a straight line is predicted if $WQ[RBO_2]/CV$ is plotted against $[BO_2^-]$. The slope, K_1/K_2, and intercept, $1/K_2$, of this line provide a method for finding the equilibrium constants for reactions (1) and (2).

Experimental

Reagents.—Diethylene glycol (DEG), ethylene glycol (EG) and 1,2-propylene glycol (PG) were obtained from Eastman and used without further purification. Glycerol (GL) from J. T. Baker Chemical Company was also used without further purification. Three samples of 2,3-butylene glycol (BG) were used. The first from Celanese Corporation of America was a mixture of *meso* and *d,l*-forms. The second from the National Research Council of Canada was found to be a mixture of the *meso* and *l*-forms by chromatographic investigation and measurement of the optical rotation. The third sample from Schenley Distillers was similarly found to be a mixture of *meso* and *d*.

Experimental Procedure.—To test the validity of equation 3, a column of Dowex 1-X8, 100–200 mesh was equilibrated with a solution of sodium borate of the desired concentration. Each glycol was then eluted separately with this solution to determine U^*, the volume of effluent at which the peak concentration of the glycol appears. The quantity of glycol present in an effluent fraction was determined by oxidation with dichromate in 50% sulfuric acid and subsequent measurement of the absorbance of the resultant Cr(III).[5] The interstitial volume, V, of a 3.90-cm.² column of Dowex 1-X8, 100–200 mesh was previously found[6] from eight determinations to be 46 ± 0.4% of the bed volume,

(1) J. X. Khym and L. P. Zill, *J. Am. Chem. Soc.*, **74**, 2090 (1952).

(2) A. J. P. Martin and R. L. M. Synge, *Biochem. J.*, **35**, 1385 (1941).

(3) S. W. Mayer and E. R. Tompkins, *J. Am. Chem. Soc.*, **69**, 2866 (1947).

(4) J. Beukenkamp, W. Rieman and S. Lindenbaum, *Anal. Chem.*, **26**, 505 (1954).

(5) R. Sargent and W. Rieman, *Anal. Chim. Acta*, **14**, 381 (1956).

(6) W. Rieman and S. Lindenbaum, *Anal. Chem.*, **24**, 1199 (1952).

TABLE I

THE EVALUATION OF EXPERIMENTAL DATA FOR FIGURE 1

Eluent	$[BO_2^-]$	0.02477	0.09341	0.2326	0.5062	0.8931
	$[OH^-]$	0.0005	0.00075	0.00204	0.00458	0.00795
Column	Height, cm.	6.2	10.0	10.5	11.9	14.9
	V	11.1	17.9	18.9	21.3	26.7
Effluent from KCl Wash	OH^-, meq.	1.14	0.86	0.57	0.65	1.43
	BO_2^-, meq.	22.75	38.74	44.55	55.62	78.86
$WQ[RBO_2]$		22.48	37.07	40.15	44.84	55.01
U^*	EG	50.5	77.5	74.4	73.1	82.5
	PG	80.3	118	105	97.6	110
	BG, m	83.3	130	123	120	146
	BG, d, l	...	...	245	173	187
	GL	280	264	163	113	106
$\dfrac{WQ[RBO_2]}{CV}$	EG	0.571	0.622	0.723	0.866	0.986
	PG	.325	.371	.466	.588	.660
	BG, m	.311	.331	.386	.454	.462
	BG, d, l	...	...	.177	.295	.344
	GL	.0836	.151	.279	.489	.694

V_b. The fundamental equation of the plate theory, $U^* = CV + V$, may then be employed to calculate C for each glycol. The eluent was then drained to the top of the resin bed, and the borate and hydroxide ions on the resin and in the interstitial solution were replaced by washing with a solution of potassium chloride. An aliquot of the collected effluent was titrated with hydrochloric acid to the methyl red end-point to determine the total base, i.e., BO_2^- + OH^-. Another aliquot was saturated with mannitol which complexes borate ion and allows the determination of hydroxide ion by a potentiometric titration with hydrochloric acid. The quantity of hydroxide ion is subtracted from the quantity of total base to obtain the quantity of borate ion. Since the quantities of borate and hydroxide ions found in this manner are the sum of the quantities present on the resin and in the interstitial solution of eluent, the quantity of each ion on the resin is found by subtracting the amount, $V[BO_2^-]$ or $V[OH^-]$, present in the interstitial solution. Thus WQ, the total capacity, is the sum of RBO_2 and ROH measured in milliequivalents.

Results

The results of the elutions (on different columns) for five concentrations of sodium borate are given in Table I. Figure 1 represents a plot of these results for ethylene glycol, 1,2-propylene glycol, the *meso* and the *d,l*-isomers of 2,3-butylene glycol and glycerol.

The predicted straight-line relationship was obtained at low concentrations of sodium borate. The curvature at concentrations above 0.3 M may be explained as being the result of two effects: (1) the neglect of activity coefficients in the aqueous and resinous phases, and (2) the salting-out effect. Approximately one-half of the observed curvature at a concentration of sodium borate of 0.893 M has been shown[7] to be due to a selective salting-out of the glycol from the aqueous to the resinous phase. The authors have employed this selective salting-out as a chromatographic method of separating mixtures of polyglycols that are difficult to separate by conventional techniques.[8]

Equilibrium Constants.—Because of the linearity of the curves at low concentrations, the intercept and limiting slope can be used to find the true equilibrium constants for reactions (1) and (2).

(7) R. Sargent, doctor's thesis, Rutgers University, 1956.

(8) R. Sargent and W. Rieman, *J. Org. Chem.*, **21**, 594 (1956).

These are given for each glycol in Table II, lines 1 and 2. In order to facilitate the calculation of the position of the peak of the elution graph, empirical values of K_2 (Table II) may be used
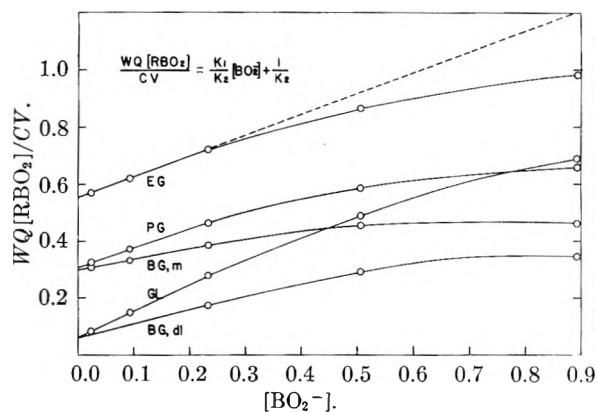
Fig. 1.

which will account for the curvature. These values are obtained by solving equation 3 for K_2, the experimental values obtained for K_1 and $WQ[RBO_2]/CV$ being used.

TABLE II

EQUILIBRIUM CONSTANTS

Concn. of BO_2^-, M	EG	PG	BG *meso*	BG *d,l*	GL
K_1 ..	1.30	2.12	1.18	8.41	14.8
K_2 0.0	1.80	3.22	3.33	17.0	15.9
.2	1.80	3.24	3.33	17.0	15.9
.4	1.86	3.40	3.41	17.5	16.7
.6	1.97	3.68	3.70	18.8	17.9
.8	2.10	4.14	4.21	21.9	19.5

Table III presents a comparison of our values for K_1 with experimental results of other investigators. G. Roy, *et al.*,[9] determined this constant (K_{cl}) by observing the change in pH caused by adding a known amount of glycol to a borate buffer.

(9) G. Roy, A. Laferriere and J. Edwards, private communication,

A measure of the extent of complex formation with boric acid is given by a quantity, Δ, Table III, which is the difference between the specific conductance of an equimolar mixture (0.5 M) of glycol and boric acid and the sum of the conductances of the unmixed solutions of the same concentration. Negative Δ values are probably the result of the presence of trace quantities of base that was used to neutralize the glycol prior to the measurement of conductance. This base would neutralize the hydrogen ions released in the formation of the complex and would lower the conductance.

TABLE III

Glycol	K_1	$K_{c1}{}^a$	$K_{18}{}^b$	$\Delta^{c,d} \times 10^6$
EG	1.30	1.85	0.14	-1.0
PG	2.12	3.10	0.44	-0.7
BG, *meso*	1.18	} 3.45^e	...	-1.3
BG, *d,l*	8.41		...	$+4.7$
GL	14.8	16.0	0.77	$+11.9$

^{a} G. Roy, A. Laferriere and J. Edwards, private communication. ^{b} J. Boeseken, *Rec. trav. chim.*, **40**, 353 (1921). ^{c} P. Hermans, *J. Chim. Phys.* ^{d} J. Boeseken and R. Cohen, *Rec. trav. chim.*, **47**, 845 (1928). ^{e} Probably a mixture of *meso* and *d,l*-forms

K_{18} = (glycol–acetone complex) (water)/(glycol) (acetone).

$\Delta = K_{(0.5\ M\ glycol\ +\ 0.5\ M\ HBO_2)} - (K_{0.5\ M\ glycol} + K_{0.5\ M\ HBO_2})$

The reaction between a glycol and acetone is similar to the complexation reaction of the glycol with borate because the quantity of product formed is dependent upon the favorability of the positions of the hydroxyl groups. The equilibrium constants for this reaction at 18°, designated by K_{18} in Table III, shows a distinct parallel to both Δ and K_1 values.

These comparisons show that the values of K_1 as obtained by anion-exchange chromatography are in the order expected. The determination of K_1 (and K_2) by this method is subject to less experimental error than a determination of Δ from conductance or pH measurements with boric acid as the complexing agent.

Separations.—The separation of one glycol from another can be accomplished readily with an eluent solution of sodium borate if the ratio of the values of C is greater than or equal to 1.3. The data presented in Tables II and III have been used to develop chromatographic methods for the separation of the glycols, which will be reported elsewhere. Polyglycols and monohydric alcohols do not interfere with the determination of vicinal glycols because they are eluted from the column very rapidly.

INFRARED SPECTRA OF SOME REACTION PRODUCTS OF OCTAFLUOROISOBUTENE

By Ernest Halpern and Jerome Goldenson

Chemical Corps Chemical and Radiological Laboratories, Army Chemical Center, Maryland

The infrared spectra (2 to 15 μ) of 13 new fluoroörganic compounds are presented. Included are the spectra of a number of fluorinated ethers and carbonyl compounds. Characteristic details of the spectra used to assist in the identification of their structure are discussed. The linear relationship reported in the literature[1] between the C=O absorption wave length and the sum of the effective electro-negativities of the substituents on the carbon was extended for application to the types of fluorinated carbonyl compounds included in this report.

In connection with a study of the reaction of alcohols with octafluoroisobutene,[2] methods were required to determine and identify the structure of the reaction products. Since the inertness of fluorinated compounds makes them difficult to characterize chemically, infrared spectroscopy was used to aid in establishing their structures. In the work, the infrared spectra of 13 new fluoroörganic compounds were obtained and are presented here for identification purposes.

Experimental

Fluoroörganic Compounds.—All the compounds used in this work were prepared by the group under Drs. F. W. Hoffmann and T. C. Simmons.[2,3] Evidence for their structure was based on the method of synthesis and nuclear magnetic resonance spectra in addition to the infrared spectra presented here. Fluorine, carbon, hydrogen and nitrogen analyses were determined for liquids and molecular weights for gases; molar refractions were also determined for some of the liquids.[2] Purities were 98% or better in all of the compounds. The compounds, spectrum numbers sample phase and cell thicknesses are given in Table I.

TABLE I

LIST OF FLUOROÖRGANIC COMPOUNDS AND SPECTRA NUMBERS

Compound	Spectrum	Sample phase	Cell thickness, mm.
$(CF_3)_2CHCF_2OC_2H_5$	1	4% soln. in CCl_4	0.109
$(CF_3)_2CHCF_2O_nC_3H_7$	2	Liquid	.023
$(CF_3)_2CHCF_2O_nC_4H_9$	3	Liquid	.023
$(CF_3)_2C=CFOCH_3$	4	Liquid	.023
$(CF_3)_2C=CFOC_2H_5$	5	Liquid	.023
$(CF_3)_2C=CFO_nC_3H_7$	6	Liquid	.023
$(CF_3)_2C=CFOCH(CH_3)_2$	7	Liquid	.023
$(CF_3)_2C=CFO_nC_4H_9$	8	Liquid	.023
$(CF_3)_2CHCOF$	9	Gas	100.0
$(CF_3)_2CHCONH_2$	10	4% soln. in CCl_4	0.1092
$(CF_3)_2CHCOO_nC_3H_7$	11	Liquid	0.023
$(CF_3)_2NCOOC_2H_5$	12	10% soln. in CCl_4	0.109
$(CF_3)_2NCOF$	13	Gas	100.0

Determination of Infrared Spectra.—The spectra were determined with a Perkin–Elmer Model 21 recording spectrometer equipped with a sodium chloride prism. A slit program of 960, a response of 1, a gain of 5, a speed of 6 and a suppression of 0 were used in all cases.

(1) R. E. Kagarise, *J. Am. Chem. Soc.*, **77**, 1377 (1955).

(2) R. J. Koshar, T. C. Simmons and E. W. Hoffmann, presented at the 130th A.C.S. Meeting, Atlantic City, N. J., Sept. 1956.

(3) F. W. Hoffmann, T. C. Simmons, E. R. Larsen, F. E. Rogers, R. J. Koshar, H. V. Holler, B. S. Singleton, J. E. Mulvaney, K. E. Paulson, R. E. Sparks and R. B. Beck, private communication.
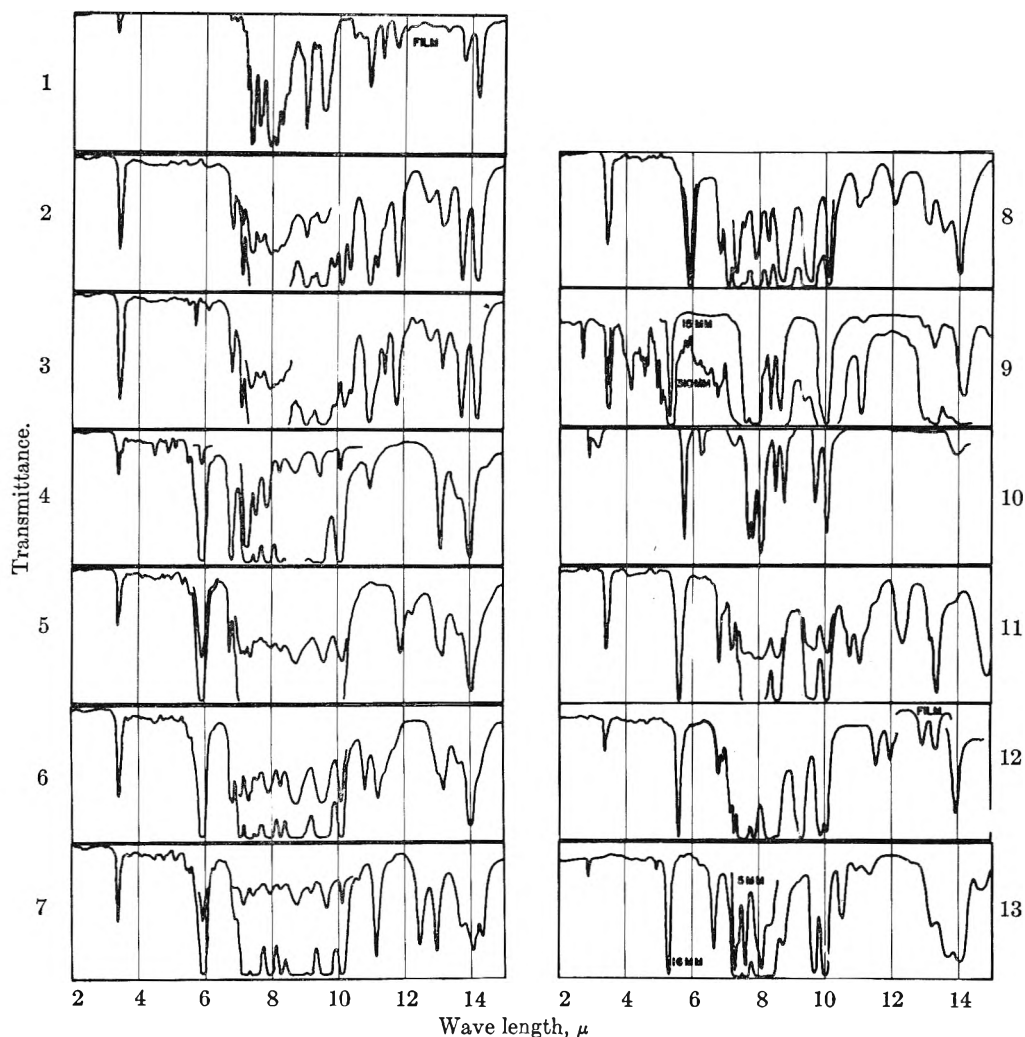
Fig. 1.—Infrared absorption spectra of fluoroörganic compounds: 1, $(CF_3)_2CHCF_2OC_2H_5$; 2, $(CF_3)_2CHCF_2O_nC_3H_7$; 3, $(CF_3)_2CHCF_2O_nC_4H_9$; 4, $(CF_3)_2C{=}CFOCH_3$; 5, $(CF_3)_2C{=}CFOC_2H_5$; 6, $(CF_3)_2C{=}CFO_nC_3H_7$; 7, $(CF_3)_2C{=}CFOCH(CH_3)_2$; 8, $(CF_3)_2C{=}CFO_nC_4H_9$; 9, $(CF_3)_2CHCOF$; 10, $(CF_3)_2CHCONH_2$; 11, $(CF_3)_2CHCOO_nC_3H_7$; 12, $(CF_3)_2NCOOC_2H_5$; 13, $(CF_3)_2NCOF$.

Discussion of Spectra

The compounds represented by spectra 1 through 8 were made by the addition of alcohols to octafluoroisobutene. Spectra 1 through 3 represent the saturated products and spectra 4 through 8 the unsaturated products. The saturated products of the type formula $(CF_3)_2CHCF_2(OR)$ do not show absorption in the 5 to 6.2 μ region while the unsaturated products of the type formula $(CF_3)_2C{=}CF(OR)$ show absorption at 5.9 μ. Since the starting material, octafluoroisobutene, shows absorption at 5.73 μ,[4] the reactions were readily followed by observing the disappearance of absorption at 5.73 and the appearance of absorption at 5.9 μ.

Spectrum 3 shows weak absorption at 5.7 μ due to a trace of octafluoroisobutene as an impurity. The spectrum of the methyl analog of $(CF_3)_2$-$CHCF_2(OR)$ has been reported by Weiblen.[4]

Spectra 1 to 3 are quite similar showing absorption in common at 9.0, 9.6, 10.9, 11.8, 13.2, 13.8 and 14.2 μ. Spectra 4 to 8 also show similarities

in absorption at about 8.8, 9.6, 10.1, 13.1, 13.6 and 14.1 μ.

All the compounds examined in which the $(CF_3)_2C-$ group is present (spectra 1 through 11) with one exception (spectrum 11) show medium absorption in the region of 13.0 to 13.3 μ and strong absorption in the region of 14.0–14.2 μ.

Use of Carbonyl Group Relation.—Five compounds whose spectra are included in this paper contain the carbonyl group. The Kagarise relation[1] between the sum of the Gordy scale electronegativities[5] of adjacent substituents and the stretching frequency of the carbonyl group was found to be useful in confirming the structures of these compounds and some intermediates. The equation for this relation was used in the following form, where $\mu_{C=O}$ is the wave length in microns of the $C{=}O$ stretching wave length and X is the sum of the Gordy electronegativity values of the substituents on the carbon

$$\mu_{C=O} = \frac{10,000}{1536.5 + 48.85X} \qquad \text{(I)}$$

(4) D. G. Weiblen, "Fluorine Chemistry," Vol. II, edited by J. H. Simons, Academic Press, Inc., New York, N. Y., 1954, Chapter 7.

(5) W. Gordy, *J. Chem. Phys.*, **14**, 305 (1946).

TABLE II

COMPARISON OF EXPERIMENTAL AND CALCULATED C=O ABSORPTION WAVE LENGTHS IN FLUOROÖRGANIC COMPOUNDS

Compound	Spectrum	Ref.	Sum of effective electronegativities	Calcd. $\mu_{C=O}, \mu$	Exptl. $\mu_{C=O}, \mu$	$\Delta\mu_{C=O}$, calcd.-obsd., μ
$(CF_3)_2NCOF$	13				5.30	
$CF_3CF_2CF(CF_3)CF_2COF$	a		7.06^b	5.33	5.30	+0.03
$n\text{-}C_{13}F_{27}COF$	a		7.06^b	5.33	5.32	+ .01
$(CF_3)_2CHCOF$	9		6.66	5.37	5.31	+ .06
C_2F_5COCl		6	6.10	5.45	5.51	− .06
CF_3COCH_3		7	5.59	5.53	5.63	− .10
$C_2F_5COCH_3$		7	5.47	5.55	5.65	− .10
$(CF_3)_2NCOOC_2H_5$	12		$5.02^{c,d}$	5.61	5.53	+ .08
$C_2F_5COOCH_3$		6	4.94	5.62	5.59	+ .03
$C_2F_5COOC_2H_5$		6	4.94	5.62	5.56	+ .06
$C_3F_7COOC_2H_5$		8	4.92^d	5.63	5.60	+ .03
$(CF_3)_2CHCOOC_3H_7$	11		4.52^d	5.69	5.60	+ .09
C_2F_5CHO		6	5.26	5.58	5.73	− .15
$(CF_3)_2CHCONH_2$	10		3.17^e	5.91	5.74	+ .17
$C_2F_5CONH_2$		6			5.84, 6.13	

^{a} Determined at Army Chemical Center. Spectrum not included in this paper because the preparation was not of sufficiently high purity. ^{b} The $n\text{-}C_{13}F_{27}-$ and $CF_3CF_2CF(CF_3)CF_2-$ groups were assumed to have the same effective electronegativities as the $CF_3-CF_2-CF_2-$ group (3.11). ^{c} The effective electronegativity for the $(CF_3)_2N-$ group (3.21) was obtained by substitution in equation I of $\mu_{C=O} = 5.30$ for $(CF_3)_2NCOF$. ^{d} The effective electronegativity value was assumed to be constant for OR groups (1.81).[1] ^{e} The effective electronegativity for the NH_2- group (0.46) was obtained by substitution in equation I of $\mu_{C=O} = 5.84$ for $C_2F_5CONH_2$.

To extend the applicability of equation I, it is necessary to assign electronegativity values to substituents which consist of groups of atoms. Kagarise[1] assigns an effective electronegativity to substituted methyl groups on an empirical basis by the equation

$$x_{\text{eff}} = \frac{x_C}{2} + \frac{1}{6}(x_X + x_Y + x_Z) \qquad (II)$$

where x_C, x_X, x_Y, x_Z are the Gordy electronegativity values of carbon and substituents X, Y and Z.

Equation II was used to obtain effective electronegativity values for groups such as CF_3, and in the work of this report this value was used in turn in equation II to obtain effective electronegativity values for larger groups such as CF_2CF_3 and CF_2-CF_2CF_3.

Examination of the effective electronegativity values calculated in this manner indicates certain trends of electronegativity with structure. The electronegativity of a fluorocarbon group is not appreciably affected by an increase in chain length as shown in the series
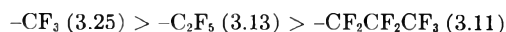
$-CF_3$ (3.25) > $-C_2F_5$ (3.13) > $-CF_2CF_2CF_3$ (3.11)

However, branching has a greater effect on the electronegativity of the substituted methyl group as

$-CF_3$ (3.25) > $-CF_2CF_3$ (3.13) > $-CF(CF_3)_2$ (3.01) > $-C(CF_3)_3$ (2.89)
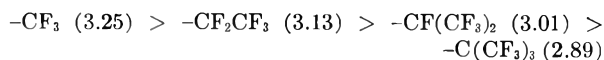
Substitution of a perfluoromethyl group by a hydrogen in $C(CF_3)_3$ decreases the electronegativity of the substituted methyl group as

$-C(CF_3)_3$ (2.89) > $-CH(CF_3)_2$ (2.71) > $-CH_2(CF_3)$ (2.52) > $-CH_3$ (2.34).
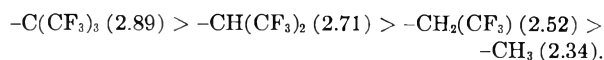
By use of the calculated effective electronegativ-

ity values and substitution in equation I, the data in Table II were obtained.

From an inspection of the data in Table II, and references 1 and 9 the similarity in shift of wave lengths between the C=O and P=O bands may be noted. Both bands shift to lower wave lengths with increase in the sum of electronegativities of the substituents on the carbon or phosphorus. The greatest deviations are noted with the two ketones, the aldehyde and amide included in the table.

An attempt was made to derive an approximate relation between the C=C absorption wave length and the effective electronegativities of the substituents on the carbons as an aid in confirming the structure of fluorinated compounds such as those represented by spectra 4 to 8. Using Gordy electronegativity values[5] and the C=C absorption wave lengths of $CF_2=CF_2$, $CF_2=CFH$, $CF_2=CH_2$ and $CH_2=CH_2$, the following equation was obtained by the method of least squares

$$\mu_{C=C} = 7.1837 - 0.11494X \qquad (III)$$

where $\mu_{C=C}$ is the wave length in microns of the C=C absorption and X is the sum of the electronegativity values of the substituents surrounding the double bond. Using equation III, poor agreement was obtained between the observed and calculated C=C absorption wave lengths for compounds containing CF_3-, C_2F_5- and RO− groups. Since the groups on each side of the C=C bond would be involved in this stretching vibration, it is thought that the effect of mass may be more pronounced on the C=C band position than is apparent with the C=O and P=O bonds, in which the oxygen vibrates independently of the masses of the groups on the C or P. Further work is planned to introduce the parameter of mass into a C=C relation.

(6) R. N. Haszeldine and K. Leedham, J. Chem. Soc., 1548 (1953).

(7) R. N. Haszeldine and K. Leedham, ibid., 3483 (1952).

(8) G. Rappaport, M. Hauptsehein, J. F. O'Brien and R. Filler, J. Am. Chem. Soc., 75, 2695 (1953).

(9) J. V. Bell, J. Heisler, H. Tannenbaum and J. Goldenson, ibid., 76, 5185 (1954).

A SCHEMATIC METHOD OF DERIVING THE RATE LAWS FOR ENZYME-CATALYZED REACTIONS

By Edward L. King and Carl Altman

Department of Chemistry, University of Wisconsin, Madison, Wisconsin

Received April 2, 1956

A schematic method of deriving the rate laws for enzyme-catalyzed reactions is described which is particularly useful for treating very complicated mechanisms. It is proved that this schematic method is valid for deriving the rate law for any enzyme catalysis mechanism regardless of the number of enzyme-containing species which are involved. Allowance for interactions which do not involve the enzyme is not within the scope of this method but is readily taken into account by usual means.

If the mechanism for an enzyme-catalyzed reaction involves n different enzyme-containing species, the usual steady-state assumption leads, after first eliminating the concentration of one of the enzyme-containing species by the relationship $[E]_0 = \Sigma(EX_i)$,[1] to a system of $n - 1$ non-homogeneous linear equations.[2] The solution of these equations for the concentrations of the several EX_i's is a straight-forward problem but one which can be tedious even when the determinant method (*i.e.*, Cramer's rule) is employed.[3,4] It is the purpose of the present communication to describe a *schematic* method of deriving the steady-state concentrations of the several enzyme containing species, EX_i, which is based upon the determinant method.

The concentration of each EX_i relative to the total concentration of enzyme, $(EX_i)/[E]_0$, is a quotient of two summations of terms, each term being the product of $n - 1$ different rate constants and the appropriate concentrations. Each term in the numerator of the expression for $(EX_m)/[E]_0$ involves the rate constants (and appropriate concentrations) associated with reaction steps which *individually or in sequence* lead to EX_m, the enzyme-containing species in question. The $n - 1$ rate constants in each term are associated with $n - 1$ reaction steps in which *each* of the $n - 1$ different enzyme-containing species EX_i ($i \neq m$) is a reactant. All of the possible combinations of $n - 1$ rate constants which conform to this requirement are present as numerator terms in the expression for $(EX_m)/[E]_0$. The denominator of the expression for $(EX_m)/[E]_0$ is the sum of the several different numerators.

A simple example will serve to illustrate this method. The mechanism involves 3 enzyme-containing species; thus each term in the expression for the relative concentration of E, ES or EP contains 2 rate constants and the appropriate

$$E + S \underset{k_2}{\overset{k_1}{\rightleftarrows}} ES \underset{k_4}{\overset{k_3}{\rightleftarrows}} EP \underset{k_6}{\overset{k_5}{\rightleftarrows}} E + P$$

concentration factors. The numerator terms can be obtained by the schematic method most simply if the mechanism is represented in triangular form

The terms are

The relative concentration of each enzyme-containing species is proportional to the summation of three terms, the schematic representations of which are shown; the proportionality constant in each case is $\{(E) + (ES) + (EP)\}^{-1}$. Thus, $(E)/[E]_0 \propto \{k_2 k_5 + k_2 k_4 + k_3 k_5\}$, $(ES)/[E]_0 \propto \{k_1 k_5(S) + k_1 k_4(S) + k_4 k_6(P)\}$, and $(EP)/[E]_0 \propto \{k_2 k_6(P) + k_1 k_3(S) + k_3 k_6(P)\}$.

Since the net rate of production of product is

$$\frac{d(P)}{dt} = \frac{\{k_5(EP) - k_6(E)(P)\}[E]_0}{(E) + (ES) + (EP)}$$

$$\frac{d(P)}{dt} = \frac{\{k_1 k_3 k_5(S) - k_2 k_4 k_6(P)\}[E]_0}{k_2 k_5 + k_2 k_4 + k_3 k_5 + (S)(k_1 k_5 + k_1 k_4 + k_1 k_3) + (P)(k_2 k_6 + k_3 k_6 + k_4 k_6)}$$

It is to be noted that the patterns of line segments which are the schematic representations of the three numerator terms in the expressions for $(EX_i)/[E]_0$ are the same for each of the enzyme-containing species; these patterns differ only with the identification of the processes by the introduction of the arrowheads. Therefore, the expression for the relative concentration of *each* enzyme-containing species in a reversible reaction involves the same number of numerator terms. If a particular reaction is being studied under concentration conditions such that it is a great distance from equilibrium, the negative term(s) in the numerator of the complete rate expression may be dropped; *the condition that the reaction is*

(1) The total stoichiometric concentration of the enzymatic sites is represented by $[E]_0$; the concentration of a species is represented by its formula enclosed in parentheses. Since the present discussion pertains exclusively to systems in which $[E]_0$ is very small compared to the concentrations of substrate, product, etc., their true concentrations are approximately equal to their stoichiometric concentrations.

(2) R. A. Alberty, *J. Am. Chem. Soc.*, **75**, 1928 (1953); footnote 7.

(3) (a) M. Bocher, "Introduction to Higher Algebra," The Macmillan Co., New York, N. Y., 1907, p. 43. (b) A. C. Aitken, "Determinants and Matrices," Oliver and Boyd, Edinburgh, 1939, Chap. 2.

(4) G. B. Kistiakowsky and W. H. R. Shaw, *J. Am. Chem. Soc.*, **75**, 866 (1953).

far from equilibrium does not, however, allow the dropping of any of the denominator terms.[5] The common procedure of dropping all (P) containing terms in treating initial velocity data may be a satisfactory practice but it cannot be justified solely by the fact that the reaction is a great distance from equilibrium. Thus, the complete rate law for the mechanism given above, when applied to a unidirectional reaction, incorporates provision for the frequently observed competitive inhibition by the product.[6]

It is of interest that one can use elementary probability considerations to compute the total number of combinations of $n - 1$ rate constants (and associated concentration factors) which are present in the expression for the relative concentration of each EX_i. If the mechanism involves m reversible steps interconverting the n different EX_i's, the total number of combinations of the m steps taken $n - 1$ at a time is

$$_mC_{n-1} = \frac{m!}{(n-1)!\,(m-n+1)!} \qquad (1)$$

Of this total number of combinations, some may contain cycles of reaction steps. Combinations containing cycles are not included since such combinations do not conform to the previously stated requirements. For every cycle consisting of r steps $(2 \leqq r \leqq n - 1)$, there are

$$_{m-r}C_{n-1-r} = \frac{(m-r)!}{(n-1-r)!\,(m-n+1)!} \qquad (2)$$

combinations which involve this cycle and which, therefore, must be subtracted from the total. As an example of the use of these equations, let us calculate the number of terms in the numerator of the expression for the relative concentration of each enzyme-containing species in the modifier mechanism which has been treated by Botts and Morales,[7] and which is outlined in the accompanying paper.[8] This mechanism can be represented
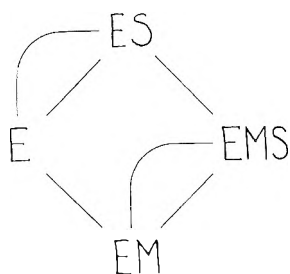
in which each line represents a reversible step. For this mechanism, $n = 4$, $m = 6$, and $r = 2$ for each of 2 cycles; thus the total number of terms in the expression for relative concentration of each EX_i is

(5) In terms of the example being discussed, the condition that the reaction is a great distance from equilibrium means that $k_1k_3k_5(S) \gg k_2k_4k_6(P)$. That this condition does not eliminate any denominator terms follows from considering the number of rate constants which are present in each denominator term. The relative magnitudes of the various denominator terms are not directly related to the thermodynamics of the over-all reaction, S = P.

(6) H. T. Huang and C. Niemann, *J. Am. Chem. Soc.*, **73**, 1541 (1951).

(7) J. Botts and M. Morales, *Trans. Faraday Soc.*, **49**, 696 (1953).

(8) E. L. King, THIS JOURNAL, **60**, 1378 (1956).

$$\left\{\frac{6!}{3! \times 3!}\right\} - 2 \times \left\{\frac{4!}{3! \times 1!}\right\} = 12$$

The twelve different patterns of line segments are
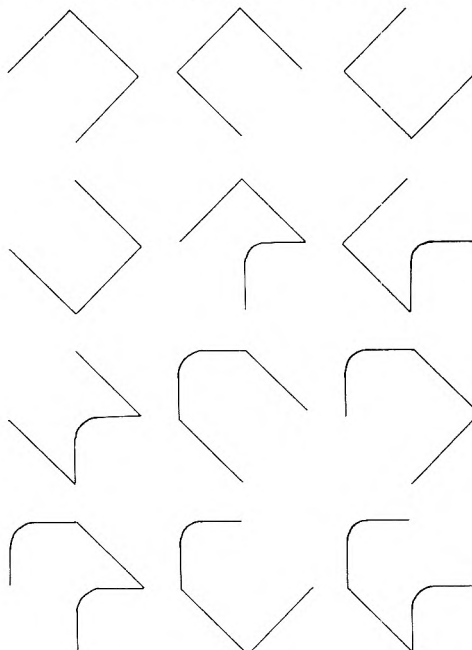
Each pattern corresponds to a term in the numerator of the expression for the relative concentration of E, ES, EM or EMS.[9]

It must be noted that for some mechanisms there may be combinations of $n - 1$ line segments which involve more than one cycle. Thus equation 2 for calculating the total number of combinations which involve a cycle will count a combination containing w cycles w times and, thus, must be used with care to assure that such a combination is subtracted from the total (given by equation 1) only once.[10]

The Basis for the Schematic Method.—The basis for the schematic method of deriving the rate law for an enzyme-catalyzed reaction can be found in the determinant solution, *i.e.*, Cramer's method,[3] for the relative concentration of each particular EX_i. Let us consider the most general case of a reaction scheme involving n enzyme-containing species, each of which can be converted to every other enzyme-containing species, EX_i. We have the n steady-state equations of the form

$$-\sum_{\substack{j=1 \\ j \neq i}}^{n} \kappa_{ij}\frac{(EX_i)}{[E]_0} + \sum_{\substack{j=1 \\ j \neq i}}^{n} \kappa_{ji}\frac{(EX_j)}{[E]_0} = 0 \qquad (3)$$

where κ_{ij} stands for the product of the rate constant *and* associated concentration factors (not including concentrations of enzyme-containing species, however) for the reaction which converts EX_i to EX_j. The use of this double subscript is a convenience in connection with the determinant notation which is to be used.[11] If more than one reversible step

(9) An appendix dealing further with this mechanism will be sent upon request.

(10) One can keep track of the combinations by numbering the m equilibria with the numbers 1 to m; it is easy, then, to compile a list of the $_mC_{n-1}$ combinations from which one can delete those containing one or more cycles.

(11) This notation has been used by F. A. Matsen and J. L. Franklin, *J. Am. Chem. Soc.*, **72**, 3337 (1950).

interconverts a particular pair of enzyme-containing species, e.g., EX_b and EX_p, both κ_{pb} and κ_{bp} are, in reality, the summations of the two or more κ's for the interconversion of these species, $\kappa_{ij} = \Sigma\kappa'_{ij}$, the κ'_{ij}'s corresponding to the individual steps.

The relative concentrations of the EX_i's are related by the equation

$$\sum_{i=1}^{n} (EX_i)/[E]_0 = 1 \qquad (4)$$

Simplicity of the determinant expression for the relative concentration of EX_m results from replacing the steady-state equation for species EX_m by equation 4 in setting up the n non-homogeneous linear equations. The use of Cramer's rule for determining the relative concentration of EX_m yields

$$\frac{(EX_m)}{[E]} = \frac{\begin{vmatrix} -\Sigma\kappa_{1j} & \kappa_{21} & \cdots & 0 & \cdots & \kappa_{n1} \\ \kappa_{12} & -\Sigma\kappa_{2j} & \cdots & 0 & \cdots & \kappa_{n2} \\ \vdots & \vdots & \vdots & \vdots & \vdots & \vdots \\ 1 & 1 & & 1 & \cdots & 1 \\ & & & & & \\ \kappa_{1n} & \kappa_{2n} & \cdots & 0 & -\Sigma\kappa_{nj} \\ -\Sigma\kappa_{1j} & \kappa_{21} & \cdots & \kappa_{m1} & \cdots & \kappa_{n1} \\ \vdots & & & \vdots & & \vdots \\ 1 & 1 & & 1 & & 1 \\ & & & & & \\ \kappa_{1n} & \kappa_{2n} & \cdots & \kappa_{mn} & -\Sigma_{nj} \end{vmatrix}} \qquad (5)$$

It follows from Cramer's rule and equation 4 that the denominator, which is the same in the expression for every $(EX_i)/[E]_0$ is the summation of the n different numerators. Thus only the numerator in this expression for $(EX_m)/[E]_0$ need be considered; this numerator reduces to the $(n-1)$ by $(n-1)$ determinant

$$(-1)^{2m} \begin{vmatrix} -\Sigma\kappa_{1j} & \kappa_{21} & \kappa_{31} & \cdots & \kappa_{n1} \\ \kappa_{12} & -\Sigma\kappa_{2j} & \kappa_{32} & \cdots & \kappa_{n2} \\ \kappa_{13} & \kappa_{23} & -\Sigma\kappa_{3j} & \cdots & \kappa_{n3} \\ & & & & \\ \kappa_{1n} & \kappa_{2n} & \kappa_{3n} & -\Sigma\kappa_{nj} \end{vmatrix} \qquad (6)$$

there being no column with m as the initial index and no row with m as the final index. (In each of the summations which are the diagonal elements, the index j assumes all possible values from 1 to n.) The index m, which corresponds to the sought for enzyme-containing species, occurs only as a final index in one term of each of the expanded diagonal elements; these diagonal elements will be represented as a_{ii}, i.e.

$$a_{ii} = \sum_{\substack{j=1 \\ j \neq i}}^{n} \kappa_{ij} \qquad i \neq m$$

The solution of this determinant, which consists of a summation of products of $n-1$ κ's (which will be called kappa products), includes only those combinations which conform to the rules already set down for the schematic derivation of the value of $(EX_m)/[E]_0$. The properties of determinants[3] lead to the following conclusions regarding (6).

(1) The column index m is not present in the determinant; thus no κ corresponding to a reaction in which EX_m is the reactant appears in any of the kappa products.

(2) All κ's with the same initial index are in the same column; thus no kappa product contains a

combination $\ldots$ $\kappa_{ij}\kappa_{im}$ $\ldots$, the κ's for two reaction steps originating with the same species.

(3) Every κ_{ij} ($i \neq m, j \neq m$) occurs two places in the determinant, once as a non-diagonal element and once in a summation a_{ii}. Because of this, certain conclusions can be drawn regarding the kappa products which contain a cycle, e.g., $\ldots$ $\kappa_{ab} \ldots \kappa_{bc} \ldots \kappa_{ca} \ldots$. The sign of this kappa product will be $(-1)^{\alpha+\beta}$ where the value of α is determined by κ's which are not involved in the cycle and β is determined by the κ's which are involved in the cycle. If the cycle consists of p different κ's, the value of β for the kappa product in which all of the κ's in the cycle arise from diagonal elements will be an even number if p is an even number and an odd number if p is an odd number. The value of β for the kappa product in which all of the κ's in the cycle arise from non-diagonal elements is determined by the number of interchanges of these κ's, initially in an ordered sequence according to the initial index, which are required to bring the second indices into their natural order; an odd number of such interchanges are required if p is an even number and thus the value of β for this kappa product will be an odd number while an even number of such interchanges are required if p is an odd number and thus the value of β for this kappa product will be an even number. Thus, the kappa products which contain cycles are cancelled since two with opposite signs are always present. (It is of interest to note that the κ's in a cycle arise either all as non-diagonal elements or all from the expanded diagonal elements.)

(4) In the ith column, are only κ's with an initial index i; thus, every kappa product contains a κ with each of the $n-1$ possible values, $i = 1$ to $i = n$ with $i \neq m$, as an initial index. In the jth row, however, are κ's with every possible value of j, $j = 1$ to $j = n$, as a final index. This is for the reason that each a_{ii} contains all possible κ_{ij}'s ($j = 1$ to $n, j \neq i$). Thus if the index m is not a final index for one of the κ's in a particular kappa product, every j which appears as a final index is also represented as an initial index and thus the kappa product must contain at least one cycle. Such a kappa product will be cancelled by an identical one with opposite sign as demonstrated under (3). If the index m is a final index for one or more of the κ's in a particular kappa product, one or more of the other possible j's will not be represented as a final index in this kappa product, but will, of course, be represented as an initial index. Thus, a sequence of reaction steps, represented in a kappa product, which terminates at EX_m originates at the EX_i with an i value not represented as a final index in the kappa product. A kappa product containing a sequence of steps terminating at EX_m which also contains a cycle of steps will be eliminated under (3).

The conclusion regarding which kappa products in determinant (6) are not allowed can really be stated with simplicity; all of the kappa products which contain cycles of steps are eliminated and all of those which do not correspond to a sequence terminating at EX_m do contain at least one cycle. The schematic method is, therefore, valid for

deriving the rate laws corresponding to *any* enzyme-catalysis mechanism in which the only interactions considered are those involving the enzyme as one of the participants.

The use of the schematic method for deriving the rate equation for enzyme-catalyzed reactions renders the treatment of a completely reversible reaction as simple as that for a more limited case.

Since, as has been mentioned earlier, the condition that the reaction is being studied at a distance from equilibrium eliminates only the negative numerator terms and does not eliminate (P) containing terms, *per se*, it seems desirable to derive the rate law on the basis of complete reversibility and then proceed to drop terms which are unimportant under the conditions being employed.

UNUSUAL KINETIC CONSEQUENCES OF CERTAIN ENZYME CATALYSIS MECHANISMS[1]

By Edward L. King

Department of Chemistry, University of Wisconsin, Madison, Wisconsin

The simple consequence of the absolute rate theory that the composition of the activated complex for a reaction is given by the form of the rate law does not apply to all limiting rate expressions arising from certain mechanisms for enzyme-catalyzed reactions. These *unusual* limiting cases may arise in mechanisms with more than one pathway for producing product (and regenerating the enzyme). Such *unusual* cases do arise if (a) the enzyme is predominantly present as an intermediate which is part of a reaction pathway *via* which most of the product is *not* being formed *and* (b) the predominant form of the enzyme is not in equilibrium with any intermediate along the reaction pathway *via* which most of the product is being formed. Alternate pathways in enzyme-catalyzed reactions cannot, therefore, be considered to be independent of one another as is true for alternate reaction pathways in uncatalyzed reactions.

Although steady-state kinetic data fall far short of completely establishing the mechanism for a chemical reaction, it is generally assumed that the order of the reaction with respect to each particular reactant gives the number of reactant molecules or ions which are incorporated into the activated complex for the reaction. This simple and useful conclusion of the absolute rate theory[2] is a consequence of the activated complex being essentially at equilibrium with the reactants.[3] In the usual Michaelis–Menten mechanism for an enzyme-catalyzed reaction, the reaction is first order with respect to the substrate at low substrate concentrations where the enzyme is predominantly present as E and is zero order with respect to the substrate at high substrate concentrations where the enzyme is predominantly present as ES. Throughout the entire concentration range, the activated complex has the composition $ES^{\ddagger}$, and thus the order of the reaction with respect to substrate is numerically equal to the average number of substrate molecules which must be added to the enzyme species to give $ES^{\ddagger}$.[4] It is the purpose of the present article,

however, to point out that certain slightly more complicated mechanisms allow the realization of limiting cases for which the order of the reaction and the composition of the activated complex are not so simply related. The mechanisms which allow these *unusual* consequences are ones in which the product can be formed (*and the enzyme regenerated*) by two or more pathways. If the enzyme is predominantly in a form which is an intermediate along one of the reaction paths at the same time that most of the product is produced *via* another reaction path, the *unusual* cases may arise.

The steady-state rate law corresponding to an enzyme catalysis mechanism is, in general, a quotient of two summations of terms. A general investigation of all possible *limiting* cases which this rate law can encompass involves considering the meaning of each numerator term coupled with each denominator term. That is, appropriate values of the rate constants and concentrations make one particular numerator term more important than all of the rest. *Under such conditions,* certain of the denominator terms *can* be important compared to all of the others and certain denominator terms *cannot* be important compared to all of the others. The physical significance of the allowed limiting cases can be discerned by considering the rate constants and concentration factors of the quotient of one numerator term and one denominator term. This can best be discussed in terms of some examples.

The steady-state rate law corresponding to the coenzyme mechanism

(1) Presented at the 129th National Meeting of the American Chemical Society, Dallas, Texas, April 8–13, 1956.

(2) S. Glasstone, K. J. Laidler and H. Eyring, "The Theory of Rate Processes," McGraw-Hill Book Co., New York, N. Y., 1941, p. 200.

(3) B. J. Zwolinski and H. Eyring, *J. Am. Chem. Soc.,* **69**, 2702 (1947).

(4) It should be noted that the mechanism: $E \rightleftharpoons E'$, $E' + S \rightleftharpoons E + P$, which bears a formal resemblance to that suggested by G. Medwedew (*Enzymologia,* **2**, 53 (1937)), yields the same rate law as the Michaelis–Menten mechanism. In this mechanism, a "special" form of the enzyme E', perhaps a particular configuration of the enzyme, reacts with the substrate to convert it to product. At low concentrations of substrate, equilibrium in the first reaction is maintained and the second reaction is rate determining. At high concentrations of substrate, the fate of almost every E' is reaction with S and the first reaction is rate determining. Thus the reaction goes from first order in substrate to zero order in substrate because the activated complex is $ES^{\ddagger}$ at low substrate concentration and is $E^{\ddagger}$ at high concentration of

substrate. This mechanism can be distinguished from the Michaelis–Menten mechanism, however, by measurements at concentrations of enzymatic sites comparable to the substrate concentration. Throughout this paper the customary concentration condition, a very low relative concentration of enzymatic sites, is assumed and thus the true concentrations of substrate, product, coenzyme and modifier are approximately equal to their stoichiometric concentrations.

$$\begin{array}{ccc} & k_1(A) \nearrow \text{EA} \searrow k_3(B) & \\ & \swarrow k_2 \quad k_4 \searrow & \\ \text{E} & & \text{EAB} \xrightarrow{k_5} \text{E + products} \\ & \nwarrow k_7 \quad k_9 \nearrow & \\ k_6(B) & \text{EB} \quad k_8(A) & \end{array}$$

may be written as the quotient of two summations of terms, the coefficients of the concentrations in the numerator being products of *four* of the nine rate constants[5,6] and in the denominator the coefficients are products of *three* of the nine rate constants. This rate equation is

$$\frac{\text{Rate}}{[\text{E}]_0} = \{k_1k_3k_5k_7(A)(B) + k_2k_5k_6k_9(A)(B) + k_1k_3k_5k_8(A)^2(B)$$
$$+ k_3k_5k_6k_8(A)(B)^2\}/\{k_1k_4k_8(A)^2 + k_1k_5k_8(A)^2 + k_1k_3k_8(A)^2(B)$$
$$+ k_3k_5k_6(B)^2 + k_3k_6k_9(B)^2 + k_3k_6k_8(A)(B)^2$$
$$+ k_2k_6k_8(A)(B) + k_1k_3k_9(A)(B) + k_1k_3k_7(A)(B)$$
$$+ k_4k_6k_8(A)(B) + k_2k_4k_8(A)(B) + k_2k_4k_8(A)$$
$$+ k_2k_5k_8(A) + k_1k_4k_7(A) + k_1k_5k_7(A)$$
$$+ k_1k_7k_9(A) + k_3k_5k_7(B) + k_3k_7k_9(B)$$
$$+ k_2k_4k_6(B) + k_2k_5k_6(B) + k_2k_6k_9(B)$$
$$+ k_2k_4k_7 + k_2k_5k_7 + k_2k_7k_9\}$$

where $[\text{E}]_0$ stands for the total concentration of enzyme and (A) and (B) stand for the concentrations of uncombined A and B.

It can be proved that 60 of the 96 possible combinations of numerator and denominator terms will not be important under any conditions. As an example consider the combination of the third term in the numerator and the fifth term in the denominator: If the third term in the numerator is dominant, it is large compared to the fourth term in the numerator, and thus the fifth term in the denominator cannot possibly be as important as the eighth term in the denominator. If

$$\{k_1k_3k_5k_8(A)^2(B)\} >> \{k_3k_5k_6k_8(A)(B)^2\}, \text{ then } k_1(A) >> k_6(B)$$

and therefore

$$\{k_1k_3k_9(A)(B)\} >> \{k_3k_6k_9(B)^2\}$$

thus, the third term in the numerator and the fifth term in the denominator *cannot* be simultaneously the dominant numerator and denominator terms. The 59 other physically meaningless combinations can be proved impossible in a similar fashion; in some proofs, the equality $k_1k_3k_7k_9 = k_2k_4k_6k_8$ must be used. Of the 36 remaining combinations of numerator and denominator terms, 32 are of a simple type; the coefficient of the concentrations in such a combination is a *single rate constant* or the product of an *equilibrium constant* and *a rate constant*. An example is the quotient of the third term in the numerator and the eighth term in the denominator, which is

$$\frac{k_8k_5}{k_9}[\text{E}]_0(A)$$

with a coefficient that is the product of an equilibrium constant k_8/k_9 and a rate constant k_5. This limiting case (the third term in the numerator and the eighth term in the denominator are the terms of predominant importance) corresponds to the dominant form of the enzyme being EB and the rate-determining step being the one with the rate constant k_5. The equilibrium constant k_8/k_9 is for

(5) L. I. Ingraham and B. Makower, THIS JOURNAL, **58**, 266 (1954).

(6) This rate law has been derived without taking into account the reverse reaction; it is applicable, therefore; only if applied to a reaction which is proceeding irreversibly and also is not subject to inhibition by product.

the reaction which converts the dominant form of the enzyme, EB, into the reactant of the rate-determining step, EAB.

The four remaining combinations cannot be eliminated and yet they are not amenable to such a simple interpretation. The four *unusual* combinations are those involving the third term in the numerator with the fourth *or* twentieth terms in the denominator and the fourth term in the numerator with the second *or* fifteenth terms in the denominator. They are

(a) $\dfrac{\text{Rate}}{[\text{E}]_0} = \dfrac{k_1k_8}{k_6}\dfrac{(A)^2}{(B)}$ (b) $\dfrac{\text{Rate}}{[\text{E}]_0} = \dfrac{k_1k_3k_5}{k_2k_6}(A)^2$

(c) $\dfrac{\text{Rate}}{[\text{E}]_0} = \dfrac{k_3k_6}{k_1}\dfrac{(B)^2}{(A)}$ (d) $\dfrac{\text{Rate}}{[\text{E}]_0} = \dfrac{k_3k_6k_8}{k_1k_7}(B)^2$

The second-order dependence upon A (or B) is surprising since no activated complex in the entire reaction mechanism contains two more A molecules (or B molecules) than are associated with any possible form of the enzyme. The physical significance of these *unusual* limiting rate expressions is clarified by a numerical example. If the concentrations of A and B are each unity and the rate constants have the values $k_1 = 10^6$, $k_2 = 10^2$, $k_3 = 10^6$, $k_4 = 10^2$, $k_5 = 10^6$, $k_6 = 10^4$, $k_7 = 1$, $k_8 = 10^2$ and $k_9 = 10^{-2}$, the situation which exists corresponds to the *unusual* combination (a). (The units of concentration and the dimensions of the rate constants are not given; they are arbitrary but must be consistent.)

(1) The numerator term $k_1k_3k_5k_8(A)^2(B)$ is at least 100-fold larger than each of the other 3 numerator terms.

(2) The denominator term $k_3k_5k_6(B)^2$ is at least 100-fold larger than each of the other 23 denominator terms and accounts for 97% of the total numerical value of the denominator.

(3) Approximately 97% of the enzyme is present as EB, 1% being present as each of the other enzyme species, E, EA and EAB.[7]

(4) Approximately 99% of the reaction occurs *via* the pathway

$$\text{E} \rightleftharpoons \text{EA} \rightleftharpoons \text{EAB} \longrightarrow \text{E + products}$$

(5) The relative concentration of E, the enzyme species which is a reactant in the rate-determining step, is given by

$$\frac{(\text{E})}{[\text{E}]_0} \cong \frac{(\text{E})}{(\text{EB})} = \frac{k_8(A)}{k_6(B)}$$

involving the ratio k_8/k_6 which is *not* an equilibrium constant. The numerator, $k_8(A)$, is the specific rate of a process which converts the predominant form of the enzyme EB into a form EAB which rapidly yields E, thus making it available for the important reaction pathway; the denominator, $k_6(B)$, is the specific rate of a process which converts E into the predominant form of the enzyme EB *thus making it unavailable* for the important reaction pathway. Thus, even though the activated complex EA‡ be essentially in equilibrium with E and A, the reactants from which it is directly formed,[3] it is not in equilibrium with the

(7) The summation of denominator terms to which the relative concentration of EB, (EB)/[E]$_0$, is proportional is $\{k_3k_5k_6(B)^2 + k_3k_6k_9(B)^2 + k_1k_3k_8(A)(B) + k_2k_4k_6(B) + k_2k_5k_6(B) + k_2k_6k_9(B)\}$.

predominant form of the enzyme, EB, and this is of great importance in connection with the relationship between the composition of the activated complex and the form of the empirical rate equation which involves the stoichiometric concentrations of the enzyme $[E]_0$ ($[E]_0 \cong (EB)$).

Case b differs from case a in that the step $EA \xrightarrow{k_3(B)} EAB$ is rate determining. Cases c and d are analogous to a and b with the predominant form of the enzyme being EA and most of the product being produced *via* the pathway

$$E \rightleftarrows EB \rightleftarrows EAB \longrightarrow E + products$$

Another mechanism which provides more than one pathway for the formation of the product is the modifier mechanism

$$E + S \underset{k_2}{\overset{k_1}{\rightleftarrows}} ES \underset{k_y}{\overset{k_x}{\rightleftarrows}} E + P$$

$$E + M \underset{k_7}{\overset{k_8}{\rightleftarrows}} EM$$

$$ES + M \underset{k_4}{\overset{k_3}{\rightleftarrows}} EMS$$

$$EM + S \underset{k_6}{\overset{k_6}{\rightleftarrows}} EMS \underset{k_\beta}{\overset{k_\alpha}{\rightleftarrows}} EM + P$$
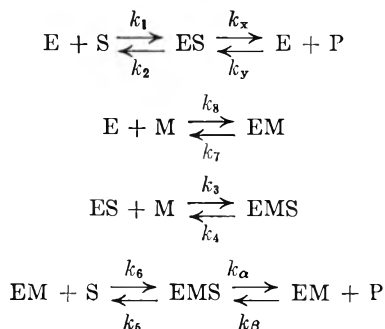
which has been treated extensively by Botts and Morales.[8] The rate law derived from this mechanism with the allowance for reversibility[9] is a quotient with twelve positive terms in the numerator (and, of course, twelve negative terms) and a forty-eight term denominator. Thus, considering only the forward reaction (*i.e.*, considering only the concentration conditions $(S)/(P) \gg k_2k_y/k_1k_x$), there are $12 \times 48 = 576$ combinations of numerator and denominator terms.[10] Of these, 434 can be shown to be impossible; *i.e.*, the particular numerator and denominator terms cannot be dominant under the same conditions.[11] A total of 112 of the combinations have simple physical significance; the coefficient of the concentrations is a *single rate constant* or *the product of an equilibrium constant*

(8) J. Botts and M. Morales, *Trans. Faraday Soc.*, **49**, 696 (1953).

(9) E. L. King and C. Altman, This Journal, **60**, 1375 (1956).

(10) An appendix summarizing the physical significant combinations will be sent upon request.

(11) In the elimination of these impossible combinations, the equalities $k_1k_3k_5k_7 = k_2k_4k_6k_8$ and $k_4k_6k_\beta k_x = k_3k_7k_\alpha k_y$ were used. Further, although the inequality $k_1k_x(S) \gg k_2k_y(P)$ which corresponds to the reaction proceeding unidirectionally eliminates *only* the negative numerator terms from the complete rate law, it does, if a certain numerator term is predominant, aid in eliminating certain denominator terms. (It is to be noted that (P)-containing terms remain in the numerator even under the condition that the reaction is proceeding unidirectionally.) For this particular mechanism, the steps $E + P \xrightarrow{k_y}$ ES and $EM + P \xrightarrow{k_\beta}$ EMS must be included if the *principle of microscopic reversibility* is not to be violated. Thus, the sequence of steps

$$E \underset{k_2}{\overset{k_1(S)}{\rightleftarrows}} ES \underset{k_4}{\overset{k_3(M)}{\rightleftarrows}} EMS \xrightarrow{k_\alpha} EM + P$$
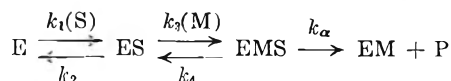
provides a pathway for formation of EM but no way for EM to yield $E + M$; the inclusion of $EM + P \xrightarrow{k_\beta} EMS$ rectifies this physically impossible situation in conformity with the *principle of microscopic reversibility*.

and a rate constant. These limiting cases correspond to the activated complex for the reaction being in equilibrium with the predominant form of the enzyme.[12] The remaining 30 limiting cases are *unusual* in the sense that the activated complex is not in equilibrium with the predominant form of the enzyme and the composition of the activated complex is not necessarily given by the concentration dependence of the rate. Twenty-six of these *unusual* limiting cases are similar to the 4 which arise in the coenzyme mechanism[5] already discussed. The larger number of *unusual* cases for modifier mechanism arise because there is the possiblity of two enzyme species not being intermediates which are a part of a reaction pathway (*i.e.*, EM and EMS are not intermediates on the pathway $E \rightleftarrows ES \rightleftarrows E + product$, and E and ES are not intermediates on the pathway $EM \rightleftarrows EMS \rightleftarrows EM + product$). It is for this reason, also, that 4 *unusual* cases can arise which are not suggested by analogy with the simpler coenzyme mechanism. These cases may arise when the two species which are not intermediates on the important reaction pathway are not in equilibrium with one another or in equilibrium with an intermediate on the important reaction pathway or rapidly converted to such an intermediate. One of these *unusual* limiting cases is

$$\frac{1}{[E]_0}\frac{d(P)}{dt} = \frac{k_1k_4k_6(S)^2}{k_8k_\alpha(M)}$$

this limiting case corresponds to the physical situation: (a) the enzyme is predominantly present as EM, (b) the product is produced predominantly by the pathway

$$E \underset{k_2}{\overset{k_1(S)}{\rightleftarrows}} ES \xrightarrow{k_x} E + P$$
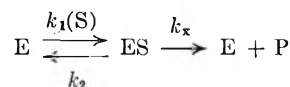
with the first step rate determining, (c) the process $E + M \xrightarrow{k_8} EM$ retards the reaction since it converts E into the predominant form of the enzyme, (d) the species EMS, which furnishes enzyme to the reaction pathway *via* the process $EMS \xrightarrow{k_4} ES + M$, is formed from EM *via* the process $EM \xrightarrow{k_6(S)} EMS$ and yields EM via the process $EMS \xrightarrow{k\alpha} EM + P$. The limiting rate expression is thus rationalized; the concentration of E, the reactant in the rate-determining step, is determined by the relationship

$$\frac{(E)}{[E]_0} \cong \frac{(E)}{(EM)} = \frac{k_4k_6(S)}{k_8k_\alpha(M)}$$

(12) Among the *usual* limiting cases is the interesting one in which the rate is proportional to (P)

$$\frac{1}{[E]_0}\frac{d(P)}{dt} = \frac{k_4k_\beta k_x}{k_3k_\alpha}\frac{(P)}{(M)}$$

this corresponds to the rate-determining step being $ES \xrightarrow{k_x} E + P$ with the concentration of ES governed by the equilibrium expression

$$\frac{(ES)}{[E]_0} \cong \frac{(ES)}{(EM)} = \frac{k_4k_\beta(P)}{k_3k_\alpha(M)}$$

EM being the predominant form of the enzyme.

in which the coefficient k_4k_6/k_8k_α is *not* an equilibrium constant.[13]

For the *usual* limiting cases, the activated complex is in equilibrium with the predominant form of the enzyme and even though the apparent rate constant is a composite of several rate constants, the temperature coefficient of the apparent rate constant is related to the enthalpy difference between the activated complex and the reactants. For the *unusual* limiting cases, such is not true; the temperature coefficient of the apparent rate

(13) A set of numerical values of the concentrations and rate constants which yields this *unusual* limiting case is: (S) = (M) = (P) = 1, $k_1 = 10^9$, $k_2 = 1$, $k_3 = 10^3$, $k_4 = 10^8$, $k_5 = 1$, $k_6 = 10^2$, $k_7 = 10^{-1}$, $k_8 = 10^5$, $k_\alpha = 10^5$, $k_\beta = 10^{-1}$, $k_x = 10^9$ and $k_y = 10^7$.

constant is *not* directly related to the enthalpy difference between the activated complex and the reactants.

If an uncatalyzed reaction (or a catalyzed reaction in which no significant amount of the catalyst is tied up as reaction intermediates) proceeds *via* more than one pathway, these pathways are completely independent. This is not true for catalyzed reactions in which a significant fraction of the catalyst (which is a catalyst for two or more of the pathways) is tied up as intermediates. The alternate pathways cannot, under such conditions, be viewed as independent and *unusual* kinetic consequences of the type outlined may arise in reactions which follow such mechanisms.

TRANSFERENCE NUMBERS IN MOLTEN SALTS

By Benson R. Sundheim

Washington Square College, New York University, New York, N. Y.

It is shown that the transference numbers of the species in a pure molten salt measured in any particular experimental arrangement may be calculated in terms of the relative masses and boundary conditions. In particular the transference number measured in the "bubble cell" type of experiment is $t_A = M_B/(M_A + M_B)$.

A pure molten salt cannot sustain a concentration gradient. For this reason, the experimental arrangement usually employed in measuring Hittorf transference numbers can give only certain results. The forces imposed by the walls of the cell or by gravity cause the transference number of the species to which the electrodes are reversible to appear to be unity.[1] It has been suggested[2,3] that an experimental arrangement which obviates the effect of gravity would enable more realistic transference numbers to be determined. Transference numbers in this sense would be based on the mobility of each ionic species "with respect to the bulk of the liquid."

Following suggestions put forward by several authors, experimenters[2,3] carried out electrolyses in cells so delicately constructed that lateral motion of the fluid within the cells could be detected. For example, in the cell pictured in Fig. 1 it was observed that electrolysis between electrodes reversible to the cations was accompanied by an increase in the volume of the cathode compartment and a corresponding decrease in the volume of the anode compartment. The interpretation heretofore made of this phenomenon was as follows: the volume change in the cathode compartment per equivalent of charge is due to the equivalent volume of the metal discharged at the electrode minus the equivalent volume of salt lost by the electrolysis plus t_+ equivalent volumes of salt due to migration into this compartment. After correcting for the volume changes at the electrode, there yet remains a decrease in volume equal to $1 - t_+ = t_-$ equivalent volumes of electrolyte.

(1) K. E. Schwarz, *Z. Elektrochem.*, **45**, 740 (1939).

(2) S. Karpachev and S. Pal'guev, *Zhur. Fiz. Khim.*, **23**, 942 (1949).

(3) F. R. Duke and R. Laity, *J. Am. Chem. Soc.*, **76**, 4046 (1954); F. R. Duke and R. Laity, This Journal, **59**, 549 (1955).

It is the purpose of this communication to demonstrate that simple considerations about the conservation of momentum lead to definite predictions about the relative motions of parts of such cells as measured in any particular arrangement and hence to predictions of the quantities which have been called transference numbers.
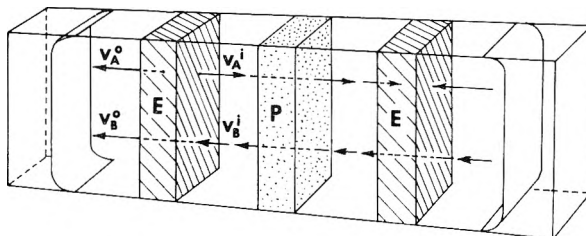
Fig. 1.—An electrolysis cell. The arrows show the motion of the ions in the various parts of the cell. For simplicity the figure shows the motion after any necessary corrections for volume changes at the electrodes are made.

Since a crucial concept in the following is the balance of momentum, we begin with the following thought experiment. Consider two separate masses of different fluids, each of which has any given momentum. Any type of interaction between the two species is permitted. The samples are allowed to collide in any way, with any sort of mixing process. The final momentum of the mixture must equal the sum of the initial momenta. Of course, kinetic energy is not conserved in such an inelastic collision unless heat is included in the kinetic energy balance. In short, the interaction of the two species according to any viscous dissipative process does not disturb the momentum balance.

A second important point is that the application of a homogeneous electric field to any neutral

sample of matter does not lead to any net body force. Although one part of a fluid may move with respect to another, momentum of an electrically neutral set of charges is conserved in a homogeneous field.

Finally, the concept of the flux of momentum in a chemical reaction must be discussed. For convenience we limit ourselves here to incompressible liquid systems. Whenever there is a volume change in a chemical reaction the chemical species come into (or out of) existence so to speak by thrusting their way against the fluid already existing. This process creates motion and hence kinetic energy but no net force and no net momentum. If the reaction is heterogeneous, taking place at an electrode for example, the momentum of the electrode must be taken into account.
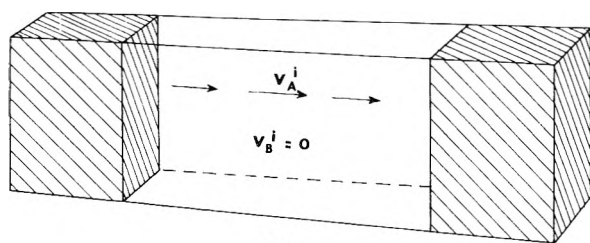
(A)
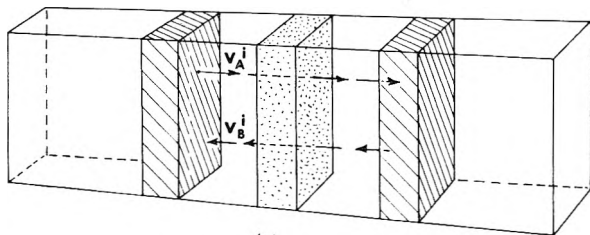
(B)
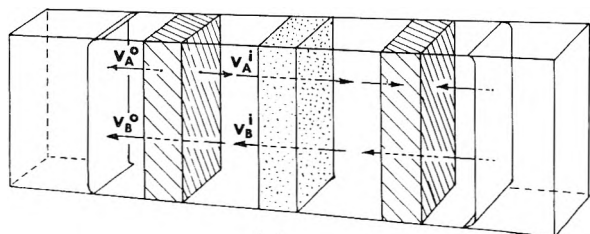
(C)

Fig. 2.—Three types of cells. The arrows show the motion of the ions. For simplicity the figures show the motion after any necessary corrections for volume changes at the electrodes have been made.

Consider the cell shown in Fig. 1. The electrodes are represented as sources adjusted so as to produce an ionic species at rates equal in magnitude and opposite in sign. The ends of the cell are open, gravity being considered absent and the cell walls of negligible mass. The liquid is incompressible and slips freely along the cell walls. There are two ionic species and the electrodes are reversible to the species A. The flow pattern is as shown in the figure. The superscript i or o serves to distinguish between portions of the fluid between the electrodes (i) and outside of the electrodes (o). The subscript E refers to the electrodes. There is

a porous plug (subscript P) inserted in the cell between the electrodes. It floats freely and because of the friction of the moving fluid has the mass average velocity of the fluid between the electrodes. All velocities are measured with reference to a coördinate system fixed in the laboratory. In the event that complex species are formed by the ions, respective velocities of the two components denote the appropriate number average velocities.

The conservation of momentum then requires

$$M_A{}^\circ \vec{v}_A{}^\circ + M_B{}^\circ \vec{v}_B{}^\circ + M_A{}^i \vec{v}_A{}^i + M_B{}^i \vec{v}_B{}^i +$$
$$M_E \vec{v}_E + M_P \vec{v}_P = 0 \quad (1)$$

The equation of continuity for each species requires that the material lost by a source appear in the liquid. Electroneutrality requires that the boundaries of the two species remain coincident. These conditions lead to the equations

$$\begin{aligned}
\vec{v}_A{}^i - \vec{v}_A{}^\circ &= \vec{q} \\
\vec{v}_B{}^i - \vec{v}_B{}^\circ &= 0 \\
\vec{v}_A{}^\circ = \vec{v}_B{}^\circ &= \vec{v}_B \\
\vec{v}_P &= \vec{v}'
\end{aligned} \quad (2)$$

where $\vec{q}$ is the strength of the source. It may be expressed in terms of the current density, the dimensions of the cell and the molar volume of the salt and it represents the volume swept out per cm.^{2} of cross-section per second by material issuing from the source. The mass average velocity, $\vec{v}^1$ of the liquid between the electrodes is defined by

$$\vec{v}' = \frac{M_A{}^i \vec{v}_A{}^i + M_B{}^i \vec{v}_B{}^i}{M_A{}^i + M_B{}^i} \quad (3)$$

Making the appropriate substitutions into equation 1, the conservation of momentum is displayed in the form

$$M_A{}^\circ \vec{v}_B + M_B{}^\circ \vec{v}_B + M_A{}^i(\vec{q} + \vec{v}_B) + M_B{}^i \vec{v}_B + M_E \vec{v}_E +$$
$$M_P \frac{M_A{}^i(\vec{q} + \vec{v}_B) + M_B{}^i \vec{v}_B}{M_A{}^i + M_B{}^i} = 0 \quad (4)$$

The masses and the strength of the source are given so that equation 4 serves to determine $\vec{v}_B$ in terms of $\vec{v}_E$. In each experimental arrangement a further relation between $\vec{v}_B$ and $\vec{v}_E$ is given, thus determining the motion of all parts of the cell and consequently determining the motions upon which transference number calculations are based.

The three experimental arrangements commonly used are shown in Fig. 2.

The ordinary arrangement of an electrolytic cell, Fig. 2A, is exposed to the leveling effect of gravity. The porous plug is omitted and the experimentally observed quantities are of course $\vec{v}_B{}^i - \vec{v}_E$ and $\vec{v}_A{}^1 - \vec{v}_E$. In this case

$$\begin{aligned}
M_P = M_A{}^\circ &= M_B{}^\circ = 0 \\
\vec{v}_B - \vec{v}_E &= 0 \\
\vec{v}_A - \vec{v}_E &= \vec{q} \\
_A = (v_A{}^i - v_E)/q &= 1
\end{aligned} \quad (5)$$

The arrangement of Fig. 2B constrains the electrodes and the porous plug to zero relative velocity.

The experimentally observed quantity is $\vec{v}_B - \vec{v}'$ after correction has been made for the volume change of the electrodes.

$$\vec{v}_B - \vec{v}' =$$

$$\frac{\vec{v}_B (M_A{}^i + M_B{}^i) - M_A{}^i (\vec{q} + \vec{v}_B) - M_B{}^i v_B{}^i}{M_A{}^i + M_B{}^i} = \frac{-\vec{q}M_A{}^i}{M_A{}^i + M_B{}^i}$$

$$t_B = (\vec{v}_B - \vec{v}_E)/(-\vec{q}) = \frac{M_A}{M_A + M_B} \qquad (6)$$

The arrangement of Figure 2C requires that $\vec{v}_E = \vec{v}_B$. The experimentally observed quantity

$$M_A{}^\circ = M_B{}^\circ = 0$$
$$\vec{v}_E = \vec{v}_B$$
$$\vec{v}_B - \vec{v}' = qM_A/(M_A + M_B)$$
$$t_B = M_A/(M_A + M_E)$$

is $\vec{v}_B - \vec{v}'$.

In addition to the motions described by the above relations certain other effects can have a bearing on the net motion. The extent of frictional drag in cells of type B is one such factor. Electrophoresis in the plug or along the walls is another. The quantities calculated above thus have the character of ideal results. The significant result is that the analysis of the relative motion of parts of an electrolysis cell does not yield information about the structure of the liquid. It is therefore seen that transference numbers in pure molten salts have little significance.

It is a pleasure to acknowledge assistance to a portion of this work by the United States Atomic Energy Commission.[4]

KINETICS OF THE REACTION BETWEEN CHROMATE AND ARSENIC TRIOXIDE IN ALKALINE MEDIUM. INDUCED REDUCTION OF OXYGEN BY THIS COUPLE[1]

BY I. M. KOLTHOFF AND MORTON A. FINEMAN[2]

Contribution from the School of Chemistry, University of Minnesota, Minneapolis, Minnesota

Received April 12, 1956

The oxidation of arsenic trioxide by potassium chromate in alkaline medium in the absence of oxygen has been found to be first order with respect to both the chromate ion and arsenic trioxide. The average value of the second order rate constant at 30° in solutions of pH 9.1 and ionic strength of 1.75 was found to be 1.61 (± 0.08) $\times 10^{-3}$ liter mole^{-1} sec.$^{-1}$. This rate constant is independent of hydrogen ion concentration at pH greater than 9.1 and increases with hydrogen ion concentration at pH smaller than 9.1. The chromate ion–arsenic trioxide reaction induces the reduction of oxygen (by arsenic trioxide) in alkaline medium. The induction factor at 40° was found to be a function of both the pressure of oxygen and the concentration of the chromate ion but apparently independent of arsenic trioxide concentration. A limiting induction factor of 4/3 was obtained. A mechanism has been proposed to account for the kinetic and the induction factor data.

The initiation of polymerization of styrene, acrylonitrile, methyl isopropenyl ketone and butadiene–styrene mixtures by the alkaline chromate ion–arsenic trioxide system has been successfully accomplished in this Laboratory.[3] An understanding of the mechanism of the over-all reaction (equation 1) between chromate and arsenic trioxide in alkaline medium and of the initiation of polymerization by this system is desirable.

$$4CrO_4{}^- + 3As_2O_3 + 10H_2O \longrightarrow 4Cr^3 + 3As_2O_5 + 20(OH)^- \qquad (1)$$
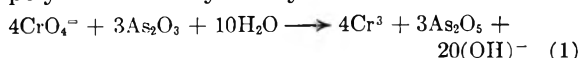
There are several experimental techniques available for studying the mechanism of initiation. These methods include: (1) the determination of the stoichiometry of the chromate ion–arsenic trioxide reaction in the absence and presence of the polymerizable monomer, (2) a kinetic investigation of the reaction in the absence and presence of monomer, (3) the identification and quantitative determination of the initiating fragment which is formed in the chromate ion–arsenic trioxide reaction and is tied up in the polymer, and (4) the investigation of other induced reactions involving the chromate ion–arsenic trioxide primary reaction in alkaline medium. With respect to the last method it should be pointed out that the initiation of polymerization with this oxidation-reduction system is an example of an induced chain reaction.[4]

In the present paper we describe a kinetic study of the oxidation of arsenic trioxide by chromate ion in alkaline medium in the absence of monomer, and the investigation of the stoichiometry of the induced reduction of molecular oxygen by the chromate ion–arsenic trioxide reaction in alkaline medium. The induced reduction of oxygen was chosen since the results will be useful not only for the interpretation of the mechanism of the primary reaction but for an understanding of the effect of oxygen in polymerization initiated by the above system.

Experimental

Materials.—Baker A.R. grade potassium chromate was

(3) I. M. Kolthoff and E. J. Meehan, *J. Polymer Sci.*, 9, 327 (1952).

(4) A. I. Medalia, *Anal. Chem.*, 27, 1678 (1955).

recrystallized from conductivity water and dried between 135 and 170°. Two batches prepared in this manner were analyzed for chromate by iodometric titration.[5] The analyses for potassium chromate were Batch A, 99.7 ± 0.1%, and Batch B, 99.6 ± 0.1%. Merck primary standard arsenic trioxide and all other chemicals of A.R. grade were used without further purification.

Analyses.—In stoichiometric investigations of induced reactions involving chromate ion and arsenic trioxide both substances must be quantitatively determined. The arsenic trioxide was determined by amperometric titration with iodine[6] in solutions buffered with borax at zero applied voltage. Chromate ion was determined polarographically at −0.80 volt (vs. S.C.E.) at a dropping mercury electrode.[7] The polarographic analysis gave a reproducibility within 4% even in the presence of the other constituents of the system.

Kinetics

Procedures.—The effects of the concentration of chromate ion, concentration of arsenic trioxide, pH, chromic ion and arsenic pentoxide on the rate of reaction were studied. The solutions of chromate ion and arsenic trioxide containing buffering agents, potassium nitrate and other reagents were made up for each run so that on mixing the ionic strength was 1.75 (±0.10) moles/liter. The initial concentrations of the reagents were calculated from the volumes and concentrations of their stock solutions and the final volume.

The solutions of arsenic trioxide and potassium chromate were deaerated at 30° for at least 15 minutes with tank nitrogen (99.5%) which had been further purified through an alkaline pyrogallol train. One-hundred ml. of the chromate solution was pipetted into a 250-ml. reaction bottle and the bubbling of the nitrogen was continued. The reaction was started by adding with a pipet 25 ml. of the arsenic trioxide solution to the reaction bottle. Zero time was taken when half of the arsenic trioxide solution had been added.

During the first 10 minutes samples of the reacting mixture were withdrawn by pipet for the determination of the arsenic trioxide. The bottles were then closed with self-sealing Buna-N gaskets held tightly by perforated metal screw caps. The remaining samples were removed with a calibrated ten-ml. syringe. The samples were run into about 120 ml. of cool borax solutions (0.04M) and quickly analyzed for arsenic trioxide. Even in the fastest reactions a negligible amount of arsenic trioxide was consumed by reaction with chromate during the actual titration.

In the faster runs, nitrogen was bubbled through the solution during the entire course of the reaction and all the samples were taken with a pipet. With this procedure of removal of each aliquot the error in time was reduced to probably less than 30 seconds.

Most of the kinetic experiments were performed in solutions buffered with borax (0.12 M) to a pH of 9.1. In those experiments conducted at other pH values, the solutions were buffered with borax and HCl for lower pH and with borax and sodium carbonate for higher pH.

Results.—By having the initial chromate ion concentration in sufficient excess over that of the arsenic trioxide concentration so that no appreciable change in chromate ion concentration occurred during the reaction, the determination of the order of the reaction with respect to arsenic trioxide is possible by the method of integration.[8] By repeating such experiments in which the chromate ion concentration is altered (but is still in large excess), the order with respect to the chromate ion can be obtained. All the kinetic data are

(5) I. M. Kolthoff and E. B. Sandell, "Textbook of Quantitative Inorganic Analysis," The Macmillan Co., New York, N. Y., 1943, p. 624.

(6) I. M. Kolthoff and J. J. Lingane, "Polarography," Interscience Publishers, Inc., New York, N. Y., 1952, p. 946.

(7) J. J. Lingane and I. M. Kolthoff, J. Am. Chem. Soc., **62**, 852 (1940).

(8) K. J. Laidler, "Chemical Kinetics," McGraw-Hill Book Co., Inc., New York, N. Y., 1950, pp. 13–18.

presented in Table I. As an illustration a few runs are plotted in Fig. 1.

TABLE I

KINETIC DATA FOR THE CHROMATE–ARSENIC TRIOXIDE[a] REACTION AT 30° IN THE ABSENCE OF OXYGEN (μ = 1.75 MOLE LITER^{-1})

	$M_A{}^\circ$ (mM)	$M_C{}^\circ$ (mM)	$M^\circ_{Cr^{+++}}$ (mM)	$M^\circ_{As_2O_5}$ (mM)	pH	k_1 (sec.$^{-1}$) × 10^4	k_2 (l. mole^{-1} sec.$^{-1}$) × 10^4
1	0.586	81.6	...	...	9.1	1.23	1.51
2	1.171	81.6	...	...	9.1	1.26	1.55
3	1.171	81.6	...	...	9.1	1.24	1.52
4	1.171	163	...	...	9.11	2.68	1.65
5	1.171	245	...	...	9.08	4.06	1.66
6	4.554	163	...	...	9.1	2.81	1.73
7	1.161	80.3	0.781	0.586	9.1	1.25	1.56
8	1.172	162	1.04	0.781	9.1	2.60	1.60
9	1.168	163	...	6.0	9.1	2.77	1.70
10	1.164	82.3	3.18	2.39	9.1	1.12	1.36
11	1.174	163	...	...	8.33	3.94	2.42
12	1.174	163	...	...	9.82	2.89	1.78
13	1.174	163	...	...	10.56	2.47	1.50

[a] Explanation of symbols: $M_C{}^\circ$ = initial concentration of chromate ions in millimoles per liter; $M_A{}^\circ$ = initial concentration of trivalent arsenic in millimoles per liter.

Employing the method of integration, the rate of reaction with respect to arsenic trioxide concentration was found to be first order for the initial 40% of the reaction. After 40% had reacted, the first-order rate constant decreased slightly as the reaction proceeded. The data in Table I reveal that an eightfold variation in initial concentration of arsenic trioxide did not influence the initial rate constant.

From the data for runs 3, 4 and 5, the rate with respect to the chromate ion concentration can be shown to be first order within the experimental error.

Since DeLury[9] has shown that the rate of oxidation of arsenic trioxide by chromate in acid media is second order with respect to hydrogen ion concentration, it was of interest to find whether the rate was dependent on hydrogen ion concentration in alkaline media. By comparing the results of runs 11, 4, 12 and 13 in Table I in which the pH was altered from 8.3 to 10.6, it is seen that the rate is independent of pH above 9.0 while the rate constant for the run at 8.3 does appear to be significantly larger.

Since the rate law goes from second order with respect to hydrogen ion concentration in acid media to zero order at pH greater than 9.0, it seems that the actual rate law which would cover the entire range of pH must be a sum of terms each one having a different dependency on hydrogen ion concentration.[10]

It was of interest to find whether the products of the reaction influenced the rate in such a way as to account for the slight decrease in the rate constant as the reaction proceeded. From the runs 3, 7 and 10, and 4, 8 and 9, there appears to be a small effect due to the products of the reaction. However, we feel that this effect is not large enough to account for the variation in rate constant as the reaction proceeded because the concentrations of

(9) (a) R. E. DeLury, THIS JOURNAL, **7**, 239 (1903); (b) **11**, 54 (1907).

(10) J. O. Edwards, Chem. Revs., **50**, 472 (1952).

the products in the actual runs were too small to cause such an effect.

The second order rate constants (k_2) have been included in Table I. The average value for k_2 for this reaction at 30° and at a pH of 9.1 at an ionic strength of 1.75 is 1.61 (± 0.08) $\times$ 10^{-3} liter mole^{-1} sec.$^{-1}$.

Induced Reduction of Oxygen

For discussing the induced reduction of oxygen by the chromate ion–arsenic trioxide reaction it is convenient to use the nomenclature of Luther and Schilow.[11] The arsenic trioxide is the actor, chromate ion is the inductor and oxygen is the acceptor. The primary reaction occurring between the chromate ion and the arsenic trioxide induces the secondary reaction between arsenic trioxide and oxygen. The induction factor (I_i) is given by the ratio of the number of equivalents of the acceptor, oxygen (E_{ox}), reduced divided by the number of equivalents of the inductor, chromate ion (E_{Cr^6}), reduced.

$$I_i = E_{ox}/E_{Cr^6} \qquad (2)$$

Nearly a century ago Kessler[12] discovered the induced reduction of oxygen by the chromate ion–arsenic trioxide reaction in alkaline medium. Except for a few experiments conducted by him, no further work has been reported in the literature on this system.

Procedure.—By measuring the amount of chromate ion and arsenic trioxide consumed in the induced reduction of oxygen, the induction factor can be calculated. For these stoichiometric experiments, most runs were performed in 250-ml. bottles or modified Kolthoff–Medalia[13] flasks. Several experiments were conducted in a Parr bomb calorimeter in order that large pressures of oxygen could be used. A few other experiments were performed in an erlenmeyer flask.

The procedure varied slightly depending on the vessel used for the experiment. When using the Kolthoff–Medalia flasks, measured volumes of each solution were placed in the two separate containers of the flask. Oxygen was bubbled through a borax buffered (0.125 M) solution containing potassium nitrate (1.50 M) and then through the solutions in the vessel for at least 25 minutes. After sealing the vessel from the air with greased, ground glass stoppers, the vessel was placed in a 40° bath for at least 15 minutes. The time was noted after the solutions were thoroughly mixed by vigorous shaking.

When using the Parr bomb calorimeter, solutions of chromate ion and arsenic trioxide saturated with oxygen at one atmosphere were mixed in a beaker placed in the bomb. The cover of the bomb was immediately tightened in place and the bomb was filled with oxygen under 10 to 15 atmospheres. The apparatus was then immersed in the 40° bath.

In the experiments performed in the 250-ml. bottles, the measured volumes of solutions of chromate ion and arsenic trioxide were mixed in the bottles and oxygen bubbled through the mixture for at least a half-hour at room temperature. The bottles, after being sealed with Buna-N gaskets tightly held metal screw caps, were placed in the constant temperature bath and zero time noted. Since under the experimental conditions the reaction between arsenic trioxide and chromate is very slow at 25°, the amount of reaction which may have occurred during the bubbling period was negligible.

Because the reaction was extremely slow, the final concentrations of arsenic trioxide and chromate ion could be determined almost simultaneously. A 25-ml. sample of the reaction mixture was quickly added to a polarographic cell

(11) R. Luther and N. Schilow, Z. physik. Chem., **46**, 777 (1903).

(12) F. Kessler, Pogg. Ann., **119**, 218 (1863).

(13) I. M. Kolthoff and A. I. Medalia, J. Am. Chem. Soc., **71**, 3777 (1949).
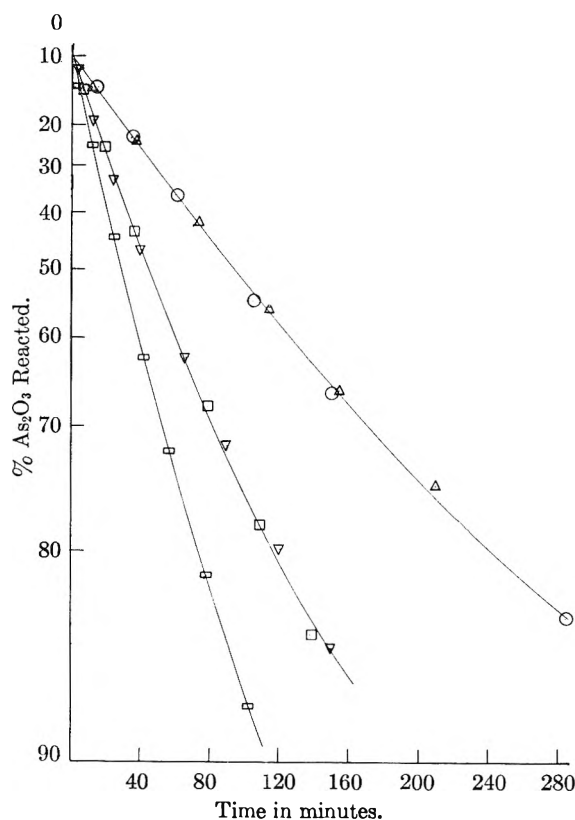
Fig. 1.—Rate of oxidation of As$_2$O$_3$ by chromate at 30.0°; μ = 1.75 molar, pH 9.1,

		$M_A°$ mM	$M_C°$ mM
☉	Run 1	0.586	81.6
△	3	1.171	81.6
☐	4	1.171	163
⊡	5	1.171	245
▽	6	4.554	163

in the 25° bath and bubbling of nitrogen was started. About five minutes later, two samples of the reaction mixture were added to 100 ml. of borax buffered solutions (0.04 M) at room temperature and immediately titrated amperometrically with iodine to determine arsenic trioxide. As soon as this was accomplished, the diffusion current of the chromate was measured at −0.80 volt (vs. S.C.E.). The total time involved for the analysis was about 25 minutes. The times listed in Table II below were recorded when the samples for arsenic trioxide determination were cooled and diluted.

Results.—According to the over-all equation for the oxidation of arsenic trioxide by chromate ion in alkaline medium (see equation 1) the theoretical reaction ratio of the number of atoms of arsenic to the number of chromium atoms reacted is 1.50. This reaction ratio was determined (see Table II, runs 1 and 2) to be 1.46. It was concluded that the analytical procedures employed were satisfactory within a few per cent.

Several runs were made to verify the fact that no measurable amount of arsenic trioxide is oxidized by oxygen in alkaline medium in the absence of chromate ion during the longest time the reactions were studied. In the most favorable case for the oxidation of arsenic trioxide by oxygen (i.e., oxygen at 15 atmospheres above the solution) only 1.7% of the oxide had reacted after 71 hours. In those runs in which the oxygen pressure was smaller than 15 atmospheres, no measurable reaction occurred. A small correction for direct oxida-

TABLE II

DATA ON THE INDUCED REDUCTION OF OXYGEN BY THE ALKALINE CHROMATE ION–ARSENIC TRIOXIDE SYSTEM

$M_{Borax} = 0.125\,M^a$, $M_{KNO_3} = 1.50\,M$, $\mu = 1.75$, $t = 40.0°$

Run	Time, hr.	Oxygen pressure (atm.)	Reaction[b] vessel	$M°C^a$ (mM)	$M°A$ (mM)	MC (mM)	MA (mM)	Eq. O_2 (meq./l.)	I_f	$1/I_f$	Estim. error in $1/I_f$	$(M_C/P_{ox})_{Av.}$ mM/atm.	Estim. error in $(M_C/P_{ox})_{Av.}$
1	24	0.0	K and M	5.60	5.94	2.73	4.02	...	...	...	...	...	...
2	53	0.0	K and M	5.60	5.94	3.48	5.02	...	...	...	...	...	...
3	70.5	0.2	Bottle	3.24	4.64	1.78	3.87	2.40	0.45	2.22	0.23	11.75	0.57
4	69.2	0.2	Bottle	2.59	4.64	1.49	3.54	2.61	0.59	1.69	.13	9.25	.34
5	70.5	0.2	Bottle	1.62	4.64	1.06	2.76	2.34	0.73	1.37	.07	5.45	.20
6	69.2	0.2	Bottle	1.30	4.64	0.88	2.39	2.14	0.81	1.23	.05	4.30	.15
7	29.5	0.2	Erlenmeyer	5.60	5.94	2.47	4.56	1.71	0.23	4.35	1.17	21.85	1.08
7	52.8	0.2		5.60	5.94	2.72	5.30	2.44	0.30	3.33	.61	21.20	0.90
8	24.0	1.0	K and M	5.60	5.94	1.81	4.52	3.61	0.67	1.49	0.31	4.70	0.18
9	52.8	1.0	K and M	5.60	5.94	2.21	5.56	4.49	0.68	1.47	0.22	4.50	.17
10	24.0	1.0	K and M	1.62	5.94	0.72	2.12	2.08	0.99	1.01	0.10	1.26	.05
11	74.0	1.0	K and M	1.62	5.94	1.18	3.67	3.80	1.07	0.93	0.04	1.03	.04
12[c]	24.0	1.0	Bottle	1.62	5.94	0.58	1.71	1.68	0.97	1.03	0.15	1.33	.05
13[c]	46.0	1.0	Bottle	1.62	5.94	1.01	3.04	3.05	1.01	0.99	.05	1.12	.04
14	71.8	1.0	K and M	1.60	5.94	1.12	3.84	4.32	1.30	0.77	.03	1.04	.05
15	74.7	1.0	K and M	0.56	5.94	0.46	1.53	1.69	1.23	0.81	.01	0.33	.01
16	118.0	1.0	K and M	2.33	7.92	1.92	5.45	5.14	0.89	1.12	0.02	1.37	0.05
17	48.0	1.0	Bottle	1.08	7.92	0.84	2.75	2.98	1.21	0.83	.02	0.66	.02
18	138.0	1.0	Bottle	0.667	7.92	0.65	2.18	2.41	1.23	0.81	.01	0.34	.01
19	95.6	1.0	Bottle	0.540	7.92	0.52	1.71	1.86	1.19	0.84	.02	0.28	.01
20	95.8	1.0	Bottle	0.333	7.92	0.32	0.98	1.00	1.04	0.96	.04	0.17	.01
21	68.7	1.0	K and M	13.00	18.60	8.04	18.13	12.14	0.50	2.00	0.15	8.97	0.33
22	65.5	1.0	K and M	10.35	18.60	7.71	17.50	11.9	0.51	1.96	.15	6.50	0.23
23	24.0	10	Bomb	1.62	5.94	0.68	2.11	2.18	1.04	0.96	0.10	0.13	0.01
24	114	15	Bomb	1.62	5.94	1.19	4.28	4.99	1.33	0.75	.02	0.07	0.003
25	161	15	Bomb	2.33	7.92	1.95	6.66	7.47	1.22	0.82	.01	0.09	.003

[a] Explanation of symbols: M_C = concn. of chromate ion; M_A = concn. of trivalent arsenic; Eq. O_2 = equiv. of oxygen. The superscript "o" refers to initial state.   [b] K and M is a Kolthoff–Medalia flask.   [c] Run at 35°.

tion has been made in the experiments conducted under 15 atmospheres of oxygen; in all other cases no correction was needed.

Three series of runs were made in which the initial concentration of arsenic trioxide and pressure of oxygen were the same in a given series while the initial chromate ion concentrations were varied (compare runs 3, 4, 5 and 6; and runs 8, 9, 10, 11, 12, 13, 14 and 15; and runs 16, 17, 18, 19 and 20 in Table II). In all cases, the induction factor increased, as the initial chromate ion concentration decreased.

In experiments in which the initial oxygen pressure was varied it was found that increasing the oxygen pressure increased the induction factor (compare runs 24 with 10, 11, 12 and 13; runs 25 and 16; and runs 7, 8 and 9).

The arsenic trioxide concentration did not appear to affect the induction factor.

It is well at this point to emphasize that the induction factors tabulated are average values of the induction factors determined at given times during the reaction period. All the essential information necessary for the determination of the induction factors is given in Table II.

Treatment of Data.—The largest induction factor observed for the induced reduction of oxygen by the chromate ion–arsenic trioxide couple was 1.33. As the conditions are altered to favor the induced reduction of oxygen, i.e., decreasing the

initial chromate ion concentration and increasing the oxygen pressure, the induction factor seems to approach a limiting value of the order of 1.33.

Assuming the error in the limiting induction factor is as much as ten per cent. and that the limiting induction factor ($I°_f$) is close to the maximum one observed, namely 1.33, then the $I°_f$ lies between 1.20 and 1.50. In order to establish the correct limiting induction factor, other information must be brought to bear on deciding its value.

From the definition of the induction factor (see eq. 2), it is seen that the limiting value of I_f is a ratio of two integers. Furthermore, the limiting ratio of the number of molecules of oxygen consumed to the number of molecules of chromate ion consumed (this ratio will be designated by ρ) must also be that of two integers. It seems reasonable to assume that the mechanism of the coupled reaction is such that both ratios, $I°_f$ and $\rho°$, are ratios of small whole numbers. From Table III one notices that when $I°_f$ is 4/3 and $\rho°$ is 1/1, both $I°_f$ and $\rho°$ are composed of the smallest whole numbers for a limiting induction factor between 1.20 and 1.50. Although Table III is not complete insofar as there are an infinite number of ratios of integers for I_f at values between 1.20 and 1.50, it can be easily demonstrated that any of those omitted will have values constructed from very large integers.

TABLE III

VARIATION OF RATIO OF OXYGEN TO CHROMATE CONSUMED
($\rho°$) AT VARYING VALUES BETWEEN 1.20 AND 1.50 OF THE
LIMITING INDUCTION FACTOR $I°_f$

$I°_f$	$\rho°$
6/5 = 1.20	9/10
11/9 = 1.22	11/12
5/4 = 1.25	15/16
9/7 = 1.29	27/28
4/3 = 1.333	1/1
11/8 = 1.38	33/32
7/5 = 1.40	21/20
10/7 = 1.43	15/14
13/9 = 1.44	13/12
3/2 = 1.50	9/8

A relation between the observed average induction factor and the ratio of the average chromate ion concentration to the average pressure of oxygen for a single experiment was derived from the mechanism proposed in the next section for the induced reduction of oxygen, namely

$$1/I_f = A + B \frac{[Cr^6]}{P_{O_2}} \qquad (3)$$

In Fig. 2 the data of the reciprocal of the induction factor *versus* the average ratio of chromate ion concentration to oxygen pressure have been plotted. For each experiment the errors for both $1/I_f$ and $[Cr^6]/P_{O_2}$ have been estimated and are given in Table II. The rectangles about each point in Fig. 1 represent these estimated errors.

The linearity of the plot in Fig. 1 is not verified conclusively by our data because of the large errors and scattering of some of the points about the best straight line. Nevertheless, considering that the oxygen pressure was varied 75-fold, the chromate ion concentration 40-fold, and the arsenic trioxide concentration 4-fold, the fit of the data to a linear equation is gratifying. The most significant feature of Fig. 2 is that a limiting induction factor does exist at zero chromate ion concentration or infinite pressure of oxygen; the limiting induction factor is 4/3 within the experimental error.

The chemical equation for the over-all induced reaction corresponding to this value of $I°_f$ may be written as

$$7H_3AsO_3 + 2CrO_4^- + 2O_2 + 5H_2O \longrightarrow 7H_3AsO_4 +$$
$$2Cr^3 + 10(OH^-) \quad (4)$$
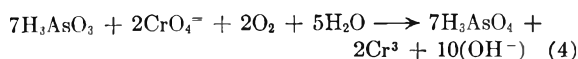
Discussion

Watanabe and Westheimer[14] have discussed the limitations which normally are imposed upon any postulated mechanism of a reaction. One of the most important is that "when relatively stable and unstable particles occur together in a reaction mixture, the unstable particles (especially when they are present at high dilution) do not react with one another to the practical exclusion of reactions between stable and unstable particles." Furthermore, with respect to the chromate ion–arsenic trioxide reaction in acid medium, Westheimer[15] points out that it is very unlikely that a tetravalent

(14) W. Watanabe and F. H. Westheimer, *J. Chem. Phys.*, **17**, 61 (1949).

(15) F. H. Westheimer, *Chem. Revs.*, **45**, 419 (1949).
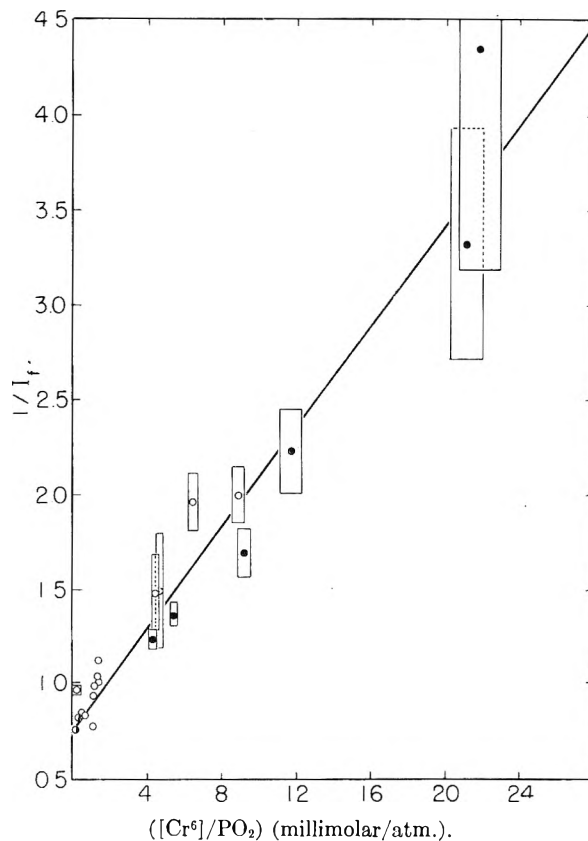
Fig. 2.—Plot of $1/I_f$ vs. ($[Cr^3]/P_{O_2}$):   ●, 0.2 atm. of oxygen; ○, 1.0; ◑, 15.

arsenic and a pentavalent chromium are produced in the initial step,[16] *i.e.*

$$Cr^6 + As^3 \rightarrow Cr^5 + As^4$$
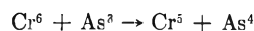
Within the limitations imposed upon a proposed mechanism and assuming that trivalent arsenic is always oxidized by a two-electron transfer, the following sequences of reactions in schemes A and B would account for the stoichiometry of the chromate–arsenic trioxide reaction in the absence of oxygen.

Scheme A

$$Cr^6 + As^3 \longrightarrow Cr^4 + As^5 \qquad (5)$$
$$Cr^4 + As^3 \longrightarrow Cr^2 + As^5 \qquad (6)$$
$$Cr^2 + Cr^6 \longrightarrow Cr^3 + Cr^5 \qquad (7)$$
$$Cr^5 + As^3 \longrightarrow Cr^3 + As^5 \qquad (8)$$

Scheme B

$$Cr^6 + As^3 \longrightarrow Cr^4 + As^5 \qquad (5)$$
$$Cr^4 + Cr^6 \longrightarrow 2\ Cr^5 \qquad (9)$$
$$Cr^5 + As^3 \longrightarrow Cr^3 + As^5 \qquad (8)$$
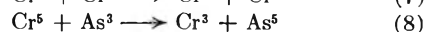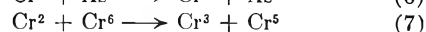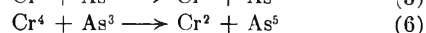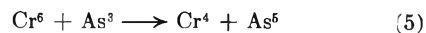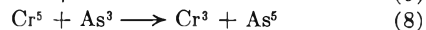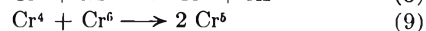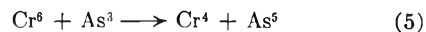
Westheimer[14] has given an excellent discussion of the induced oxidations of manganous and iodide ions by the chromate ion–arsenic trioxide reaction in acid medium. He has shown how Scheme B can account for the observed induction factors and rate data in acid media for both of these oxidations.

In alkaline medium in the presence of oxygen it is necessary to assume that the dissolved oxygen oxidizes the chromous ion (Cr^2), (that oxygen does

(16) Designations of Cr^5, Cr^4, Cr^6, As^3, As^5 are used where the nature of the particular ion or molecule of the indicated valence cannot be identified.

not oxidize Cr^5 or Cr^4 appears reasonable from estimated electrode potentials).[15] Thus it appears that Scheme A is operative in alkaline medium. The following reactions along with Scheme A would account for the induction factor

$$Cr^2 + O_2 \longrightarrow Cr^2O_2 \qquad (10)$$
$$2CrO_2 \longrightarrow (CrO_2)_2 \qquad (11)$$
$$(CrO_2)_2 + 2As^3 + 4H^+ \longrightarrow 2As^5 + 2Cr^3 + 2OH^- + H_2O_2 \quad (12)$$
$$H_2O_2 + As^3 \longrightarrow As^5 + 2OH^- \qquad (13)$$
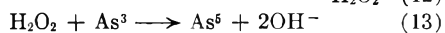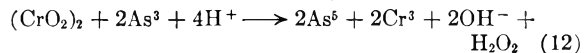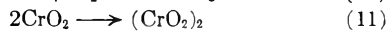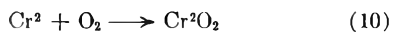
In the presence of oxygen there is competition between reactions (7) and (10). Under conditions where the limiting value of the induction factor is attained the entire sequence is given by reactions (5), (6), (10), (11), (12) and (13). Reaction (12) undoubtedly occurs in steps. It is assumed that Cr^2O_2 is relatively stable and can accumulate in the solution to give rise to reaction (11).

The rate of disappearance of arsenic trioxide has been determined in a few preliminary runs at 40° in the presence and absence of oxygen. The data are not accurate enough to be reported here, but they indicated clearly that the rate constant of disappearance of arsenic trioxide in the presence of oxygen is somewhat greater (of the order of 10 to 20%) than in its absence. Hence it may be concluded that oxygen does not affect the rate of the rate-determining reaction (5).

With respect to the initiation of polymerization by the alkaline chromate ion–arsenic trioxide oxidation–reduction system, it seems very probable that initiation occurs by way of one of the intermediates of unstable oxidation states of chromium (Cr^5, Cr^4) which are formed in the reaction mixture. At the present time we cannot venture to predict which one actually performs this function. Experiments have been carried out in which polystyrene was prepared by emulsion polymerization using the chromate–arsenic trioxide recipe.[5] Although the polystyrene was purified by repeated solution in benzene and precipitation with alcohol, its color remained slightly greenish, indicating the presence of chromium. Considering that the molecular weight of the polymer was a few million, the greenish color must have been due to some coprecipitated trivalent chromium. Therefore, it is still unknown whether an intermediate valence form of chromium initiates polymerization by adding to a monomer molecule or by the reaction $Cr^4(Cr^5) + M \rightarrow M^\bullet + Cr^3 + H^+$.

THE INTERACTION OF NITROGEN WITH A TUNGSTEN SURFACE

BY GERT EHRLICH

Contribution from General Electric Research Laboratory, Schenectady, New York

The states of binding of nitrogen adsorbed on a sparsely covered tungsten surface have been examined experimentally. In addition to a primary chemisorbed state, β, which is completely desorbed only at temperatures as high as 2000°K., two other states of lower binding energy have been isolated using the flash filament technique. One of these states, designated as α, is significantly populated at room temperature, the other, γ, can be detected only below 200°K. From the evaporation rate determined by Becker and Hartman, it is shown that nitrogen in the β-state is present on the surface as atoms, with a binding energy of ~150 kcal./g. atom. The rate of filling up of the α-levels is limited by the rate of formation of the β-state, and it is deduced that adsorption occurs on sites formed on the surface through the presence of the immobile, atomically bound β-layer; the γ-state is only weakly bound, and can be associated with physical adsorption. At 80°K., chemisorption in the β-state ceases when only part of the surface is covered—adsorption in the γ-state continues, however, indicating an activation barrier to chemisorption on some of the surface sites. Heterogeneity of binding also is indirectly indicated.

Fundamental to an understanding of the reactions that may occur between a gas and a metal surface is a knowledge of the states of binding of the adsorbed species present on the surface and their rate of formation. The kinetics of chemisorption of a diatomic gas on a metal have recently been examined[1] on the assumption that gas molecules held to the surface by dispersion forces act as a precursor to the final, chemisorbed state. Such a mechanism proved consistent with the results obtained by Becker and Hartman[2] for the adsorption of nitrogen on tungsten and their rate measurements suggest that chemisorption occurs preferentially at sites which are clustered together into regions only a few atom spacings wide, which have been associated with lattice steps on the surface.

Underlying this analysis is the assumption that only two states of binding need be considered— physical adsorption, in which molecules are weakly held to the surface by dispersion forces, and chemisorption, in which a bond comparable in energy with a primary chemical bond is formed between the adsorbed species and the surface. Actually, the nature of the interactions between a gas and a metal is far from being understood; the relation between binding and surface structure and even the more basic problem of the state of association of adatoms on a surface have not been thoroughly explored; reliable experimental data bearing on such questions are scanty. We have therefore undertaken a study of the adsorption of diatomic gases on a bare metal surface and in the following we report upon the results of our investigation of the system nitrogen on tungsten.

(1) G. Ehrlich, *Internatl. J. Phys. and Chem. of Solids*, in press.

(2) J. A. Becker and C. D. Hartman, THIS JOURNAL, **57**, 157 (1953).

In this, we have relied primarily upon the flash filament technique, not only to explore the rate of gas adsorption, but also to distinguish between the various states of binding possible on the surface. Molecules held in states of low binding energy (~10 kcal./mole and lower) would be expected to appear in detectable amounts only at low temperatures, and it is this range (100–400°K.) which we shall consider in detail here.

The Flash Filament Technique

The amount of gas adsorbed on a surface as a function of the time during which gas impinges upon it, as well as the state of the adsorbed material, can both be ascertained by the flash filament method; in this the solid under investigation, immersed in a gas, is mounted in a vacuum system in such a way as to permit rapid heating, and the amount of gas desorbed from the sample upon such heating is determined from the resulting pressure rise in the system. This idea was first made use of by Taylor and Langmuir[3] in studying the adsorption of cesium on tungsten, and the experimental arrangement in this investigation differs in only two significant ways from that of Taylor and Langmuir. Following Apker,[4] an ionization gage has been employed to monitor the gas pressure inside the system; and instead of operating at a constant pressure in a closed system we have resorted to a flow technique similar to that described by Becker and Hartman.[2] The gas is allowed to stream through a cell containing the sample and the pressure gage, and a steady state with respect to the number of molecules in the cell is established with the filament so hot that it is not adsorbing. Upon letting the sample cool, adsorption occurs, resulting in a decrease in the pressure; this is continuously indicated by the ion gage, so that the number of molecules striking the filament is known, just as in the constant pressure method of Taylor and Langmuir. The amount adsorbed at any instant can be obtained from the pressure burst upon flashing the filament, or else from the decrease in the cell pressure during the interval of adsorption. Inasmuch as we will report findings that appear to have escaped previous observers, the experimental techniques employed will be described in detail, though some aspects may have been summarized previously.[2,5]

Vacuum System.—Figure 1 shows the line used in our studies. Reagent (Airco) nitrogen is kept in a flask provided with a break-off seal, leading to trap A; the latter is equipped with a 10 mil tungsten spiral filament, which during a run is kept at ~1300°K. to remove possible contaminants in the gas. The gas pressure inside the flash filament cell is regulated with a metal valve B,[6] manufactured by the Granville–Phillips Company. The cell itself consists of an inverted ion gage G,[7] to which is joined a side arm containing the sample under investigation—a 10 mil tungsten filament F, mounted on molybdenum leads L; gas flow through the cell is restricted by the magnetically operated ground glass plates D and E, resting on ground glass shoulders, which delimit a volume of 370 cc. A second ion gage H is provided on the manifold leading to the trap I and serves both as pump and pressure measuring device. Interposed between I and two single stage mercury diffusion pumps in series is an additional trap J, immersed in liquid nitrogen to eliminate mercury vapor. Prior to incorporation in the measuring system, the cell was calibrated on an auxiliary system against a McLeod gage, yielding a gage constant for N_2 of 15 (mm. Hg)$^{-1}$.

Electrical System.—Since the flash-filament method depends upon pressure measurements during rapidly changing conditions, the gages must be operated at a constant electron current i_e, regardless of the state of contamination of the electrodes. A circuit designed by Malmberg[8] has been found very satisfactory for this purpose. The ion current of the gage i_p is amplified by a slightly modified RCA microammeter, WV-84A, the output of which is displayed on a

(3) J. B. Taylor and I. Langmuir, *Phys. Rev.*, **44**, 423 (1933).

(4) L. Apker, *Ind. Eng. Chem.*, **40**, 846 (1948).

(5) J. A. Becker, *Advances in Catalysis*, **7**, 135 (1955).

(6) D. G. Bills and F. G. Allen, *Rev. Sci. Instr.*, **26**, 654 (1955).

(7) D. Alpert, *J. Appl. Phys.*, **24**, 860 (1953).

(8) P. R. Malmberg, Westinghouse Res. Lab. Memo 60–94411, 9–16 (1953).
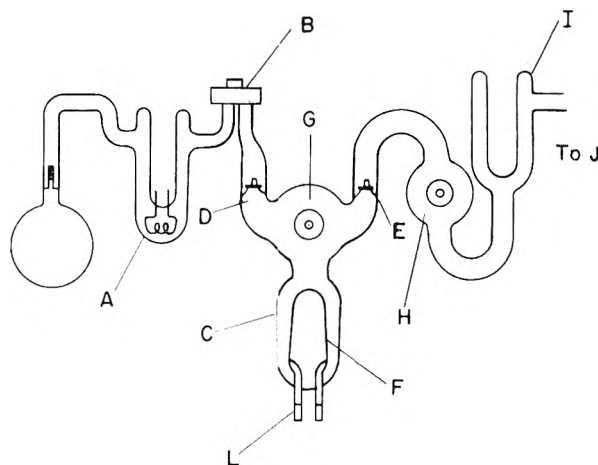
Fig. 1.—Vacuum system for flash filament determinations: A, trap; B, metal valve; C, flash filament cell; D, E, ground glass valves; F, flash filament; G, H, ionization gage; I, J, trap; L, leads.

Speedomax G recorder in which the response time for full scale deflection has been decreased below one second by altering the pen drive mechanism. For very low current measurements ($i_p < 10^{-9}$ amp.) the response time of the amplifier is too great to follow the pressure variation during a gas burst, and an Applied Physics Corporation vibrating reed electrometer has been used in its place.

The sample filament is heated by 60 cycle a.c., using a constant voltage source, which is capable of raising the filament temperature from ambient to 2200°K. within a second. By proper grounding of all equipment external to the cell, the need for an internal electrostatic shield has been obviated.

The Adsorption Sample.—A 10-mil, pre-war 218 tungsten wire, 12.15 cm. long was bent into a hair pin loop and welded to $^1/_8''$ molybdenum leads. The sample was aged in a separate vacuum system (pressure ~10^{-8} mm.) in which the filament was first maintained at 2750°K. for six hours, then at 3000°K. for 15 minutes, after which it was sealed into the cell. This treatment is designed not only to eliminate gases from the sample, but also to bring about recrystallization and thus establish a reproducible surface structure, which will not be affected by subsequent heating cycles.[5] Microscopic examination of the sample shows the wire to consist of small grains, most of which extend over the entire diameter and are between 0.5–1 mm. long; the heating schedule smooths but does not eliminate the drawing marks on the wire.

Vacuum Techniques.—To achieve suitable vacuum conditions, the line, up to the break-off seal leading to the gas bottle, is brought to 10^{-6} mm. with the diffusion pumps, leak checked, and then baked at 420° for 12 hr. or more with the valve B kept open by means of a clamp, and the ports D and E tipped to permit gas flow. To facilitate baking, the operating parts from trap A to I are mounted on a Marinite board to which an oven can be attached. Those parts not enveloped by the oven, the connections to the gas reservoir, to the trap J and to the mercury pumps, are separately baked out with heating tapes and small ovens. The trap J is cooled first, and is then immersed in liquid nitrogen. The temperature of the system is then lowered. After cooling and checking for tightness, the system is pumped down with the ion gages, and the metal parts of trap A, cell C and gage H are slowly outgassed by resistance heating, electron bombardment, and induction heating. One hour generally suffices to eliminate major contamination, and the whole system is then put through another bakeout cycle. Once a pressure $<10^{-9}$ mm. is achieved, the flash filament is carefully outgassed, and after another brief baking the system is pumped down to below 2×10^{-10} mm. The valve B is then shut, the trap A cooled in liquid nitrogen (keeping the filament hot) and nitrogen is admitted by opening the break-off with a magnetically operated hammer. After flushing the cell several times with nitrogen, the system is ready for operation.

(9) G. F. Smith, *Phys. Rev.*, **94**, 295 (1954).

Techniques of Measurement.—The pressure p_C in the flash filament cell at any instant is determined by the requirement

$$\frac{dG}{dt} = -\int \vec{j} \cdot \vec{d\tau} = \frac{V}{kT}\frac{dp_C}{dt} \qquad (1)$$

that the increase in the number of molecules G within the volume V of the cell be equal to the flux of gas, $\int \vec{j} \cdot \vec{d\tau}$ through the surface τ delimiting the cell interior. Here *all* molecular currents $\vec{j}$ must be included, and it is this requirement which defines the operating conditions of a cell, as is apparent on considering a measuring cycle. The course of the pressure during such a cycle is shown schematically in Fig. 2. A steady state pressure p is established with the filament hot, *i.e.*, $dG/dt = 0$; the filament heating is interrupted at time t_0 and adsorption is allowed to occur until an arbitrary time t_1. Here the sample is heated rapidly, and the gas accumulated on the filament is evolved, leading to the pressure burst at time t_2. Once the steady-state pressure is regained, a measuring cycle can again be started.
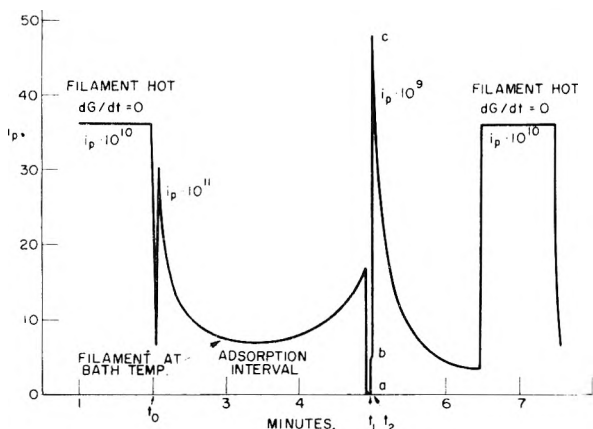
Fig. 2.—Typical measuring cycle. Trace of ion current i_p of gage in flash filament cell (operating at electron current $i_e = 5 \times 10^{-4}$ amp.) as a function of time.

If the cell has been properly prepared then, during the hot interval, the only source of gas will be the controlled supply entering the port D, the only sinks the port E, through which gas can escape to the pumps, and the ion gage, which, in monitoring the pressure continuously removes gas molecules by ionization or dissociation.[7] Under these ideal conditions, the flow of gas *into* the cell is given by $-\int \vec{j} \cdot \vec{d\lambda}$, and depends only upon the leak rate S_B of the valve B, and the pressure p_A of the gas reservoir. Since p_A is generally $>>10^{-3}$ mm., the condition $p_A >> p_C$ holds, and (neglecting a small contribution of port D)

$$-\int \vec{j} \cdot \vec{d\tau} = \frac{S_B}{kT_A}(p_A - p_C) = \mathfrak{F}_A \qquad (2)$$

Provided the reservoir temperature remains constant, the pressure in A will remain unaffected by the flow into the cell, which is thus equal to the constant $\mathfrak{F}_A$. The rate at which molecules stream through port E is given by

$$\int \vec{j} \cdot \vec{d\tau} = -\frac{S_E}{kT_C}(p_C - p_B) \qquad (3)$$

and the loss due to the pumping action of the gage by

$$\int_\tau^{\tau - (\tau_D + \tau_E)} \vec{j} \cdot \vec{d\tau} = \frac{-S_G}{kT_C}(p_C - p_0) \qquad (4)$$

where S_G is the pumping speed of the gage at the set electron current, and p_0 the ultimate pressure achievable, which again satisfies the condition $p_C >> p_0$. From the steady-state requirement, we find, if $p_C >> p_B$, that

$$\mathfrak{F}_A = -\frac{p_C}{kT_C}(S_E + S_G) \qquad (5)$$

When the heating of the filament is discontinued, then in addition to the two terms in (5), we must account for the

loss of molecules at the filament due to adsorption, and at the leads and walls, which during the heating of the filament are themselves warmed, and upon cooling can also act as sinks (to which we assign a strength S_W) or, under some conditions, as sources. The instantaneous pressure within the cell is now determined by

$$\frac{V}{kT_C}\frac{dp_C}{dt} = \mathfrak{F}_A + \frac{p_C}{kT_C}(S_E + S_G + S_W + S_F) \qquad (6)$$

and since $\mathfrak{F}_A$ is constant the introduction of two additional sinks will cause the pressure to drop to a lower value at which a new steady state, $dp_C/dt = 0$, will be maintained. The sink strengths S_W as well as S_F decrease as the amount of gas adsorbed increases, and we must expect thereafter a gradually increasing pressure. It should be noted that the representation of the net rates of adsorption by $(p_C/kT_C)S$ is straightforward only if adsorption occurs as a reaction of the first order with respect to gas, and evaporation from the surfaces is negligibly small.

Upon flashing the filament, the gas adsorbed on it during the cold interval is evolved at a rate $\mathfrak{F}_F$, and the pressure in the cell rises rapidly as a result of this additional source, with an over-all variation

$$\frac{V}{kT_C}\frac{dp_C}{dt} = \mathfrak{F}_A + \mathfrak{F}_F + \frac{p_C}{kT_C}(S_E + S_G + S_W + S_F) \qquad (7)$$

until all the gas is given off. The number of molecules desorbed from the filament during the flash is obtained by integration over the time during which desorption occurs, and is

$$n = \int_{t_1}^{t_2} \mathfrak{F}_F \, dt = \frac{V}{k}\int_{t_1}^{t_2}\frac{1}{T_C}\frac{dp_C}{dt} \, dt - \int_{t_1}^{t_2}\mathfrak{F}_A \, dt - \frac{1}{k}\int_{t_1}^{t_2}\frac{p_C}{T_C}(S_E + S_G + S_W + S_F) dt \qquad (8)$$

For sufficiently small $(t_2 - t_1)$, the number n is just equal to the number of molecules adsorbed during the cold interval between $t = t_0$ and $t = t_1$ and can therefore also be obtained from (6) by integrating over this interval, that is

$$n = \int_{t_0}^{t_1}\frac{S_F}{kT_C}p_C \, dt$$

The instantaneous net rate of adsorption on the filament likewise can be obtained in two different ways: either from (7) by solving for $(p_C/kT_C)S_F$ or alternatively, by constructing a curve of n *versus* t, using (8) and differentiating this with respect to time.

These procedures become significant only if the quantities entering (7), and (8) are experimentally accessible, however, and the experimental conditions must be designed to minimize the contributions of factors which cannot be readily accounted for quantitatively. In determining n from (8), it is apparent that considerable simplification results if the terms on the right for the number of molecules entering from the reservoir during the time interval $(t_2 - t_1)$ necessary for desorption and for the depletion of molecules within the cell due to the action of ports, ion gage, glass wall and filament are small compared with the gas evolved from the filament during the flash. This condition could be easily satisfied by keeping $\mathfrak{F}_A$, the rate of inflow, at a minimum and by reducing $(S_E + S_G)$ as well as $(t_2 - t_1)$; these requirements are, however, mutually contradictory if the kinetics of adsorption are of interest. The value of S_E can be made as small as that of S_B ($\sim 10^{-11}$ cc./sec.) by resorting to an improved valve, S_G can be minimized by operating the ionization gage at a low electron current i_e, $\mathfrak{F}_A$ can be decreased by adjusting valve B, and the time interval $(t_2 - t_1)$ can be cut down by increasing the power input to the filament. However, to elucidate the kinetics, it is necessary to know not only n, but also $1/p_C \, dn/dt$. If $\mathfrak{F}_A$ is greatly reduced, not only does the time interval $(t_1 - t_0)$ necessary to achieve a given coverage become excessively long, but it becomes more difficult to measure the instantaneous pressure, which will also be lowered. Similarly, reduction of S_G results in a proportionate lowering of the ion current, and therefore a decrease in the signal to noise ratio. A decrease in S_E, on the other hand, will prolong the time necessary for establishment of a steady state and therefore will enhance the contribution of S_W and S_F. An increase in the power input to the filament, to decrease the desorption time, may result in excessive heating of the wall, etc.

The conditions under which measurements have generally been carried out have been adjusted to make the sum of the last two terms of (8) less than 5% of the term accounting for the pressure peak, and corrections have been calculated using values for $(S_E + S_G + S_W)$ obtained from the experimentally observed decrease in the pressure following a gas burst. The instantaneous temperature of the gas evolved upon heating the filament will of course be greater than that of the cell walls. However, the cell is designed so that gas from the filament must, before entering the gage, collide with the walls, which are maintained at a constant temperature by an oil thermostat; this of course limits operations to wall temperatures at which condensation of gas evolved from the filament is not appreciable. Under these conditions, T_C can be considered constant, and (8) can be approximated by

$$n = \frac{V\Delta p_C}{\kappa T_C} \qquad (9)$$

These general considerations also dictate the dimensions of the cell and sample used. To increase the response upon flashing the filament, the ratio of the filament area to the cell volume should be increased. This is limited by the size of the electrode structures and the need for large passageways between sample tube and gage to prevent pressure gradients. Increasing the size of the filament not only may result in mechanical instability but also brings with it a reduced cooling rate and a lower and more difficultly measurable steady-state pressure. Also adsorption immediately upon shutting off the heating current does not take place at the bath temperature; measurements become significant only when the filament reaches its steady-state temperature and the early stages of adsorption may thus become inaccessible.

It should be apparent that the same factors enter the determination of n, and $(1/p_C)(dn/dt)$, by the alternative route using (7). However, whereas during the flash the correction factors $(S_E + S_G + S_W)$ can be kept at a readily determined minimum value, the adsorption on the walls and depletion through gage and port during the interval $t_1 - t_0$ enter more significantly and can lead to appreciable errors in assigning the total amount of adsorption on the filament. Corrections necessitated by adsorption on the walls in particular can only be evaluated indirectly, and determination of n and dn/dt from (7), though quite rapid, has been used only to check qualitatively the results obtained by direct flashing of the filament.

Operating at an emission current i_e of 5×10^{-4} amp., with the exit port E completely closed, $(S_E + S_G + S_W)$ for our system was determined as 28 cc./sec. The rate of gas inflow was varied between 7×10^{10} to 2×10^{12} molecules/sec. During the interval necessary to establish a steady-state pressure with the filament hot, the filament leads have been found to rise 85° above the bath temperature, but return to within 5° of the latter 1.5 minutes after shutting off the heating current. The lag in the temperature rise of the leads upon heating the filament is sufficient to prevent evolution of gas from the leads during the one second period necessary to measure desorption from the filament; the temperature rise during this interval is less than 10°. The large diameter of the leads necessary to accomplish this, however, also results in a cooling of the filament near the point of juncture, sufficient to prevent removal of gases from this section. Assuming that chemisorbed material is not removed below 1400°K., we can correct the total length,[10] to give an effective filament length of 11.63 cm. and a geometric surface area of 0.92 cm.², which we have employed in calculating the amount of adsorption per unit area. This section of the filament, permanently covered with adsorbed gas, also acts as a barrier to the transport of gas to the clean sections through surface diffusion of chemisorbed material from the leads. The lifetime of physically adsorbed gases at room temperature is so short that only $\sim 10^3$ atom sites can be visited before evaporation, and therefore the bulky leads cannot act in this fashion as a significant gas source.

The flash filament method depends, in essence, upon the rapid measurement of gas pressures in a flow system. Just as a McLeod gage cannot be applied to the study of condensable gases, so the ionization gage cannot be used,

without special precautions, in the study of gases that are dissociated at hot filaments. This, of course, circumscribes the technique described here, as will appear in detail in a later report.

Experimental Results

The State of Binding of Nitrogen.—The structure of the gas burst evolved from the tungsten filament upon heating it after an interval of adsorption at room temperature[11] is shown in Fig. 3,
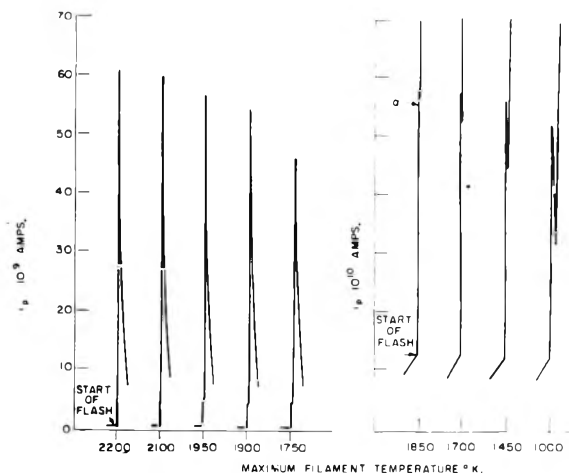
Fig. 3.—Dependence of pressure peak on filament temperature at constant $(t_1 - t_0)$. Trace of ion current for gage operating at $i_e = 5 \times 10^{-4}$ amp.: (a) ion current amplification on recorder 100×10^{-4} amp. full scale; (b) ion current amplification 100×10^{-10} amp. full scale.

for a series of progressively lower filament currents (*i.e.*, lower steady-state temperatures). Above 2100°K., the peak height is insensitive to a further temperature increase—all the gas has been desorbed from the filament; below this temperature, however, the peak height decreases as the maximum temperature is decreased. With a heating current small enough to raise the temperature to only 1700°K., and therefore also with a smaller rate of heating, a second peak at the foot of the larger one can be clearly resolved and by resorting to a higher amplification of the ion current, this can be enlarged suitably for measurement. The height of this (α) peak, as appears from 3b, is fairly insensitive to the power input to the filament; the same value is found for the α peak for maximum filament temperatures from 1400–1850°K. From a qualitative estimate of the heating curve of the sample an upper limit of 800°K. can be set for the temperature at which the material constituting the α peak is completely desorbed.

That the low temperature α-peak is real, and not due to possible transients in the measuring devices, is demonstrated by the recorder traces in Fig 4a; here the burst structure for a fixed time $(t_1 - t_0)$ is compared with that obtained after briefly flashing the filament to a low temperature (<800°K.). After such a preliminary heating, the α-peak has been significantly diminished, yet the larger, high temperature β-peak has not been affected. During the evolution of the α-peak the temperature of the lead–filament junction rises less than 2°, and such an indirect heating can therefore

(10) I. Langmuir, S. MacLane and K. B. Blodgett, *Phys. Rev.*, **35**, 478 (1930).

(11) For a preliminary account of these effects see (a) G. Ehrlich, *J. Chem. Phys.*, **23**, 1543 (1955); (b) **24**, 482 (1956).
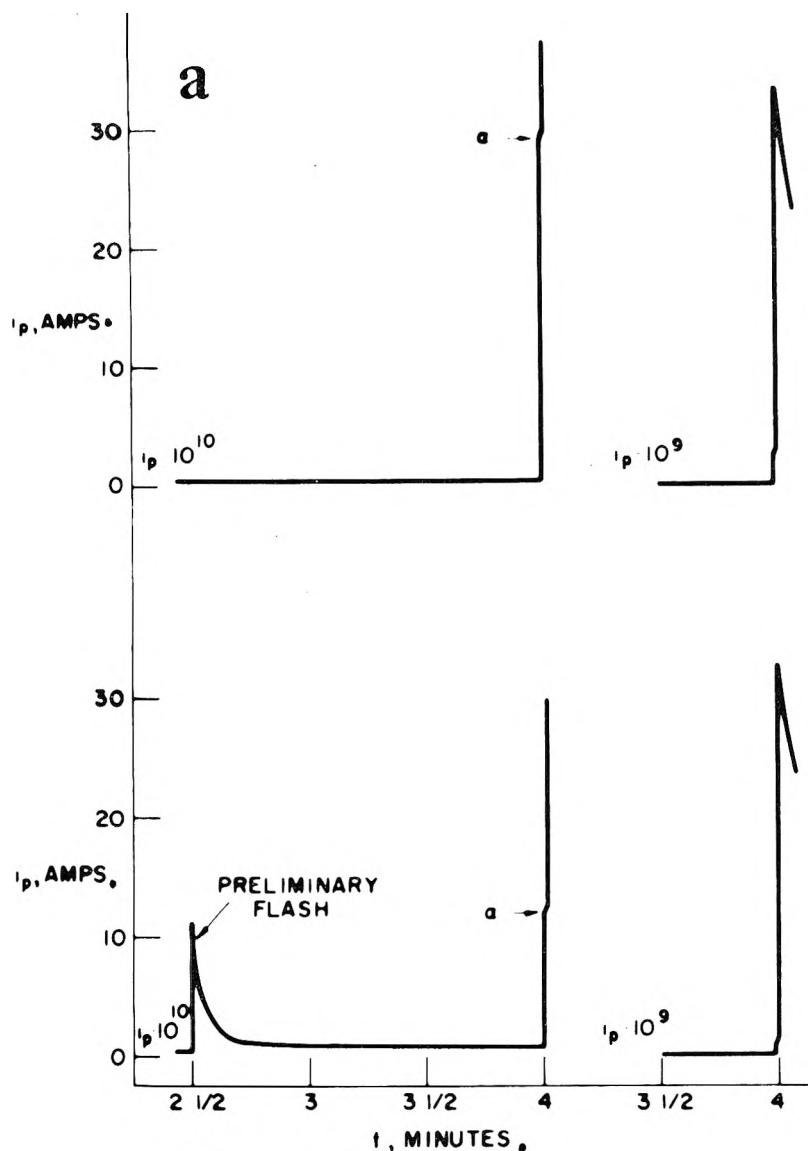
Fig. 4a.

also be eliminated as a source of this effect. The presence of an α-peak has been observed on three different filaments in different vacuum systems, using several nitrogen sources; it is found as well when a tungsten filament is mounted on leads of nickel, on which no adsorption of nitrogen has been observed around room temperature. The interaction of nitrogen with the hot filament of the ion gage, or the production of ions, is not responsible for the peak structure either—the same effects are found if during the interval of adsorption, the operation of the gage is discontinued. Only the α- and β-peak contribute significantly to the number of adsorbed molecules at room temperature, and higher, as is evident from the shape of the gas bursts observed after adsorption at 196°K. Even at this low temperature, no additional peaks can be resolved—only at 80°K. does a third peak, γ, become important.[11b]

In ascertaining the course of adsorption, the α- and β-peaks are determined separately because of the limitations of the ion current detecting system;

to measure the α-peak, the power input to the filament has to be lowered to achieve a time interval of 0.7 sec. between the start of heating and the evolution of β, and the β-peak is therefore partly lost. The amount of gas in the β-peak is obtained as the difference between the total peak height, as found with a heating current sufficient to raise the filament temperature above 2200°K., and that of α; i.e., it corresponds to bc in Fig. 2. That the detecting system does not introduce an error $>10\%$ in the determination of α has been demonstrated both by heating the flash filament more slowly and by resorting to a detector with a rise-time $<10^{-3}$ sec. A sample plot for n_α, n_β and $k_1 p$, the impingement rate, obtained in this fashion for a filament maintained at 298°K. during the period of adsorption is given in Fig. 5. The relationship between the material in α and β is most clearly shown in Fig. 6, however. Here the number of α molecules recorded for a given number of β is plotted for temperatures from 196–334°K.; at any given temperature, data for only a single run are included. The initial steady-state pressures for these differ by a factor of two, however, and the explicit dependence of the increasing portion of these curves upon pressure, if any, is within the limit of error of the measurements. For small values of n_β ($<50 \times 10^{12}$ molecules/cm.²) a single curve fits all data points. The higher the temperature of adsorption, however, the lower the value of n_β at which a maximum in n_α is recorded and beyond which the population of the latter decreases. The interpretation of the two peaks, α and β, in terms of two different states of adsorption—one stable only for temperatures below 800°K., the other one up to 2000°K.—is further supported by the results of kinetic measurements reported below.

The Rate of Adsorption.—For a first-order reaction between gas and surface, the rate of adsorption dn/dt is related to the pressure through the condition of mass balance

$$dn/dt = k_1 ps - D \qquad (10)$$

$k_1 p$ gives the rate of impingement of molecules on unit area, s the fraction of these that are adsorbed, and D the rate at which evaporation from the surface occurs. Above $T = 190°K.$ only α- and β-species appear in significant numbers, and we shall consider their rate of formation independently,
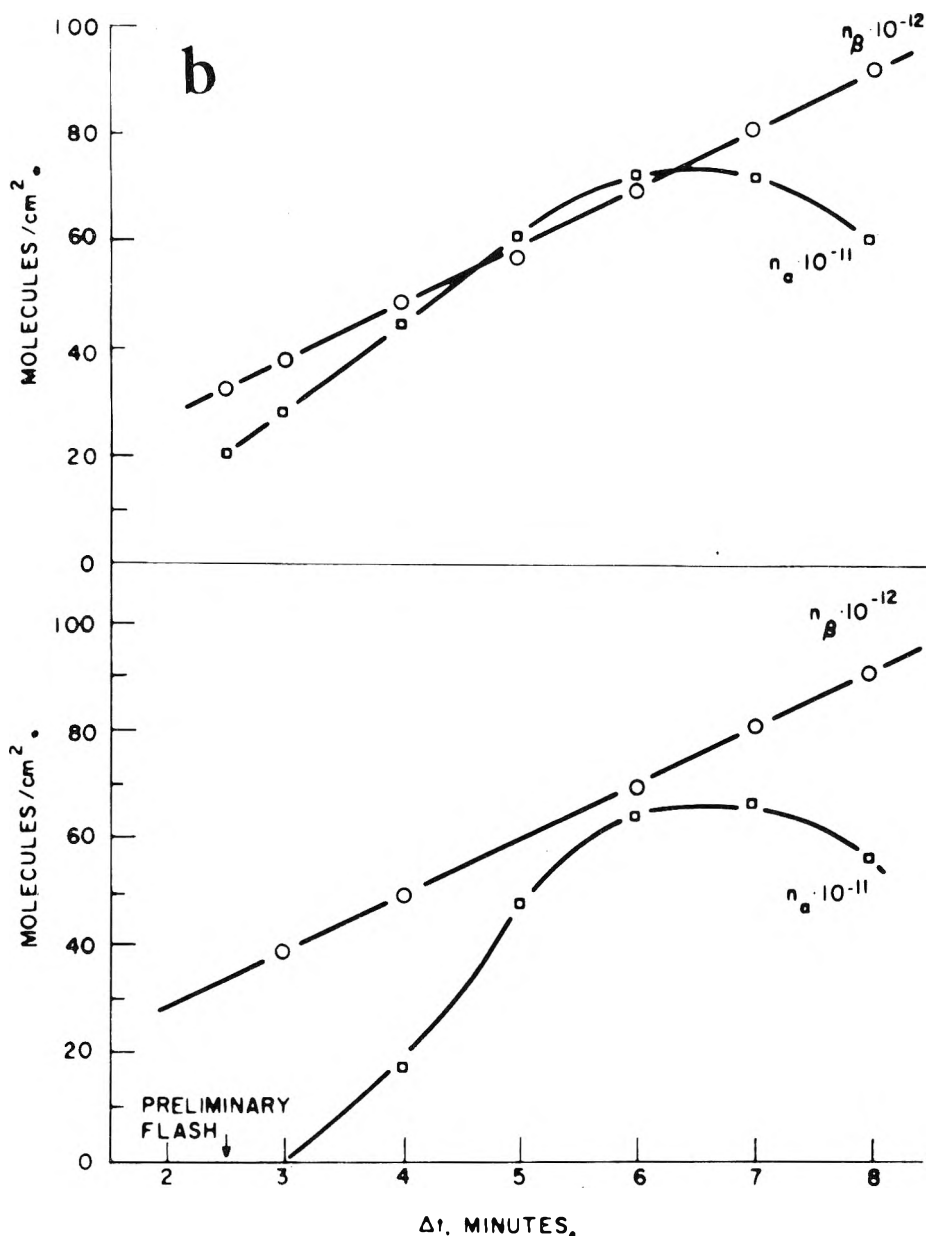
Fig. 4.—Effect of preliminary low temperature flash upon α- and β-pressure peaks. Ion gage electron current $= 5 \times 10^{-4}$ amp., $T = 336°$K.: (a) trace of ion current recorder; (b) adsorption in state α and β at 336°K. as a function of the time of adsorption.

applying a relation of the form of (10) to the analysis. By the procedures outlined above, we obtain for any given adsorption temperature a grid plot,[2] in which the rate of adsorption in the β-state, dn_β/dt, is graphed against the impingement rate $k_1 p$ for different constant values of n_β, the number of molecules adsorbed. The slope at constant n gives the sticking coefficient s_β, the intercept the evaporation rate D_β. Under the conditions of our experiments (maximum adsorption temperature 373°K., maximum cover $\sim 2 \times 10^{14}$ molecules/cm.²) the evaporation rate, as shown in the previous section, is negligibly small; the dependence of the sticking coefficient for β-species upon the temperature as well as the amount adsorbed so obtained is given by the plots in Fig. 7.

Qualitatively, these curves are very similar to those found for the total rate of adsorption by Becker and Hartman.[2] At the lowest temperatures, and at low coverage, the value of s_β is constant on increasing n_β; it decreases only when an appreciable portion of the surface has been filled. At the higher temperatures, the sticking coefficient not only has a lower value, it also decreases at a smaller cover n_β. It should be noted that our results differ in two significant ways, however—the absolute values of the sticking coefficients are lower than found by Becker and Hartman, as is the coverage (θ_c) at which the sticking coefficient decreases. At 298°K. we find a sticking coefficient s_β for a sparsely covered tungsten surface of ~ 0.1, compared with 0.55 previously reported; the sticking coefficient s_β decreases for $n_\beta > 50 \times 10^{12}$ molecules/cm.², whereas the previous investigators found it constant till 125×10^{12} molecules/cm.² had been adsorbed.
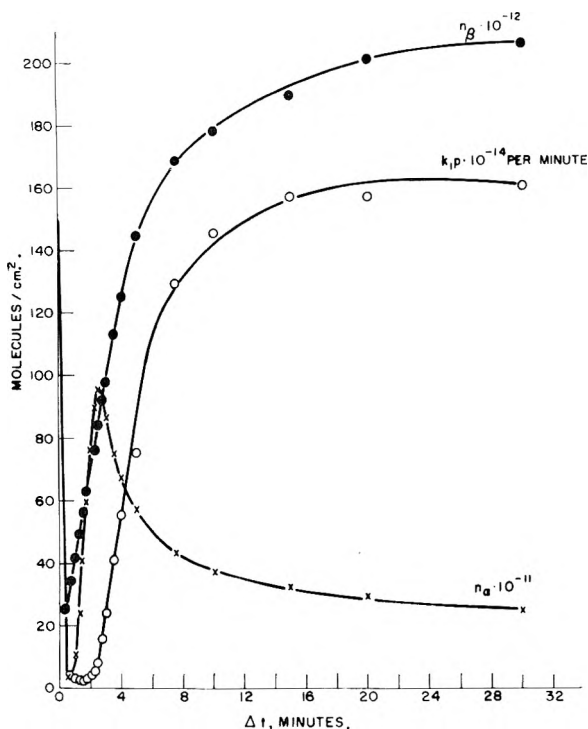
Fig. 5.—Adsorption of nitrogen on tungsten filament at 298°K.; n_β = number of molecules adsorbed in β state per cm.^{2}; n_α = number of molecules adsorbed in α state per cm.^{2}; k_1p = number of molecules impinging per cm.^{2} per minute.
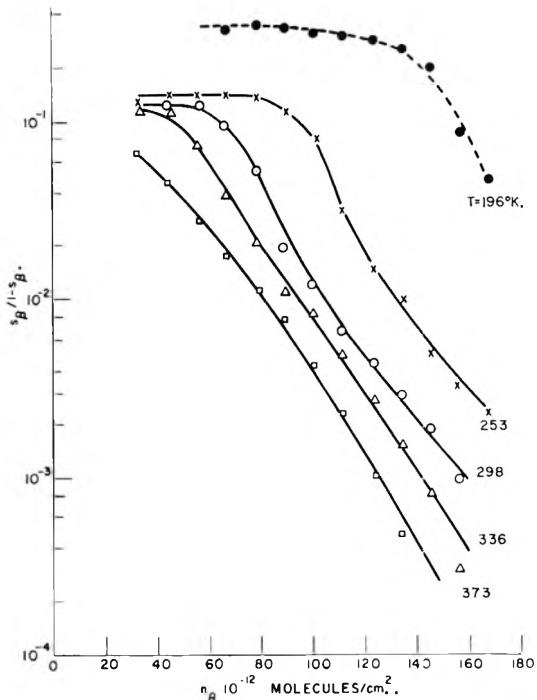
Fig. 7.—The dependence of sticking coefficient for nitrogen in state β upon coverage (n_β) and temperature.
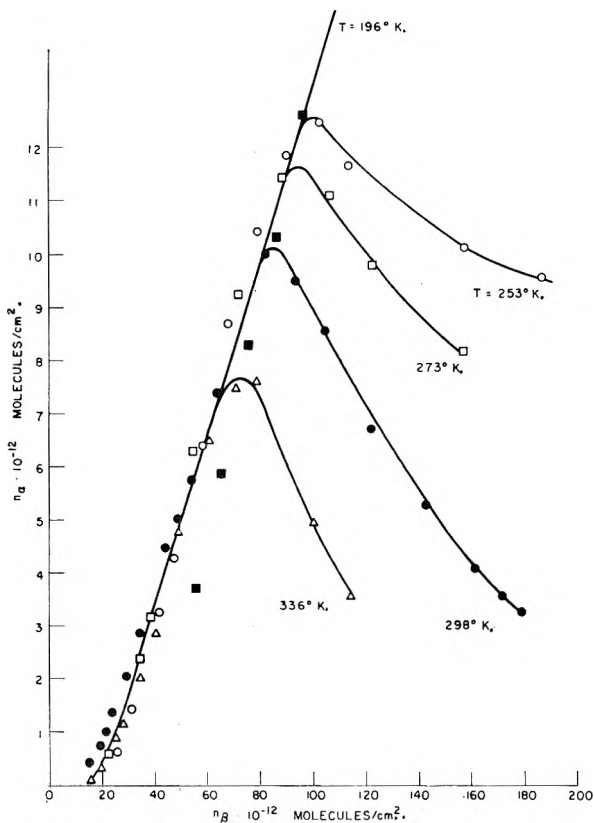
Fig. 6.—Dependence of adsorption in state α upon population of state β.

Fig. 8.—Adsorption of nitrogen in states β and γ on tungsten, sample at 80°K.

For the lowest temperature examined, T = 80°K., adsorption cannot be followed by the usual

methods, inasmuch as immersion of the cell in liquid nitrogen results in condensation of gas evolved from the flash filament and thus prevents
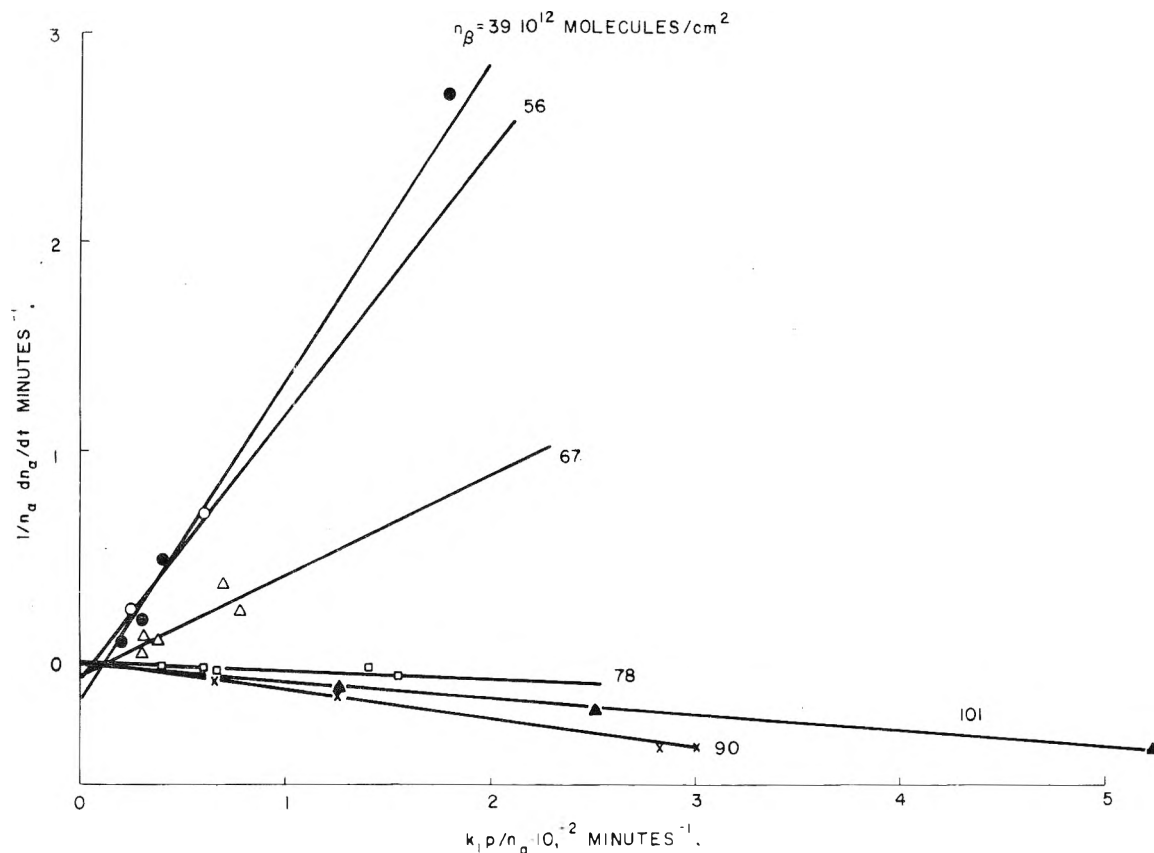
Fig. 9.—The rate of adsorption of nitrogen in state α on tungsten at $T = 336°$K.

detection.[12] Measurements carried out with a stream of gas at 310°K., impinging upon the filament kept at 80°K., are recorded in Fig. 8. We have refrained from evaluating a sticking coefficient, inasmuch as experimental observations are still preliminary and inasmuch as under the conditions of the experiment—a hot gas impinging upon a cold surface—the condensation coefficient of nitrogen onto tungsten may well be less than unity. The initial rate of formation of the β-state appears at least twice as rapid under these conditions as at 300°K., however.

The rate behavior of r_α can also be recorded on a grid graph similar to that used to ascertain s_β. For the adsorption step, we can write $dn_\alpha/dt = pk_1s_\alpha$, where $s_\alpha = s_\alpha(n_\alpha, n_\beta)$; inasmuch as our data indicate an essentially constant relation between n_α and n_β, we are justified in writing $s_\alpha = s_\alpha(n_\beta)$. Our results also indicate, however, that for n_α we must consider the depletion step, and for this we propose a trial term of the form $n_\alpha D_\alpha$, in which the specific rate $D_\alpha = D_\alpha(n_\beta)$. If this is indeed warranted, then a plot of $(1/n_\alpha \ dn_\alpha/dt)_{n_\beta=\text{const.}}$ against k_1p/n_α should yield a straight line of slope s_α and intercept D_α. The data for the rate of formation of n_α at 336°K. is shown in Fig. 9, and within the limits of error of the data points a straight line graph can be obtained. For $n_\beta > 70 \times 10^{12}$ molecules/cm.², however, we find $s_\alpha < 0$, indicating that our assumption concerning the rate

of depletion of n_α is unjustified, and that D_α depends upon the rate of impingement of gas or equivalently, upon dn_β/dt. Such a relation is apparent from Fig. 6 as well—the decrease in n_α with increasing n_β at constant T, is such as to indicate dn_α/dn_β is constant for varying pressures.

The double flash experiments already referred to provide additional information concerning the rate of growth of the α-peak. Figure 4b gives the variation of n_α and n_β with time as observed in an ordinary measuring cycle, and also the effect of subjecting the filament to a preliminary flash at an intermediate time. The height of the β-peak is not significantly affected by such a preliminary flash; however, the α-peak $^1/_2$ minute after the preliminary flash, is still absent; it then approaches, but does not achieve, the same height usually found, but with a rate approximately twice as high. In other words, the α-species are adsorbed at a finite rate, small compared with the rate of impingement or dn_β/dt, and this rate depends upon the number of α species already present. A comparison of the rate of formation of α and β also establishes that the former cannot be an impurity effect. At 196°K., the ratio dn_α/dn_β is found to be 0.13, and $s_\beta \sim 0.25$; this implies that for the α-peak to be due to an impurity, it would have to be present in the gas admitted at a minimum concentration of 3% (assuming a sticking coefficient of unity)—a hundred-fold greater than the impurity content given by mass spectrometric analysis.

(12) Measurements on germanium which may be suspect because they have been carried out under these conditions are reported by J. T. Law, This Journal, 59, 543 (1955).

The Adsorption of Nitrogen on Tungsten

The Mechanism of the Formation of State β.—
It has been shown in a preceding paper[1] that a sticking coefficient significantly less than unity yet independent of the amount chemisorbed (n_β) is evidence for a reaction limited by the rate of diffusion of physically adsorbed gas over the surface, and occurring at patches of unusual reactivity, which have been tentatively identified with lattice steps present on the surface. For a temperature at which x_s, the root mean square distance between the point of arrival and departure of a physically adsorbed molecule, is small compared with the separation of the active (A) patches, the sticking coefficient s_β, in the region where it is independent of the amount chemisorbed, reduces to

$$s_\beta = A_A \left(1 + \frac{x_s}{a}\right) \tag{11}$$

here A_A gives the fraction of the total surface area occupied by active A patches of characteristic dimension a. The variation of the sticking coefficient with temperature is dictated by $\Delta H_{-1}^* - \Delta H_s^*$, the difference between the heat of activation for desorption and surface diffusion of the precursor, and is given by

$$\frac{\partial \ln s_\beta}{\partial \frac{1}{kT}} = \frac{\Delta H_{-1}^* - \Delta H_s^*}{2} \left(1 - \frac{a}{x_s} \cdots\right) \tag{12}$$

At higher coverages, the more complete expression

$$s_\beta = A_A \left(1 + \frac{x_s}{a}\right) \frac{k_2}{k_2 + k_{-1A} + 4dx_s^{-1}\frac{k_{AB}}{a}} \tag{13}$$

must be resorted to, since the rate constant of chemisorption k_2, which decreases with the amount chemisorbed, may then no longer dominate over the rate constant for evaporation k_{-1A} and surface diffusion k_{AB} of the physically adsorbed precursor and the sticking coefficient will become dependent upon the amount of material chemisorbed. For the high temperature range in which $a > x_s$, the rate is given by

$$s_\beta = A_A \frac{k_2}{k_2 + k_{-1A} + \frac{k_{AB}}{a}\frac{4d}{x_s + 4d}} \tag{14}$$

d being the interatomic distance on the surface, and the dependence upon temperature is found to be

$$\frac{\partial \ln s_\beta}{\partial \frac{1}{kT}} = \Delta H_{-1}^* - \Delta H_2^* \tag{15}$$

where ΔH_{-1}^* is the heat of activation for desorption of the precursor, and ΔH_2^* that for transfer from the precursor to the chemisorbed state.

This kinetic scheme, however, does not account for the presence of molecules in an intermediate state of binding, such as the α-state which has been demonstrated here. The data presented above suffice to show that our previous considerations are *not* affected by this. If nitrogen in state α were to participate as an intermediate in the formation of β, we expect that depletion of the population, n_α, in this state would diminish the rate of formation of β. This, however, is not indicated by the results in Fig. 4b—the rate of

formation of β is not affected, within the limit of error, by the removal of the α-species by a low temperature flash, although this permanently lowers the concentration in this state. Also, regardless of the mechanism by which β is formed, the ratio of the rate of formation of β, dn_β/dt, to the concentration of precursor, n_1, at a fixed value of n_β must be constant and independent of the pressure. This condition is *not* satisfied by the α-material. As appears from Fig. 6, the concentration n_α is initially independent of pressure and is determined by n_β only, the rate dn_β/dt, on the other hand, varies directly with pressure. The presence of molecules in a binding state of low energy is demanded by the mechanism proposed; that species of this kind *are* present is indicated by the fine structure of the gas burst, evolved from a filament on which adsorption has occurred at $80°K$.[11b] The additional γ-peak, which is obtained only at this low temperature, varies in size directly with the pressure, and thus *may* constitute the precursor.

To account for the adsorption of nitrogen in the α-state, we need add only a term k_α, the rate constant for the formation of α, in the denominator of (13) and (14), provided we remain in a region where evaporation is negligible. As mentioned above, the rate of chemisorption found for the β-state is considerably less than that reported previously, as is the coverage (θ_C) at which the sticking coefficient becomes dependent upon the amount of material on the surface. Even at as low a temperature as $336°K$. the sticking coefficient depends upon cover in the limit $\theta \rightarrow 0$. In the temperature range over which s_β is initially constant, and for which the rate is diffusion limited, the activation term $\Delta H_{-1}^* - \Delta H_s^*$ is found to be ~ 2.5 kcal./mole, in agreement with the value deduced from Becker's data. The lower value of the sticking coefficient, and of θ_C, as well as of the temperature at which the rate appears to become reaction controlled, can all be reconciled by a lower value of A_A, the fraction of the surface occupied by reactive strips. We must conclude that on a polycrystalline filament the active strips are spread farther apart than on a rolled tungsten ribbon of coarse crystals, as used by Becker and Hartman. Such treatment tends to orient the crystals so that (100) is parallel to the plane of rolling, and [110] is parallel to the direction of rolling[13]; even severe heat treatment, sufficient to cause appreciable evaporation, does not eliminate this texture.[14] Unfortunately, we cannot conclude from this that crystal planes with an orientation close to (100) are particularly active in adsorption, inasmuch as we have no information on the relative density of steps on the samples used. The interesting point that *is* raised by the interpretation of the kinetics as occurring at active regions is the extraordinary reactivity that must be associated with these. A sticking coefficient independent of cover depends on the fact that a molecule which encounters an active region will have a negligibly small probability of being evaporated. As previously pointed out, the dimen-

(13) W. G. Burgers and J. J. A. Van Amstel, *Physica*, **3**, 1064 (1936).
(14) L. Apker, private communication.

sions of the active region are such that their association with lattice steps is a tempting one. For these, there would be significant spilling over of conduction electrons into the troughs, which may contribute to the ease with which chemisorption (and as will be shown later, disruption of the bond between nitrogen atoms) occurs; another effect which may contribute, however, is the stronger binding due to dispersion forces which can be expected at a lattice step, and which would prolong the time interval during which reaction can occur.

The continuing adsorption of nitrogen, once the active (step) sites have been filled, has been associated with the presence of other sites of lower reactivity on the surface. In Fig. 8, the course of adsorption on a filament cooled with liquid nitrogen ($T = 80°K.$) is recorded. Significantly the adsorption in the β-state ceases at this low temperature once n_β reaches a value of 100×10^{12} molecules/cm.^{2}, in contrast with the continued growth of the population of this level at higher temperatures. From the temperature range over which the γ peak can be isolated, we infer that it is due to gas held to the surface by dispersion forces; adsorption in the γ-state, at 80°K., continues until it is more than twice the size of β. This, of course, is the low temperature behavior that *would* be expected for sites with an activation energy such that conversion from the physically adsorbed to the chemisorbed state is slow, yet for which the activation energy for desorption from the physically adsorbed state is still higher, so that gas is irreversibly bound in this state.[15] The rapid initial formation of β indicates a lower activation energy for the active sites.

Measurement of chemisorption at these temperatures may elucidate the variation in reactivity of different gases found for the same surface. For example, the sticking coefficient of carbon monoxide on a sparsely covered tungsten filament at 300°K. is three times that of nitrogen and remains constant at this high value up to $n_\beta \sim 240 \times 10^{12}$ molecules/cm.^{2}.[16] This difference *may* be due to a dependence of the rate of CO adsorption upon crystallographic surface features different from those important for N$_2$, and should be revealed, in a higher value of A_A, by such measurements.

The Nature of Nitrogen in State α.—In order to interpret properly the experimental results on the adsorption state of low binding energy which we have designated as α, we must consider the measurements which indicate its presence. These consist of observations of the rise in the pressure in the cell upon raising the filament to $T < 800°K.$, and indicate those entities that are desorbed in this temperature range. If there are species present on the surface in binding levels of low energy, the possibility exists that, upon increasing the temperature, these may be transferred to more stable levels, and would therefore eventually be desorbed in a higher temperature range, together with molecules that were initially adsorbed in a tightly bound state. The absence of gas evolution at a low temperature thus does not constitute evidence for the absence of levels of low binding energy if gas is found that can be desorbed at a higher temperature. Although for nitrogen the observation of gas desorption proves the existence of states of low binding energy, their occupation can be inferred only if it can be shown that transfer to a different state has not occurred during the flash.

As is apparent in Fig. 6, the quantity of nitrogen adsorbed in the α-state is defined, for low coverages at least, by the amount of material in the β-state; for approximately nine molecules in β there appears a single one in α. From this we can draw two conclusions. First, over the range of temperatures and coverages for which this holds, the α-levels are not depopulated by conversion to β, or by evaporation. Loss by conversion during a flash would have to occur above this temperature range, and here it would have to compete with evaporation. The α-pressure peak as shown in Fig. 3b is not sensitive to the power input, suggesting that the amount lost is not appreciable. Second, the material in state α is irreversibly adsorbed, the population being independent of temperature or pressure. The constant relation between the population of state α and β can be accounted for if the rates of formation of both species are determined by the same limiting step—such as diffusion to active sites—and if the number of α and β sites differ. The same relation could be obtained if an α-site were formed by the adsorption of nitrogen in state β. We can distinguish between these two possibilities by comparing the dependence of the rate of formation of β upon n_β, as shown in Fig. 7, with that of n_α upon n_β, in Fig. 6. The value of n_α reaches a maximum at a value of n_β somewhat larger than that for which the sticking coefficient becomes markedly dependent upon the cover. Inasmuch as the decrease in the sticking coefficient has been associated with a change from a diffusion controlled to a reaction controlled rate,[1] the maintenance of a linear relation between α and β when the mechanism of formation of the latter has undergone a change, eliminates the possibility of a common controlling step. A scheme whereby an α site is formed through the adsorption of β is not subject to such a difficulty.

The formation of such sites has been considered by Roberts,[17] who pointed out that the adsorption of diatomic molecules, without lateral interaction, in an immobile layer corresponded to a random array of pairs of sites and as such would leave a number of single sites unoccupied. These could not accommodate both atoms of a molecule, but could still hold the molecule, although more weakly; it is tempting to speculate that this could be due to the presence of strongly bound β-species, which induce surface states[18] that can form one electron bonds with the molecule, as envisioned by Pollard.[19] Here we shall not concern ourselves, however, with the nature of the bond formed, but will con-

(15) G. Ehrlich, THIS JOURNAL, **59**, 473 (1955).

(16) G. Ehrlich, to be published.

(17) J. K. Roberts and A. R. Miller, *Proc. Cambridge Phil. Soc.*, **35**, 293 (1939).

(18) C. A. Coulson and G. R. Baldock, *Disc. Faraday Soc.*, **8**, 27 (1950).

(19) W. G. Pollard, *Phys. Rev.*, **56**, 324 (1939).

centrate on the phenomenology of the α-state. Underlying Roberts' model are the equivalent assumptions that a diatomic molecule is adsorbed, without losing its molecular identity, through interactions between two adjacent lattice sites and the atoms, and that the adsorbed molecule is immobile, or, that the adsorption is accompanied by rupture of the molecular bond and that the adatoms so formed in adjacent lattice sites are immobile. For adsorption of the latter kind (which will be shown to correspond to the system nitrogen on tungsten) on a uniform crystal surface, and assuming no lateral interactions between adatoms, the fraction of the total number of sites which are surrounded by occupied sites, and thus could conceivably constitute an α-site, has been given as $(1 - \theta)/(3\theta/4 - \theta)^4$. For $\theta = 1/2$, this would predict that for every molecule in state α there would be ~7 in β, close to the experimentally determined value. However, it also follows that initially the number of α-species would be negligible, but would increase very rapidly at higher values of n_β. As appears from Fig. 6, an essentially linear relation between α and β holds even at the smallest values of n_β experimentally accessible, and this explanation does not appear correct. However, on a nonuniform surface there are other opportunities for forming gaps inaccessible to a diatomic molecule as a whole, beyond those considered by Roberts. Thus, *for example*, the regions on which adsorption occurs most rapidly have been associated with lattice steps, and these, above absolute zero, must be kinked.[20] For tungsten at the maximum flash temperature (~2200°K.) the kinks are separated from one another by ~15 atom distances. An unoccupied site between a kink and a filled site could, conceivably, form a well for an α-nitrogen. Moreover, if chemisorption in the β-state occurs solely on a step, the number of nearest neighbors, and therefore the dependence upon θ, would be reduced, so that the relation between α and β could in this way approach that experimentally observed.

The view that α-nitrogen is bound on sites that are created by the adsorption of nitrogen in the β-state offers a ready explanation for the possibility of isolating an α-peak in the pressure burst at all. The relatively low temperature ($T < 800°K.$) at which α is completely evolved indicates that it is thermodynamically less stable than the β-state. To account for the existence of α at all we must therefore assume a barrier to the conversion to β. Physically, this is most readily visualized if the α-sites are surrounded by sites on which β cannot be formed. To bring nitrogen from an α to a β-site, an activation energy equal at least to that for evaporation out of α minus that for evaporation from the physically adsorbed state will have to be gained; that is, the barrier to surface diffusion away from such a site does not differ significantly from that for evaporation and these processes will be competitive. This is in contrast to the diffusion between equivalent sites for physically adsorbed molecules,[21] or between chemisorbed adatoms.[22]

(20) W. K. Burton, V. Cabrera and F. C. Frank, *Phil. Trans. Roy. Soc.*, **A243**, 299 (1951).

(21) F. C. Tompkins, *Trans. Faraday Soc.*, **46**, 569 (1950).

(22) R. Gomer and R. Wortman, *J. Chem. Phys.*, **23**, 1741 (1955).

in which the barrier amounts to a small fraction (less than $1/3$) of that to evaporation.

It appears from Fig. 9 that the process whereby the concentration of α is depleted at higher values of n_β does not explicitly depend upon n_α. The rate of adsorption in the β-state appears as the rate determining step, which is consistent with the picture of irreversible binding of α during the initial stages of chemisorption. The activation energy for the depletion step, deduced from the temperature dependence, is ~2.5 kcal./mole. Although molecular binding in the α-state is the most appealing and offers a consistent interpretation of all the facts known at present, the data do not so far permit a proof of this, or deduction of the driving force for the depletion of the α-state. Both matters will be considered in a future report on the details of the desorption steps.

The Nature of Nitrogen in State β.—Although there is indirect evidence, such as the evolution of atoms from a hot tungsten filament in a gas atmosphere and the occurrence of exchange reactions on surfaces, that upon chemisorption homonuclear diatomic molecules may lose their molecular identity and be adsorbed as atoms, investigations of the kinetics of the desorption step, which should establish this, have been very limited. The work of Becker and Hartman appears to be the first and only study of the desorption of molecules in which the rate has actually been followed directly, through measurement of the quantity of gas adsorbed. In this connection, the isolation of a state of adsorption of low binding energy (the α state) is of interest since it permits a *preliminary* attempt to interpret their rate measurements.

In Fig. 10a the rate of evaporation of nitrogen on tungsten (at constant coverage) has been plotted on a log scale against reciprocal absolute temperature. It is apparent that for $T > 900°K.$ the data at low cover can be adequately approximated by a straight line, but that this *fails* to account for the evaporation rate at lower temperatures. Such a behavior is to be expected from our own work which indicates the presence of adsorbed material in a distinct state of weak binding (α), and qualitatively, the results of Becker and Hartman for evaporation below $T = 1100°K.$ are in agreement with ours concerning the temperature range and onset of evaporation of α. Their data for higher temperatures are presumably not in serious error due to failure to isolate the α state, since in this range it is unstable and the population in it negligible; the activation energy for the desorption of nitrogen in this range ($1100° < T < 1500°K.$) i.e., for the β-state, obtained from the slope of the plot in Fig. 10a, is 71 kcal./mole. This value appears to describe the data for those coverages for which sufficient data are given, i.e., up to $n_\beta = 172 \times 10^{12}$ molecules/cm.²; for the latter, however, the fit is much poorer. The variation of the rate with the amount chemisorbed is more uncertain, both because of the difficulties in making such measurements and because of the evolution of α. At high enough T, not only should the rate of desorption of β outweigh that of α, so that the error incurred by failure to separate the two

should be diminished, but the rate also becomes more readily measurable. In Fig. 10b the desorption at 1400°K. has been plotted against the square of the amount chemisorbed—and an adequate straight line is obtained. For lower desorption temperatures, the agreement is much poorer; a dependence upon a power >2 seems indicated—and we must consider as *tentative* the deduction that desorption is a second-order reaction, with a rate law $D_\beta = n_\beta^2\ 2.4 \times 10^{-4}\ \exp(-71 \cdot 10^3/RT)$ molecules/cm.² sec.

These results are to be compared with those previously reported by Bosworth and Rideal[23] and van Cleave.[24] It is conceivable that the low binding energies found by these investigators for nitrogen on tungsten referred to nitrogen in the α-state; a more likely explanation of the discrepancy between their findings and ours is the possibility of contamination of the surfaces used in their work. An additional limitation on the work of Bosworth[25] lies in the fact that particularly at low temperatures ($T = 80°$K.) the contact potential will not be significantly affected by the species present in the greatest numbers—the molecules physically adsorbed.

From the analysis of the data of Becker and Hartman, it does appear that, upon adsorption in the β-state, nitrogen molecules are dissociated and exist on the surface as atoms. If we accept the validity of Gomer's[22] measurements on the onset of surface diffusion of hydrogen and oxygen adsorbed on tungsten, as well as his correlations with the heats of adsorption per atom, then we can expect the onset of surface diffusion for nitrogen at approximately the same temperature as for oxygen, that is, at 450°K. or higher. This is of twofold interest. First of all, it indicates that the model for the formation of the α state presented in the previous section, involving singularities in an immobile adsorbed layer, is consistent with the available evidence. Secondly, inasmuch as desorption measurements are carried out above $T = 1000°$K., a mechanism for the transfer of atoms over the surface exists under the conditions of measurement, and the temperature coefficient of the evaporation rate from a non-uniform surface thus gives an average heat of activation for desorption from the sites present on the particular surface.[26] Beeck[27] has reported a differential heat of adsorption of nitrogen on an evaporated tungsten film at room temperature of 95 kcal./mole, significantly higher than the heat term deduced from the rate measurements. At room temperature, the chemisorbed nitrogen should be immobile, and Beeck's experimental value thus refers to the heat of adsorption for sites of high reactivity. Although the validity of the technique for the production of such films is in serious doubt,[28] contamination or incomplete adsorption on the metal

(23) R. C. L. Bosworth and E. K. Rideal, *Physica*, **4**, 925 (1937).

(24) A. B. van Cleave, *Trans. Faraday Soc.*, **34**, 1174 (1938).

(25) R. C. L. Bosworth, *J. Proc. Roy. Soc. N. S. Wales*, **79**, 166 (1946).

(26) We do not agree that the temperature coefficient gives a minimum heat of desorption from the weakest binding sites, as suggested by R. Gomer, *Advances in Catalysis*, **7**, 93 (1955).

(27) O. Beeck, *ibid.*, **2**, 151 (1950).

(28) T. W. Hickmott and G. Ehrlich, to be published.

Fig. 10.—Desorption of nitrogen from tungsten as reported by Becker and Hartman.[2] One layer ($\theta = 1$) = 1.25 × 10¹⁴ molecules/cm.²; (a) evaporation rate as a function of $1/T$; (b) evaporation rate at $T = 1400°$K. as a function of coverage.

could lead to values of the heat which are too low, and if we accept the experimental data as correct, we must conclude that this discrepancy between the calorimetric heat and that observed from rate measurements is due to the presence of binding sites of different strength on the metal. This *may* be expected from the well established dependence of surface tension and work function on the orientation of the crystal surface exposed, and a variation of heat of adsorption with crystal plane has actually been deduced from field emission studies of oxygen on tungsten by Becker.[5] This, however, is a particularly complicated system, for which the interpretation of the emission patterns is even more uncertain than usual[5,26,29] and such a conclusion appears premature. Since only very limited experimental studies on desorption are so far available, a more detailed examination of this question will be delayed till the completion of experimental work now in progress.

Becker[2,5] has interpreted his results on both adsorption and desorption on the assumption that a second, atomic layer, is formed on top of the first, once 1.25 × 10¹⁴ molecules have been adsorbed per sq. cm. Our own analysis associates the break in the plot of sticking coefficient *versus* amount adsorbed with a filling up of reactive A sites, with adsorption continuing thereafter, still on the metal,

(29) E. W. Müller, *Z. Elektrochem.*, **59**, 372 (1955).

but on less reactive sites as well as on those A sites not filled. The break is determined by the rates of the processes that compete with chemisorption for molecules physically adsorbed. Only at a temperature such that the rate of these processes is negligibly small compared with chemisorption does θ_C give a true measure of the "active" area on the surface—as we have found at $T = 80°K$. A reaction on a uniform surface, with only alternate sites filled, as envisioned by Becker,[5] cannot do justice to the experimentally determined kinetics of chemisorption. Moreover, the interpretation of the desorption data, offered in support of the two-layer model, does not appear valid. As indicated, the heat of desorption appears constant within the experimental error, even in the range of formation of the "second layer," and there seems to be no change in the mechanism of desorption; the constancy of the heat of desorption upon increasing the amount of material adsorbed also shows that, up to $n_\beta = 172 \times 10^{12}$ molecules/cm.[2] at least, interaction between adatoms is small. Since the data available at the moment are not extensive, a further examination of the kinetics of desorption is indicated, however.

The salient facts regarding the interaction of nitrogen with a tungsten surface that emerge from these studies are that adsorption may occur in at least three distinct binding states—one in which primarily dispersion forces are at play, and two, designated as α and β, respectively, in which the binding is sufficiently strong to be termed chemi-

sorption. In the β-state nitrogen is present as atoms, with a binding energy of ~150 kcal./g. atom. Below 450°K., the chemisorbed species so formed should be immobile. The rate of formation of this state is rapid at special active strips, presumably lattice steps, and occurs at temperatures as low as 80°K.; adsorption in the β-state occurs at other lattice sites as well, but by a process with a higher activation barrier which prevents chemisorption at 80°K. Simultaneous with adsorption of nitrogen in the β-state is the formation of the α-state, which is dictated by the rate of growth of β, and presumably occurs through the adsorption of molecules on singularities in the atomic layer first formed. At temperatures below 100°K., a third state, γ can be detected, and it is this binding level that is most densely populated at 80°K. At this temperature adsorption in the γ state competes successfully with chemisorption.

Experimental work still in progress has shown that other diatomic molecules can also exist in a number of different binding states on a tungsten surface, although the details of the interactions differ from those found for nitrogen.[30] The presence of chemisorbed entities adsorbed with a low binding energy may be significant in affecting catalytic reactions—so far, however, no experimental work has been carried out under conditions that would help to elucidate this question.

(30) T. W. Hickmott and G. Ehrlich, J. Chem. Phys., 24, 1263 (1956).

CORRELATION OF PHYSICAL PROPERTIES OF NORMAL ALKYL SERIES OF COMPOUNDS[1]

By Kun Li, Raymond L. Arnett, Morton B. Epstein, Rita B. Ries, Louise P. Bitler, Janet M. Lynch and Frederick D. Rossini

Contribution from Petroleum Research Laboratory, Carnegie Institute of Technology, Pittsburgh, Pennsylvania

Methods of correlation of the physical properties of various normal alkyl series of compounds are described. The properties are for the liquid state and include molal volume, density, molal refraction and refractive index, at 25°, and the normal boiling point at 1 atmosphere. The compounds treated include the normal alkyl series of the alkanes, 1-alkenes, cyclopentanes, cyclohexanes, benzenes, 1-alkanethiols, 2-alkanethiols, 1-alkanols, 2-alkanols and alkanoic acids.

I. Introduction

The American Petroleum Institute Research Project 44 has been engaged since 1942 in collecting, analyzing, correlating, calculating and critically selecting values of properties of hydrocarbons and related compounds.[2-4] In this work, one of

(1) This investigation was performed under the American Petroleum Institute Research Project 44 in the Petroleum Research Laboratory of the Carnegie Institute of Technology, Pittsburgh, Pennsylvania.

(2) F. D. Rossini, K. S. Pitzer, W. J. Taylor, J. P. Ebert, J. E. Kilpatrick, C. E. Beckett, M. G. Williams and H. G. Werner, "Selected Values of Properties of Hydrocarbons," National Bureau of Standards Circular 461, U. S. Government Printing Office, Washington, D. C., 1947.

(3) F. D. Rossini, K. S. Pitzer, R. L. Arnett, R. M. Braun and G. C. Pimentel, "Selected Values of Physical and Thermodynamic Properties of Hydrocarbons and Related Compounds," Carnegie Press, Carnegie Institute of Technology, Pittsburgh, Pennsylvania, 1953.

the important tie lines for the reference of values of isomeric molecules is the series of normal alkyl compounds for the different homologous series. The general formula of such a homologous series may be taken as

$$Y-(CH_2)_m-H \tag{1}$$

where m represents the number of carbon atoms in the normal alkyl chain and Y represents the given end group, containing one or more carbon atoms, which may be a methyl group, CH_3-, a cyclopentyl group, C_5H_9-, a cyclohexyl group, $C_6H_{11}-$, a phenyl group, C_6H_5-, a vinyl group, C_2H_3-, an acetylenic group, C_2H-, or $HOCH_2-$, or $HSCH_2-$, etc. The

(4) "Selected Values of Properties of Hydrocarbons and Related Compounds," Loose-leaf data sheets, American Petroleum Institute Research Project 44, Carnegie Institute of Technology, Pittsburgh, Pennsylvania.

first members of the foregoing series are, respectively, methane, cyclopentane, cyclohexane, benzene, ethylene, acetylene, methanol and methanethiol (methyl mercaptan).

It was desired to obtain values for the simple physical properties for each member of such homologous series of compounds up to near C_{20}, and in some cases to near C_{40}. It was found that for each homologous series there were a number of the compounds which had not yet been synthesized in a pure state with measurements of properties reported. Further, for some of the compounds which had been prepared, the reported measurements were not sufficiently reliable. In order to obtain values for the compounds which had not yet been synthesized, and to obtain more reliable values for those compounds for which the reported data were inadequate, recourse was had to the correlation of the values of the properties with molecular structure.

To do this properly requires very reliable data on the first several members of a given homologous series of compounds and on two or three compounds in the range of 10 to 20 carbon atoms in the normal alkyl chain. With reliable data on five or six compounds so selected, it is possible to obtain reliable values for from 10 to 25 other members of the given homologous series without experimental data on these latter compounds.

The present paper explains the procedures which have been in use since about 1946 in the work of the American Petroleum Institute Research Project 44 on the evaluation of values of properties for the members of homologous series of compounds, and presents the background and procedures for the properties of molal volume and density, molal refraction and refractive index and boiling point.

II. General Considerations

It has long been known that the value of a physical property for a pure compound can be correlated with the structure of the molecules of which it is composed. In order to represent a given property in terms of molecular structure, one may assume a function, G, representing the property, which is expressed in terms of i independent structural variables, $z_1 \ldots z_i$, and of j adjustable parameters, $a_1 \ldots a_j$. That is

$$G = f(z_1 \ldots z_i, a_1 \ldots a_j) \qquad (2)$$

In equation 2, the z's are known from the structure of the molecule and the a's are adjusted to fit the experimentally observed values of the given property.

In dealing with the members of a homologous series of compounds, of the general formula given by equation 1, a simplification occurs since the difference from member to member, beginning with $m = 0$ and continuing to the higher members of the series, is the addition of one CH_2 group in the normal alkyl chain. In this case, only one structural variable, z, is needed, that pertaining to the number of carbon atoms in the normal alkyl chain, and we may write

$$G = f(z, c_1 \ldots a_j) \qquad (3)$$

Starting with the first member of the homologous series

$$Y-H \qquad (4)$$

one sees that each succeeding member of the series is produced from the preceding member by the addition of one carbon atom and two hydrogen atoms, into the chain

$$\begin{array}{c} H \\ | \\ -C- \\ | \\ H \end{array} \qquad (5)$$

It is clear that a very rough first approximation is that the change in the value of the given property will be approximately the same from member to member in the homologous series. Further, it is clear that the actual differences in the value of the property will tend to approach constancy as one goes to large values of m. In terms of the increment in the value of the property per CH_2 group, one can say that the increment per CH_2 group will approach a constant value, or the difference in successive values of the increment per CH_2 group will approach zero, as m increases. The rate at which the differences in successive values of the increment per CH_2 group approach zero will vary greatly with the property under consideration. In any case, for any given property, the increment per CH_2 group will approach a constant value for m equal to infinity and this limiting constant value of the increment per CH_2 group will be independent of the end group Y, for the given property, under specified conditions. That is to say, for the compound represented by equation 1, we can express the value of the given property, G, by the equation

$$G = G_0 - am + f(m) \qquad (6)$$

where a is a constant for all homologous series independent of the end group, Y, $f(m)$ is a function of which the derivative with respect to m goes to zero for m equal to infinity, and G_0 is a constant for each series. As previously mentioned, the end group Y is always selected so as to contain at least one carbon atom.

III. Molal Volume and Density

1. **Review of Previous Work.**—The molal volume has long been recognized as an approximately additive property. Aranda[5] and Komoshilov[6,7] developed linear equations for the homologous series of paraffin hydrocarbons. Calingaert and co-workers[8] and Huggins[9,10] put forward more accurate equations for the molal volume for the liquid at 20°, in terms of the number of carbon atoms in the molecule. Kurtz and co-workers[11,12] recommended a general equation for the molal volume of liquid hydrocarbons.

(5) V. G. Aranda, *Anal. real soc. españ. fís. y quim. (Madrid)*, **34**, 513 (1936).

(6) N. F. Komoshilov, *Zhur. Obshchei Khim.*, **9**, 701 (1939).

(7) N. F. Komoshilov, *ibid.*, **10**, 945 (1940).

(8) G. Calingaert, H. A. Beatty, R. C. Kuder, and G. W. Thompson, *Ind. Eng. Chem.*, **33**, 103 (1941).

(9) M. L. Huggins, *J. Am. Chem. Soc.*, **63**, 116 (1941).

(10) M. L. Huggins, *ibid.*, **76**, 843 (1954).

(11) S. S. Kurtz and M. R. Lipkin, *Ind. Eng. Chem.*, **33**, 779 (1941).

(12) S. S. Kurtz and A. Sankin, *ibid.*, **46**, 2186 (1954).

Mibashan[13] related molal volume to normal boiling point. Francis[14] correlated the density with the number of carbon atoms. Smittenberg and Mulder[15] proposed the following equation for the density of a homologous series of compounds

$$d = d_\infty + k'/(n + z') \qquad (7)$$

Here n is the number of carbon atoms, d_∞ is the limiting value of the density for an infinitely long chain, and k' and z' are arbitrary constants for given homologous series. This relation gave remarkable accord with the experimental values for the individual compounds.

2. Method Used in the Present Work.—In the work of the API Research Project 44, the reference data were taken for the liquid at 25°. Accurate data on the densities of the API Research hydrocarbons of the series of normal paraffins (n-alkanes) and the normal monoölefins (1-alkenes) up to C_{16} were available.[16] These two normal alkyl series were used as the primary basis for developing the correlation.

Plots of the molal volume, V, against m, the number of carbon atoms in the normal alkyl chain, for these two normal alkyl series, n-alkanes and 1-alkenes, yielded lines which were nearly straight and had almost identical slopes. A sensitive test for linearity was performed by plotting, against m, the residual volumes, defined as the differences between the experimental values and corresponding values calculated from the equations representing the straight line in each case. Definite departures from linearity, greater than the uncertainty of the data, were indicated, and it was decided to include in the equation a term involving $f(m)$

$$V = V_0 + a_v m + f(m) \qquad (8)$$

In accordance with the discussion presented earlier in this paper, the change of molal volume with the number of carbon atoms in the normal alkyl chain approaches a limiting constant value as m increases without limit. This requires that $df(m)/dm$ in equation 8 becomes zero, with dV/dm becoming equal to a_v.

It was found that plotting $(m - 1)$ times the residual volume against the $1/(m - 1)$ yielded a straight line within the significance of the data. This meant that the residual volume, or $f(m)$, could be expressed as a second degree equation in $1/(m - 1)$, or

$$f(m) = b_v/(m - 1) + c_v/(m - 1)^2 \qquad (9)$$

Then the final equation for the molal volume becomes

$$V = V_0 + a_v m + b_v/(m - 1) + c_v/(m - 1)^2 \qquad (10)$$

where the constants V_0, a_v, b_v and c_v are evaluated from the experimental data. It is to be noted that, as previously indicated

$$dV/dm = a_v; \quad \text{as } m \longrightarrow \infty \qquad (11)$$

This means that a_v will have the same value for all normal alkyl series. Since density is the molecular weight divided by molal volume, M/V, then the limiting value of density, as m approaches infinity, will be

$$d_\infty = 14.026/a_v \qquad (12)$$

where 14.026 is the molecular weight of one CH_2 group.

For all the normal alkyl series examined in this investigation, Equation 10 holds satisfactorily for values of m greater than one.

3. Results of the Present Work.—Equation 10 was fitted to the best available data on the molal volume, at 25° and one atmosphere, of the n-alkanes and 1-alkenes[2-4,16,17] by means of the method of least squares.

From the data on the twelve n-alkanes, C_5 to C_{16}, inclusive, the value of a_v in Equation 10 for the series of n-alkanes at 25° was found to be 16.4867 ml./mole, with a standard deviation of ±0.0090 ml./mole. Correspondingly, the data on the twelve 1-alkenes, C_5 to C_{16}, inclusive, yielded, for the value of a_v in Equation 10 for the series of 1-alkenes at 25° and 1 atmosphere 16.4834 ml./mole, with a standard deviation of ±0.0049 ml./mole. For all normal alkyl series, a weighted mean value of a_v equal to 16.4841±0.0043 ml./mole at 25° and 1 atmosphere was selected. With this value of a_v, values of the other constants, V_0, b_v and c_v were recalculated for the series of n-alkanes and the series of 1-alkenes. The limiting value of density, d_∞, corresponding to the selected value of a_v, becomes 0.85088 g./ml. at 25°.

With the value of a_v thus predetermined, only three constants, V_0, b_v and c_v, were required to be evaluated in applying equation 10 to the data on other normal alkyl series. Eight other homologous series of compounds were thus investigated. Wherever the data warranted, the method of least squares with appropriate weighting was used.

Table I gives the values of the constants of equation 10 for calculating the molal volume for the liquid at 25° for ten normal alkyl series of compounds, including n-alkanes, 1-alkenes, cyclopentanes, cyclohexanes, benzenes, 1-alkanethiols, 2-alkanethiols, 1-alkanols, 2-alkanols and alkanoic acids. The last column of Table I gives the root mean square or standard deviation of the calculated from the experimental values of density. These standard deviations are of the same magnitude as the uncertainties in the experimental data.

From the values of the molal volume calculated from the constants given in Table I for each series, it is possible to calculate the density, for the liquid at 25° and 1 atmosphere, for each of the compounds of each of the series.

IV. Molal Refraction and Refractive Index

1. Review of Previous Work.—As far back as 1893, Eykman[17] reported the additivity of the molal refraction, $R = V(n_D - 1)$, of CH_2 groups in homologous series for the liquid state. Following Eykman's work, many linear equations have been proposed by different investigators.[9,12,18] Equations for refractive index have been de-

(13) A. Mibashan, *Trans. Faraday Soc.*, **41**, 374 (1945).

(14) A. W. Francis, *Ind. Eng. Chem.*, **33**, 554 (1941).

(15) J. Smittenberg and D. Mulder, *Rec. trav. chim.*, **67**, 813 (1948).

(16) D. L. Camin, A. F. Forziati and F. D. Rossini, This Journal, **58**, 440 (1954); D. L. Camin and F. D. Rossini, *ibid.*, **59**, 1173 (1955).

(17) J. F. Eykman, *Rec. trav. chim.*, **12**, 157 (1893).

(18) J. P. Wibaut and S. L. Langedijk, *ibid.*, **59**, 1220 (1940).

TABLE I

VALUE OF THE CONSTANTS OF EQUATION 10 FOR MOLAL VOLUME, FOR THE LIQUID AT 25° AND 1 ATMOSPHERE, FOR VARIOUS NORMAL ALKYL SERIES

$a_v = 16.4841$ ml./mole for all series.   The series is represented by the general formula, $Y-(CH_2)_m-H$, where the end group Y always contains one or more carbon atoms.

Normal alkyl series	No. of compd. used to evaluate the constants	V_0, ml./mole	Values of the constants b_v, ml./mole	c_v, ml./mole	Root-mean-square or stand. dev. in density, g./ml.
n-Alkanes	12	45.82233	14.56329	−4.56336	0.000048
1-Alkenes	12	57.08054	10.37057	−5.33246	.000037
n-Alkyl cyclopentanes	3	95.80176	−0.74372	+1.64148	...
n-Alkyl cyclohexanes	3	110.53675	−0.81676	1.02295	...
n-Alkyl benzenes	3	91.99335	−5.03136	4.71845	...
1-Alkanethiols	6	59.61365	−5.09148	5.03934	.000038
2-Alkanethiols	5	77.53475	−4.61859	4.64630	.000148
1-Alkanols	7	43.56824	−3.74475	3.36719	.000135
2-Alkanols	5	61.65620	−6.88659	7.21123	.000134
n-Alkanoic acids	6	43.84111	−1.17385	−1.09678	.00078

veloped by Schoorl[19] in terms of molecular weight and by Francis[13] in terms of the number of carbon atoms. Mibashan[12] also correlated refractive index with the normal boiling point.

Smittenberg and Mulder[14] proposed for the refractive index an equation of the form similar to their equation for density

$$n_D = n_\infty + k/(n + z) \qquad (13)$$

Here, n_∞ is the limiting value of refractive index for an infinite number of carbon atoms in the normal alkyl chain and has the same value for different homologous series.

2. Method Used in the Present Work.—The accurate data obtained on the series of normal paraffins of the API Research hydrocarbons[2-4,15,16] indicate that the Lorentz–Lorenz molal refraction

$$R = V(n^2 - 1)/(n^2 + 2) \qquad (14)$$

is linear with the number of carbon atoms within the significance of the data

$$R = R_0 + a_R m \qquad (15)$$

Here, m is the number of carbon atoms in the normal alkyl chain, and a_R is the constant increment per CH_2 group, which is the same for different homologous series. Equation 15 holds satisfactorily for values of m greater than one.

3. Results of the Present Work.—Equation 15, with R taken as given by equation 14, was fitted to the best available data on molal volume and refractive index for the sodium-D spectral line, at 25° and one atmosphere, for the n-alkanes and 1-alkenes[2-4,15,16] by means of the method of least squares.

From the data on the twelve n-alkanes, C_5 to C_{16}, inclusive, the value of a_R in equation 15 for the series of n-alkanes at 25° was found to be 4.64290 ml./mole, with a standard deviation of ±0.00039 ml./mole. Correspondingly, the data on the twelve 1-alkenes, C_5 to C_{16}, inclusive, yielded, for the value of a_R in equation 15 for the series of 1-alkenes at 25° 4.64109 ml./mole, with a standard deviation of ±0.00034 ml./mole. These data indicate an apparently fortuitous small value of the standard deviation for each series which is considerably smaller than the difference in the experi-

(19) N. Schoorl, "Organische Analyse," Vol. II, third edition D. B. Centen, Amsterdam, 1937, p. 39.

mental value of a_R for the two series of compounds. In the same manner as was done for the molal volume, one value of a_R was selected to be used for all different normal alkyl series. A weighted mean value of a_R was arbitrarily taken as 4.64187 ml./mole. This mean value is 0.00103 and 0.00078 ml./mole within the experimental values for the n-alkanes and 1-alkenes, respectively.

Using this selected value of a_R, the value of R_0 was calculated for each of the homologous series under investigation, by the method of least squares, with appropriate weighting. Table II gives the calculated values of R_0 for ten normal alkyl series of compounds, including n-alkanes, 1-alkenes, cyclopentanes, cyclohexanes, benzenes, 1-alkanethiols, 2-alkanethiols, 1-alkanols, 2-alkanols and alkanoic acids. The last column of Table II gives the root mean square or standard deviation of the calculated from experimental values of refractive index. These standard deviations are of the same magnitude as the uncertainties in the experimental data.

From the values of molal refraction calculated from the constants given in Table II, it is possible to calculate the refractive index, for the sodium-D spectral line for the liquid at 25° and 1 atmosphere, for each of the compounds of each of the series, using the value of molal volume from Table I, using the equation

$$(n^2 - 1)/(n^2 + 2) = R/V \qquad (16)$$

Writing equations 10, 14, and 15 together, one has

$$\begin{aligned} R/V &= (n^2 - 1)/(n^2 + 2) \\ &= (R_0 + a_R m)/[V_0 + a_v m + \\ &\quad b_v/(m - 1) + c_v/(m - 1)^2] \end{aligned} \qquad (17)$$

As m approaches infinity, the limit of R/V is the value per CH_2 group and becomes

$$(R/V)_\infty = [(n^2 - 1)/(n^2 + 2)]_\infty = a_R/a_v \qquad (18)$$

Substituting the numerical values of a_R and a_v, one obtains

$$a_R/a_v = 0.2815968 \qquad (19)$$

and, from equation 18

$$n_\infty = 1.47510 \qquad (20)$$

for the liquid at 25° and the sodium-D spectral line.

TABLE II

VALUES OF THE CONSTANTS OF THE EQUATION FOR MOLAL REFRACTION, $R = V(n^2 - 1)/(n^2 + 2) = R_0 + a_R m$, FOR THE LIQUID AT 25° AND THE SODIUM-D SPECTRAL LINE, FOR VARIOUS NORMAL ALKYL SERIES

$a_R = 4.64187$ ml./mole for all series. The series is represented by the general formula, $Y—(CH_2)_m—H$, where the end group Y always contains one or more carbon atoms.

Normal alkyl series	No. of compd. used to evaluate the constants	Value of R_0 ml./mole	Root-mean-square or stand. dev. in refractive index
n-Alkanes	12	6.72066	0.000052
1-Alkenes	12	10.93704	.000046
n-Alkyl cyclopentanes	3	23.14251	.000048
n-Alkyl cyclohexanes	3	27.76551	.000016
n-Alkyl benzenes	3	26.55060	.000052
1-Alkanethiols	6	14.50273	.00012
2-Alkanethiols	5	19.17105	.00021
1-Alkanols	7	8.23182	.00046
2-Alkanols	4	12.85626	.00019
n-Alkanoic acids	6	8.26657	.00033

V. Normal Boiling Point

1. Review of Previous Work.—The relationships involving the normal boiling points of compounds of homologous series have been very extensively studied in the past, with the series of normal paraffins having received the greatest amount of attention. In 1842, Kopp[20] stated that in any given homologous series the increase in boiling point on the addition of a CH_2 group is constant. Thirty-five years later, Schorlemmer[21] pointed out that Kopp's statement was somewhat inaccurate. In the following years, Goldstein[22] and Young[23] formulated relations for the difference in boiling point between two successive members of a homologous series of compounds. Expressions of different forms and degrees of complexity for the normal boiling point of members of homologous series have been proposed by Mills,[24] Hinrichs,[25] Walker,[26] Boggio-Lera,[27] and Ramage.[28]

In 1916, Plummer[29] suggested that one should distinguish three different classes of homologous series and that their boiling point relations should be treated differently. The first class involves marked association among the molecules; the second class, slight association among the molecules; and the third class, no association.

More recent correlations include those of Young,[30] Cox,[31] Aten,[32] Merkel,[33] Burnop,[34] Kinney,[35] and Francis.[14]

(20) H. Kopp, Ann., **41**, 169 (1842).

(21) C. Schorlemmer, Chem. News, **25**, 101 (1877).

(22) M. Goldstein, Ber., **12**, 689 (1879).

(23) S. Young, Phil. Mag., **9**, 1 (1905).

(24) E. J. Mills, ibid., **17**, 173 (1884).

(25) G. Hinrichs, Z. physik. Chem., **8**, 229 (1891).

(26) J. Walker, J. Chem. Soc., **65**, 193 (1894).

(27) E. Boggio-Lera, Gazz. chim. ital., **29**, 441 (1899).

(28) H. Ramage, Proc. Cambridge Phil. Soc., **xii**, 445 (1904).

(29) H. C. Plummer, Phil. Mag., **32**, 371 (1916).

(30) S. Young, Proc. Roy. Irish Acad., **B38**, 65 (1928).

(31) E. R. Cox, Ind. Eng. Chem., **27**, 1423 (1935).

(32) A. H. W. Aten, J. Chem. Phys., **5**, 260 (1937).

(33) J. H. C. Merkel, Koninkl. Ned. Akad. Wetenschap. Proc., **40**, 164 (1937).

(34) V. C. E. Burnop, J. Chem. Soc., 826 (1938).

(35) C. R. Kinney, Ind. Eng. Chem., **32**, 559 (1940).

Egloff, Sherman and Dull[36] adopted Plummer's[29] logarithmic formula

$$T = a \log (n + b) + k \qquad (21)$$

and found that the boiling points of aliphatic homologous series of compounds could be represented rather accurately by this simple formula, with the same value of a and b being used for the different series. Subsequently, this same formula was applied to the homologous series of other types of compounds by using a different value of a for each series, with the same value of b being used for all series.[37-39]

2. Method Used in the Present Work.—Because of the great increase in the precision and accuracy of our present-day data, it was necessary to seek some new form of equation to satisfy the needs of the API Research Project 44 in correlating the data on normal boiling points for many different series of normal alkyl compounds.

In view of the moderate success achieved by previous correlations involving a logarithmic function, it appeared logical to take as a first approximation the following

$$t = t_0 + c_t' \log (m - 1) \qquad (22)$$

However, a plot of boiling point against $\log (m - 1)$ indicated that one or more additional terms were required to bring accord with the experimental data on the first several members of the series. Then the following form of equation was taken

$$t = t_0 + c_t' \log (m - 1) + f(m) \qquad (23)$$

In equation 23, the form of the function, $f(m)$, could be determined from the accurate data recently reported by the API Research Project 6 on the boiling points of the normal paraffins and the normal monoölefins (1-alkenes), each series from C_5 to C_{16}, inclusive.[15,16] Careful comparison of these data with equation 23 made it evident that the function, $f(m)$, had to be something more than a simple power series.

Differentiation of equation 23 with respect to m gives

$$dt/dm = c_t/(m - 1) + d[f(m)]/dm \qquad (24)$$

A plot of the data in the form of $(m - 1)dt/dm$ against m showed that $(m - 1)dt/dm$ increases with increasing values of m and rapidly approaches a limit, in a form resembling an exponential curve. Then the data were plotted in the form of $(m - 1)dt/dm$ against $e^{-b_t(m - 1)}$, and a reasonably good straight line was obtained when a suitable value of b_t was used. Then we have

$$(m - 1) dt/dm = -d_t e^{-b_t(m-1)} + c_t \qquad (25)$$

or

$$dt/dm = -d_t e^{-b_t(m-1)}/(m - 1) + c_t/(m - 1) \qquad (26)$$

Equation 26 gives a limit of zero for dt/dm as m increases to infinity.

Integrating equation 26 from $m = 2$ to any

(36) G. Egloff, J. Sherman and R. B. Dull, THIS JOURNAL, **44**, 730 (1940).

(37) N. Corbin, M. Alexander and G. Egloff, Ind. Eng. Chem., **38**, 156 (1946).

(38) W. D. English and R. V. V. Nicholls, J. Am. Chem. Soc., **72**, 2764 (1950).

(39) W. D. English, ibid., **74**, 2927 (1952).

<div align="center">

TABLE III

VALUES OF THE CONSTANTS OF THE EQUATION FOR THE NORMAL BOILING POINT,

$$t = t_0 + c_t' \log (m - 1) - d_t \left\{ \int_{b_t}^{\infty} e^{-u} \, d \ln u - \int_{u}^{\infty} e^{-u} \, d \ln u \right\}$$

</div>

$u = b_t(m - 1)$, and $b_t = 0.1505$ for all normal alkyl series.   The series is represented by the general formula, $Y-(CH_2)_m-H$, where the end group Y always contains one or more carbon atoms.   (The values of the definite integrals are given in Table IV.)

Normal alkyl series	No. of compd. used to evaluate the constants	t_0, °C.	Values of the constants c_t', °C.	d_t, °C.	Root-mean-square or stand. dev. in normal b.p., °C.
n-Alkanes	12	− 47.2841	570.5673	225.3648	0.044
1-Alkenes	12	− 9.4932	550.2697	226.0561	.047
n-Alkyl cyclopentanes	3	+103.4316	471.4638	204.8897	...
n-Alkyl cyclohexanes	6	130.9469	449.4821	196.1562	.21
n-Alkyl benzenes	6	133.2915	439.1626	190.3216	.25
1-Alkynes	4	5.3599	542.2579	229.9587	.036
1-Alkanethiols	6	69.3654	513.3685	224.4221	.30
2-Alkanethiols	5	83.9546	484.5158	210.2326	.088

given higher value of m, one obtains

$$t = t_0 + c_t \int_2^m dm/(m - 1) - d_t \int_2^m [e^{-b_t(m-1)}/(m - 1)] dm \quad (27)$$

or

$$t = t_0 + c_t \ln (m - 1) - d_t \int_2^m [e^{-b_t(m-1)}/(m - 1)] dm \quad (28)$$

The lower limit of $m = 2$ for the integration was taken for simplification of the mathematical operations and also because it was not necessary to include the first member of the series in the correlation. The last term in equation 27 may be transformed. Let

$$u = b_t(m - 1), \text{ or } m = (u/b_t) + 1 \quad (29)$$

then

$$dm = du/b_t \quad (30)$$

and

$$\int_2^m [e^{-b_t(m-1)}/(m - 1)] dm = \int_{b_t}^u (b_t e^{-u}/u) du/b_t \quad (31)$$

$$= \int_{b_t}^u e^{-u} d \ln u$$

But

$$\int_{b_t}^u e^{-u} d \ln u = \int_{b_t}^{\infty} e^{-u} d \ln u - \int_u^{\infty} e^{-u} d \ln u \quad (32)$$

The values of the two definite integrals on the right side of equation 32 may be found in certain mathematical tables.[40]

The complete equation then may be written, from equations 28, 31 and 32, as

$$t = t_0 + c_t' \log (m - 1) - d_t \left\{ \int_{b_t}^{\infty} e^{-u} d \ln u - \int_u^{\infty} e^{-u} d \ln u \right\} \quad (33)$$

where $u = b_t(m - 1)$.

The value of b_t is determined as follows. Differentiating equation 25 with respect to m gives

$$d[(m - 1)dt/dm]/dm = b_t d_t e^{-b_t(m-1)} \quad (34)$$

Taking the logarithm of both sides of this equation, one obtains

$$\ln\{d[(m - 1)dt/dm]/dm\} = -b_t(m - 1) + \ln(b_t d_t) \quad (35)$$

A plot of $\ln\{d[(m - 1)dt/dm]/dm\}$ against $(m - 1)$ yields a straight line, the slope of which is $-b_t$, with intercept equal to $\ln (b_t d_t)$.

Although the evaluation of b_t in this way may seem somewhat tedious, it has been found that one value of b_t can be made to serve for substantially all normal alkyl series of compounds. Moreover, it is found that the value of d_t, the coefficient of the definite integrals in equation 33, has nearly the same value for the series of normal alkanes and the 1-alkenes. These findings are in accord with the fact that the differences in normal boiling points between normal alkanes and 1-alkenes having the same value of m fall on a straight line when plotted against $\log (m - 1)$. This latter fact would be true when the values of the definite integrals in equation 33 are the same for the two corresponding compounds of the two series, that is, when the values of b_t and d_t are the same for the two compounds. This means also that the values of b_t and d_t so determined may be utilized in some measure to evaluate data for other normal alkyl series for which the data may be very meager.

By the method of least squares, the data on the series of normal alkanes and 1-alkenes yielded a value of $b_t = 0.1505 \pm 0.0027$.

For the normal alkyl series of oxygen compounds, it was found that plots of $(m - 1)dt/dm$ against $e^{-b_t(m - 1)}$ yielded curves which departed from linearity. This departure was not unexpected since the correlation was based primarily on the simple hydrocarbons which have an intermolecular behavior appreciably different from that of organic oxygen compounds.

As in the case of molal volume and molal refraction, it was found that the first member of the series can not readily be included in the correlation. Hence, equation 33 may be used to calculate values of normal boiling points for m greater than one.

3. Results of the Present Work.—In Table III are given values of the constants, t_0, b_t, c_t and d_t, required for calculating the normal boiling points for the compounds of eight different normal alkyl

(40) "Tables of Sine, Cosine and Exponential Integrals," Vol. I, Prepared by the Federal Work Agency, Works Projects Administration for the City of New York, New York, 1940.

TABLE IV

VALUES OF THE DEFINITE INTEGRALS IN THE EQUATION FOR CALCULATING NORMAL BOILING POINTS

$u = b_t(m - 1);\quad b_t = 0.1505;\quad \int_{b_t}^{\infty} e^{-u}\, d \ln u = 1.461598$

Value of m	$\int_u^{\infty} e^{-u}\, d \ln u$	$\int_{b_t}^{\infty} e^{-u}\, d \ln u - \int_u^{\infty} e^{-u}\, d \ln u$
2	1.461598	0.000000
3	0.903213	0.558385
4	.623211	0.838387
5	.452555	1.009043
6	.338771	1.122827
7	.258833	1.202765
8	.200710	1.260888
9	.157408	1.304190
10	.124556	1.337042
11	.099279	1.362319
12	.079610	1.381988
13	.064165	1.397433
14	.051942	1.409656
15	.042235	1.419363
16	.034495	1.427103
17	.028158	1.433440
18	.023122	1.438476
19	.018972	1.442626
20	.015647	1.445951
21	.012893	1.448705
22	.010671	1.450927
23	.008824	1.452774
24	.007325	1.454273
25	.006075	1.455523
26	.005056	1.456542
27	.004204	1.457394
28	.003506	1.458092
29	.002922	1.458676
30	.002441	1.459157
31	.002039	1.459559

TABLE IV (Continued)

Value of m	$\int_u^{\infty} e^{-u}\, d \ln u$	$\int_{b_t}^{\infty} e^{-u}\, d \ln u - \int_u^{\infty} e^{-u}\, d \ln u$
32	.001706	1.459892
33	.001427	1.460171
34	.001196	1.460402
35	.001002	1.460596
36	.000841	1.460757
37	.000706	1.460892
38	.000593	1.461005
39	.000498	1.461100
40	.000419	1.461179

series. The last column of the table gives the root mean square or standard deviation.

In Table IV are given values of the definite integrals for values of m from 2 to 40.

It should be noted that when one value of the constant b_t is common to a number of series of compounds, equation 33 may be simplified to

$$t = t_0' + c_t' \log (m - 1) + d_t \int_u^{\infty} e^{-u}\, d \ln u \quad (36)$$

where

$$t_0' = t_0 - d_t \int_{b_t}^{\infty} e^{-u}\, d \ln u \quad (37)$$

VI. Conclusion

By means of the methods described in the present report, values were calculated for the properties of molal volume, density, molal refraction, refractive index and boiling point for two hundred compounds for which experimental data are nonexistent or inadequate. The many individual values so calculated appear in the tables of the API Research Project 44.[4]

The work is being extended to cover additional series, in particular with respect to the property of boiling point for the normal alkyl series of alcohols.

PHYSICAL PROPERTIES OF 2,4,6-TRI-DIMETHYLAMINOMETHYL-PHENOL TRIACETATE[1]

By A. BONDI AND H. L. PARRY[2]

Shell Development Company, Emeryville, California

In order to elucidate the mechanisms of curing of EPON® resins with amine salts, the dissociation equilibria of the triacetate of 2,4,6-tri-(dimethylaminomethyl)-phenol in non-aqueous media have been investigated. In the temperature range 20–80° it has been found that 1. Ionic dissociation in solution is negligible (ca. 0.01–0.1%) and changes little, if any, with temperature. 2. Molecular dissociation into free amine and free acid, either in the melt or in solution, is of the order of 20–25% at 80°. From the rate of cure of EPON resins observed with this salt, one would assume that the salt is dissociated to more than 70% at 80°. This discrepancy is reconciled by the suggestion that the first and rate-determining step in the reaction is the removal of acetic acid from the catalyst by esterification with some of the epoxide. Several previously unexplained observations are also explained by such a mechanism.

The cure of certain epoxy resins catalyzed by amines is often too rapid. Delay of cure until the resin is heated has been accomplished through the use of the corresponding amine carboxylates. Re-

lease of the amine by thermal dissociation at the intended curing temperature was held responsible for this effect. In the course of time, some doubts arose regarding the correctness of this mechanism. A quantitative investigation of the extent of molecular and ionic dissociation of a typical amine salt was therefore undertaken to clarify the mode of

---

action of these amine carboxylate catalysts.

Properties and Structure of the Amine Salt.—
All of the work was done on the triacetate of 2,4,6-tri-(dimethylaminomethyl)-phenol (TDMP). The commercial TDMP was purified by fractional distillation *in vacuo* and was neutralized with the stoichiometric amount of Analytical Grade Glacial Acetic Acid. The physical properties of the TDMP and of the triacetate are given on Table I. The molecular structure of the salt is indicated on Fig. 1.

The molal volume of the salt is 51 cm.³ less than that of the physical mixture of the two components would have been. The shrinkage per amine acetate group, 16.9 cm.³, corresponding closely to the 17.4 cm.³ observed for piperidine propionate[3] is about two-thirds of that accompanying covalent, *e.g.*, C–C bond formation, indicative of the strength of the bond.

The dipole moment of so complicated a molecule as TDMP can hardly be interpreted in an unambiguous manner. The same applies to that of the triacetate. The probably nearly random orientation of the amine dipoles would lead to an average dipole moment of about 1 *D* for the TDMP. The observed value of about 3.4 *D* must therefore be connected with phenolate formation of one or both of the *ortho* methyl amino methyl groups.[4] The large dipole moment of the triacetate is of the order expected if the randomly oriented salt bonds are of the length indicated above. Clarification of this point requires experiments with simple model compounds. (The dipole moments given in Table I are just a by-product of the electrical measurements carried out for the study of ionic dissociation.)

Fig. 1.—Configuration of TDMP-triacetate.
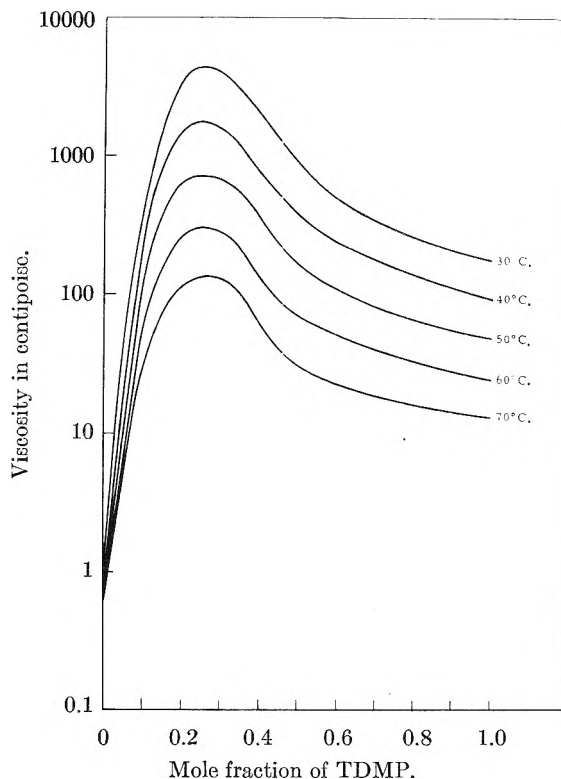
Fig. 2.—Viscosity *vs.* composition for the system TDMP-acetic acid at various temperatures.

TABLE I

Physical   Properties   of   2,4,6-Tri-(dimethylamino-methyl)-phenol (TDMP) and of its Triacetate

	TDMP	TDMP-Triacetate
Density at 30°, $d^{30}{}_4$, g. cm.$^{-3}$	0.973	1.0684
Expansion coefficient (30–100°), °C.$^{-1}$		5.8×10^{-4}
Viscosity, at 30°, poise	1.5[a]	32.7
50°, poise	0.4[a]	3.97
82°, poise	..	0.44
Dipole moment,[b] in toluene, at 30°, *D*	3.3	7.0
at 90°, *D*	3.5	4.3

[a] Approximate values, obtained with a Brookfield viscometer. [b] Calculated by means of Guggenheim's method from dielectric constant measurements at 10 kc./sec.

The high viscosity of the TDMP-triacetate is its most peculiar physical property. The more than 20-fold increase in viscosity as TDMP is neutralized with acetic acid is illustrated by the curves of Fig. 2. The similarity of the slope of the viscosity–temperature curve of the triacetate to that of about equiviscous hydrocarbons, shown on Fig. 3, threw doubt on the idea that the salt is extensively dissociated at 80 to 100°, for in that case the viscosity of the salt should have been of the order of that of a physical mixture of TDMP and acetic acid, or about 50 times less than actually observed.

(3) E. B. R. Prideaux and R. N. Coleman, *J. Chem. Soc.*, 1346 (1936); 4 (1937).

(4) This surmise has been confirmed by the measurements of J. R. Hulett, *et al.* (*J. Chem. Soc.*, 3901 (1955)) who found that trimethylaminephenolate exhibits a dipole moment of 3.24 *D*.

Molecular Dissociation.—Amine carboxylate salts can dissociate into uncharged, molecular species and into charged, ionic components. The extent to which they will do so depends strongly on the environment into which they have been placed. Vapor pressure measurements (with a simple U-tube tensiometer) on the pure triacetate gave the results shown in Table II. After correction for dimerization in the vapor[5] the activity of acetic acid in the system could be evaluated. If the acetic acid forms an ideal solution in the TDMP acetate, the activity is a direct measure of the degree of dissociation of the salt. The model system acetic acid–isoöctylphenol exhibited the behavior of a nearly perfect solution (Table III). This finding supported the assumption that acetic acid forms a sufficiently nearly ideal solution in the salt to permit the identification of the activity of acetic acid (*cf.* Table II) with the degree of molecular dissociation of the triacetate.

(5) O. Redlich, Shell Development Company, private communication.
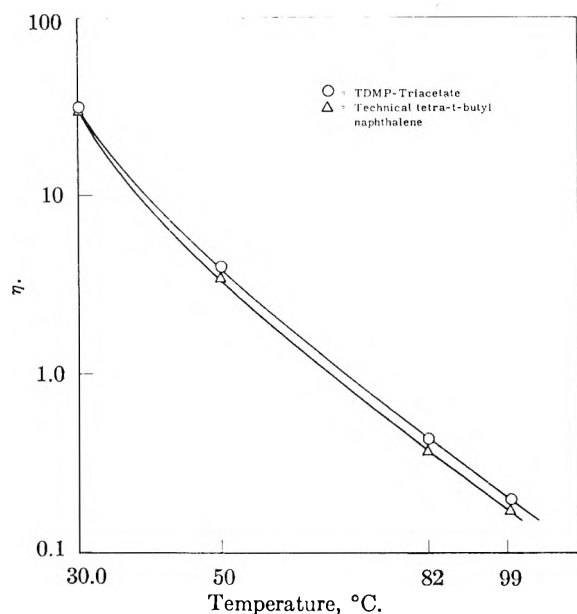
Fig. 3.—Comparison of the viscosity–temperature curves of TDMP-triacetate and a hydrocarbon.

TABLE II

VAPOR PRESSURE AND DERIVED DATA FOR TDMP-TRI-ACETATE

Temp., °C.	40	60	80
Vapor pressure, mm.	1	6	19
Apparent activity of AcOH, a_1'	0.032	0.068	0.094
Corrected activity^a of AcOH, a_1	0.10	0.17	0.19
Activity coefficient of AcOH, γ_1	0.14	0.23	0.26

^{a} Corrected for dimerization of acetic acid in the vapor phase.

TABLE III

SOLUTION CHARACTERISTICS FOR THE SYSTEM ACETIC ACID–p-ISOÖCTYLPHENOL

Concn. of AcOH, mole fraction	0.0	0.1	0.4
M.p., °C.	85.8^a	81.9	61.4
Activity coefficient of isooctyl-phenol, γ_2	..	1.03	1.06
Vapor pressure, mm. at ( ) °C.	..	10(85)	52(80)
Apparent activity of AcOH, a_1'	..	0.04	0.26
Corrected activity^b of AcOH, a_1	..	0.097	0.40
Activity coefficient of AcOH, γ_1	..	0.97	0.99

^{a} Heat of fusion of p-isoöctylphenol at its melting point = 22.6 cal./g. = 4,600 cal./mole (kindly determined by Mr. C. Busso). ^{b} Corrected for dimerization of AcOH in the vapor phase.

The over-all dissociation of the salt in 2-butanone was measured ebullioscopically. The results are shown in Fig. 4. Owing to the smallness of the ionic dissociation, the data of Fig. 4 are essentially a measure of the degree of molecular dissociation[6] (in 2-butanone) at 80°.

Ebullioscopic measurements in benzene, by contrast, indicated rather strong association of the TDMP-triacetate in non-polar solvents. Similar association of organic electrolytes in non-polar

solvents had been observed by Walden[8,9] and others.[10] Cryoscopic measurements in benzene, surprisingly enough, do not show any strong signs of association or dissociation.

Between the butanone, the melt and benzene, essentially just the ends of the "polarity" spectrum have been covered. They do not provide sufficient information to discern the parameter which determines the extent of molecular dissociation. Rough interpolations might be made on the basis of cohesive energy density, dielectric constants or other measures of cohesive forces in liquids.

Ionic Dissociation.—The only convenient measure of ionic dissociation in non-electrolytes is the electrical conductivity K, or more specifically the Walden product $\Lambda\eta$ of equivalent conductance Λ and viscosity η. According to an empirical rule proposed by Walden[9] and, more recently, given theoretical justification by Eyring and co-workers,[11] the degree of dissociation α is approximately $(\Lambda\eta)/b$. The numerical constant b is 0.6 according to Walden's experiments, and this is the value we shall use, keeping in mind, however, that it is probably just a number of the order of one.

The change of $\Lambda\eta$ as the TDMP is titrated with acetic acid is shown on Fig. 5. It is apparent that one of the three amine groups is rather weaker than the other two, both of which are of about equal strength and exhibit a degree of dissociation of the same order as that of melts of strong electrolytes. The titration curve of TDMP in aqueous solution, shown on the same figure, also indicates the greater strength of two of the amine groups as compared with the third one. The aqueous solution is colored intensely yellow until the neutralization of the first two amine groups.

The color suggests that the great strength of the first two amine groups may be due to resonance of the unpaired electrons of the nitrogen atom *ortho* to the phenol group between the phenolate and the hydrochloride bond. Interestingly, Gemant had suggested a very similar structure to explain the unusually high electrical conductivity of the ternary salt amine–carboxylic acid–phenol in hydrocarbon solutions.[12] The very different quantitative relations in the non-aqueous and in the aqueous case derive from the fact that the TDMP is a strong base in water but a nearly neutral body in non-aqueous environments. The dissociation constants of the "strong" amine groups differ from that of the "weak" one by a factor somewhat less than 10^3 in water, and slightly more than 10^2 in the TDMP salt melt.

The temperature coefficient of $\Lambda\eta$ of the melt, and hence of α, is slightly negative and would probably be nearly zero if the competing thermal (molecular) dissociation were taken into account. This result is in agreement with the theory,[11] which exhibits no temperature factor in the formula for $\Lambda\eta$.

(6) The activity coefficient of acetic acid in the related solvent 2-heptanone[7] (the only applicable literature data that were found) is sufficiently close to unity to warrant simple conversion of the activity to the degree of dissociation of the salt in 2-butanone solution.

(7) D. F. Othmer and R. F. Benenati, *Ind. Eng. Chem.*, **37**, 299 (1945).

(8) P. Walden, *Z. physik. Chem.*, **A157**, 389 (1931).

(9) P. Walden and E. J. Birr, *ibid.*, **A131**, 1, 21, 31 (1928); **A160**, 45, 57, 161 (1932).

(10) M. Centnerszwer and Iazniewski, *ibid.*, **A160**, 257 (1932).

(11) S. Glasstone, K. Laidler and H. Eyring, "Theory of Rate Processes," McGraw-Hill Book Co., New York, N. Y., 1941.

(12) A. Gemant, *J. Chem. Phys.*, **14**, 424 (1946).

Ionic dissociation of TDMP and of its triacetate in solution in toluene and 2-butanone is primarily a function of the dielectric constant ϵ of the solution and of the temperature T. All of the solution data of this investigation and the comparable data of Gemant[12] can be plotted against the variable $(\epsilon T)^{-1}$ as had first been proposed by Mecke for the evaluation of non-aqueous electrolyte solutions.[13] Such a plot is shown in Fig. 6.

While the aminophenol exhibits no anomaly, i.e., its dissociation is a unique function of ϵT, the dissociation of the triacetate salt may involve a further variable, in that the dissociation at the higher temperature appears to be systematically smaller than that at 30°. This deviation reflects only the "loss" of ionogens due to simultaneous molecular dissociation. The data can be brought to coincidence on a single line (within the rather poor experimental accuracy) by correcting for molecular dissociation in butanone.

The quantitative evaluation of the dissociation constant from the degree of dissociation requires either the knowledge or an assumption of the stoichiometry of the dissociation process in the solution. Assumption of dissociation like a uni-univalent electrolyte leads to the relation $K_i = \alpha^2$ at low degrees of dissociation. The process suggested by the melt data, namely, the simultaneous dissociation of both *ortho* acetate groups, leads to $K_i = \alpha^3$ at low degrees of dissociation. The thermodynamic parameters which can be obtained from the information in Fig. 6 are

$$\Delta F_i = RT \ln K_i = Q_n + \frac{A_i}{\epsilon} - 2T \, \Delta S_i$$

where Q_n = heat of neutralization of the ions, A_i = work of dissociation = $R(\partial \log K_i / \partial (\epsilon T)^{-1}) T$, and ΔS_i = entropy of dissociation = $R \ln K_i$ at $(\epsilon T)^{-1} = 0$. The resulting data are assembled in Table IV. It is noteworthy, and of course to be expected, that the value of Q_n is essentially identical for the solutions in toluene and in 2-butanone. The magnitude of the parameters does not differ very much from the values published for other non-aqueous ionized systems.

TABLE IV

Thermodynamic Properties Governing the Ionic Dissociation of TDMP-Triacetate in Two Solvents at 30°

Solvent	Free energy of dissociation ΔF_i, kcal./mole	Heat of neut., Q_n, kcal./mole	Work of ion separation, A_i, mole	Entropy dissociation, ΔS_i, e.u.
Toluene	30.6	24.08 ⎫	⎫	
2-Butanone	10.3	24.37 ⎬	56.6 ⎬	27.4

The *dissociation of TDMP triacetate in the resin system* can now be estimated by interpolation between the data for toluene solution ($\epsilon_{25} \sim 2.38$) and 2-butanone ($\epsilon_{20} = 18.5$), since the dielectric constant of the liquid resin precursor (EPON 828) is about 8.3.[14] At the usual concentration of catalyst (about 8%w.) and at 80°, the observed cure temperature, ionic dissociation of the salt

(13) R. Mecke and H. Zeininger, Z. Elektrochem., **52**, 49 (1948); **54**, 174 (1950).

(14) Kindly determined by Dr. C. H. Klute in this Laboratory.
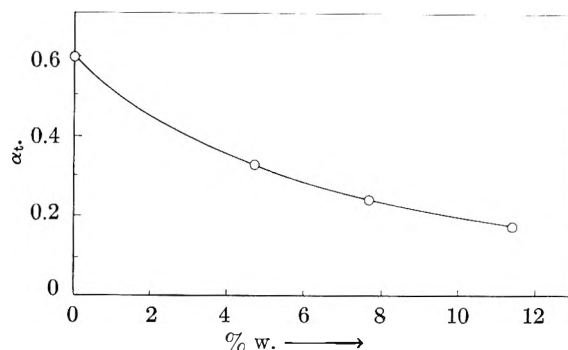
Fig. 4.—Total degree of dissociation of TDMP-triacetate in 2-butanone at 80° (from ebullioscopic data).
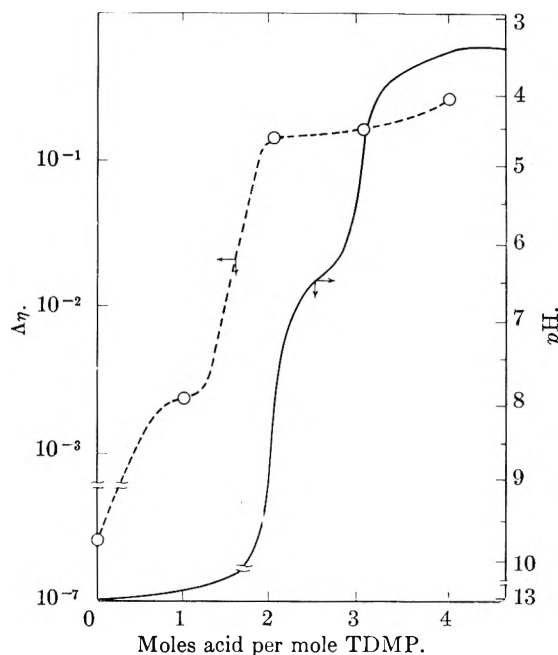
Fig. 5.—Change of ionic dissociation of TDMP upon additions of acid at 30°. Broken curve shows the change of $\Delta\eta$ of the melt upon addition of acetic acid, the continuous curve gives the change of pH of an aqueous solution of TDMP upon addition of HCl.

should be of the order of 0.01%. Molecular dissociation should be less than 25% (the extent observed in butanone solution) and probably more than about 8%, the linear interpolation value.

Catalytic Activity of the Salt.—Quantitative evaluation of the reactivity of cross-linking catalysts is exceedingly difficult owing to the lack of simple means to estimate the reaction rate. An approximate measure of the reaction rate is the rate of heat release in this exothermic reaction. For rapid evaluation it is convenient to conduct the reactions adiabatically by simply following the temperature rise of a thermocouple embedded in the center of a 2-inch cube of polymer during the curing process. A few measurements have also been carried out (by Dr. D. J. Meier) in the more nearly isothermal differential thermal analyses. Evaluation of the reaction rate from the adiabatic experiments indicated that the triacetate of a given amount of TDMP exhibits about 70 to 80% of the activity of the free amine. The differential thermal analyses, shown in Fig. 7, demonstrate also in a qualitative
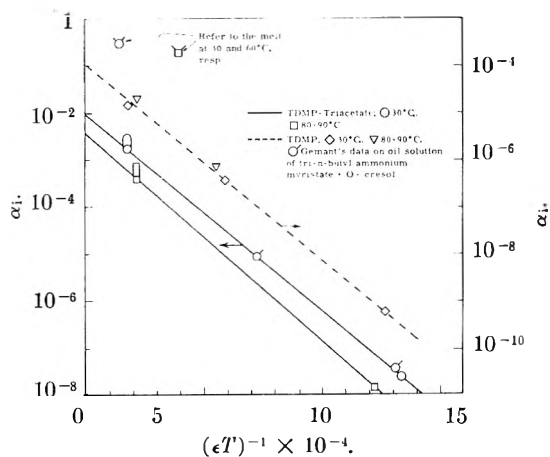
Fig. 6.—Relation between degree of ionic dissociation, α_i dielectric constant ϵ of the solution and temperature.

manner how much more the amine triacetate catalyzed reaction resembles that catalyzed by the same amount of free amine than that catalyzed by half the amount of free amine.

While the higher total heat release during the acetate catalyzed reaction is undoubtedly real (it is displayed also in the adiabatic reaction and can be associated with the esterification of the acetic acid by epoxide groups), the early hump in the triacetate curve "C" is probably an instrumental artifact.
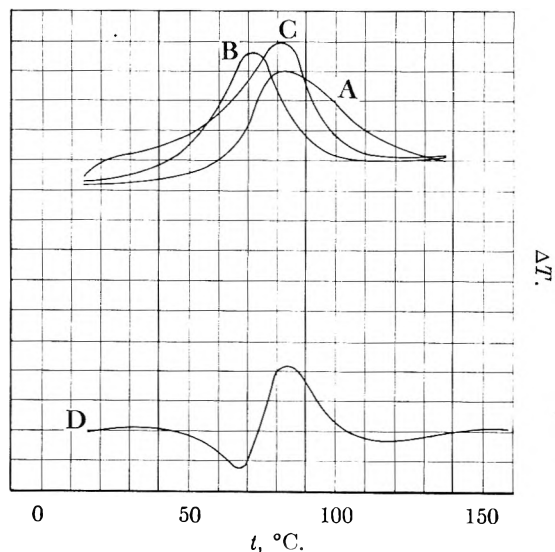
Fig. 7.—Differential thermal analysis of the catalyzed condensation (curing) of epoxide resin EPON 828: A, catalyzed by 5 parts TDMP; B, catalyzed by 10 parts TDMP; C, catalyzed by 10 parts TDMP + 6.8 parts acetic acid; D, the temperature differential between samples B and C in a repeat run. The heating rate of the reference cell was uniformly 1°/min.; ΔT in arbitrary units.

The relatively small differences between the curves B and C are accentuated in curve D, depicting the temperature difference between an acetate and a free amine catalyzed polymer during the curing process. This measurement shows the low temperature start of the reaction by the free amine and the higher heat release rate of the acetate catalyzed reaction once it gets underway.

The "degree of cure" of the finished resin as measured by physical properties, such as thermal shock resistance, also indicates an activity of the amine triacetate equivalent to more than 60% of the amine contained therein.

The temperature coefficient of catalyst activity is apparent from the "pot life" of the monomer-catalyst mixture. For the triacetate it is >18 hr. at room temperature, >2.5 hr. at 60° and at 80° full cure is obtained within 2 hr. For TDMP the corresponding figures are 0.5 hr. at room temperature and full cure at 80° in less than 1 hr., at 5.5% amine.

Proposed Mechanism of Polymerization Catalysis by Amine Carboxylates.—The sharp temperature dependence and the high amine-equivalence of the reactivity of the amine carboxylate catalyst appear incompatible with the small temperature coefficient and the relatively small extent of dissociation (molecular and ionic) of this salt, estimated in the previous sections. If there were a mechanism, however, which withdrew the acid from the partially dissociated salt, all of the amine would become ultimately available as catalyst for the curing reaction. The rate at which the acid was withdrawn would then determine rate at which the catalyst became available and thereby, in effect, the reactivity of the catalyst. The temperature coefficient of catalyst reactivity would then not be the relatively low heat of dissociation (of TDMP-triacetate) but the probably large energy of activation of the acid withdrawal reaction.

Such an acid withdrawal reaction is the well-known esterification of epoxides to form glycol monoesters. As a typical reaction mixture contains 0.52 eq./100 g. of epoxy groups and 0.05 eq./100 g. of acetic acid (in the catalyst), the latter can be removed easily by esterification without markedly affecting the over-all polymer. The epoxide esterification rate is, indeed, sharply temperature dependent, should be proportional to the concentration of reactants, and is catalyzed by the amounts of ionized acid available from the amine salt. The "activation temperature" of the catalyst is then just the point at which acid is esterified at the rate at which amine has to be available to sustain the rapid EPON condensation reaction. Unfortunately, this picture must remain qualitative as long as there are no quantitative data on the epoxide acetylation rate.

The proposed mechanism is supported by indirect evidence. EPON 828 resin containing TDMP carboxylate exhibits neutral pH before beginning the reaction but becomes basic rapidly as soon as gelation commences. If the acid had not been consumed, the reaction should have remained neutral. The ~15% increase in total heat release brought about by the acetic acid is in agreement with expectation from the known values of the heats of epoxide condensation and esterification. Moreover, if the amine carboxylate had remained in the resin, its electrical properties should have reflected the very high conductivity of that salt. Actually, however, the electrical properties of resin cured with amine carboxylate are virtually in-

distinguishable from those cured with free amine (Table V). This observation, in the face of the notorious sensitivity of the dissipation factor to conducting impurities, precludes the presence of more than traces of amine carboxylate in the cured resin. The proposed mechanism of catalysis appears to be well supported by the properties of the material.

TABLE V

COMPARISON OF ELECTRICAL PROPERTIES[a] OF EPON CAST-INGS CURED WITH FREE AMINE AND WITH AMINE CARBOXYL-ATE

Property		TDMP	TDMP-car-boxylate
Dielectric constant, at 21°, $f = 10^2$ c./sec.		3.93	3.66
$f = 10^7$		3.78	3.42
85°, $f = 10^2$		4.32	3.80
$f = 10^7$		3.33	2.80
Dissipation factor, at 21°, $f = 10^2$ c./sec.		0.003	0.003
$f = 10^7$		0.018	0.021
85°, $f = 10^2$		0.03	0.01
$f = 10^7$		0.03	0.03

[a] Kindly determined by Dr. C. H. Klute.

After completion of this manuscript, Shechter and Wynstra[15] presented a series of papers giving rather good experimental evidence for the postulated ion catalyzed epoxide–carboxylic acid reaction in the presence of tertiary amine. But their data are still insufficient for quantitative evaluation of the mechanism.

Conclusions.—1. The bond between tertiary amines and carboxylic acids appears to be quite strong, as judged by molar volume contraction when they form the salt. 2. Molecular dissociation of the phenolic amine carboxylate (TDMP-triacetate) under consideration at 80° is of the order of 20% in the melt and in 2-butanone solution and is essentially absent in toluene solution. 3. Ionic dissociation—measured by the Walden product $\Lambda\eta$—is rather extensive in the melt (about 20%), but for all solutions tested it is small and its

(15) L. Shechter and J. Wynstra, Div. of Paint Plastics and Printing Ink Chemistry, Am. Chem. Soc. Meeting, Cincinnati, April, 1955, preprint p. 280.

logarithm is an inverse function of the product ϵT. 4. The TDMP as triacetate exhibits within 70 to 80% of the reactivity of the free amine as epoxide resin curing catalyst. 5. The contradictory nature of the small extent of dissociation and the catalytic activity of the amine carboxylate is resolved by proposing that the catalytic activity of this salt is determined by the rate at which the acid component is esterified by the bulk monomer rather than by the extent of amine salt dissociation. This mechanism is supported by several auxiliary observations.

Experimental

The electrical conductivity measurements on the melt were carried out with blacked platinum electrodes and a Leeds and Northrup Resistance Bridge.

The electrical measurements on the solutions were carried out in a Balsbaugh cell.[16] The a.c. dielectric constant and dissipation factor were measured with a Type 716C General Radio Bridge and a suitable oscillator. The d.c. conductivity was determined with the aid of a wide range electronic multimeter.[17–19]

Because of the very pronounced polarization effects (time variable resistance values) with most of the solutions in low voltage d.c. measurements, the a.c. conductivity results were employed in the calculation of equivalent conductance Λ, wherever possible. The dissipation factors in the butanone solutions were too large, however, to permit accurate a.c. measurements. The d.c. conductivity of these solutions was therefore measured under a potential of 95 volts to overpower the polarization effects. A disagreeable side effect of this high voltage was rapid electrolysis of the more concentrated triacetate solution to an unidentified insoluble compound and considerable heat liberation. Only the conductivity determined at low concentrations in butanone has therefore been used for the calculations. Even these are probably not very accurate.

(16) J. C. Balsbaugh and A. H. Howell, *Rev. Sci. Instr.*, **10**, 194 (1939).

(17) C. J. Penther and A. Bondi, THIS JOURNAL, **57**, 540 (1953).

(18) A. A. Maryott and E. R. Smith, "Table of Dielectric Constants of Pure Liquids," Natl. Bur. Stand. Circular 514, 1951.

(19) Rohm and Haas Co., Catalog of Dimethylaminomethyl Phenols, 1947.

THE LIQUID DENSITY, VAPOR PRESSURE AND CRITICAL TEMPERATURE AND PRESSURE OF NITROGEN TRIFLUORIDE[1,2]

By Roger L. Jarry and Henry C. Miller

Pennsylvania Salt Manufacturing Co., Research and Development Department,
Whitemarsh Research Laboratories, Wyndmoor, Pa.

The liquid density of nitrogen trifluoride has been measured over the temperature range 78 to 170°K. These data have been fitted to the equation $d(\text{g./cm.}^3) = 2.103 - 3.294 \times 10^{-3}\, T - 4.675 \times 10^{-6}\, T^2$. The estimated uncertainty in the measured values is ±0.1%. Vapor pressures have been measured to the critical point and are represented to a precision of ±0.17 atm. by the equation $\log_{10} P(\text{atm.}) = 4.27264 - 613.330\, T^{-1}$. The vapor pressures have been measured to one atmosphere with a higher order of precision and the data have been fitted to the Antoine equation: $\log_{10} P(\text{mm.}) = 6.77966 - 501.913/T - 15.37$. The normal boiling point calculated from the Antoine equation is 144.10°K. Temperature was known in all cases to ±0.05°. The critical temperature is 233.90 ± 0.10°K., the critical pressure is 44.72 ± 0.17 atm.

Introduction

As part of a program at this Laboratory on the physical properties of fluorine compounds, various properties of nitrogen trifluoride have been measured. The temperature range over which the liquid density had been previously measured by Ruff[3] has been considerably extended by this study. Vapor pressures were checked against the data of Pierce and Pace[4] and extended to the critical point. The high vapor pressures and the critical constants have not appeared in the literature heretofore.

Apparatus and Procedure.—The density was measured between 97 and 170°K. using an all-metal apparatus, described in a previous publication.[5] This system allowed measurements to be made to 5 atm. pressure. For the lower temperature measurements a dilatometer comprising a glass bulb of about 4 cm.³ volume connecting to the gas system by means of 2 mm. i.d. capillary tubing was used. Ten cm. of this capillary tubing immediately above the bulb was calibrated along with the bulb using mercury. The bulb of the dilatometer was enclosed in a copper block and a second block placed about the capillary tubing above the calibrated section. This upper block was equipped with a heat leak which dipped into the refrigerant used, liquid nitrogen. The entire assembly was enclosed within a vacuum shield. By means of heaters on the two blocks and the heat leak the temperature of the blocks could be adjusted so as to have a minimum temperature differential over the calibrated 10 cm. of the capillary. By this means measurements could be made over the full length of the calibrated section.

The nitrogen trifluoride was condensed into the measuring devices from calibrated volumes in an air thermostat. Since the range of determinations in the two devices overlapped, and the dilatometer required several fillings, the precision of filling by the volumation method could be readily checked.

Vapor pressures were measured in the metal system in which the density device had been replaced by a nickel container connected by means of $^1/_8$ in. nickel tubing to the sensing unit. Pressures to two atmospheres were read on a mercury manometer by means of a cathetometer to a precision of ±0.05 mm. Pressures to the critical point were taken on a 1000 p.s.i.g. Bourdon gage with an accuracy of ±0.25% of the total scale.

Critical temperature was measured on samples sealed in 2 mm. i.d. capillary tubing. This tube was placed directly into a bath of cold acetone; temperature was controlled by a heater immersed in the bath and/or the addition of cold acetone. The disappearance and reappearance of the meniscus was noted by several observers and an average value of temperature used.

Temperature was measured by means of a capsule type platinum resistance thermometer, or by means of thermocouples which had been compared with the thermometer. The thermometer had been compared with the National Bureau of Standards temperature scale. During the equilibrium periods of 15–20 min. during which measurements were taken the temperature drift in the metal system or the dilatometer were no more than 0.002°/min. and 0.004°/min., respectively.

Material.—The nitrogen trifluoride was prepared by the electrolysis of molten ammonium bifluoride as described by O. Ruff and co-workers.[6] A nickel anode was used to prevent the formation of carbon tetrafluoride. The crude gas resulting from the electrolysis was purified by low temperature filtration and distillation using a still set-up and controls as described by Booth and Jarry.[7] As a check of the purity, both infrared spectra and the freezing point were determined. The infrared scans were compared with the data of Wilson and Polo[8] and later of Pace and Pierce.[9] The spectra found for the purified material corresponded to the later work with its inclusion of two peaks, at 7.8 and 6.45 μ which appear to be part of the nitrogen trifluoride spectra and were not reported by Wilson and Polo. The freezing point was determined on two samples and gave an average value of 66.49°K. as compared to the value of 66.37°K. given by Pierce and Pace.[10]

Preliminary toxicity studies were made on the crude nitrogen trifluoride (approx. 90% NF₃, the remainder probably N₂O). These tests indicated a moderate degree of hazard. The main toxic effect of this compound appears to be irritation of the lung tissue comparable to the nitrogen oxides, but requiring higher concentrations, and recovery from non-lethal exposure seems to be rather complete. Irritation of the external mucous membranes cannot be used as a warning sign as this appears at concentrations (4000 p.p.m.) affecting the lungs.

Results and Discussion

The data for the liquid density are given in Table I, and have been fitted to the equation

$$d = 2.103 - 3.294 \times 10^{-3}\, T - 4.675 \times 10^{-6}\, T^2 \quad (1)$$

where d is the density in g./cm.³ at the absolute temperature T.

Deviations between the experimental and values calculated using eq. 1 are given in column 3 of Table I. A comparison with the previous data of Ruff[3] shows good agreement, with his data being generally 0.2–0.3% lower. The precision of these measurements is estimated to be ±0.1%. The volume values for the glass bulb were corrected using the

(1) Presented at the Delaware Valley Regional Meeting, Philadelphia, February 16, 1956.

(2) This paper represents the results of one phase of research carried out under Contract No. 18(600)-761, supported by the United States Air Force through the Air Force Office of Scientific Research of the Air Research and Development Command.

(3) O. Ruff, *Z. anorg. allgem. Chem.*, **197**, 273 (1931).

(4) L. Pierce and E. L. Pace, *J. Chem. Phys.*, **23**, 551 (1955).

(5) R. L. Jarry and H. C. Miller, *J. Am. Chem. Soc.*, **78**, 1552 (1956).

(6) O. Ruff, J. Fischer and F. Lutz, *Z. anorg. allgem. Chem.*, **172**, 417 (1928).

(7) H. S. Booth and R. L. Jarry, *J. Am. Chem. Soc.*, **71**, 971 (1949).

(8) M. K. Wilson and S. P. Polo, *J. Chem. Phys.*, **20**, 1716 (1952).

(9) E. L. Pace and L. Pierce, *ibid.*, **23**, 1248 (1955).

(10) L. Pierce and E. L. Pace, *ibid.*, **22**, 1271 (1954).

TABLE I

THE DENSITY OF LIQUID NITROGEN TRIFLUORIDE BETWEEN
78 AND 170°K. (0°C. = 273.16°K.)

Temp., °K.	Density, g./cm.^{3}	Dev. obsd. − calcd.	Temp., °K.	Density, g./cm.^{3}	Dev. obsd. − calcd.
78.05	1.819	0.002	119.53	1.643	0.001
79.10	1.814	.001	124.50	1.621	.000
79.44	1.812	.001	129.42	1.600	.001
81.68	1.802	−.001	131.06^a	1.593	.002
87.23	1.780	.000	134.23	1.580	.003
87.66	1.775	−.003	135.35^a	1.574	.003
92.22	1.760	.001	139.16	1.558	.004
94.27	1.748	−.002	139.94^a	1.552	.002
97.01	1.740	.001	144.00	1.536	.004
99.45	1.727	−.002	144.66^a	1.530	.002
101.79	1.720	.000	149.34^a	1.508	.001
104.07	1.708	−.001	153.93^a	1.484	−.001
109.91	1.683	−.002	158.53^a	1.461	−.003
114.79	1.663	.000	164.16^a	1.434	−.002
119.47	1.643	.001	169.54	1.406	−.004

^{a} Indicates the measurements made in the metal apparatus.

expansion coefficient data for Pyrex glass of Buffington and Latimer.[11] Temperature was known to ±0.05°.

The vapor pressure results are given in Table II. The data to one atmosphere were fitted to the Antoine equation by the method described by C. B. Willingham, et al.,[12] and the following equation derived

$$\log_{10} P(\text{mm.}) = 6.77963 - \frac{501.913}{T - 15.37} \quad (2)$$

The normal boiling point calculated using eq. 2 is 144.10°K., in good agreement with that of Pierce and Pace,[4] 144.15°K. The vapor pressure data to the critical point were fitted by the method of least squares to the equation

$$\log_{10} P(\text{atm.}) = 4.27264 - \frac{613.33}{T} \quad (3)$$

Deviations between the experimental and calcu-

(11) Buffington and Latimer, *J. Am. Chem. Soc.*, **48**, 2305 (1926).
(12) C. B. Willingham, *et al.*, *J. Research Natl. Bur. Standards*, **35**, 219 (1945).

TABLE II

THE VAPOR PRESSURE OF NITROGEN TRIFLUORIDE
(0°C. = 273.16°K.)

Temp., °K.	Pressure, mm.	Dev. obsd. − calcd. mm.	Temp., °K.	Pressure, atm.	Dev. obsd. − calcd. atm.
89.33	1.00	0.01	148.97	1.388	0.043
94.14	2.59	.03	153.80	1.884	.043
98.99	5.92	−.07	158.67	2.558	.004
103.87	12.84	.01	163.52	3.374	.049
108.58	24.79	−.05	168.40	4.326	.055
113.70	47.39	.04	173.36	5.551	.122
118.49	81.64	−.09	178.27	6.912	−.106
123.16	132.83	.01	183.16	8.544	.149
127.61	203.16	−.02	188.03	10.380	.129
131.95	297.96	−.13	193.15	12.490	−.009
136.08	418.31	−.14	198.06	15.006	+.011
140.17	573.08	+.39	203.14	17.796	−.126
144.18	764.26	+.21	208.02	20.925	−.172
			217.94	28.272	−.464
			222.96	32.830	−.326
			227.81	37.863	−.187
			232.78	43.510	.076

lated values for these two equations are given in column three of Table II. Temperature was known in these measurements to 0.05°. The heat of vaporization at the normal boiling point calculated using eq. 2 and a gas imperfection of −3.78%, derived from the Berthelot equation, is 2769 cal./mole. This value is the same as that obtained experimentally by Pierce and Pace.[4]

The critical temperature was determined to be 233.90 ± 0.10°K. From this value the critical pressure was calculated using eq. 3 to be 44.72 ± 0.17 atm.

A BOILING POINT METHOD FOR DETERMINATION OF VAPOR PRESSURES OF MOLTEN SALTS

BY J. L. BARTON AND H. BLOOM

Auckland University College, Auckland, New Zealand

A method has been developed for determining vapor pressure of fused salts by measuring their boiling points over a range of measured constant pressures. Superheating was prevented by passing a slow stream of nitrogen bubbles through the melt and the temperature of the boiling liquid was measured directly. The reliability of the method has been demonstrated for NaCl, KCl, CdCl₂, and PbCl₂. The heats of vaporization and normal boiling points of the four salts have been calculated.

In only very few cases are the vapor pressures of molten salts known to a reasonable degree of accuracy.[1] Many methods have hitherto been used for such determinations, but the results of different investigators vary considerably. The

(1) K. K. Kelley, Bureau of Mines Bull. No. 383 (1935).

purpose of this investigation was to develop a reliable method for the measurement of vapor pressure of fused salts and to establish accurate vapor pressure data for pure NaCl, KCl, CdCl₂ and PbCl₂ prior to an investigation of binary mixtures of these salts.

The methods available for determination of vapor pressure may be divided into two categories: absolute and non-absolute

Non-absolute methods include the Knudsen effusion and the transpiration techniques. Both require a knowledge of the molecular weight of the vapor. As it is becoming increasingly evident that salt vapors at high temperatures do not always consist of the simplest molecular species,[2,3] methods which require a knowledge of molecular weight of the vapor are best avoided. These methods are, however, useful in obtaining information on the molecular weight of vapors when the vapor pressure is known. The transpiration method has yet other disadvantages—the possibility of under-saturation of the gas stream, thermal segregation and diffusion. This method has been used extensively by Jellinek and co-workers.[4]

Absolute methods may be divided into boiling point and static techniques. Both have been used for molten salts. Static methods have certain disadvantages, viz., the difficulty of removing all adsorbed gases from the sample before sealing it off and the difficulty of finding suitable refractory materials to form the relatively complicated high temperature part of the apparatus.

Rodebush and Dixon[5] developed a "quasi-static" method in which the sample is not sealed off. This method does not suffer from the drawbacks of static methods.

In the present investigation, a boiling point method was considered attractive because of its fundamental simplicity and because small amounts of gaseous impurities in the sample do not cause error. The main difficulties lie in the measurement of temperature and the elimination of superheating. A boiling point method was used by von Wartenburg, et al.,[6-8] to determine the vapor pressures of some thirty-three salts, but otherwise it has been used for molten salts in only a few instances.[9,10] Previous investigators using this method have not generally attempted to eliminate superheating. At moderate temperatures, the effect of superheating may be avoided by measuring the temperature of the condensing vapor. At high temperatures, however, the rapid interchange of heat between a thermocouple in the vapor and the walls of the container (which are generally at a higher temperature) can lead to erroneous results. The error may be reduced by radiation shields. In the present investigation the temperature of the boiling liquid was measured after ascertaining that superheating had been prevented.

Preliminary investigations showed that without adequate precautions the melts tended to superheat, particularly at pressures less than 50 mm.

This superheating probably accounts for the irregularities in the data reported by previous investigators who used boiling point methods. Superheating was prevented in this case by passing a slow stream of nitrogen bubbles through the melt. It will be shown from the steady boiling temperatures that true vapor pressures of the molten salts can be derived.

Experimental

Materials Used.—Sodium and potassium chlorides were of analytical reagent quality. Lead chloride was precipitated from a solution of analytical reagent lead nitrate by analytical reagent hydrochloric acid.[11] Cadmium chloride was prepared from electrolytic cadmium (supplied by the Electrolytic Zinc Co. of Australia, Ltd.) and gaseous chlorine.[12]

Apparatus.—Heating was carried out in a 13% rhodium-platinum wound electric furnace controlled by variable voltage transformers. The temperatures of the furnace and the inside melt were measured by standardized 13% rhodium–platinum versus pure platinum thermocouples and a Tinsley precision potentiometer. The refractory tubes were of impervious mullite or silica. Silica was found to be quite satisfactory as high as 1300° provided oxygen was completely excluded. The melt (3 to 4 cm. in depth) was held in a refractory tube of length 18 inches, closed at the bottom. The length of the tube situated in the furnace was approximately 8 inches. Into the melt was inserted a double bore insulator (24 inches long) of sillimanite, the lower end being 0.5 cm. from the bottom of the tube. This insulator conducted the thermocouple into the melt, the wires being bent upwards so as to situate the junction just below the surface of the melt. Pure dry nitrogen was passed into the melt at a rate of approximately 2 bubbles per second through the bores of the insulator, the rate of bubbling (indicated by a butyl phthalate bubbler) being controlled by a valve similar in principle to that described by Wansbrough–Jones.[13] Sealing of the upper end of the boiling point apparatus was accomplished by a rubber gland which had holes for the admission of tubes containing the thermocouple, etc. To prevent overheating of this gland, a silica air condenser was inserted into the boiling point tube through a hole in the gland to lower the condensation level of the vapor. The boiling tube was lagged with asbestos wool for 4 inches above the level of the furnace to prevent solidification of the liquid condensed salt in this region. Pressure in the apparatus was controlled by a rotary oil pump connected to two Lewis type manostats[14] in series. The first contained a fine sintered glass disk for rough control of pressure and the second, a medium porosity disk for fine control of the pressure in the boiling point apparatus. Stability was accomplished by allowing a controlled leak of air into the high pressure end of the manostat system. Pressure was measured by a closed end mercury manometer read by means of a precision cathetometer. Pressure remained constant to ±0.1 mm. throughout an experiment.

Procedure.—With the apparatus assembled as above, the furnace temperature was raised at the rate of 2–10° per minute, while a steady stream of nitrogen was being bubbled throughout the melt. The boiling point was indicated by the steady temperature maintained by the thermocouple in the melt in spite of the continued rise of temperature registered by the furnace thermocouple. This procedure was repeated for various applied pressures from 15 mm. to about ²/₃ atmosphere.

Accuracy.—Temperature was measured to ±0.5° and pressure to ±0.1 mm.

Results and Discussion

The vapor pressure (P) may be expressed as a function of temperature $(T°,K.)$ by equations of the type

(2) L. Brewer and J. S. Kane, THIS JOURNAL, **59**, 105 (1955).

(3) E. W. Dewing, ibid., **77**, 2639 (1955).

(4) K. Jellinek and G. A. Rosner, Z. physik. Chem., **A143**, 51 (1929); H. Hintz and K. Jellinek. Z. Elektrochem., **42**, 187 (1936).

(5) W. H. Rodebush and A. L. Dixon, Phys. Rev., **26**, 851 (1925).

(6) H. von Wartenburg and P. Albrecht, Z. Elektrochem., **27**, 162 (1921).

(7) H. von Wartenburg and H. Schulz, ibid., **27**, 568 (1921).

(8) H. von Wartenburg and O. Bosse, ibid., **28**, 384 (1922).

(9) L. Hackspill and R. Grandadam, Ann. Chim., **5**, 218 (1926).

(10) D. N. Tarasenkov, A. N. Grigorovich and A. V. Bogoslovskaya, J. Gen. Chem. (USSR), **5**, 924 (1935).

(11) H. Bloom and D. Rhodes, THIS JOURNAL, **60**, 791 (1956).

(12) J. Barton, H. Bloom and N. E. Richards, Chem. and Ind., 439 (1956).

(13) O. H. Wansbrough-Jones, Proc. Roy. Soc. (London), **A127**, 530 (1930).

(14) J. M. O'Gorman, Ind. Eng. Chem. (Anal. Ed.), **19**, 506 (1947).

$$\log_{10} P = \frac{-\Delta H_0}{2.303R} T^{-1} + \frac{\Delta C_p}{2.303R} \log_{10} T + I \quad (1)$$

ΔH = heat of vaporization per mole, ΔC_p = heat capacity of vapor minus heat capacity of liquid and I is an integration constant. The values of ΔC_p used are for NaCl, -7; KCl, -7; CdCl$_2$, -10 and PbCl$_2$, -13.2 cal. deg.$^{-1}$ mole^{-1}. Similar values are used by Kelley.[1] In each case equation 1 with the experimentally determined constants ΔH_0 and I expresses the relation between experi-
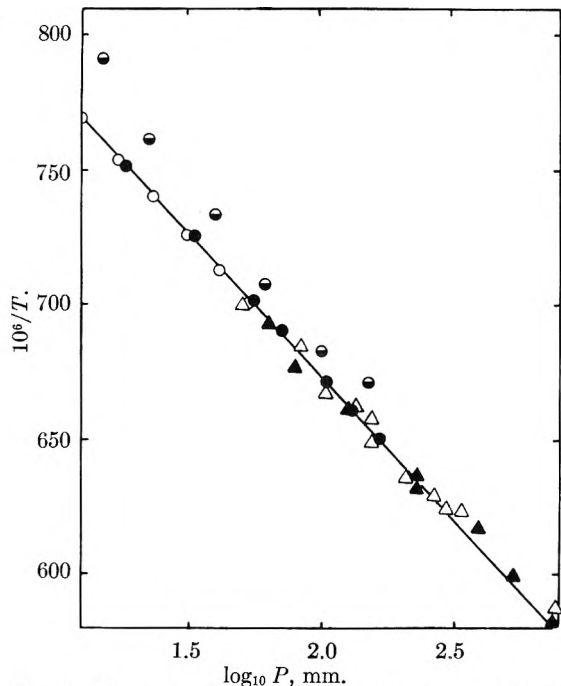
Fig. 1.—Vapor pressure of NaCl: this work, ●; Horiba and Baba,[20] ◐; Fiock and Rodebush,[15] ○; Ruff and Mugden,[21] ▲; Von Wartenburg and Albrecht,[6] △.
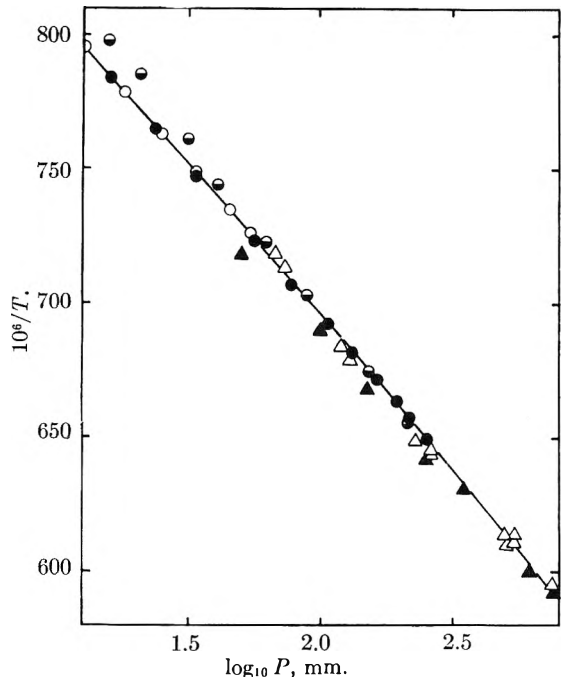
Fig. 2.—Vapor pressure of KCl: this work, ●; Horiba and Baba,[20] ◐; Fiock and Rodebush,[15] ○; Ruff and Mugden,[21] ▲; Von Wartenburg and Albrecht,[6] △.
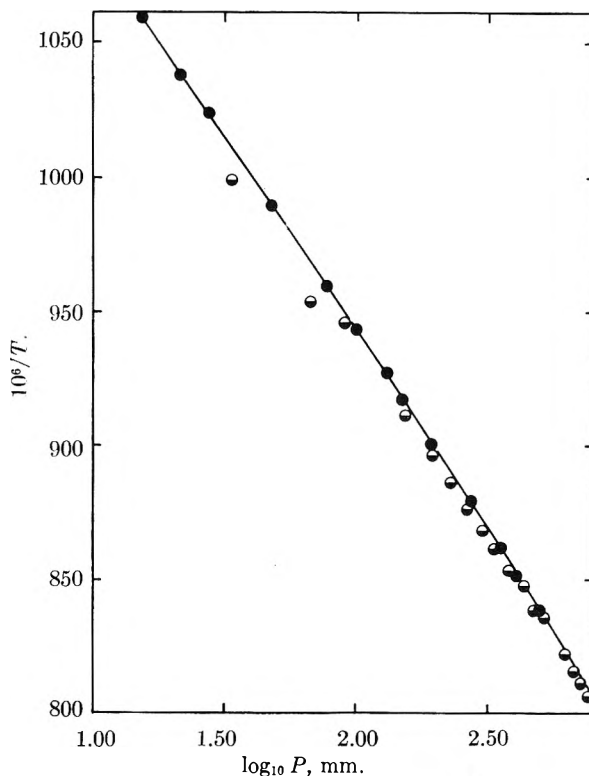
Fig. 3.—Vapor pressure of CdCl$_2$: this work, ●; Maier[16] ◐.
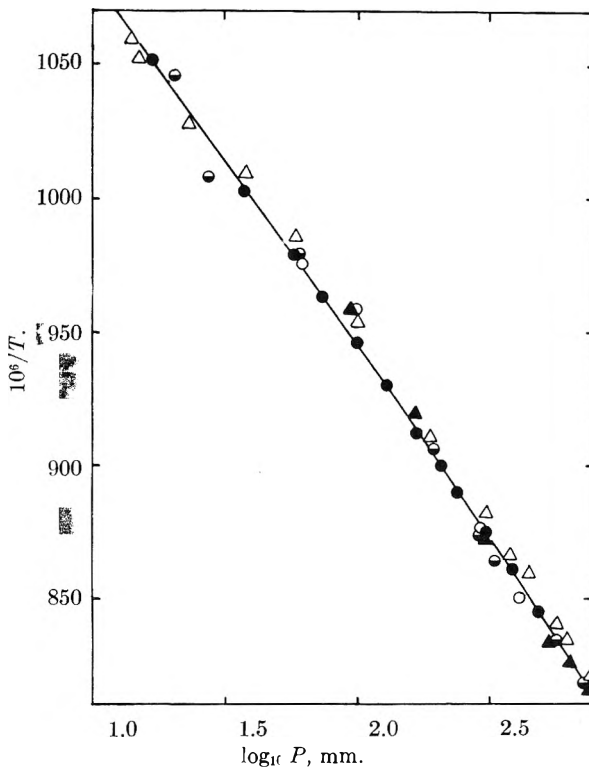
Fig. 4.—Vapor pressure of PbCl$_2$: this work, ●; Maier,[16] ◐; Jahn-Held and Jellinek,[19] ○; Von Wartenburg and Bosse,[8] ▲; Tarasenkov, et al.,[10] △.

mental values of log P and T to within 1%. In all cases the boiling point from equation 1 can be estimated within experimental accuracy (standard deviation ±1°).

The relation between log P and T for the salts investigated is shown in Table I.

TABLE I

VAPOR PRESSURE EQUATIONS

(P in mm. T in °K.)

NaCl $\log_{10} P = -11,495T^{-1} - 3.526 \log_{10} T + 20.929$

KCl $\log_{10} P = -11,023T^{-1} - 3.526 \log_{10} T + 20.798$

CdCl$_2$ $\log_{10} P = -9,183T^{-1} - 5.04 \log_{10} T + 25.907$

PbCl$_2$ $\log_{10} P = -10,168T^{-1} - 6.65 \log_{10} T + 31.726$

The experimental results, together with those of previous investigators, are shown in Figs. 1, 2, 3 and 4, respectively. In each figure the derived vapor pressure equation of Table I is represented by the solid line.

The heat of vaporization is obtained from the measured values of the constants in equation 1. The values of heats of vaporization for the salts investigated are given in Table II, in which they are compared with earlier results quoted by Kelley.[1]

TABLE II

HEAT OF VAPORIZATION ΔH, KG. CAL. MOLE^{-1}

	This work	Kelley	Source of Kelley's data
NaCl	$52.6 - 7.0 \times 10^{-3}T \pm 0.4$	$52.8 - 6.9 \times 10^{-3}T$	15
KCl	$50.4 - 7.0 \times 10^{-3}T \pm 0.2$	$50.6 - 7.0 \times 10^{-3}T$	15
CdCl$_2$	$42.0 - 1.0 \times 10^{-2}T \pm 0.2$	$42.3 - 1.0 \times 10^{-2}T$	16–18
PbCl$_2$	$46.5 - 1.32 \times 10^{-2}T \pm 0.2$	$45.8 - 1.32 \times 10^{-2}T$	16, 17

NaCl and KCl.—The measurements by Fiock and Rodebush[15] are the most self consistent of any previous investigations on these salts. (The standard deviations of temperature from the equations they derive are no higher than ±0.8°). The "quasi-static" method employed by these investigators has been checked carefully by Rodebush and Dixon[5] for mercury giving results which were in excellent agreement with previously accepted

(15) E. F. Fiock and W. H. Rodebush, J. Am. Chem. Soc., **48**, 2522 (1926).

(16) C. G. Maier, Bureau of Mines Technical Paper No. 360 (1925).

(17) B. Greiner and K. Jellinek, Z. physik. Chem., **A165**, 97 (1933).

(18) F. Volmer, Physik. Z., **30**, 590 (1929).

(19) W. Jahn-Held and K. Jellinek, Z. Elektrochem., **43**, 491 (1937).

(20) S. Horiba and H. Baba, Bull. Chem. Soc. Japan, **3**, 11 (1928).

figures—hence the values by the former authors for the vapor pressures of NaCl and KCl are considered to be reliable. A comparison of the present heat of vaporization values with those of Fiock and Rodebush shows satisfactory agreement. The heats of vaporization (in kg. cal. mole^{-1}) obtained by Fiock and Rodebush are 43.1 ± 0.2 for NaCl and 41.7 ± 0.2 for KCl. At the mean temperatures of their experiments, the values calculated from our equations are 43.2 ± 0.4 (1339°K.) and 41.4 ± 0.2 (1279°K.), respectively. At a given vapor pressure our measured temperature is an average of 4° higher for NaCl and 1.5° lower for KCl, than the corresponding values of Fiock and Rodebush. From our results we have calculated the boiling point at 760 mm. pressure, obtaining for NaCl, 1734°K. (cf. von Wartenburg and Albrecht[6] 1712°, Ruff and Mugden[21] 1715°, Kelley[1] 1738°), and for KCl, 1686°K. (cf. von Wartenburg and Albrecht[6] 1690°, Ruff and Mugden[21] 1688° and Kelley[1] 1680°).

CdCl$_2$.—The best previous data are those of Maier[16] who claimed only "technical accuracy." From Fig. 3, it can be seen that Maier's results have considerable scatter at pressures less than approx. 100 mm. The equations for ΔH from Table II, show that our value agrees very well with that calculated by Kelley. Our value of the boiling point at 760 mm. is 1233°K. (cf. Maier[16] 1243°, Kelley[1] 1240°).

PbCl$_2$.—Our data are more self consistent than that of previous investigators especially at pressures below 200 mm. Kelley's estimate of ΔH for this salt is approximately 1 kcal. too low. Our value of the boiling point at 760 mm. is 1224°K. (cf. von Wartenburg and Bosse[8] 1227°, Maier[16] 1227°, Tarasenkov, et al.,[10] 1215° and Kelley[1] 1227°).

(21) O. Ruff and S. Mugden, Z. anorg. allgem. Chem., **117**, 147 (1921).

THE REACTION BETWEEN PU(III) AND OXYGEN IN AQUEOUS SULFATE SOLUTIONS[1]

BY T. W. NEWTON AND F. B. BAKER

University of California, Los Alamos Scientific Laboratory, Los Alamos, New Mexico

Received May 7, 1956

The rate of oxidation of Pu(III) by oxygen in aqueous sulfate solutions has been investigated at 25° at an ionic strength of 2. The initial reaction is $2Pu(III) + 2H^+ + O_2 = 2Pu(IV) + H_2O_2$. Its rate was found to be first power in O_2, second power in Pu(III), zero power in Pu(IV), and essentially zero power in H^+ concentration. The rate depends on the $SO_4^=$ concentration in a complicated way which may be explained on the basis of reaction by two parallel paths, one involving two and the other involving three sulfate groups in the activated complexes. In one run at 35° the rate was found to be about 2.9 times as fast as at 25° in solutions with the same concentrations of reactants. This leads to an over-all average activation energy of about 19 kcal.

Introduction

It is known that the oxidation of Pu(III) to Pu(IV) by oxygen is very slow in solutions of HCl or $HClO_4$.[2] In these solutions the potential for oxidation of Pu(III) to Pu(IV) is about -0.98 v.[3] In sulfuric acid solutions the reaction is measurably fast.[4] In 1 M H_2SO_4 the potential is about -0.75 v.[5] Many oxidations by oxygen in acid solutions are believed to involve H_2O_2 as an intermediate. The $H_2O_2-O_2$ couple has a potential of -0.68 v., and thus only strong reducing agents can form enough H_2O_2 to make the oxidation fast.[6] It has been suggested[4] that perhaps sulfate increases the rate of oxidation of Pu(III) because the existence of very stable Pu(IV)–$SO_4^=$ complexes makes Pu(III) a stronger reducing agent.

The purpose of the present investigation was to determine the rate law for the oxidation of Pu(III) by oxygen and to learn something of the mechanism of the reaction. It was found that relatively large amounts of H_2O_2 are formed as an intermediate in the oxidation and that although the rate depends strongly on the sulfate concentration, it does not depend on the Pu(IV) concentration. Thus the increased rate in sulfuric acid solutions is not due to the fact that Pu(III) is a better reducing agent there.

Experimental

Apparatus.—The oxidations were carried out in a cylindrical, jacketed Pyrex reactor of about 500-ml. capacity. Thermostated water was circulated through the jacket. Oxygen was introduced below the liquid surface and the contents of the reactor were stirred with a hollow Pyrex stirrer. The shaft of this stirrer emerged from the reactor through a Teflon bearing which was supported by a glass tube mounted in a rubber stopper in the top of the reactor. The stirrer was fashioned so that gas from above the liquid was pumped down through the hollow shaft and dispersed from holes in the rotating stirrer tips in the form of many tiny bubbles. A Teflon valve at the bottom of the reactor enabled samples to be withdrawn for analysis.

Spectrophotometric measurements were made with a Cary Recording Spectrophotometer, Model 14, No. 5. Potentiometric measurements were made with a Beckman Model G pH meter. A saturated calomel electrode was used for reference. This electrode was connected to the experimental solutions by means of a bridge containing 1 M H_2SO_4.

Reagents.—Stock solutions of $Pu(ClO_4)_3$ in $HClO_4$ were prepared by dissolving pure plutonium metal in standardized concentrated acid and diluting the resulting solution to the desired concentration. Stock solutions of $Fe(ClO_4)_2$ in $HClO_4$ were prepared by dissolving reagent grade iron wire in standardized dilute acid and diluting. The $HClO_4$ solutions were prepared by diluting concentrated acid and were standardized by titration. The perchloric acid used for the solutions described above was prepared by distilling reagent grade concentrated acid under reduced pressure. Stock solutions of Na_2SO_4 were prepared from reagent grade material which had been recrystallized from boiling water. Stock solutions of $NaClO_4$[7] were prepared by neutralizing reagent grade Na_2CO_3 with reagent grade $HClO_4$ and boiling out the CO_2. These last two stock solutions were analyzed by evaporating known volumes and heating to constant weight at 140°. The water used in all the solutions and experiments was doubly distilled, the second distillation from alkaline $KMnO_4$. The oxygen was from the laboratory supply and the air was water pumped from the room. These gases were purified by passing over CuO at about 700° and then scrubbing with alkaline $KMnO_4$ and dilute acid.[7] Before passing them into the reactor they were saturated with water vapor by passing them through a solution with a composition similar to that of the experimental one.

Rate Measurements.—The proper amounts of the various stock solutions, except for the plutonium, were put into the thermostated reactor. Oxygen (or air) was passed through the stirred solutions for at least 10 minutes before the plutonium stock solution was added. Periodically, samples were withdrawn for analysis as described below.

To show that the reaction was homogeneous, and not catalyzed by surfaces of the reactor, two separate experiments were made. In the first, the glass surface was increased by a factor of about 11 by the use of glass wool, and in the second the Teflon surface was increased by a factor of about 170. In neither of these runs was the rate increased by more than 5% compared with a similar run without glass wool or Teflon scrap. It has been concluded that the reaction is predominantly homogeneous.

The small effect found here due to glass wool is to be contrasted with that found for the oxygen oxidation of Fe(II) in phosphoric acid solutions.[8] For that reaction, Cher and Davidson found that when the glass surface was increased

(1) This work was done under the auspices of the U. S. Atomic Energy Commission. Presented in part at the 129th ACS Meeting in Dallas, Texas, April, 1956.

(2) R. E. Connick and W. H. McVey, paper 3.9, and K. A. Kraus and J. R. Dam, Paper 4.14. in "The Transuranium Elements," edited by G. T. Seaborg, J. J. Katz and W. M. Manning, National Nuclear Energy Series, Division IV, Vol. 14B, McGraw-Hill Book Co., Inc., New York, N. Y., 1949.

(3) R. E. Connick and W. H. McVey, J. Am. Chem. Soc., **73**, 1798 (1951); S. W. Rabideau and J. F. Lemons, ibid., **73**, 2895 (1951).

(4) R. E. Connick, in "The Actinide Elements," edited by G. T. Seaborg and J. J. Katz, National Nuclear Energy Series, Division IV, Vol. 14A McGraw-Hill Book Co., Inc., New York, N. Y., 1954, Chap. 8.

(5) J. J. Howland, Jr., J. C. Hindman and K. A. Kraus, ref. 2, Paper 3.3.

(6) W. M. Latimer, "The Oxidation States of the Elements and Their Potentials in Aqueous Solutions," Second Edition, Prentice-Hall, Inc., New York, N. Y., 1952, p. 44.

(7) A run made with recrystallized $NaClO_4$ gave a rate constant differing by less than 1% from that obtained from a similar run using non-recrystallized material. A run made with untreated oxygen gave rates essentially the same as a similar run using purified oxygen. Thus, either there are no critical impurities in these reagents, or the purification procedures removed none of them.

(8) M. Cher and N. Davidson, J. Am. Chem. Soc., **77**, 793 (1955).

by a factor of 15.8, the rate was increased by a factor of 1.78.

The measured rates were not limited by the rate of solution of oxygen in the experimental solutions. Except where it has been otherwise indicated, all runs were made at a stirring rate of 2000 r.p.m. or greater. At this rate, a great many very fine bubbles were stirred into the solution. To show that this gave an adequate rate of solution of oxygen, two runs were made which were identical except that in one the stirring rate was 2100 r.p.m., and in the other it was only 1000 r.p.m. At this lower rate, only a few bubbles were stirred into the solution. Conditions were chosen so that the rate of the reaction was as large as any studied. The apparent second-order rate constant for the run at the lower stirring rate was 0.994 as great as for the other. This difference is well within the experimental error; so it has been concluded that the rate of solution of oxygen is very large compared with its rate of reaction with Pu(III).

Analytical Methods.—Rate runs were made both with and without Fe(II) which was added in some of the runs to keep the H_2O_2 concentrations very low. The analyses, which were made periodically to determine the rate of the reaction, were different in these two types of runs.

In runs without Fe(II), H_2O_2 was detected in the partially oxidized solutions of Pu(III) by means of the characteristic spectral absorption produced when titanyl sulfate was added. The H_2O_2 concentrations, during the course of a run, were determined by subtracting the spectrophotometrically determined Pu(III) concentrations from the sums of the Pu(III) and H_2O_2 concentrations. These sums were determined by titrating aliquots from the reactor in the following way. The 13.81-ml. aliquot was quickly pipetted into an excess, 5.00 ml., of standard $KMnO_4$ in 20 ml. of 3 M H_2SO_4; this stopped the reaction by oxidizing the Pu(III) to Pu(IV) and the H_2O_2 to oxygen. The time of the analysis was taken as the time at which half the aliquot had been delivered. Nitrogen was bubbled through the solution to remove the dissolved oxygen, and 5.00 ml. of standard $FeSO_4$ (an excess) was added to reduce the unreacted $KMnO_4$. The excess Fe(II) was then determined by a potentiometric titration with standard $K_2Cr_2O_7$ solution. At the end-point of this titration, all the plutonium present was quantitatively Pu(IV). The flow of nitrogen was maintained during the titration.

The Pu(III) concentrations were determined spectrophotometrically by measuring the absorbances[9] of samples from the reactor at 4815 and 6005 Å. Where necessary, readings were made as a function of time and extrapolated to the time at which the sample was taken. At the wave lengths used, both Pu(III) and Pu(IV) absorb significantly; therefore the necessary molar absorptivities[9] were determined from the absorbances of analyzed mixtures. These mixtures were prepared by oxidizing known concentrations of Pu(III) with oxygen, so significant amounts of H_2O_2 were present. Thus the Pu(III) concentrations could not be determined by simple titrations to Pu(IV), but were calculated from separate determinations of the sums and of the differences of the concentrations of Pu(III) and H_2O_2. The sums were determined as already described, and the differences were determined as follows. An aliquot of the mixture was pipetted into 5.00 ml. of standard $FeSO_4$ in 20 ml. of 3 M H_2SO_4, which had been swept with nitrogen. This reduced the H_2O_2 to H_2O. The solution was then partially oxidized with 5.00 ml. of standard $KMnO_4$ and then titrated potentiometrically with standard $K_2Cr_2O_7$ as before. The amounts of standard $FeSO_4$ and $KMnO_4$ were made the same for this procedure as for the one above so that the blank corrections would be the same in both procedures.

In the runs in which Fe(II) had been added, a rapid oxidation–reduction equilibrium involving Pu(III), Pu(IV), Fe(II) and Fe(III) was set up (reaction (5), *vide infra*). In these runs the Pu(III) concentrations were calculated from the sums of the Pu(III) and Fe(II) concentrations and the equilibrium quotient

$$K_5 = [Pu(III)][Fe(III)]/[Pu(IV)][Fe(II)]$$

where the quantities in brackets represent the concentrations in the indicated oxidation states. The concentration of Pu(III) is the solution of the equation

(9) H. K. Hughes, *Anal. Chem.*, **24**, 1349 (1952).

$$(K_5 - 1) [Pu(III)]^2 + (T - K_5P - K_5T - F) [Pu(III)] + K_5PT = 0$$

where T is the sum of the Pu(III) and Fe(II) concentrations, P is the total plutonium concentration and F is the total iron concentration.

The sums of the Pu(III) and Fe(II) concentrations were determined by titration in the same way as described for the Pu(III)–H_2O_2 sums except that Ce(IV) was used as the initial oxidizing agent. It was found that partially reduced Ce(IV) is more stable than partially reduced $KMnO_4$.

The equilibrium quotients, K_5, were calculated for the various experimental solutions from the formal potentials for the Pu(III)–Pu(IV) and the Fe(II)–Fe(III) couples. These formal potentials were determined in the various experimental solutions by applying the Nernst equation to the potentiometric titration curves of Pu(III) and Fe(II). The equilibrium quotients were calculated from the equation

$$0.059 \log K_5 = E_{Pu} - E_{Fe}$$

where E_{Pu} and E_{Fe} are the formal potentials of the plutonium and iron couples, respectively. The values found for K_5 in the experimental solutions are listed in Table III.

Results and Discussion

Runs without Fe(II).—Two rate runs were made, during which H_2O_2 and Pu(III) concentrations were determined as a function of time, as previously described. It is postulated that the reactions which take place are

$$Pu(III) + 1/2 O_2 + H^+ = Pu(IV) + 1/2 H_2O_2 \quad (1)$$

$$Pu(III) + 1/2 H_2O_2 + H^+ = Pu(IV) + H_2O \quad (2)$$

$$Pu(IV) + 1/2 H_2O_2 = Pu(III) + 1/2 O_2 + H^+ \quad (3)$$
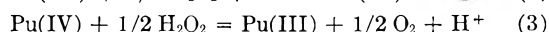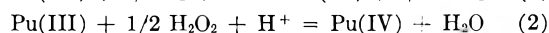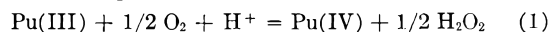
This reaction scheme requires that $d[Pu(III)]/dt = R_3 - R_1 - R_2$, $2 d[H_2O_2]/dt = R_1 - R_2 - R_3$, and $R_1 - R_3 = d[H_2O_2]/dt - 1/2 d[Pu(III)]dt$, where the R's are the rates of the individual reactions given above. The rates $d[Pu(III)]/dt$ and $d[H_2O_2]/dt$ were determined from plots of concentration *vs.* time, and the quantity $(R_1 - R_3)$ was determined as a function of the concentrations of Pu(III) and H_2O_2. It seemed likely that $R_1 = k_1'[Pu(III)]^2$ and $R_3 = k_3[H_2O_2][Pu(IV)]^2$, where k_1' is an apparent second-order rate constant, since during a run, P_{O_2}, $[H^+]$ and $[SO_4^=]$ remained essentially constant. The rate law for reaction (1) was suggested by that of the reaction between Fe(II) and O_2.[10] Since reaction (3) is the reverse of reaction (1), its rate law was chosen so that the ratio of the reverse and forward rates gives the equilibrium quotient.[11]

If these rate laws are the correct ones, a plot of $(R_1 - R_3)/[Pu(III)]^2$ *vs.* $[Pu(IV)]^2[H_2O_2][Pu(III)]^{-2}$ should be a straight line with a slope of k_3 and an intercept of k_1'. When the data were plotted in this way, essentially straight lines resulted. The data for one of these runs are shown in Table I. The plots for both runs are shown in Fig. 1. The points scatter considerably, but indicate that k_1' is about 1.93 M^{-1} min.$^{-1}$ and that k_3 is about 9.5×10^2 M^{-2} min.$^{-1}$. These runs were made in solutions with $P_{O_2} = 0.75$ atm. and 0.3 M in $HClO_4$ and 0.4 M in Na_2SO_4.

(10) P. George, *J. Chem. Soc.*, 4359 (1954); A. B. Lamb and L. W. Elder, Jr., *J. Am. Chem. Soc.*, **53**, 137 (1931).

(11) The back reaction may be a little more complicated than indicated here. The equilibrium quotient for reaction (1) was estimated from the ratio of k_1 and k_3, this together with the potential of the H_2O_2–O_2 couple led to a potential for the Pu(III)–Pu(IV) couple which agreed with a direct determination in a solution with the same acid and salt concentrations to within only 0.05 v.

Table I

Oxidation of Pu(III) by O₂

Conditions: 25° P_{O_2} = 0.75 atm., total Pu = 5.36 × 10⁻³ M, 0.3 M HClO₄, 0.4 M Na₂SO₄

Time, min.	Pu(III), $M \times 10^4$	$-d\,Pu(III)/dt$, M min.⁻¹ $\times 10^6$	H₂O₂, $N \times 10^4$	$d\,H_2O_2/dt$, N min.⁻¹ $\times 10^6$
0	52.3	44.2	1.1	27.4
20	43.5	43.0	6.3	22.0
40	35.5	36.0	9.6	11.2
60	29.5	26.7	11.0	0
80	24.8	18.9	10.2	− 4.0
100	21.7	13.9	9.1	− 5.3
120	19.3	10.2	8.1	− 5.1
140	17.5	7.7	7.0	− 4.8
160	16.2	5.6	6.2	− 4.2
180	15.0	4.2	5.2	− 3.6

Runs with Fe(II) Present.—In order to remove the complications arising from reactions (2) and (3), the main series of runs was made with Fe(II) present. In addition to the reactions given above, it is postulated that the following occur also

$$Fe(II) + 1/2\,H_2O_2 + H^+ = Fe(III) + H_2O \quad (4)$$

$$Fe(II) + Pu(IV) \rightleftarrows Fe(III) + Pu(III) \quad (5)$$
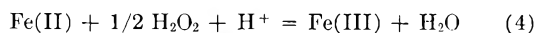
Reaction (4) is very fast, but its kinetics have been studied.[12] The reaction between Fe(II) and O₂ has been neglected here because it is very slow.[10] Reaction (4) keeps the H₂O₂ concentration at such a low level that reactions (2) and (3) may be neglected. Under these conditions $R_1 = R_4 = -\frac{1}{2}\,d[Pu(III) + Fe(II)]/dt$. At various times the sums of the Pu(III) and Fe(II) concentrations were determined by titration and the Pu(III) concentrations were calculated as previously described. A small correction for the H₂O₂ present was made. Its concentration was estimated from the rate of reaction (4) using the rate constant reported by Rigg, et al.[12] Rates were determined from the slopes of plots of [Pu(III) + Fe(II)] vs. time.

The course of a typical run is indicated by the data shown in Table II. Here the rate, R_1, and the concentrations of Pu(III), Fe(II) and H₂O₂ are given as a function of time. When $R_1/[Pu(III)]$ was plotted against [Pu(III)], a good straight line through the origin resulted, showing that, indeed, $R_1 = k_1'[Pu(III)]^2$. This run gave 1.94 M^{-1} min.⁻¹ for the value of k_1'. Two other runs, again made in 0.3 M HClO₄ and 0.4 M Na₂SO₄, gave 1.97 and 1.99 M^{-1} min.⁻¹. These values are in good agreement with the two runs made without Fe(II); this indicates that Fe(II) probably reacts only as indicated in equations (4) and (5).

The runs discussed above were made in solutions in which the H⁺ concentration was about 0.095, the SO₄⁼ concentration was about 0.195, and the HSO₄⁻ concentration was about 0.205 M. These concentrations were calculated under the assumption that the acid dissociation quotient of HSO₄⁻ is about 0.09 at unit ionic strength.[13] These concentrations lead to an ionic strength of 1.09.

For studying the effect of O₂, H⁺ and SO₄⁼ on the rate solutions with an ionic strength of 2 were

(12) T. Rigg, W. Taylor and J. Weiss, J. Chem. Phys., 22, 575 (1954).

(13) E. Eichler and S. Rabideau, J. Am. Chem. Soc., 77, 5501 (1955).
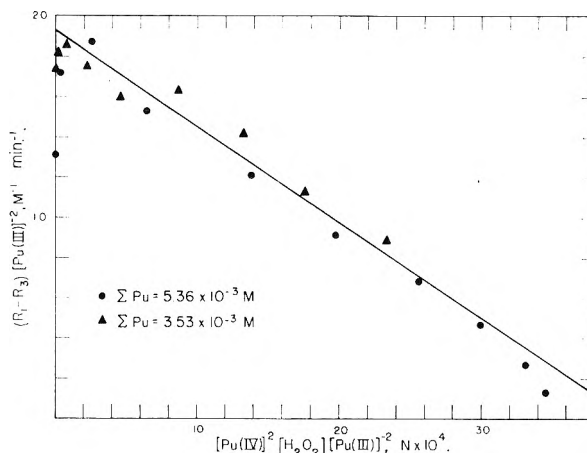
Fig. 1

Table II

Oxidation of Pu(III) by O₂ with Fe(II) Present

Conditions: 25°, P_{O_2} = 0.745 atm., total Pu = 2.64 × 10⁻³ M, total Fe = 5.6 × 10⁻⁴ M, 0.30 M HClO₄ and 0.40 M Na₂SO₄.

Time, min.	Pu(III), $M \times 10^4$	Fe(II) $M \times 10^4$	R_1, M min.⁻¹ $\times 10^6$	R_1 (calcd.),[a] M min.⁻¹ $\times 10^1$
5	25.2	4.2	11.8	12.3
35	21.3	2.1	8.9	8.8
65	17.7	1.2	6.1	6.1
95	15.0	0.9	4.3	4.4
125	13.0	.7	3.3	3.3
185	10.1	.4	2.2	2.0
245	8.0	.3	1.5	1.25
305	6.6	.25	1.0	0.85
365	5.7	.2	0.7	0.6
425	5.0	.2	0.4	0.5

[a] Calculated using $R_1 = 1.94\,[Pu(III)]^2$.

chosen. The acid and salt concentrations in these solutions are given in Table III. The concentrations of free H⁺ and free SO₄⁼ were calculated from the concentrations of HClO₄ and Na₂SO₄ by assuming that the acid dissociation quotient of HSO₄⁻ is 0.1 in solutions with an ionic strength of 2. This value is not in agreement with that given by Zebroski, et al.,[14] but has been confirmed by pH and extinctiometric measurements.[15]

Table III

Acid and Salt Concentrations

Solution[a]	HClO₄, M	Na₂SO₄, M	NaClO₄, M	H⁺, M	SO₄⁼, M	HSO₄⁻, M	K_5
a	0.10	0.15	1.55	0.05	0.10	0.05	4.9
b	.20	.20	1.40	.10	.10	.10	4.4
c	.40	.30	1.10	.20	.10	.20	4.4
d	.60	.40	0.80	.30	.10	.30	4.8
e	.80	.50	0.50	.40	.10	.40	5.6
f	.13	.06	1.75	.10	.03	.03	11.1
g	.17	.14	1.55	.10	.07	.07	5.2
h	.30	.40	0.90	.10	.20	.20	3.7
i	.40	.60	0.40	.10	.30	.30	3.3

[a] Ionic strength of all solutions is 2.0 if K_a for HSO₄⁻ is 0.1.

Oxygen Dependence.—The oxygen dependence was studied by comparing the rates in runs made

(14) E. L. Zebroski, H. W. Alter and F. K. Heumann, ibid., 73, 5646 (1951).

(15) Use was made of the effect that the sulfate ion concentration has on the absorption spectrum of the uranyl ion.

with air passing through the reactor with similar runs made with oxygen. The results of these experiments are shown in Table IV. The column headed "Oxidation range" gives the range in which data were collected for the evaluation of the apparent second-order rate constant. In the air runs which gave rise to the values 1.05, 1.07 and 1.10 for the oxygen dependence, it was noticed that the apparent second order rate constants drifted upward as the runs proceeded. It was thought that this might be due to a small amount of inhibitor which was being oxidized slowly. In the air runs marked with an a in Table IV, a small amount of Pu was oxidized with oxygen before any Fe was added. This treatment removed the trend and brought the apparent oxygen dependence closer to unity. It has been concluded that at least the middle half of the oxidation occurs predominantly by a mechanism which is first order in the oxygen pressure.

TABLE IV

EFFECT OF OXYGEN PRESSURE

Temperature, 25°

Solution	Total Pu $M \times 10^3$	Total Fe, $M \times 10^4$	P_{O_2}, atm.	Oxidation range, %	Apparent 2nd-order rate const., M^{-1} min.$^{-1}$	Apparent O_2 dependence
h	2.4	9.8	0.742	20–83	2.85	
	3.1	9.8	.740	41–86	2.88	
	4.8	9.8	.154	10–65	0.531	1.07
	3.1	9.8	.156	12–52	0.556	1.05
	3.1	9.8	.156	35–71	0.591^a	1.01
i	2.4	8.1	.733	37–82	3.25	
	3.1	9.9	.734	57–86	3.27^a	
	4.8	9.8	.154	19–68	0.585	1.10
	3.1	9.9	.152	39–71	0.646^a	1.03

^{a} Fe added after a small amount of Pu had been oxidized with oxygen.

Hydrogen Ion Dependence.—The effect of H^+ on the rate of the reaction in the presence of Fe^{++} has been studied at a constant $SO_4^=$ concentration of 0.10 M. The results of these experiments are shown in Table V. The apparent second-order rate constants were corrected to 1 atm. of O_2 by assuming a first power oxygen dependence. The solubility of oxygen in solutions of constant ionic strength but of varying concentrations of $HClO_4$ and Na_2SO_4 was found to be constant to within 1%.[16] The rate decreases approximately linearly with increasing H^+ concentration. This effect is probably due to a combination of three factors. (1) A medium effect: the solution with the lowest H^+ concentration was 1.55 M in $NaClO_4$ whereas the solution with the highest H^+ was only 0.5 M in $NaClO_4$. (2) An incorrect estimate of the acid dissociation quotient for HSO_4^-: this would lead to varying concentrations of $SO_4^=$. (3) A path for the reaction which involves hydrolyzed plutonium species: this last explanation cannot be the most important one for, if it were, the effect of varying H^+ concentration would be given approximately by $k = k_0(1 + a/[H^+])$ where a and k_0 are constants. This last expression does not describe the experimental results.

(16) The authors are grateful to Mr. T. N. Sarachman for making these measurements.

Sulfate Ion Dependence.—The effect of $SO_4^=$ on the rate of the reaction in the presence of Fe^{++} has been studied at a constant H^+ concentration of 0.10 M. The results of these experiments are shown in Table VI, and in Fig. 2. The apparent second-order rate constants were corrected to 1 atm. of O_2 in the same way as before. The rate is strongly dependent on the sulfate concentration but not in any simple way. It is reasonable to assume that different activated complexes with different numbers of $SO_4^=$ groups attached are simultaneously important. This suggests the following general mechanism

$Pu^{+++} + iSO_4^= \rightleftarrows Pu(SO_4)_i^{+3-2i}$ (rapid and reversible)

$Pu(SO_4)_i^{+3-2i} + O_2 \rightleftarrows O_2 \cdot Pu(SO_4)_i^{+3-2i}$ (rapid and reversible)

$Pu(SO_4)^{j+3-2j} + O_2 \cdot Pu(SO_4)_i^{+3-2i} = \begin{bmatrix} \text{intermediate which} \\ \text{reacts rapidly with} \\ H^+ \text{ to give products} \end{bmatrix}$ (rate determining)
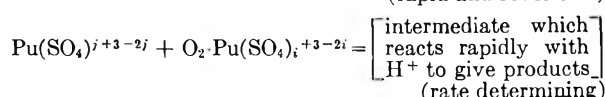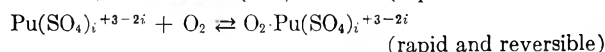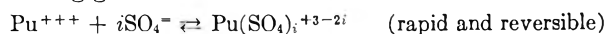
where $i = 0, 1, 2, \ldots$, and $j = 0, 1, 2, \ldots$. The intermediate might be similar to one of the Pu(IV)–H_2O_2 complexes studied by Connick and McVey,[17] or it might be two singly hydrolyzed Pu(IV)–$SO_4^=$ complexes plus an H_2O_2 molecule.

TABLE V

EFFECT OF HYDROGEN ION CONCENTRATION

Temperature, 25°, sulfate concentration, 0.10 M.

Soln.	H^+, M	Total Pu, $M \times 10^3$	Total Fe, $M \times 10^4$	P_{O_2}, atm.	Oxidation range, %	Rate constant M^{-1} atm.$^{-1}$ min.$^{-1}$	Calcd.^{a} rate constant M^{-1} atm.$^{-1}$ min.$^{-1}$
a	0.05	2.4	6.5	0.741	25–75	2.28	2.34
b	.10	2.4	9.8	.736	11–72	2.30	2.28
		3.1	33.1	.725	18–66	2.25	
c	.20	2.4	9.8	.732	13–70	2.23	2.14
d	.30	2.4	9.8	.731	10–68	1.98	2.01
e	.40	2.4	9.8	.737	8–67	1.85	1.88
		2.4	9.8	.738	10–68	1.87	

^{a} Calculated assuming $k = 2.41 [1 - 0.55(H^+)]$.

TABLE VI

EFFECT OF SULFATE ION CONCENTRATION

Temperature, 25°, hydrogen ion concentration, 0.10 M.

Soln.	$SO_4^=$, M	Total Pu, $M \times 10^3$	Total Fe, $M \times 10^4$	P_{O_2}, atm.	Oxidation range, %	Rate constant M^{-1} atm.$^{-1}$ min.$^{-1}$	Calcd.^{a} rate constant M^{-1} atm.$^{-1}$ min.$^{-1}$
f	0.03	4.8	9.8	0.726	8–55	0.325	0.324
g	.07	4.4	9.8	.740	38–77	1.39	1.40
b	.10	2.4	9.8	.736	11–72	2.30	2.24
		3.1	33.1	.725	18–66	2.25	
h	.20	2.4	9.8	.742	20–83	3.84	3.94
		3.1	9.8	.740	41–86	3.89	
i	.30	2.4	8.1	.733	37–82	4.43	4.39
			9.9	.734	57–86	4.46	

^{a} Calculated using $k = 3.3f_1f_1 + 21.3f_1f_2$, where f_1 is the fraction of the Pu(III) in the first sulfate complex, and f_2 is the fraction in the second complex.

With a scheme as general as this, it is very unlikely that a unique description of what actually is occurring is possible. However, by making some reasonable assumptions about the sulfate complexes of Pu(III), we are able to interpret our experimental observations in terms of only two reaction paths. These are the ones with two and

(17) R. E. Connick and W. H. McVey, reference 2, Paper 4.12.

three $SO_4^=$ groups in the activated complex. This assumption and the mechanism above lead to the following rate law

$$\text{Rate} = [\text{Pu(III)}]^2[O_2][k_{11}f_1f_1 + k_{12}f_if_2] \quad (6)$$

where the k's are the rate constants for the indicated paths, f_1 is the fraction of the Pu(III) in the form of the first complex and f_2 is the fraction in the form of the second. These f's are calculated from the appropriate association quotients. Since these quotients have not been determined they were estimated as follows. The association quotient of $CeSO_4^+$ at ionic strength 2 is about 10.[18] Since Pu^{+++} has very nearly the same radius as Ce^{+++},[19] it has been assumed that the association quotient for $PuSO_4^+$ is 10 also. No information is available on complexes such as $Pu(SO_4)_2^-$ but its association quotient is undoubtedly less than that for the first complex. We have assumed that $[Pu(SO_4)_2^-]/[PuSO_4^+][SO_4^=] = 5$. The calculated values in Table VI and the solid line in Fig. 2 are based on these assumptions. The agreement between calculated and observed apparent second-order rate constants does not support the precise values assumed for the association quotients, but probably does support the idea that in the sulfate range investigated, the two most important paths are those with two and three $SO_4^=$ groups in the activated complexes. By means of least squares, k_{11} and k_{12} were found to be 3.33 and 21.3 M^{-1} atm.$^{-1}$ min.$^{-1}$, respectively.

Effect of Temperature.—The effect of temperature on the rate of the reaction has been investigated only briefly. One run was made at 35°; the acid and salt concentrations were those of solution b in Table III. The apparent rate constant was found to be 5.18 M^{-1} atm.$^{-1}$ min.$^{-1}$. For comparison with data taken at 25° it is necessary to correct for the difference in oxygen solubility at the two temperatures. It has been found that at 35° oxygen is about 12% less soluble in $HClO_4$, Na_2SO_4 $NaClO_4$ mixtures with ionic strengths of 1.1, than at 25°.[16] At 35° and at ionic strength of 2 the acid dissociation quotient for HSO_4^- is probably about 0.08; this leads to a free sulfate concentration of 0.093 M. At 25° a solution with this sulfate concentration and saturated with oxygen at 0.88 atm. would have an apparent second-order rate constant of 1.8 M^{-1} min.$^{-1}$. The average activation energy (RT^2 d ln k/dt) is then calculated to be 19 kcal. If the

(18) T. W. Newton and G. M. Arcand, *J. Am. Chem. Soc.*, **75**, 2449 (1953).

(19) Reference 6, page 297.
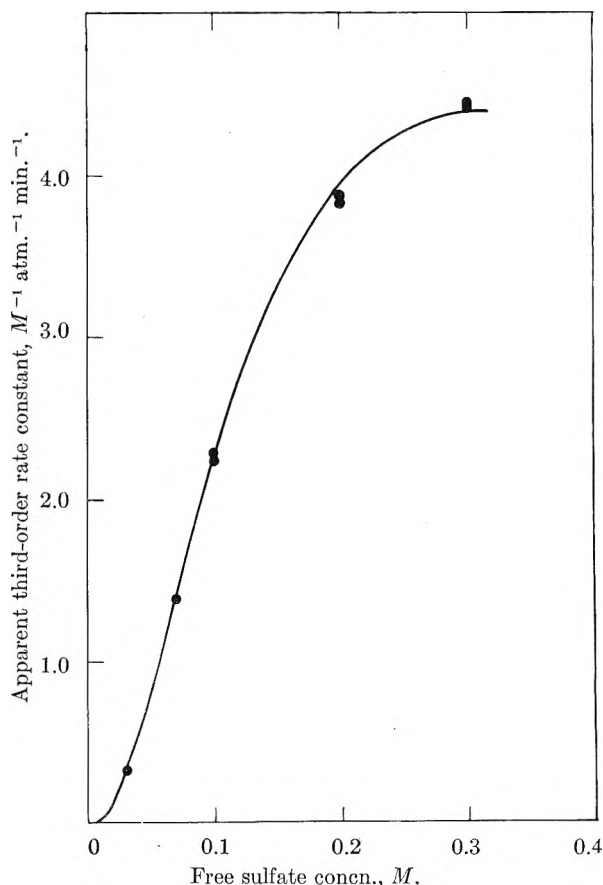
Fig. 2.

mechanism which is proposed above is correct, this value is an average for the two paths and includes the heats of formation of the Pu(III)–$SO_4^=$ complexes.

NOTE ADDED IN PROOF.—In a discussion of this paper with Prof. G. Scatchard the following two points were brought out. (1) In equation (6) the term $k_{11}f_1f_1$ should be replaced by $k_{11}f_1f_1 + k_{02}f_0f_2$ in order to allow for the other, but kinetically indistinguishable, path leading to an activated complex with two $SO_4^=$ groups. (2) If $K = [Pu(SO_4)_2^-]/[PuSO_4^+][SO_4^=]$ is not assumed to be 5, but is taken as an adjustable parameter, a least squares treatment gives it a value of 4.2 and leads to a slightly better fit of the data.

PHASE RELATIONS IN THE SYSTEM CALCIUM BROMIDE, CALCIUM OXIDE AND WATER

By A. C. Nixon and R. E. Smith

Shell Development Company, Emeryville, California

Isotherms for the system calcium bromide–calcium oxide–water were determined at 40, 50 and 60°. Existence of the complex salts $CaBr_2 \cdot 3CaO \cdot 16H_2O$ ($D_{1\cdot3\cdot16}$) and $3CaBr_2 \cdot 4CaO \cdot 16H_2O$ ($D_{3\cdot4\cdot16}$) was confirmed. The decomposition temperature of $D_{1\cdot3\cdot16}$ is 52.5°. $D_{3\cdot4\cdot16}$ appears to be stable below 100°, at which temperature water is lost. The heat of formation of $D_{1\cdot3\cdot16}$ is approximately 1100 kcal.

Introduction

This paper describes the results of an investigation of the ternary system calcium bromide–calcium oxide–water at 40, 50 and 60°. A previous investigation by Milikan[1] established the existence of two complex salts, $CaBr_2 \cdot 3CaO \cdot 16H_2O$ ($D_{1\cdot3\cdot16}$) and $3CaBr_2 \cdot 4CaO \cdot 16H_2O$ ($D_{3\cdot4\cdot16}$), and defined the phase diagram at 25°. He reported a decomposition temperature of 49.2° for $D_{1\cdot3\cdot16}$.[1] Our data indicate that this value is low.

The current work employed the "wet residue" method of Schreinemakers.[2] In connection with the application of this method a useful experimental technique was developed during this study. The decomposition temperatures of $D_{1\cdot3\cdot16}$ and $D_{3\cdot4\cdot16}$ were investigated by thermal analyses.

Experimental

Chemicals.—Calcium oxide was prepared by two methods. In the first method a selected sample of Mallinckrodt Chemical Works reagent grade calcium acetate was calcined at 1050 to 1100° for approximately 20 hours. In the second method a selected sample of Allied Chemical and Dye Corporation Baker and Adamson reagent grade CaO was recalcined and used without further purification. The impurity level for both samples, as determined by emission spectrometric analysis, varied from 0.4 to 0.8%; the chief impurity was strontium.

Calcium bromide was prepared initially by the reaction between hydrobromic acid and calcium oxide followed by concentration and repeated crystallizations. Later in the work a selected sample of J. T. Baker Chemical Co. reagent grade calcium bromide was used without further treatment. The maximum impurity level for both samples was 0.1 to 0.2%.

Distilled water was employed in all experiments.

Analytical Methods.—Bromide was determined by the Volhard method[3] for total halides. Calcium oxide was determined by titration with 0.1 N HNO_3, using phenolphthalein as an indicator. Total calcium was determined either by the volumetric oxalate method[4] or by the Versenate method[6] for total cations. The Versenate method gave calcium values which checked to within 1% of the oxalate method for a few test samples. The total calcium value, used as a cation check, gave closures which showed an average deviation of 1% for all experiments. Water was determined by difference.

Equipment.—The bulk of the experimental work was performed in a stoppered test-tube type cell equipped with a sintered glass liquid phase sampler and a stainless steel stirrer. This assembly was contained in a constant temperature water bath controlled to ±0.2°. Equilibrium periods of 24 to 48 hours were allowed.

A portion of the work employed a useful equipment variation in which the equilibrium cell was attached to a

phase separating cell containing a sintered glass filter plate but separated by a puncturable rubber diaphragm. After charging the equilibrium cell the mounted assembly was immersed in a constant temperature water-bath and vented after reaching the bath temperature. The cell was rotated end-over-end at approximately 30 revolutions per minute for 24 hours. The liquid phase was sampled by (1) slightly elevating the unit to allow connection of a vent line to the liquid sample bottle, (2) rotating the assembly and puncturing the rubber diaphragm with a stainless steel wire, and (3) attaching an air line to permit pressure filtration of the slurry. A Dow-Corning medium porosity (fine series) sintered glass filter was employed. Only at the time of actual manipulation were the connections above the surface of the bath. After the filtration was completed the assembly was removed from the bath, dismantled and a sample of the solid filter cake was taken.

This experimental device prevents the vapor loss normally found with all packing gland-type stirrers. As a result, it provides a check on the accuracy of each experiment since the composition of the charge lies on a straight line connecting the compositions of the two phases, when plotted on a three component diagram.

Results and Discussion

Equilibrium data for the system calcium oxide–calcium bromide–water at 40, 50 and 60° are presented in Tables I, II and III, respectively. The solubility data for calcium oxide in water and for calcium bromide in water were taken from the literature.[6] The corresponding equilibrium phase diagrams are shown in Figs. 1, 2, and 3. In these diagrams the composition of the liquid phase has been intentionally shifted away from the calcium bromide–water axis to clarify the diagram. The
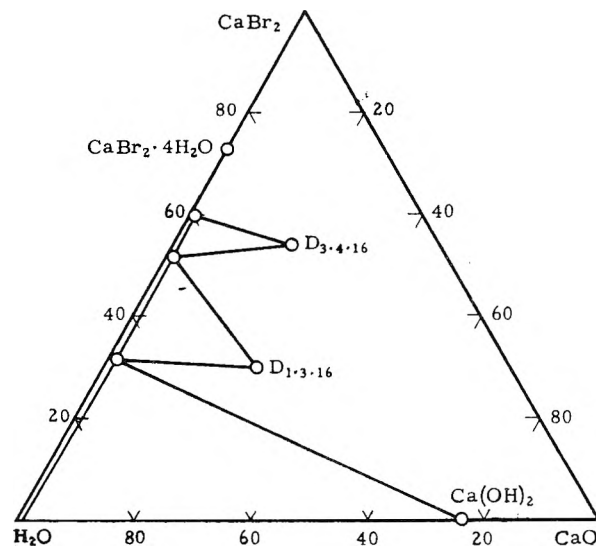
Fig. 1.—System $CaO–CaBr_2–H_2O$ at 40°, weight percentages.

(1) J. Milikan, *Z. physik. Chem.*, **92**, 59 (1918).

(2) F. A. H. Schreinemakers, *ibid.*, **11**, 81 (1893).

(3) "Scott's Standard Methods of Chemical Analysis," 5th ed., Vol. 1, D. Van Nostrand Co., Inc., New York, N. Y., 1939, p. 192.

(4) Ref. 3, p. 211.

(5) G. Schwarzenbach, and W. Biedermann, *Helv. Chim. Acta*, **31**, 678 (1948).

(6) N. A. Lange, "Handbook of Chemistry," 3rd ed., Handbook Publishers, Inc., Sandusky, Ohio, 1939, p. 1024.

compositions of the field intersection points at these temperatures, including the 25° data by Milikan,[1] are presented in Table IV.

TABLE I

THE SYSTEM CALCIUM OXIDE–CALCIUM BROMIDE–WATER AT 40°, WEIGHT PERCENTAGES

	Liquid phase			Wet residue phase	
CaO	CaBr₂	H₂O	CaO	CaBr₂	H₂O
0.11	0	99.9	...	...	...
.045	12.9	87.1	31.3	7.66	61.0
.13	22.5	77.4	33.2	12.2	54.6
.13	28.2	71.7	40.5	12.8	46.7
.18[a]	30.4[a]	69.4[a]	15.6[a]	28.9[a]	55.5[a]
.21	32.3	67.5	25.5	25.8	48.7
.16	36.5	63.4	14.8	33.6	51.6
.16	37.9	61.9	11.6	34.5	53.9
.24	41.6	58.2	16.2	35.7	48.1
.41	50.0	49.6	10.8	42.6	46.6
.55[a]	52.1[a]	47.4[a]	12.1[a]	42.8[a]	45.1[a]
.70	52.5	46.8	13.1	43.7	43.2
.45	54.0	45.6	11.0	53.6	35.4
.35	55.3	44.4	11.0	54.5	34.5
.26	58.5	41.2	9.45	56.7	33.8
.25	59.5	40.3	8.33	58.2	33.5
.20	61.7	38.1	5.45	62.7	31.8
	68.0	32.0	...	...	...

[a] Modified apparatus.

TABLE II

THE SYSTEM CALCIUM OXIDE–CALCIUM BROMIDE–WATER AT 50°, WEIGHT PERCENTAGES

	Liquid phase			Wet residue phase	
CaO	CaBr₂	H₂O	CaO	CaBr₂	H₂O
0.097	0	99.9	...	...	...
.045	9.24	90.7	36.2	5.5	58.3
.15	14.0	85.8	30.5	7.89	61.6
.092	15.1	84.8	30.5	9.58	59.9
.12	18.8	81.1	29.3	13.8	56.9
.11	22.8	77.1	31.4	13.6	55.0
.14	34.6	65.3	32.9	19.8	47.3
.10	35.4	64.5	46.5	13.8	39.7
.21	37.2	62.6	40.9	17.3	41.8
.30	40.3	59.4	12.6	35.6	51.8
.30[a]	40.6[a]	59.1[a]	28.5[a]	25.4[a]	46.1[a]
.14	41.9	58.0	13.1	36.6	50.3
.68	47.7	51.6	12.2	40.6	47.2
.74	49.1	50.2	9.91	42.9	47.2
.89	51.4	47.7	14.7	42.1	43.2
1.07	51.5	47.4	9.11	49.1	41.8
0.68	52.6	46.7	11.5	53.3	35.3
.46	55.3	44.2	10.3	54.6	35.1
.38	59.1	40.5	6.79	61.5	31.7
.30	59.7	40.0	11.2	57.0	31.8
0	72.0	28.0	...	...	...

[a] Modified apparatus.

TABLE III

THE SYSTEM CALCIUM OXIDE–CALCIUM BROMIDE–WATER AT 60°, WEIGHT PERCENTAGES[a]

	Liquid phase			Wet residue phase	
CaO	CaBr₂	H₂O	CaO	CaBr₂	H₂O
0.088	0	99.9	...	...	...
.33	24.5	75.2	37.9	13.4	48.7
.28	34.4	65.3	32.9	19.5	47.6
.40	42.3	57.3	45.9	16.7	37.4
1.26	51.6	47.1	5.98	49.1	44.9
1.20	52.4	46.4	8.15	52.3	39.5
0.38	56.5	43.1	9.75	55.4	34.9
.37	59.8	39.8	8.41	64.1	27.5
.27	61.1	38.6	5.99	60.0	34.0
0	73.5	26.5	...	...	...

[a] All except first four in modified apparatus.

Milikan[1] reported a decomposition temperature of 49.2° for D₁.₃.₁₆; however, the 50° isotherm shows that D₁.₃.₁₆ is stable at this temperature. This salt was prepared by precipitation from a supersaturated solution and was separated from
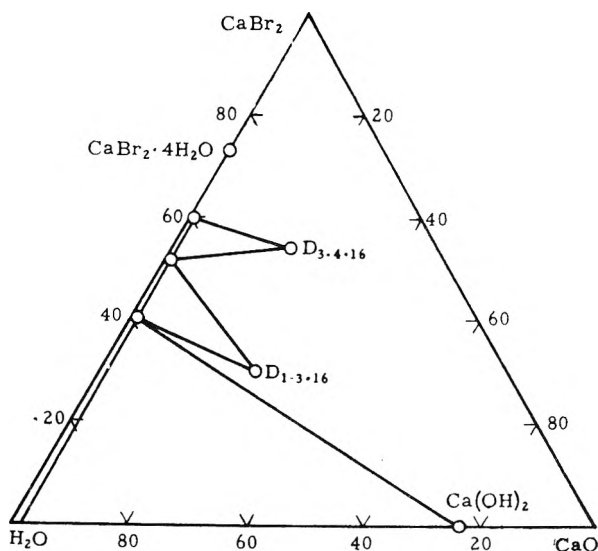
Fig. 2.—CaO–CaBr₂–H₂O at 50°, weight percentages.
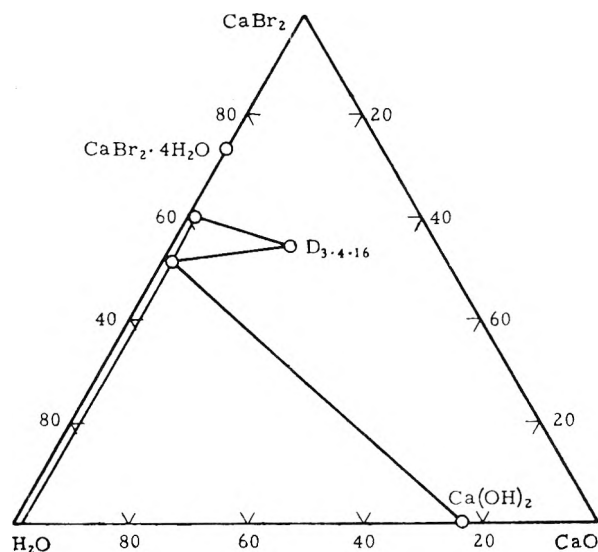
Fig. 3.—CaO–CaBr₂–H₂O at 60°, weight percentages.

TABLE IV

EQUILIBRIUM FIELD INTERSECTION COMPOSITIONS IN WEIGHT PERCENTAGES

Temp., °C.	Ca(OH)₂-D₁.₃.₁₆		D₁.₃.₁₆-D₃.₄.₁₆		D₃.₄.₁₆-CaBr₂·xH₂O		
	CaBr₂	CaO	CaBr₂	CaO	CaBr₂	CaO	x
25	20.8	0.38	54.3	0.11	60.0	0.20	6
40	31[a]	0.70	52.5	0.22	59.5	.25	4
50	40.4	1.07	51.5	0.30	59.5	.32	4
60	52.0[b]	1.25[b]	...	...	59.8	.35	4

[a] Obtained two values: 32.3 and 30.4. [b] Ca(OH)₂-D₃.₄.₁₆ field.

the mother liquor by centrifuging. The white crystals, after drying between filter papers, appeared to be stable and non-hygroscopic. Freezing point determinations on this sample indicate that the formation temperature of D₁.₃.₁₆ is 52.5°. Warming curves attempted in a modified Rossini-type apparatus gave high results (54.8°), but this is believed due to poor heat transfer between the crystals and the benzene suspending agent. Based on the heat input to the benzene-crystal slurry and

the warming curve, the heat of formation of $D_{1.3.16}$ is approximately 1100 kcal.

The complex $D_{3.4.16}$ was prepared in a similar manner. A simple warming experiment showed no evidence of decomposition below approximately 100°, at which temperature some water loss

occurred.

The authors wish to express their appreciation to Shell Development Company for permission to publish this work, and to R. C. Hurlbert for assistance in evaluation of the heat of formation of $D_{1.3.16}$.

REACTION OF ACTIVE NITROGEN WITH METHYL CYANIDE[1]

BY W. FORST[2] AND C. A. WINKLER

Contribution from the Physical Chemistry Laboratory, McGill University, Montreal, Canada

Received May 21, 1956

The reaction of active nitrogen with methyl cyanide was studied at five temperatures in the range 90 to 460°. The main products were hydrogen cyanide and hydrogen. Smaller amounts of cyanogen, methane, ethane, ethylene, acetylene and (probably) methylisonitrile were also recovered. The yields of primary products, in relation to the methyl cyanide flow rate, indicate complete consumption of active nitrogen at each temperature, but the maximum yield increased markedly with increase of temperature.

Introduction

Previous studies in this Laboratory have shown that, although reactions of active nitrogen with hydrocarbons yield mainly hydrogen cyanide, small amounts of cyanogen may also be formed. The present study was made to determine whether, with the CN group present in methyl cyanide, reaction of this molecule with active nitrogen would reveal another aspect of active nitrogen reactions that might be useful in their interpretation.

Experimental

The apparatus was similar to that described in an earlier paper.[3] The molecular nitrogen flow rate was 5.98×10^{-5} mole/sec., corresponding to an operating pressure of 1.03 mm. in the system. Methyl cyanide "chemically pure" was purchased from Brickman and Company, Montreal, and was purified as outlined previously.[3]

Condensed products of the reaction were distilled into a low temperature still of the type described by Le Roy.[4] The C_2 hydrocarbons were distilled at −140° and analyzed on a mass-spectrometer.[5] The excess of the reactant and the products were condensed on $N/2$ KOH frozen in liquid nitrogen. Upon melting, the solution was divided into three aliquots. In one aliquot, total cyanide ($= a$) was determined by titration with silver nitrate[6]; the second aliquot was acidified with dilute sulfuric acid (1:10) and boiled $1/2$ hour. The ammonia so formed ($= b$) was determined by Kjeldahl distillation. The third aliquot was transferred into a tube, frozen in liquid nitrogen, and an equal volume of concentrated sulfuric acid slowly added. The tube was then evacuated, sealed and digested for 12 hours at 150°. Total ammonia ($= c$) was then determined in another Kjeldahl distillation. Cyanogen ($= d$) was determined in a separate experiment by the method of Rhodes.[7] Net hydrogen cyanide was given by the difference ($a - d$), and unreacted methyl cyanide by ($c - a - b$). In the absence of any reaction products easily hydrolyzable by dilute acids, the determination of cyanogen as ammonia (b), or by the direct method (d) should have yielded identical results. However, the result (b) was consistently higher than the result (d), and the discrepancy was attributed to

the presence of methylisonitrile in the reaction products. Methylisonitrile was identified by its hydrolytic products, *i.e.*, methylamine and formic acid, which were detected in the acidified reaction mixture by tests due to Valton[8] and Grant,[9] respectively. No attempt was made to determine the methylisonitrile quantitatively, in view of the small amounts involved (at most 3% of total products at 235°). The difference ($b - d$) was assumed to represent methylisonitrile, and the carbon and hydrogen balances calculated on this basis were between 99 and 101%.

Non-condensable reaction products were withdrawn from the nitrogen stream with a Toepler pump and analyzed on the mass spectrometer.

Experiments were made at 90, 160, 245, 345 and 460°.

Results

The results for all the products exclusive of methane are summarized in Figs. 1, 2 and 3. No methane was found at 90°; the results of analyses at 460° were:

MeCN flow rate, mole/sec. $\times 10^6$	Methane yield. mole/sec. $\times 10^6$
3.5	0.00
8.1	.00
15.5	.184

The data for methylisonitrile are uncertain, *i.e.*, the amounts calculated might represent methylisonitrile plus other unidentified components. At lower temperatures these results were fairly reproducible, but at 345 and 460° the reproducibility became very poor and no consistent data could be obtained.

Discussion

In discussing the results, the assumption will be made that the reactive species in active nitrogen is atomic nitrogen in the ground state, for reasons indicated elsewhere.[10]

Since the main products of the reaction were hydrogen and compounds containing a carbon–nitrogen bond, it would appear that the initial attack of the nitrogen atom was at a carbon atom in the methyl cyanide molecule. Seven possible

(1) With financial assistance from the National Research Council of Canada.

(2) Holder of National Research Council Bursary and Studentships, 1952-1955.

(3) W. Forst and C. A. Winkler, *Can. J. Chem.*, **33**, 1814 (1955).

(4) D. J. Le Roy, *Can. J. Res.*, **28B**, 492 (1950).

(5) The authors are indebted to Dr. H. I. Schiff for permission to use the mass spectrometer, and to Dr. D. Armstrong for the analyses.

(6) I. M. Kolthoff and V. A. Stenger, "Volumetric Analysis," Vol. II, John Wiley and Sons, New York, N. Y., 2nd Ed., 1947.

(7) F. H. Rhodes, *J. Ind. Eng. Chem.*, **4**, 652 (1912).

(8) P. A. Valton, *J. Chem. Soc.*, **127**, 40 (1925).

(9) W. M. Grant, *Anal. Chem.*, **20**, 267 (1948).

(10) (a) H. G. V. Evans and C. A. Winkler, *Can. J. Chem.*, in press; (b) H. G. V. Evans, G. R. Freeman and C. A. Winkler, *ibid.*, in press.

reactions may be suggested, of which three are highly endothermic and a fourth[11] may be ruled out on evidence available. The only three exothermic reactions are all spin disallowed.[10a] They are[12]

$$N + CH_3CN \longrightarrow 2HCN + H + 19 \text{ kcal.} \quad (1)$$
$$N + CH_3CN \longrightarrow C_2N_2 + H_2 + H + 7 \text{ kcal.} \quad (2)$$
$$N + CH_2CN \longrightarrow HCN + CN + H_2 + 9 \text{ kcal.} \quad (3)$$
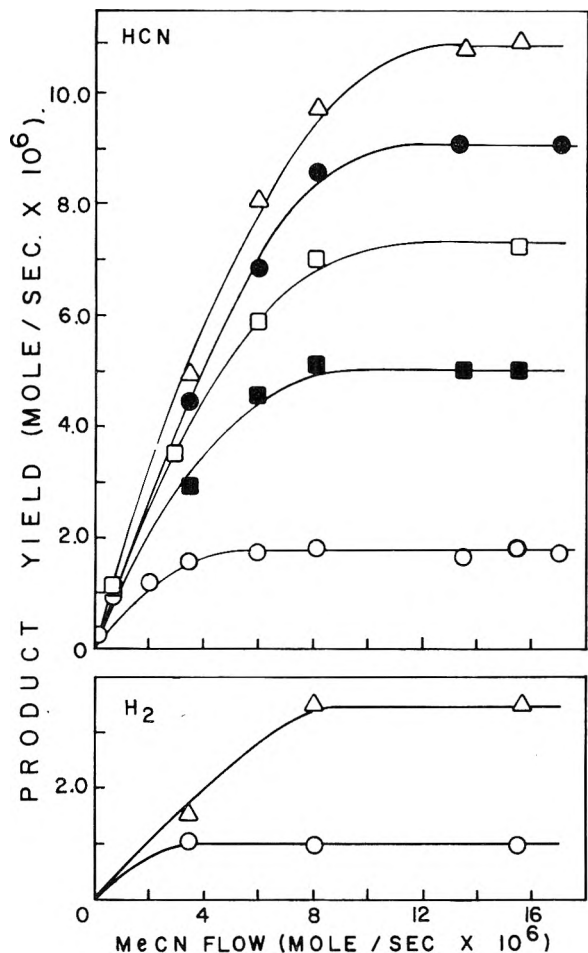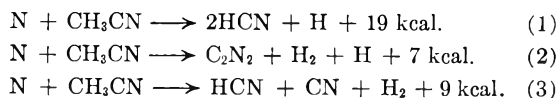
Fig. 1.—Dependence of hydrogen cyanide and hydrogen yields on methyl cyanide flow rate: ○, $90 \pm 30°$ (temp.); ■, $160 \pm 15°$; □, $245 \pm 10°$; ●, $345 \pm 5°$; △, 460 ± 5.

(11) The reaction $N + CH_3CN \rightarrow CH_3C + N_2 + ?$ kcal. seems unlikely since studies in this Laboratory have shown that no C_2 hydrocarbons are formed when active nitrogen is introduced into excess hydrogen cyanide; H. Brody, M. Sc. thesis, McGill University, 1955.

(12) The approximate heats of reaction were calculated from heats of formation published by the National Bureau of Standards in "Selected Values of Chemical Thermodynamic Properties," Nat. Bur. Stand. Washington, 1952, supplemented by

Substance	Heat of formation (kcal./mole)	Reference
CN	-93	L. Brewer, L. K. Templeton, and F. A. Jenkins, *J. Am. Chem. Soc.*, **73**, 1462 (1951); C. A. McDowell and J. W. Warren, *Trans. Faraday Soc.*, **48**, 1084 (1952).
N	-112	A. E. Douglas, THIS JOURNAL, **59**, 109 (1955).
CH_2CN	-70	Rough estimate
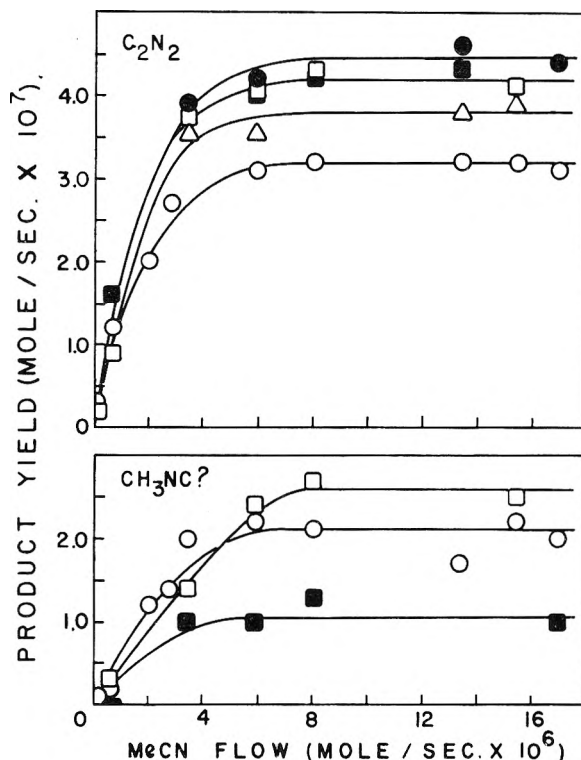
Fig. 2.—Dependence of cyanogen and isonitrile (?) yields on methyl cyanide flow rate (symbols have same significance as in Fig. 1).
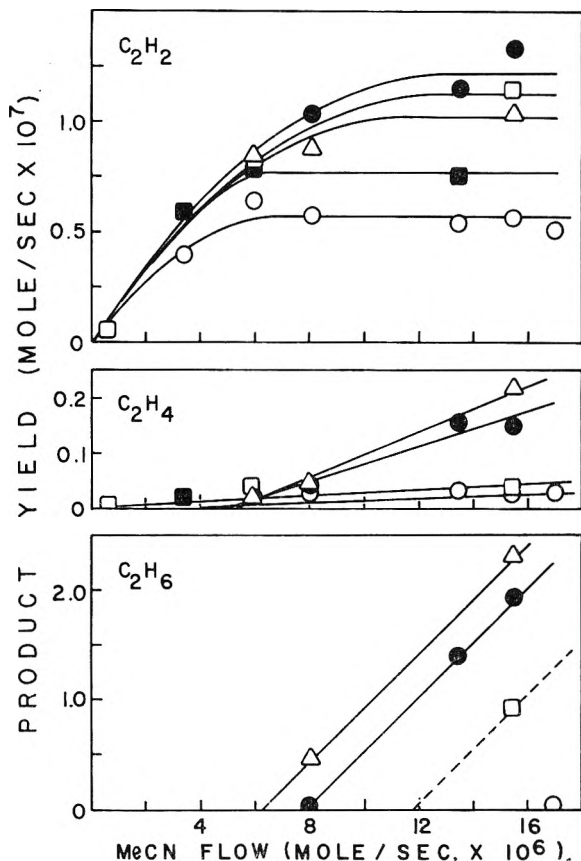
Fig. 3. Dependence of acetylene, ethylene and ethane yields on methyl cyanide flow rate (symbols have same significance as in Fig. 1).

All three reactions will produce the entities H and CN in the ratio 3:2, *i.e.*, three hydrogen atoms are formed for every two CN radicals when no attention is paid to the state of combination. A simple material balance requires that the yield of final products in each case must obey the relation

(yield of H_2) = $^1/_4$(yield of HCN) + $^3/_2$(yield of C_2N_2)

Inspection of Figs. 1 and 2 shows that this relation is approximately satisfied at both 90 and 460°. The agreement obviously means only that any one of the three reactions, or any combination of them, is not inconsistent with the experimental results.

It has not been possible to assess the relative importance of reactions 1, 2 and 3 except by comparison with the reaction of active nitrogen with methyl chloride.[13] In that reaction, neither cyanogen chloride nor chlorine was found among the products. By analogy, it might be inferred that the production of HCN in reaction 1 is probably large compared with the extent of its formation in reaction 3, or through C_2N_2 and CN produced in reactions 2 and 3, respectively.

The plateaus on the curves of Figs. 1, 2 and 3 indicate that, irrespective of mechanism assumed, the amounts of the primary products formed in the initial step (or steps) remain constant above a certain critical flow rate of methyl cyanide at each temperature. The only explanation seems to be that all the available nitrogen atoms are consumed when the methyl cyanide flow rate exceeds the critical values, and that the number of nitrogen atoms participating in product formation is quite different at different temperatures. Similar though less accentuated behavior has been observed in the reaction of methyl chloride with active nitrogen.[13] The observation can be explained if it is assumed that the reactant acts as an efficient catalyst for the recombination of nitrogen atoms; a mathematical analysis of the problem is projected for a further publication.

The ethane found in the reaction products at higher temperatures, and at methyl cyanide flow rates above the critical values, presumably resulted from recombination of methyl radicals formed[3] in the reaction

$$H + CH_3CN \longrightarrow HCN + CH_3 \qquad (4)$$

At lower methyl cyanide flow rates, where nitrogen atom consumption was incomplete, methyl radicals should be destroyed rapidly[14] and ethane production correspondingly insignificant, as observed.

The few data for methane content of the products suggest that the pattern of methane production was similar to that for ethane and that methane also resulted from reactions of methyl radicals

$$CH_3 + H \longrightarrow CH_4 \qquad (5)$$
$$CH_3 + H_2 \longrightarrow CH_4 + H \qquad (6)$$
$$CH_3 + CH_3CN \longrightarrow CH_4 + CH_2CN \qquad (7)$$
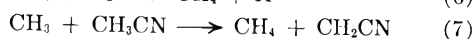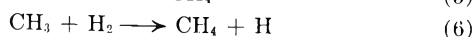
Reactions 6 and 7 are known to have activation

energies of about 10 kcal.[15,16] and should occur at appreciable rates at 345° and 460°. Hence, reactions 4 and 6 could lead to methyl radical production by a chain mechanism. This apparently does not occur, however, since the straight lines representing the production of ethane (Fig. 3) do not have a common origin nor do they have different slopes at different temperatures, corresponding to different extents of a chain reaction. In the absence of a chain reaction, there should be a methyl cyanide flow rate above which ethane production from recombination of methyl radicals should become constant. Apparently this flow rate was not attained for the conditions of the present experiments. Further, the recovery of ethane at 460° at a lower methyl cyanide flow rate than at 345° may be attributed to an increase, with temperature, of the rate of reaction 4, and may also indicate that there is more rapid consumption of nitrogen atoms at the higher temperature.

The pattern of acetylene production (Fig. 3) suggests that acetylene is a primary product from the attack of active nitrogen on methyl cyanide. It seems necessary to assume that acetylene is formed in a drastic disruption of the methyl cyanide molecule, perhaps in a sequence such as

$$CH_3CN + N \longrightarrow CH_3CN \cdot N$$
$$CH_3CN \cdot N + N \longrightarrow N_2 + \text{reactive fragments}$$
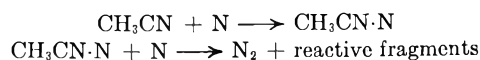
which would be expected to accompany catalyzed recombination. The recombination of two nitrogen atoms makes available more than 200 kcal. and there should be a good chance that the methyl cyanide part of the complex receives enough energy to dissociate into reactive fragments. Among the possible fragments are CH, CH_2, CH_3 and CN. Acetylene might then result from recombination of CH radicals, or from interradical reactions such as[17]

$$CH_2 + CH_3 \longrightarrow C_2H_2 + H_2 + H$$
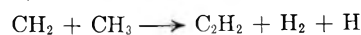
The presence of ethylene in the products may also be explained by interaction of radicals formed by fragmentation of the parent molecule, *e.g.*

$$2CH_2 \longrightarrow C_2H_4$$
$$CH + CH_3 \longrightarrow C_2H_4$$
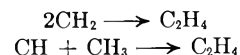
At low methyl cyanide flow rates, some of the fragments might be involved in subsequent reactions, such as

$$CH_2 + N \longrightarrow CN + H_2$$
$$CH + N \longrightarrow CN + H$$
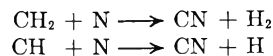
It seems reasonable to assume that some of the CN radicals produced directly or indirectly in the fragmentation of the methyl cyanide molecule should recombine to cyanogen. If these fragments were the only source of cyanogen, the following relation might be expected at high methyl cyanide flow rates and at low temperatures

$$C_2H_2 + C_2H_4 \geq C_2N_2$$

The fact that this relation is not satisfied (Figs.

(13) H. B. Dunford, H. G. V. Evans and C. A. Winkler, *Can. J. Chem.*, **34**, 1074 (1956).

(14) D. A. Armstrong and C. A. Winkler, *ibid.*, **33**, 1649 (1955).

(15) M. H. J. Wijnen and E. W. R. Steacie, *Disc. Faraday Soc.*, **14**, 118 (1953).

(16) M. H. J. Wijnen and E. W. R. Steacie, *J. Chem. Phys.*, **22**, 1074 (1954).

(17) H. Wiener and M. Burton, *J. Am. Chem. Soc.*, **75**, 5815 (1953).

2 and 3) suggests that reactions 2 and 3 may contribute appreciable cyanogen to the products.

The formation of some methylisonitrile in the methyl cyanide–nitrogen atom reaction is difficult to explain. It might arise from a reaction between CH_3 and CN radicals, or conceivably from an inversion reaction of the type reported by Ogg and Polanyi[18]

$$CN + CH_3CN \longrightarrow CH_3NC + CN - 15 \text{ kcal.}$$

However, the endothermicity of such a reaction would seem to require the participation of excited CN radicals.

(18) R. A. Ogg and M. Polanyi, *Trans. Faraday Soc.*, **31**, 482 (1935).

FORMATION CONSTANTS OF SOME METAL DERIVATIVES: S-ALKYL CARBOXYLIC ACIDS

By Roger J. Irving[1] and W. Conard Fernelius

Contribution from The College of Chemistry and Physics, The Pennsylvania State University, University Park, Pennsylvania

Formation constants are reported for the compounds $C_2H_5SCH_2COOH$, $C_2H_5SCH_2CH_2COOH$ and $o\text{-}C_2H_5SC_6H_4COOH$ with the following metals: Cu, Ni, Pb, Cd, Co, Zn, Mg. The order of stability for the metal derivatives of a given ligand is different in some respects from that previously established for coördination through oxygen and/or nitrogen. Five-membered chelate rings are more stable than six-membered rings. For these sulfur-containing ligands $\log K_2 > \log K_1$ with some metals, in contrast to the situation usually found for ligands coördinating through oxygen, nitrogen, nitrogen and oxygen, and nitrogen and sulfur. Difficulties encountered in the study of sulfur compounds are discussed.

Introduction

Since 1941 a good deal of information has accumulated on the relative stabilities of metal coördination compounds.[2-5] The data demonstrate the existence of several regularities among the properties of coördination compounds.[5-8] However, if one lists the ligand molecules or anions for which data on formation constants exist, one sees that these ligands all coördinate through the atoms oxygen and nitrogen: *oxygen only*, β-diketones, *o*-hydroxyaldehydes, tropolone, hydroxyquinones, kojic acid, etc.; *nitrogen only*, diamines, polyamines, *o*-phenanthroline, dimethylglyoxime, etc.; *oxygen and nitrogen simultaneously*, amines containing –O– and –OH, 8-quinolinol, amino acids, the "complexones," *o*-hydroxy azo dyes, etc. Although many familiar ligands coördinate through sulfur, very few data on formation constants exist for such ligands: *sulfur only* apparently none; *sulfur and nitrogen simultaneously*, amines containing –S– and –SH,[9,10] *o*-aminobenzenethiol[11]; *sulfur and oxygen simultaneously*, *o*-mercaptobenzoic acid.[12] Furthermore, these data are not suffi-

ciently numerous to permit one to judge whether the same regularities which hold for coördination through oxygen and nitrogen, are valid for coördination through sulfur. The present report is a preliminary account of an investigation begun in an effort to furnish formation constant data for sulfur-containing ligands.

Experimental

S-Ethylmercaptoacetic Acid, $C_2H_5SCH_2COOH$.—This compound was obtained by the action of ethyl mercaptan on monochloroacetic acid in alkaline solutions[13]: pale yellow liquid with an unpleasant odor; b.p. 117° at 11 mm., d^{20}_4 1.152; lit. values b.p. 117.8° at 11 mm., d^{20}_4 1.1518, 90% yield.

β-(S-Ethylmercapto)-propionic Acid, $C_2H_5SCH_2COOH$. —β-Chloropropionic acid (5.5 g.) was dissolved in 10 ml. of water containing 2.5 g. of sodium hydroxide. To the cooled solution (ice-bath) was added with constant stirring an ice-cold solution of 3.5 ml. of ethyl mercaptan and 2.5 g. of sodium hydroxide in 5 ml. of water. After the mixture was allowed to stand at room temperature for several hours, it was again cooled in ice and carefully made acid to litmus with 20% sulfuric acid. The solution was repeatedly extracted with ether, and the extract dried over calcium chloride. After removal of the ether, the oil was distilled *in vacuo* to yield a pale yellow oil soluble in water and readily soluble in dioxane; b.p. 127° at 12 mm., d^{20}_4 1.143, n^{25}_D 1.482, yield 3.8 g. (68% based on chloropropionic acid), neut. equiv., 134.0 g., theoretical 134.2 g., molar refraction 33.46 cc., calcd. 33.42 cc.

o-(S-Ethylmercapto)-benzoic Acid, $C_2H_5SC_6H_4COOH$.—Thiosalicylic acid (7.2 g.) was added to a solution of 5 g. of sodium hydroxide in 10 ml. of water and 50 ml. of alcohol. This mixture was refluxed with 3.9 ml. of ethyl iodide for 2 hours. On cooling and acidification with dilute hydrochloric acid (litmus as indicator) the compound separated as a white powder.[14] It was recrystallized twice from water; yield 95%, m.p. 135°; lit. value 134–135°.

2,3-Dimercaptopropanol was purchased from the Delta Chemical Works. Mercaptoacetic acid, cysteine hydrochloride, and methionine were obtained from Distillation Products Industries. Dioxane was purified by Eigenberger's procedure[15] and stored over activated alumina in a brown bottle to minimize the formation of oxidizing decomposition products on standing.

(1) New South Wales University of Technology, Sydney, Australia.

(2) J. Bjerrum, "Metal Ammine Formation in Aqueous Solution," P. Haase and Sons, Copenhagen, 1941.

(3) J. Bjerrum, *Chem. Revs.*, **46**, 381 (1950).

(4) A. R. Burkin, *Quart. Rev.*, **5**, 1 (1951).

(5) A. E. Martell and M. Calvin, "Chemistry of the Metal Chelate Compounds," Prentice–Hall, Inc., New York, N. Y., 1952.

(6) M. Calvin and K. W. Wilson, *J. Am. Chem. Soc.*, **67**, 2003 (1945).

(7) H. Irving and R. J. P. Williams, *Nature*, **162**, 746 (1949).

(8) (a) L. G. Van Uitert, W. C. Fernelius and B. E. Douglas, *J. Am. Chem. Soc.*, **75**, 2736 (1953); (b) L. G. Van Uitert and W. C. Fernelius, *ibid.*, **76**, 379 (1954).

(9) E. Gonick, W. C. Fernelius and B. E. Douglas, *ibid.*, **76**, 4671 (1954); C. R. Bertsch, W. C. Fernelius and B. P. Block, THIS JOURNAL, **60**, 384 (1956).

(10) G. L. McIntyre, Jr., Dissertation, The Pennsylvania State University, 1953.

(11) R. C. Charles and H. Freiser, *J. Am. Chem. Soc.*, **74**, 1383 (1952).

(12) T. Foley and R. C. Anderson, *ibid.*, **70**, 1195 (1948); **71**, 909 (1949); **72**, 5609 (1950); R. C. Anderson and S. E. Turner, *ibid.*, **71**, 912 (1949).

(13) J. P. Claesson, *Bull. soc. chim.*, [2] **23**, 444 (1875).

(14) Farbwerke vorm. Meister Lucius und Brüning, German Patent 203,882; *Chem. Zentr.*, **79**, II, 1791 (1908).

(15) E. Eigenberger, *J. prakt. Chem.*, **130**, 75 (1931).

TABLE I

FORMATION CONSTANTS OF METAL DERIVATIVES OF SULFUR-CONTAINING ACIDS IN 50% DIOXANE AT 30°

Metal Ion	S-Ethylmercaptoacetic acid			β-(S-Ethylmercapto)-propionic acid			o-(S-Ethylmercapto)-benzoic acid		
	Max. $\bar{n}$	log K_1	log K_2	Max. $\bar{n}$	log K_1	log K_2	Max. $\bar{n}$	log K_1	log K_2
H$^+$		−5.56			−6.34			−6.17	
Cu^{++}	2	4.55	3.60	2.5	4.2	a	2.0	4.16	3.30
Pb^{++}	1.7	3.97	2.90	2.2	4.34	3.57	2.0	4	d
Cd^{++}	0.8	3.45	...	2.1	3.17	3.55	2.0	3.34	3.35
Zn^{++}	1.0	3.14	...	2.0	3.02	3.22	2.0	2.87	3.52
Ni^{++}	0.9	3.12	...	1.7	2.86	3.38	1.7	2.37	3.62
Co^{++}	0.9	3.06	...	2.0	2.8 b	2.0	2.0	3.1	e
Mg^{++}	...	...	...	1.8	3.0 av. c		2.0	2.18	3.29

^{a} When $\bar{n}$ 0.7, a hydroxy species formed. ^{b} Likely, but not certain, value. ^{c} Value from formation curve because calculations from twelve sets of n values gave unreal roots in every case. ^{d} Even at small n values, hydroxy species formed. ^{e} Even at low pH values, hydroxy species formed.

The potentiometric titrations were performed at 30° by a modified form[16,17] of the procedure described by Calvin and Wilson,[6] with 0.1 mmole of metal ion as nitrate and 0.4 mmole of ligand present in 100 ml. of 50% dioxane. Calculations were made as described by Block and McIntyre.[18]

Results

The results are assembled in Table I. In several instances (EtSCH$_2$COOH with Cu, Pb, Cd; EtSCH$_2$CH$_2$COOH with Cu, Pb, Cd, Co*; o-EtSC$_6$H$_4$COOH with Pb, Cd) doubling the concentration of ligand (0.8 mmole of ligand to 0.1 mmole of metal ion) resulted in higher $\bar{n}$ values than those given in the table. (The variations were particularly large in the case marked*). However, in such cases calculations at the higher concentration for the case $N = 2$ yielded the same values for log K_1 and log K_2 as calculations at the lower concentration for the case $N = 2$.

No calculations of formation constants is possible when the acid dissociation constants of the ligand acids are not known. Simple titration in aqueous solution is not suitable for determination of the dissociation constants of very weak acids. Nevertheless, worthwhile information can be obtained by titrating such acids in the presence of metal ions and observing the relative displacements of the titration curves from that of the weak acid alone.

With 2,3-dimercaptopropanol (BAL), the ions, Cu^{++}, Ni^{++}, Pb^{++} and Zn^{++} gave precipitates above pH 3 in water. The Pb^{++} and Zn^{++} compounds were insoluble in all mixtures of water–dioxane up to 75% dioxane. The complexes of BAL with Cu and Ni are quite stable as shown by the lowering of the pH of BAL in the presence of metal ions, while Mg shows no evidence of coördination. From a solution of pH 10 where the ratio of BAL to Ni^{++} was 2:1, a soluble green compound was isolated. Calcd. for Ni(SCH$_2$CHSH·CH$_2$OH)$_2$: Ni, 19.4. Found: Ni, 20.6.

Although mercaptoacetic acid is essentially mono-

basic (pK_D = 5.3, pK_{D2} = 11) in titration with base, it is definitely dibasic when titrated in the presence of Ni^{++} and the titration curve shows strong coördination. The mercapto acid oxidizes readily.

Titration curves of aqueous solutions of cysteine in the presence of Cu^{++}, Ni^{++}, Zn^{++}, Pb^{++}, Cd^{++} and Co^{++} give evidence of coördination while those in the presence of Mn^{++} and Mg^{++} do not. The curves in general follow a complicated pattern above pH 5 due to oxidation,[19] precipitation, or formation of basic metal cysteinates. Cystine hydrochloride could not be studied, as it is insoluble in both water and water–dioxane mixtures.

Dissociation constants (pK_D) from the neutralization curve of methionine, CH$_3$SCH$_2$CH$_2$CHNH$_2$-COOH are 2.94 and 9.15.[20]

Methionine in 50% dioxane coördinates strongly with several metal ions and from the titration curves the order of stability is Cu > Ni > Zn > Co > Cd.

Discussion

The choice of suitable ligands coördinating through sulfur for potentiometric study is not easy despite their wide use in analytical chemistry. Many of the most interesting compounds are not suitable for study because of (1) lack of solubility of ligand and/or metal derivatives, (2) ease of hydrolysis, and (3) ease of oxidation of –SH groups to disulfides. Further, those sulfur compounds which are neither weak acids or bases cannot be studied by potentiometric titration.

The results tabulated in Table I show that like the chelate rings containing nitrogen and oxygen, the five-membered chelate rings containing sulfur are more stable than six-membered rings.

The increase in $\bar{n}$ values upon increasing the concentration of ligand is very unusual. If this increase in n is real and if it can be assumed that >S and –COO$^-$ are held with greatly different intensity, then it seems reasonable that the neutral species

(16) L. G. Van Uitert and C. G. Haas, Jr., J. Am. Chem. Soc., **75**, 451 (1953); L. G. Van Uitert, W. C. Fernelius and B. E. Douglas, ibid., **75**, 457 (1953).

(17) B. E. Bryant, W. C. Fernelius and B. E. Douglas, ibid., **75**, 3784 (1953).

(18) B. P. Block and G. H. McIntyre, Jr., ibid., **75**, 5667 (1953).

(19) M. P. Schubert, ibid., **53**, 3851 (1931).

(20) O. H. Emerson, P. L. Kirk and C. L. A. Schmidt, J. Biol. Chem., **92**, 449 (1931), give 2.28 and 9.21 at 25°.
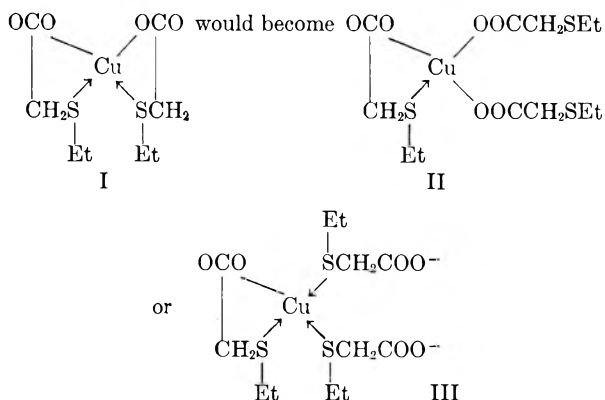
I seems more likely because many compounds of Cu and Pt of this type with sulfur-containing ligands are known.

The most important conclusion to be drawn from Table I is that for the three ligands the strength of bonding as indicated by log K_1 values is Co < Ni < Cu > Zn which is the same order of stability as for ligands containing oxygen and/or nitrogen. Irving and Williams[21] in a comprehensive study of the problem show that in the first transition series the stability order of the divalent metals is a direct consequence of their ionization potentials and ionic radii. The empirical order Cu > Ni > Pb > Co > Zn > Cd > Mg[8b,22] holds with minor variations for many oxygen and nitrogen type ligands, but lead and cadmium fall out of line when the ligand contains sulfur: Cu > Pb > Cd > Zn > Ni.

For the great majority of cases of metal ion coordination studied so far log K_n > log K_{n+1}. In several instances in Table I, log K_2 > log K_1. This situation is in direct contradiction to the view held by Bjerrum[23] that there is a statistical decrease in the numerical values of succeeding formation constants. Even though this may well be an over simplification omitting such factors as steric hindrance, type of hybrid orbitals formed, or possible rearrangement of orbitals, the instances where log K_2 > log K_1 are few in number

(21) H. Irving and R. J. P. Williams, *J. Chem. Soc.*, 3192 (1953).

(22) D. P. Mellor and L. Maley, *Nature*, **159**, 370 (1947); **161**, 436 (1948).

(23) Ref. 2, pp. 40-4.

Ag^{+}-NH₃: log K_1 = 3.19; log K_2 = 3.83[24]

Ag^{+}-monoamines[9,25]

Zn^{++}-NH₃: log K_1 = 2.37; log K_2 = 2.44; log K_3 = 2.50; log K_4 = 2.15[26]

Fe^{++}-dipyridyl: log K_1 = 4.26; log K_2 < 5; log K_3 > 7.3[27]

Fe^{++}-o-phenanthroline: log K_1 = 5.19; log K_{1-3} = 21.3

so that log K_2 and log K_3 are probably both greater than log K_1.[28] The abnormally high second and third formation constants of ferrous ion with dipyridyl and o-phenanthroline have been explained on the basis of "orbital stabilization." The evidence of an electronic rearrangement lies in the change from paramagnetism to diamagnetism.[21] No explanation of the reversal of order of formation constants in the case of Ag^{+} and Zn^{++} has been proposed. The general reversal of order for these sulfur-containing ligands makes a study of these ligands particularly important.

Several earlier workers have studied the metal derivatives of cysteine.[19,29-33] The Ni^{++}, Co^{++}, Co[+++] and Fe^{++} derivatives have been definitely established (in some cases more than one for a given ion). The Ni^{++} compound is stable; the Co^{++} compound oxidizes readily to a substance which seems to contain Co[+++] and some cystine; the Fe^{++} compound is stable but the Fe[+++] compound formed on oxidation is unstable so that cystine is the product.

(24) Ref. 2, pp. 130-6.

(25) R. J. Bruehlman and F. A. Verhoek, *J. Am. Chem. Soc.*, **70**, 1401 (1948).

(26) Ref. 2, pp. 152-64.

(27) P. Krumholz, *J. Am. Chem. Soc.*, **71**, 3654 (1949).

(28) T. S. Lee, I. M. Kolthoff and D. L. Leussing, *ibid.*, **70**, 2348 (1948); I. M. Kolthoff, D. L. Leussing and T. S. Lee, *ibid.*, **72**, 2173-7 (1950).

(29) A. Rosenheim and I. Davidsohn, *Z. anorg. Chem.*, **41**, 231 (1904).

(30) C. Neuberg and P. Mayer, *Z. physiol. Chem.*, **44**, 498 (1905).

(31) W. Cremer, *Biochem. Z.*, **132**, 426 (1928); **194**, 231 (1928); **201**, 489 (1928); **206**, 228, 236 (1929).

(32) L. Michaelis, *J. Biol. Chem.*, **83**, 191 (1929); **84**, 777 (1929); L. Michaelis and S. Yamaguchi, *ibid.*, **83**, 367 (1929).

(33) H. B. Vickery and C. S. Leavenworth, *ibid.*, **86**, 129 (1930).

KINETIC STUDY OF THE TRIFLUOROACETONITRILE–BUTADIENE CYCLIZATION[1]

BY JOHN M. S. JARVIE AND GEORGE J. JANZ

Contribution from the Department of Chemistry, Rensselaer Polytechnic Institute, Troy, N. Y.

A kinetic study of the trifluoroacetonitrile–butadiene cyclization reaction in the temperature range 350–520° is reported. The reaction is homogeneous and second order, the rate expression being $k_2 = 2.1 \times 10^9 e^{-21,500/RT}$. Comparison of these data with the kinetic parameters of normal diene reactions, at high temperatures, shows that this reaction is an example of a Diels–Alder process in which the dihydro-cyclic adduct loses hydrogen spontaneously under the conditions of the reaction to form 2-trifluoromethylpyridine. From consideration of the entropies of activation, it follows that the transition state, while similar to that in the normal Diels–Alder process, may be more bonded in structure.

The reaction of cyanogen and related nitriles with 1,3-dienes to form 2-substituted pyridines; *i.e.*

$$\text{(diene)} + C\!\!-\!\!R \longrightarrow \text{(pyridine)} + H_2 \qquad (1)$$

has been studied by Janz and co-workers[2] in the homogeneous gas phase and over catalyst surfaces. More recently it was observed[3] that with trifluoroacetonitrile and butadiene, reaction proceeds readily without the presence of catalysts at 400° with the formation of 2-trifluoromethylpyridine as product. The present communication describes a kinetic study of this reaction in the temperature range 350–520°. A discussion of the result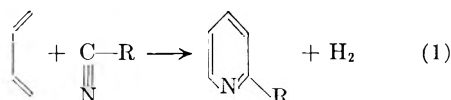s in the light of the high temperature Diels–Alder and the cyanogen–butadiene reactions gives a further insight on the mechanism of this generalized cyclization-dehydrogenation reaction.

Experimental

Description of Flow Apparatus.—The system used was an all glass apparatus, having a preheater maintained at about 250° so that the gases entering the reaction zone were of sufficiently high temperature to prevent any cooling at the entrance. The gas flows were controlled by two needle valves (Edwards and Co.) and read on rotameters (Emil Greiner) which had been calibrated previously for both trifluoroacetonitrile and butadiene. The nitrogen flow was measured by a capillary type flowmeter. The temperature in the reaction zone was measured by means of six chromel–alumel thermocouples placed in a well over the length of the reactor.

The trifluoroacetonitrile (Columbia Organic) and butadiene (Matheson) were transferred from the cylinders supplied by the manufacturers to glass cylinders and were degassed on a vacuum system. The glass cylinder of butadiene was placed in an ice–water mixture previous to the commencement of a run and the trifluoroacetonitrile cylinder in an acetone–chloroform mixture to which Dry Ice was added until the temperature was constant in the range −62 to −58°.

The product and the unreacted reactants were collected in two Dry Ice traps and two liquid nitrogen traps. The system was flushed for 30 minutes with nitrogen before and after each experiment. It was found that all the product was collected in the first Dry Ice trap in addition to most of the butadiene. These were subsequently separated by a simple distillation. The trifluoroacetonitrile was collected as a white solid in the liquid nitrogen traps. A summary of experiments completed is given in Table I. From a consideration of the limits of error in the operation of flow

methods, a variation of 10% is possible in the rate constant. However, for internal consistency the values given in Table I are shown with more significant figures than are necessary. An experiment designed to correlate the amount of hydrogen evolved with the pyridinic product formed (runs 37 and 39) utilized a Toepler pump and a calibrated volume to collect this gas. The number of moles of hydrogen was calculated from the pressure and volume of the gas thus collected escaping from the liquid nitrogen traps in the reaction system.

Determination of 2-Trifluoromethylpyridine for Rate Calculations.—In the initial stage of this work, it was thought the refractive index would afford a means of determining the amount of trifluoromethylpyridine present in the product. It was found that this method gave unsatisfactory results, probably because the other substances present interfere with the refractive index determination, which was based on a calibration assuming only trifluoromethylpyridine and vinylcyclohexene as products.

The ultraviolet spectra of 2-trifluoromethylpyridine and 3-vinylcyclohexene-1 were examined in order to find out if trifluoromethylpyridine could be determined in the presence of vinylcyclohexene and the other products formed. The spectrum of trifluoromethylpyridine in alcohol is shown in Fig. 1. Two maxima were observed close together at 251 and 256 mμ and having extinction coefficients of 1685 and 1784, respectively. The spectrum of vinylcyclohexene in alcohol in the same region showed a peak at 273 mμ and ϵ 4.5. The values obtained for the extinction coefficient over the range 220–340 mμ did not exceed 8, while in the region 250–260 mμ the extinction coefficient had the value of about 4. From this it is apparent that the interference in the spectrum of trifluoromethylpyridine caused by the presence of vinylcyclohexene is exceedingly small and may be considered negligible in the use of ultraviolet analysis for the quantitative determination of the trifluoromethylpyridine.

A distillation of the reaction product was carried out to separate the fraction boiling higher than trifluoromethylpyridine. A study of the ultraviolet spectrum showed that the higher boilers did not interfere with the determination of trifluoromethylpyridine. It follows that this method for the determination of trifluoromethylpyridine in the presence of vinylcyclohexene and the high boilers is satisfactory.

Results and Discussion

The forms of the kinetic rate equations in flow systems have been considered by Harris[4] in detail. For a second-order process, where the limiting cases of complete and negligible diffusion can be neglected; *i.e.*, for low conversions, the rate law has the form

$$k_2 = \frac{V_1^2}{V_r}\left(\frac{N_C}{N_{A_1}N_{B_1}}\right) \text{ cc. mole}^{-1}\text{ sec.}^{-1} \qquad (2)$$

in which V_1 is the volume of the gases entering the reaction zone, V_r, at the temperature and pressure of the reaction, and N_{A_1}, N_{B_1}, N_C are the moles of trifluoroacetonitrile, butadiene and trifluoromethylpyridine per second flowing through the reaction

(1) Part XI in the series, "The Reaction of Cyanogen and Related Nitriles with 1,3-Dienes." Presented before the General Session, Petroleum Division, American Chemical Society, Atlantic City, September, 1956.

(2) G. J. Janz and co-workers, *J. Am. Chem. Soc.*, **76**, 6377 (1954); **77**, 3014 (1955).

(3) J. M. S. Jarvie, W. E. Fitzgerald, and G. J. Janz, *ibid.*, **78**, 978 (1956).

(4) G. M. Harris, THIS JOURNAL, **51**, 505 (1947).

TABLE I

RUN DATA FOR BUTADIENE–TRIFLUOROACETONITRILE REACTION

Run	Partial pressure of reactants (atm.) CF₃CN	C₄H₆	N₂	Contact time (sec.)	Conversion × 10², % CF₃CN	C₄H₆	Temp., °K.	Rate constant, cc. moles⁻¹ sec.⁻¹
5	0.383	0.413	0.205	39.3	6.45	5.98	666	219
6	.367	.292	.402	29.6	3.79	3.98	678	243
7	.254	.253	.492	23.4	1.63	1.64	687	156
12	.478	.522	...	41.1	9.82	10.33	672	252
13	.387	.400	.213	37.8	15.32	14.80	718	596
14	.371	.327	.302	31.5	5.27	5.98	688	289
15	.406	.384	.210	37.0	17.01	18.00	722	708
16	.396	.390	.215	35.2	44.43	45.10	776	2060
17	.407	.389	.205	35.5	18.22	19.08	733	795
18	.377	.396	.227	41.0	12.49	11.90	703	444
19	.402	.386	.212	38.9	7.85	8.18	694	298
20	.254	.260	.486	26.1	2.21	2.17	672	179
21	.198	.190	.612	19.0	0.567	0.592	674	87.1
22	.354	.354	.292	35.5	4.38	4.37	668	191
23	.442	.558	...	38.0	10.13	8.01	683	268
24	.399	.503	.098	40.6	7.10	5.64	671	192
25	.408	.498	.094	36.6	22.42	18.36	715	721
26	.551	.449	...	36.6	20.89	25.66	726	757
27	.574	.426	...	37.5	24.31	32.74	749	934
28	.618	.382	...	30.1	35.71	57.80	796	2030
29	.597	.403	...	38.5	10.13	15.01	696	373
30	.588	.412	...	43.5	1.95	2.79	630	56.3
31	.422	.356	.216	12.1	0.121	0.148	675	16.1
32(P)ᵃ	.613	.388	...	47.1	9.48	14.99	688	293
33(P)ᵃ	.484	.296	.220	36.3	4.98	8.14	688	261
37	.595	.405	...	39.7	10.90	16.00	696	387 (402)ᵇ
39	.475	.525	...	39.6	14.00	12.69	693	383 (386)ᵇ

ᵃ (P) Reactor packed with Pyrex chips. ᵇ ( ) In Rate Constant column refers to k_2 calculated from moles of hydrogen evolved.

zone. In the present case, this relation can be expressed by the equation

$$k_2 = \frac{\text{(fractional conversion of CF}_3\text{CN)}}{\text{(contact time)(partial pressure of C}_4\text{H}_6)} \quad (3)$$

for convenience of calculation. The rate constants, k_2, reported in Table I were computed in this manner.

Kinetic Results

The effects of contact time, partial pressures and surface area were investigated to test the validity of the rate equation, and the order of the reaction. The dependence of the rate constant on the contact time was investigated at 400°. The data (runs 5, 6, 7, 12, 20, 21, 23, 24 and 31, Table I) were extrapolated to this exact temperature using the slope of the Arrhenius plot. It was found that at contact times greater than 30 sec., the rate constant was independent of time. The failure of the rate law at contact times less than 30 sec. is not understood, but may be, in part, due to the fact that temperature equilibrium may not be attained by the gases. In the present work, the contact times used at all temperatures were greater than 30 sec.

The rate constants, normalized to 420°, for the variation in partial pressures with nitrogen gas (runs 6, 13, 18, 22 and 24, Table I) and in the molar ratios of reactants (runs 6, 13, 22, 24, 26 and 29, Table I) were constant (338 ± 18) within the experimental limits of error. The homogeneity of this reaction was established using a reaction vessel packed with Pyrex chips to increase the surface area fiftyfold (runs 32 and 33).

The temperature dependence of the rate constant was investigated to obtain the parameters of the Arrhenius equation. The plot of log k_2 and $1/T°$K. is linear over the whole range investigated. The rate equation for this process,
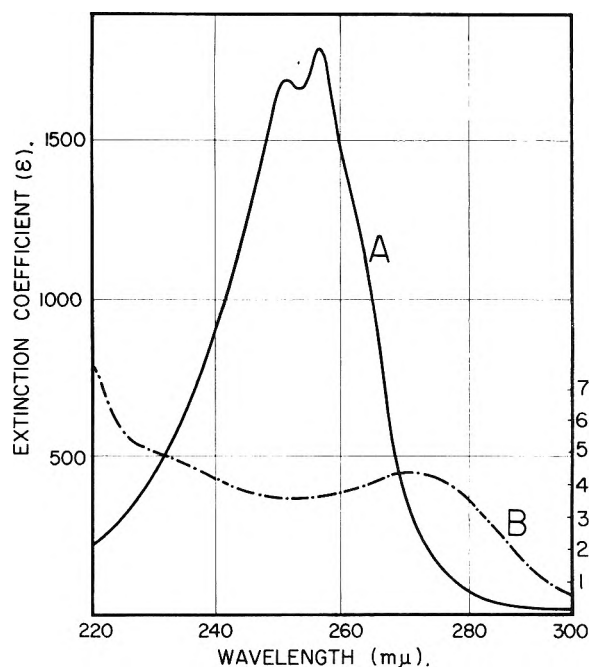

Fig. 1.—Ultraviolet absorption spectra of trifluoromethyl-pyridine and 3-vinylcyclohexene-1 in alcohol: A, trifluoromethylpyridine; B, 3-vinylcyclohexene-1.

accordingly, is

$$k_2 = 2.1 \times 10^9 \, e^{-21,500/RT} \qquad (4)$$

the reaction being second order over-all, but first order with respect to each of the reactants, butadiene and trifluoroacetonitrile, respectively. The rate constants, interpolated at even temperatures, are given in Table II.

TABLE II

RATE CONSTANTS[a] FOR THE TRIFLUOROACETONITRILE–BUTADIENE REACTION OVER THE TEMPERATURE RANGE 350–520°

Temp., °C.	k_2, cc. moles^{-1} sec.$^{-1}$	Temp., °C.	k_2, cc. moles^{-1} sec.$^{-}$
350	58.1	440	528
360	76.6	450	649
370	101	460	802
380	131	470	982
390	169	480	1190
400	210	490	1430
410	274	500	1720
420	345	510	2070
430	429	520	2470

[a] Interpolated from the experimental results plotted as log k_2 against $1/T°$K.

The reaction of trifluoroacetonitrile with butadiene may be formulated as
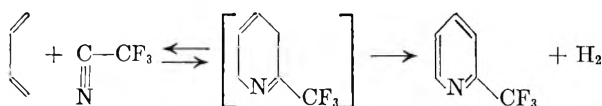
in which the dihydropyridine derivative postulated above corresponds to the normal adduct in an orthodox Diels–Alder association reaction. Theoretical considerations[5] on the stability of dihydropyridine relative to pyridine show that the dihydro compound is thermodynamically quite

Diene	Dienophile	Temp. range (°C.)
Butadiene	Acrolein	155–322
Butadiene	Crotonaldehyde	242–300
Butadiene	Butadiene	173–386
		418–650
Butadiene	Ethylene	487–648
Butadiene	Cyanogen	325–450
Butadiene	Trifluoroacetonitrile	357–523

unstable, and thus, if formed under conditions favoring aromatization, would be expected to pass over to the pyridinic product. A hydrogen–pyridinic product balance in the ratio of 1.0/1.0 accordingly is predicted for the over-all process under consideration. In the present work an experiment was devised in which the amount of hydrogen evolved during the reaction could be collected. The results (runs 37, 39, Table I, 4.64 × 10^{-2}, 4.46 × 10^{-2}, and run 39, 3.40 × 10^{-2}, 3.75 × 10^{-2} moles of hydrogen and trifluoromethylpyridine,

(5) P. J. Hawkins and G. J. Janz, *J. Chem. Soc.*, 1479 (1949).

(6) G. Kistiakowsky and J. Lacher, *J. Am. Chem. Soc.*, **55**, 4109 (1933).

(7) M. G. Evans and E. Warhurst, *Trans. Faraday Soc.*, **34**, 614 (1938).

(8) G. Kistiakowsky and J. Ransom, *J. Chem. Phys.*, **7**, 373 (1939).

(9) D. Rowley and H. Steiner, *Faraday Soc. Disc.*, **10**, 198 (1951).

(10) P. J. Hawkins and G. J. Janz, *J. Am. Chem. Soc.*, **74**, 1790 (1952).

respectively) confirmed the prediction above; *i.e.*, that hydrogen is produced in the same molar ratio as the pyridinic product.

An insight on the mechanism of this reaction can be gained by comparison of the kinetic results with other high temperature homogeneous gas phase reactions. A summary of the pertinent data is given below.

The entropies of activation, ΔS^*, have been calculated from the absolute rate theory equations[11] for two typical Diels–Alder type reactions as well as for the trifluoromethylpyridine and cyanogen cyclizations. The Arrhenius A factor and the energy of activation for the trifluoroacetonitrile–butadiene reaction fall within the range (10^9–10^{10}, 20–24 kcal.) for typical Diels–Alder association reactions. It follows from this that the kinetic parameters of the present system may be attributed to a rate-controlling step similar to that for the Diels–Alder addition, *i.e.*, the cyclization step. The kinetics of the diene associations at high temperatures in the homogeneous gas phase have been discussed recently in detail.[9] It was shown that a cyclic transition complex was in best accord with all available rate data. The entropy of activation in the trifluoroacetonitrile–butadiene cyclization is about 2 to 4 e.u. more negative than that in the orthodox Diels–Alder associations. If significant, this indicates that the transition complex has a more bonded structure in this cyclization than in the comparable diene associations.

It is of interest to compare the kinetic results reported for the cyclization of cyanogen with butadiene[10] with the present work. The energy of activation for the former is 5 to 10 kcal./mole higher, and the frequency factor 10^2 higher than that obtained for the trifluoroacetonitrile–butadiene cyclization, and the orthodox Diels–Alder reactions.

A Factor	ΔE	ΔS^*	Ref.
1.46 × 10^9	19.7		6
0.9 × 10^9	22.0		7
9.2 × 10^9	23.69	−16.9	8
1.4 × 10^{11}	26.8		9
3.0 × 10^{17}	27.5	−14.5	9
1.6 × 10^{12}	31.6	−11.8	10
2.1 × 10^9	21.5	−19.4	This work

The entropy of activation calculated for the cyanogen–butadiene reaction (−11.8 e.u.) is considerably greater than the values found for the present system and the related diene associations. A comparison of the rotational entropy increments accompanying the configurational changes when butadiene and cyanogen approach the position for 1,4-addition (−6 e.u.), with the loss in translational entropy in the formation of a bonded cyclic complex (−40 e.u.), indicates that the transition complex must have greater looseness than in the other reactions. The orientation of butadiene and cyanogen into the position for 1,4-addition accounts for approximately one half of the entropy of activation, so that the degree of bond formation in the transition complex must be quite incipient.

(11) S. Glasstone, K. Laidler and H. Eyring, "Theory of Rate Processes," McGraw-Hill Book Co., New York, N. Y., 1941, p. 198.

The use of trifluoroacetonitrile in the dienes–nitriles cyclization has also been of interest since the (CN) group is coupled with a group having a very strongly electrophilic nature. Of the nitriles previously studied (HCN, CH_3CN, C_2H_5CN, C_6H_5CN, CH_2=CH—CN and $(CN)_2$) only cyanogen reacted at an appreciable rate in the homogeneous gas phase. In the present instance, the high reactivity of the (CN) group in trifluoroacetonitrile may be attributed to the polarization of the dieno-philic link by the proximity of the CF_3 group with its strong electrophilic properties. A study of importance of this effect in the mechanism in the homogeneous gas phase reaction is in progress.

A STUDY OF THE CONDUCTANCE BEHAVIOR OF SOME UNI-UNIVALENT ELECTROLYTES IN DIMETHYL SULFOXIDE AT 25°[1]

BY PAUL G. SEARS, GEORGE R. LESTER AND LYLE R. DAWSON

Department of Chemistry, University of Kentucky, Lexington, Kentucky

Received May 24, 1956

The conductances of nineteen uni-univalent electrolytes in dimethyl sulfoxide have been measured at 25° for solute concentrations ranging from 3–700 × 10⁻⁵ N. In every case, excellent agreement exists between the experimentally observed behavior and that predicted theoretically by the Onsager equation. The limiting equivalent conductance of each electrolyte has been evaluated by an extrapolation of a Shedlovsky plot of Λ'_0 versus C. Limiting ionic equivalent conductances which are based upon the equal conductances of the *n*-octadecyltrimethylammonium and the *n*-octadecyl sulfate ions agree within 2–5% with those which are based upon an assumed constancy of the limiting conductance–viscosity product of the tetra-*n*-butylammonium ion in non-aqueous solvents. The conductance behavior of electrolytes in dimethyl sulfoxide closely resembles that for the same electrolytes in dimethylformamide and in pyridine.

Introduction

Dimethyl sulfoxide (CH_3SOCH_3) is a recently introduced, versatile solvent which now has become available commercially as a relatively inexpensive, very pure product. It is characterized by a broad, convenient liquid range (18.4–189°), a moderate viscosity (0.0196 poise), a relatively high dielectric constant (46.6), and extensive dissolving power. Its high Trouton constant (29.5)[2] is evidence that it is an associated liquid. The structural aspects of dimethyl sulfoxide indicate that it should function as an electron-donor solvent; hence, its solutions might be expected to exhibit solute–solvent interactions similar to those which have been observed for solutions of the same solutes in dimethylformamide, acetone or pyridine. The objectives of this research, therefore, have been to investigate the potentialities of dimethyl sulfoxide as an electrolytic solvent through a study of the conductimetric behavior of several electrolytes and to compare the pattern of results for dimethyl sulfoxide solutions with those which have been reported for solutions of the same electrolytes in other electron-donor solvents.

Experimental

1. Purification of Solvent.—Dimethyl sulfoxide, which was supplied as 99.9% pure by the Stepan Chemical Company, was refluxed for several hours in contact with calcium oxide and then was fractionated through an efficient distillation column at a reduced pressure of approximately 5 mm. The middle fractions thus obtained were fractionated one or more times at the same pressure until the dimethyl sulfoxide which finally was retained had a conductivity which did not exceed 3 × 10⁻⁸ ohm⁻¹ cm.⁻¹ as well as the desired density, viscosity and dielectric constant.

2. Purification of Salts.—Tetra-*n*-butylammonium and trimethylphenylammonium iodides and sodium benzenesulfonate (all Eastman Kodak Co. grade) were recrystallized three times from methanol or ethanol–ether mixtures. Trimethylphenylammonium benzenesulfonate (practical grade) was treated with bone-black prior to several recrystallizations from methanol. These salts were dried to constant weight *in vacuo* at 70°.

The purification and the drying of the potassium and sodium salts have been described in previous papers.[3,4]

The following salts were furnished in purified form by E. D. Wilhoit[5]: potassium *n*-octadecyl sulfate, m.p. 179–181°; *n*-octadecyltrimethylammonium nitrate, m.p. 200–202°; *n*-octadecyltrimethylammonium iodide, m.p. 234–236°.

3. Apparatus and Procedure.—The bridge, cells, bath and temperature control and procedure of the conductance measurements have been described previously.[3,6] The dielectric constant of each fraction of dimethyl sulfoxide was determined at ten megacycles using the equipment and procedure which have been described by Leader.[7] The viscosity of each fraction of dimethyl sulfoxide was measured using size-50 Cannon–Fenske viscometers which were calibrated by the Cannon Instrument Company. Kinetic energy corrections were assumed to be negligible.

The following data for dimethyl sulfoxide at 25° were used in the calculations: density, 1.096 g./ml.; viscosity, 0.0196 poise; dielectric constant, 46.6. Values of the fundamental constants were taken from a 1952 report of the Subcommittee on Fundamental Constants.[8]

Results

Corresponding values of the equivalent conductance, Λ, and the concentration in gram equivalents per liter, C, are presented in Table I for each of the

(1) Taken from a thesis submitted by George R. Lester in partial fulfillment of the requirements for the degree of Master of Science.

(2) T. B. Douglas, *J. Am. Chem. Soc.*, **70**, 2001 (1948).

(3) D. P. Ames and P. G. Sears, THIS JOURNAL, **59**, 16 (1955).

(4) P. G. Sears, R. K. Wolford and L. R. Dawson, *J. Electrochem. Soc.*, accepted.

(5) E. D. Wilhoit, Dissertation University of Kentucky, 1956.

(6) P. G. Sears, E. D. Wilhoit and L. R. Dawson, *J. Chem. Phys.*, **23**, 1274 (1955).

(7) G. R. Leader, *J. Am. Chem. Soc.*, **73**, 856 (1951).

(8) F. D. Rossini, F. T. Gucker, H. L. Johnston, L. Pauling and G. W. Vinal, *ibid.*, **74**, 2699 (1952).

nineteen electrolytes which were studied. The maximum experimental error inherent in these data is estimated to be 0.15%.

Table I

Equivalent Conductances of Some Electrolytes in Dimethyl Sulfoxide at 25°

$C \times 10^4$	Λ	$C \times 10^4$	Λ	$C \times 10^4$	Λ
(a) Potassium iodide		(b) Sodium iodide		(c) Potassium bromide	
0.7092	37.81	0.5083	37.24	1.529	37.83
2.317	37.41	2.718	36.75	5.175	37.32
8.123	36.91	6.335	36.30	10.88	36.80
13.30	36.31	13.44	35.74	23.27	36.04
19.72	35.99	22.59	35.25	35.89	35.38
26.96	35.67	32.92	34.82	52.52	34.92
(d) Sodium bromide		(e) Potassium thiocyanate		(f) Sodium thiocyanate	
1.432	37.40	1.331	42.90	1.434	42.36
4.147	36.95	4.212	42.44	3.080	42.02
10.44	36.31	8.292	41.97	8.865	41.36
22.12	35.57	16.07	41.41	18.33	40.64
24.52	35.01	25.53	40.88	29.87	40.04
50.71	34.45	37.47	40.30	44.48	39.43
(g) Potassium nitrate		(h) Sodium nitrate		(i) Potassium perchlorate	
1.005	40.95	2.669	39.81	1.867	38.44
3.546	40.44	6.451	39.26	3.641	38.15
7.064	39.96	13.04	38.60	9.470	37.58
15.46	39.13	23.05	37.91	19.13	36.96
25.55	38.44	35.72	37.15	27.39	36.52
36.45	37.87	51.76	36.41	37.66	36.13
(j) Sodium perchlorate		(k) Potassium picrate		(l) Sodium picrate	
0.7860	37.86	0.4676	31.36	0.9568	30.65
4.644	37.24	2.045	30.95	4.799	30.07
8.771	36.88	5.198	30.53	8.257	29.69
14.25	36.49	12.09	30.02	15.84	29.20
22.19	36.06	19.71	29.62	25.21	28.75
44.51	35.25	29.64	29.15	37.51	28.23
(m) Tetra-n-butylammonium iodide		(n) Tri-methylphenyl-ammonium iodide		(o) Tri-methylphenyl-ammonium benzenesulfonate	
1.970	34.25	2.126	37.05	1.810	30.21
4.117	33.98	5.120	36.68	5.282	29.71
8.550	33.54	12.00	36.07	9.224	29.37
14.19	33.15	23.98	35.33	20.19	28.62
22.46	32.67	38.30	34.66	33.35	27.97
31.42	32.29	49.00	34.29	43.71	27.57
(p) Sodium benzenesulfonate		(q) n-Octadecyl-trimethyl-ammonium nitrate		(r) n-Octadecyl-trimethyl-ammonium iodide	
2.768	29.73	0.2830	36.71	0.2882	33.53
6.521	29.29	0.9595	36.71	1.260	33.26
15.14	28.58	3.216	36.10	2.995	32.95
31.83	27.67	6.574	35.70	5.410	32.68
51.63	26.89	10.26	35.37	8.983	32.33
66.97	26.41	(s) Potassium n-octadecyl sulfate			
		0.3018	24.17		
		1.141	23.97		
		3.004	23.69		
		6.324	23.34		
		9.647	23.08		

Discussion

For each salt in dimethyl sulfoxide, a linear plot of the equivalent conductance *versus* the square root of the concentration was obtained for concentrations less than 2×10^{-3} N. The data which are presented in Table II show in each case that excellent agreement exists between the limiting experimental and the theoretical Onsager[9] slopes and therein indicate that the salts are completely dissociated in dimethyl sulfoxide. At concentrations greater than 2×10^{-3} N, the slopes of the plots of Λ *versus* $\sqrt{C}$ exhibit various types of minor deviations from those predicted theoretically; however, these deviations are somewhat expected inasmuch as the Onsager equation is a limiting expression and applies only to very dilute solutions.

Table II

Test of Onsager's Equation for the Conductances of Some Uni-univalent Salts in Dimethyl Sulfoxide at 25°

Salt	Λ_0	Theor. slope (S_T)	Exptl. slope (S_E)	% Dev. $(S_E - S_T)$ $100/S_T$
KI	38.2	−55	−54	−2
NaI	37.6	−55	−50	−9
KBr	38.4	−55	−53	−4
NaBr	38.0	−55	−54	−2
KSCN	43.5	−58	−55	−5
NaSCN	43.0	−57	−56	−2
KNO₃	41.5	−57	−60	5
NaNO₃	40.8	−56	−60	7
KClO₄	39.1	−55	−53	−4
NaClO₄	38.3	−55	−50	−9
KPi[a]	31.7	−52	−49	−6
NaPi	31.1	−52	−49	−6
Bu₄NI	35.0	−53	−48	−9
Me₃PhNI	37.8	−55	−56	2
Me₃PhNSO₃Ph	30.9	−51	−52	2
NaSO₃Ph	30.6	−51	−52	2
Me₃OctdNNO₃[b]	37.0	−54	−50	−7
Me₃OctdNI	33.8	−53	−49	−7
KOctSO₄	24.5	−48	−44	−8

[a] Pi represents picrate.   [b] Octd represents octadecyl.

Values of the limiting equivalent conductances of the salts in dimethyl sulfoxide were determined by mathematically extrapolating plots of the Shedlovsky rearrangement and extension of the Onsager equation.[10] This modified equation which may be written in general form as

$$\frac{\Lambda + \beta\sqrt{c}}{1 - \alpha\sqrt{c}} = \Lambda_0' = \Lambda_0 + BC \qquad (1)$$

reduces to the following expression for dimethyl sulfoxide solutions at 25°

$$\frac{\Lambda + 35.7\sqrt{c}}{1 - 0.502\sqrt{c}} = \Lambda_0' = \Lambda_0 + BC \qquad (2)$$

The plot of Λ_0' *versus* C for each salt is linear over the entire concentration range which was studied. The results are summarized in Table III.

Numerous combinations of the values of Λ_0 in Table III provide substantiation of the Kohlrausch law of independent ionic migrations for dimethyl sulfoxide solutions. The values of B (and also of

(9) L. Onsager, *Physik. Z.*, **28**, 277 (1927).
(10) T. Shedlovsky, *J. Am. Chem. Soc.*, **54**, 1405 (1932).

TABLE III

DATA DERIVED FROM PLOTS OF Λ_0' *versus* C FOR SOME SALTS IN DIMETHYL SULFOXIDE AT 25°

Salt	Λ_0	B	Salt	Λ_0	B
KI	38.2	90	KPi	31.7	90
NaI	37.6	100	NaPi	31.1	55
KBr	38.5	90	Bu₄NI	35.0	80
NaBr	38.0	60	Me₃PhNI	37.9	50
KSCN	43.5	100	Me₃PhNSO₃Ph	30.9	8
NaSCN	43.0	65	NaSO₃Ph	30.6	8
KNO₃	41.5	-80	Me₃OctdNNO₃	37.0	90
NaNO₃	40.8	-95	Me₃OctdNI	33.8	150
KClO₄	39.1	115	KOctdSO₄	24.5	110
NaClO₄	38.3	145			

B' which can be calculated by dividing B by Λ_0) do not show any consistent parallelism with those which have been observed for solutions of the same electrolytes in water or in hydrogen cyanide.[11]

Several methods have been used to approximate limiting ionic equivalent conductances in non-aqueous solvents. Thompson and Kraus[12] have suggested that the limiting equivalent conductances of the n-octadecyltrimethylammonium and the n-octadecyl sulfate ions should be equal and therefore can be evaluated by halving the value of Λ_0 for n-octadecyltrimethylammonium n-octadecylsulfate. Then utilizing the data for additional salts in which one of these ions is present, other ionic conductances can be calculated. Although n-octadecyltrimethylammonium n-octadecyl sulfate is virtually insoluble in dimethyl sulfoxide, the value of its limiting equivalent conductance has been calculated indirectly by two combinations of the values of Λ_0 for potassium n-octadecyl sulfate, potassium nitrate, n-octadecyltrimethylammonium nitrate, potassium iodide and n-octadecyltrimethylammonium iodide. Taking the limiting conductance of each of the two large ions in dimethyl sulfoxide as 10.0 ohm⁻¹ cm.² equiv.⁻¹, other ionic conductances were calculated. The results are summarized in Table IV.

TABLE IV

LIMITING EQUIVALENT CONDUCTANCES OF IONS IN DIMETHYL SULFOXIDE AT 25° BASED UPON THE METHOD OF THOMPSON AND KRAUS

Cation	$\Lambda_0{}^+$	Anion	$\Lambda_0{}^-$
K⁺	14.4	SCN⁻	29.2
Me₃PhN⁺	14.1	NO₃⁻	27.0
Na⁺	13.8	ClO₄	24.6
Bu₄N⁺	11.2	Br⁻	24.2
Me₃OctdN⁺	10.0	I⁻	23.8
		Pi⁻	17.3
		PhSO₃⁻	16.8
		OctdSO₄⁻	10.0

The constancy of the conductance–viscosity product for the tetra-n-butylammonium ion was suggested initially by Pickering and Kraus[13] as a basis for approximating limiting ionic conductances. Healey and Martell[14] and also McDowell

and Kraus[15] have discussed the applications of this method. Assuming the value of the conductance–viscosity product of the tetra-n-butylammonium ion in dimethyl sulfoxide to be 0.208 ± 0.009 ohm⁻¹ cm.² equiv.⁻¹ poise, values of anionic limiting conductances were calculated which were 2–5% greater than those based on the n-octadecyltrimethylammonium n-octadecyl sulfate method.

If the limiting ionic conductance data in Table IV are considered to be reasonably reliable, it is interesting to note that the conductance–viscosity product for the picrate ion in dimethyl sulfoxide is approximately 0.34 ohm⁻¹ cm.² equiv.⁻¹ poise. This appears to be an unusually high value for the product although Kraus[16] has emphasized the unusual nature of the product for the picrate ion in other electron-donor solvents such as pyridine and nitrobenzene.

TABLE V

RATIOS OF THE LIMITING EQUIVALENT CONDUCTANCES OF SOME POTASSIUM AND SODIUM SALTS IN DIMETHYLFORMAMIDE, PYRIDINE AND ACETONE TO THOSE IN DIMETHYL SULFOXIDE AT 25°

Salt	$\dfrac{\Lambda_0(DMF)^a}{\Lambda_0(DMSO)^b}$	$\dfrac{\Lambda_0(Pyridine)}{\Lambda_0(DMSO)}$	$\dfrac{\Lambda_0(Acetone)}{\Lambda_0(DMSO)}$
NaI	2.18	2.00	5.07
KI	2.16	2.10	5.06
NaPi	2.16	1.95	5.26
KPi	2.16	2.07	5.23
NaBr	2.19	2.05	5.11
KBr	2.18	2.16	5.11
NaClO₄	2.14	1.94	5.06
KClO₄	2.12	2.04	5.01
NaSCN	2.08	. . .	4.64
KSCN	2.07	. . .	4.63
NaNO₃	2.15	1.95	4.91
KNO₃	2.13	2.04	4.86
Mean	2.14 ± 0.07	2.03 ± 0.09	5.00 ± 0.37

a DMF represents dimethylformamide. *b* DMSO represents dimethyl sulfoxide.

Series of decreasing limiting conductances for the cations and the anions in dimethyl sulfoxide are discernible from the arrangement of the data in Table IV. A comparison of the pattern of behavior of ionic species in dimethyl sulfoxide with patterns for the same species in other electron-donor solvents yielded some interesting correlations. Ratios of the limiting equivalent conductances of some potassium and sodium salts in dimethylformamide,[3,4] in acetone,[17] and in pyridine[18] to those in dimethyl sulfoxide are presented in Table V. These data indicate that the pattern of behavior of electrolytes in dimethyl sulfoxide most closely resembles the patterns for the same electrolytes in dimethylformamide and in pyridine.

At 25° the $\Lambda_0\eta_0$ product for a typical electrolyte such as sodium bromide in dimethyl sulfoxide, in pyridine, in dimethylformamide and in acetone is 0.743, 0.685, 0.663 and 0.587 ohm⁻¹ cm.² equiv.⁻¹ poise, respectively. These values provide evidence that the sizes of the solvodynamic units of the sol-

(11) C. A. Kraus, THIS JOURNAL, **58**, 673 (1954).

(12) W. E. Thompson and C. A. Kraus, *J. Am. Chem. Soc.*, **69**, 1016 (1947).

(13) H. L. Pickering and C. A. Kraus, *ibid.*, **71**, 3288 (1949).

(14) F. H. Healey and A. E. Martell, *ibid.*, **73**, 3296 (1951).

(15) M. J. McDowell and C. A. Kraus, *ibid.*, **73**, 3293 (1951).

(16) C. A. Kraus, *Ann. N. Y Acad. Sci.*, **51**, 789 (1949).

(17) M. B. Reynolds and C. A. Kraus, *J. Am. Chem. Soc.*, **70**, 709 (1948).

(18) W. F. Luder and C. A. Kraus, *ibid.*, **69**, 2481 (1947).

ute in dimethyl sulfoxide are relatively less than those of the same solute in the other solvents.

EQUILIBRIA IN THE TERNARY SYSTEM MgCl₂–BaCl₂–H₂O BETWEEN 18 AND 100°

By Gunnar O. Assarsson

Chemical Laboratory of the Geological Survey of Sweden, Stockholm 50, Sweden

The ternary system MgCl₂–BaCl₂–H₂O was examined within the temperature range 18–100°. There occur three phases of barium chloride: dihydrate, monohydrate and anhydrous salt. The solubility of barium chloride in saturated magnesium chloride solutions is insignificant. Thus, it is possible to determine the lowest formation temperature of barium chloride monohydrate only as being < 45°. The lowest formation temperature of anhydrous barium chloride is at 83 ± 3°. The formation of the phases was confirmed by X-ray exposure in a heating camera. Two isotherms, 50 and 100°, and a synoptic diagram of the ternary system are given.

In some earlier papers,[1] we have published the results of investigations concerning the equilibria in some of the aqueous systems of alkaline earth and alkali chlorides. To complete the survey, knowledge is required of the systems containing these chlorides and barium chloride. Also the chlorides of Li, Cs and Rb could be taken into consideration in the final summing up of the results, but the systems containing these chlorides are believed to have been studied elsewhere.[2] The results from the investigation of barium chloride together with magnesium chloride will now be presented.

Experimental

The experiments were performed as earlier described. Magnesium and barium were separated and determined gravimetrically using the same method as for magnesium and strontium.[1]

The Barium Chloride Hydrates Occurring in the System.—The earlier known phases of the barium chloride are the dihydrate, the monohydrate and the anhydrous salt.

Barium chloride dihydrate has been investigated by Tovborg–Jensen.[3] It is monoclinic, belonging to the space group P21/n, and its lattice parameters are $a = 7.136$, $b = 10.86$, $c = 6.738$ Å., $\beta = 90°57'$.

Barium chloride monohydrate was first described by Skey and Davis[4] as tetragonal, and later by Kirschner[5] as orthorhombic. Skey and Davis' preparation was obtained from a barium chloride solution containing hydrochloric acid, Kirschner's preparation from nearly pure methyl alcohol. Experiments performed in connection with the present investigation showed that these two preparations do not have identical X-ray patterns. The preparation obtained by Kirschner's method contains methyl alcohol. Later Pinsker[6] determined the structure of the compound using the electron diffraction method and found the monohydrate to be orthorhombic, having the unit cell dimensions $a = 4.51$, $b = 9.02$, $c = 11.28$ Å. The monohydrate is usually prepared by dehydration of the dihydrate between 45 and 60°. For identification of the monohydrate in the equilibrium studies described below,

X-ray photographs of analytically controlled preparations of this kind (55°), were compared with those of preparations obtained at 70–80° by diffusion of solutions containing hydrochloric acid (20–30%) into a barium chloride solution. The X-ray patterns of these latter preparations were shown to be identical with those of the monohydrate prepared by dehydration at 55°. The measurements were in very good agreement with those listed in the card catalog of A.S.T.M.[7] On comparison with values obtained by calculations based on Pinsker's unit cell dimensions the agreement between observed and calculated d-values and intensities was generally tolerable. It should be kept in mind that the monohydrate may be rather easily dehydrated during bombardments of the electrons under the low pressure conditions of an electron diffraction apparatus.

Anhydrous barium chloride has been examined by Döll and Klemm[8] who have calculated its orthorhombic cell dimensions per analogia $a = 7.823$, $b = 9.33$, $c = 4.948$ Å. The anhydrous barium chloride can easily be prepared by dehydration of the hydrates in a thermostat at temperatures higher than 80°. Preparations of this kind (100°) were used for comparison of the X-ray patterns of the phases in the equilibrium experiments described below; the measurements of the diffractions were in very good agreement with those given by Döll and Klemm.

A hemihydrate of barium chloride seems also to exist, being formed on cautious dehydration of the dihydrate at 70–85°. However, as it is metastable it has not been observed among the phases of the aqueous systems.

Results

The solids in equilibrium with solutions of the system include no double salt within the temperature range investigated. The principal interest is therefore connected with the changes in the isothermally invariant equilibria and the lowest formation temperature of the hydrates of barium chloride. As the saturated magnesium chloride solutions have a dehydrating effect on barium chloride dihydrate, barium chloride monohydrate and anhydrous barium chloride must be formed at temperatures which are low compared with the corresponding ones in the pure aqueous system (102° for the monohydrate, 268° for the anhydrous salt[9]). In an accurate determination of the lowest formation temperature of the phases some difficulties were encountered. The experiments were

(1) G. O. Assarsson and A. Balder, This Journal, **58**, 416 (1954) and literature there cited.

(2) *Cf.* Y. Y. Dodonov, L. V. Eferova and V. S. Kolosova, *Doklady Akad. Nauk S.S.S.R.*, **63**, 301 (1948); V. E. Plyushchev and N. F. Markovskaya, *J. Obshchei Khim.*, **24**, 1302 (1954) and other Russian authors.

(3) A. Tovborg-Jensen, *Kgl. Danske Videnskaps Selskab. Mat. fys. Meddel.*, **22**, No. 3 (1945) (English).

(4) W. Skey and E. H. Davis, *Trans. New Zealand Inst.*, **3**, 220 (1870).

(5) A. Kirschner, *Z. physik. Chem.*, **76**, 176 (1911).

(6) G. Pinsker, *Zhurn. Fiz. Khim.*, **23**, 1058 (1949).

(7) Alphab. and numer. index of X-ray diffraction data A.S.T.M. Spec. Techn. Publ. No. 48 B, 1950.

(8) W. Döll and W. Klemm, *Z. anorg. allgem. Chem.*, **241**, 248 (1939).

(9) G. I. Hüttig and Chr. Slonim, *Z. anorg. allgem. Ch.*, **181**, 66 (1929); A. Benrath, *ibid.*, **247**, 147 (1941).
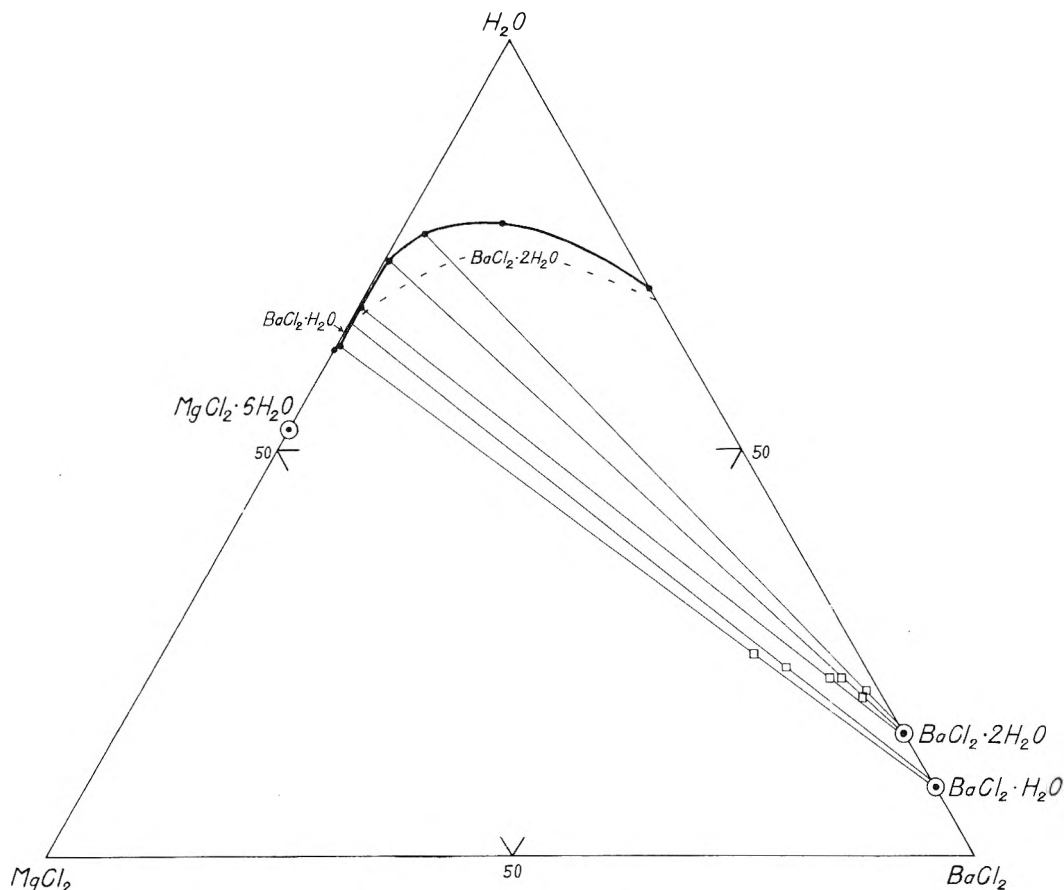
Fig. 1.—The ternary system MgCl₂–BaCl₂–H₂O: the isotherm at 50°.

Table I

The System MgCl₂–BaCl₂–H₂O Experiments for Reaching Equilibria Close to the Isothermally Invariant Points

Symbols: Ba 2 = BaCl₂·2H₂O Ba 1 = BaCl₂·H₂O, Ba = BaCl₂; Mg 6 = MgCl₂·6H₂O; X = controlled with X-ray photographs.

Temp., °C.	Compd. added	Soln. MgCl₂	BaCl₂	Wet residue MgCl₂	BaCl₂	Phase formed
25.0	Ba	35.7	.05	19.8	45.6	Ba 1 + Ba X
	Ba 1	35.7	.05	14.1	56.3	Ba 1
	Ba 2	35.7	.05	6.9	69.8	Ba 2
36.0	Ba 1	36.4	.05	8.2	70.0	Ba 1
	Ba 2	36.4	.05	7.0	70.3	Ba 2
42.0	Ba 1	36.9	.05	6.2	74.1	Ba 1
	Ba 2	36.9	.05	4.2	75.8	Ba 2
45.0	Ba 1	37.0	.05	17.1	54.6	Ba 1 X
	Ba 2	37.0	.05	10.9	64.3	Ba 1 X
47.0	Ba 1	37.2	.05	10.3	67.1	Ba 1 X
	Ba 2	37.2	.05	6.5	75.8	Ba 1 X
70.0	Ba 2	35.2	.2	11.1	64.6	Ba 1
	Ba 2	30.5	.4	7.1	72.7	Ba 1
	Ba 1	29.6	.5	5.4	72.3	Ba 2
	Ba 2	26.2	1.1	4.6	72.9	Ba 2
81.0	Ba	39.8	.15	16.8	55.5	Ba 1 X
	Ba 1	39.8	.15	12.6	64.0	Ba 1
	Ba 2	39.8	.15	14.8	59.5	Ba 1
83.0	Ba	39.9	.15	19.6	49.0	Ba X
	Ba 1	39.9	.15	12.2	64.4	Ba 1 X
	Ba 2	39.9	.15	10.4	69.0	Ba 1
85.0	Ba	40.0	.15	15.2	61.6	Ba
	Ba 1	40.0	.15	12.2	68.8	Ba

25 and 36°: equilibrium not reached

performed by saturating the solutions with magnesium and barium chloride, filtering off the undissolved solids, and afterwards adding a small amount of barium chloride. The analyses of the solids formed showed, however, that they were dependent upon the type of hydrate of barium chloride which was added. At 25° up to about 40° the solid contained dihydrate when dihydrate was added, and monohydrate and anhydrous salt when the solid added was the monohydrate and/or anhydrous salt. The results were similar even when the samples were shaken in the thermostat for a day, for a week or for longer time. Thus, equilibrium could not be reached.

At first, when the temperature was about 45° or higher, there did occur a rather complete transformation of the dihydrate into the monohydrate. Some of these analyses are listed in Table I. It seems to be impossible to reach equilibrium for these reactions within a reasonable time, obviously because of the insignificant solubility of barium chloride in the saturated magnesium chloride solutions which produces a coating of hydrated salt round the grains of the salt added. As a real equilibrium cannot be reached in practice, the lowest formation temperature of barium chloride monohydrate cannot be determined; it can only be concluded that it is somewhat below 45°.

When the solutions are not concentrated, the transformation of the unstable into the stable phase is performed more easily, as shown by the isotherm at 50° (Table II, Fig. 1). For the same reason the transition temperature of monohydrate-anhydrous barium chloride is not determined
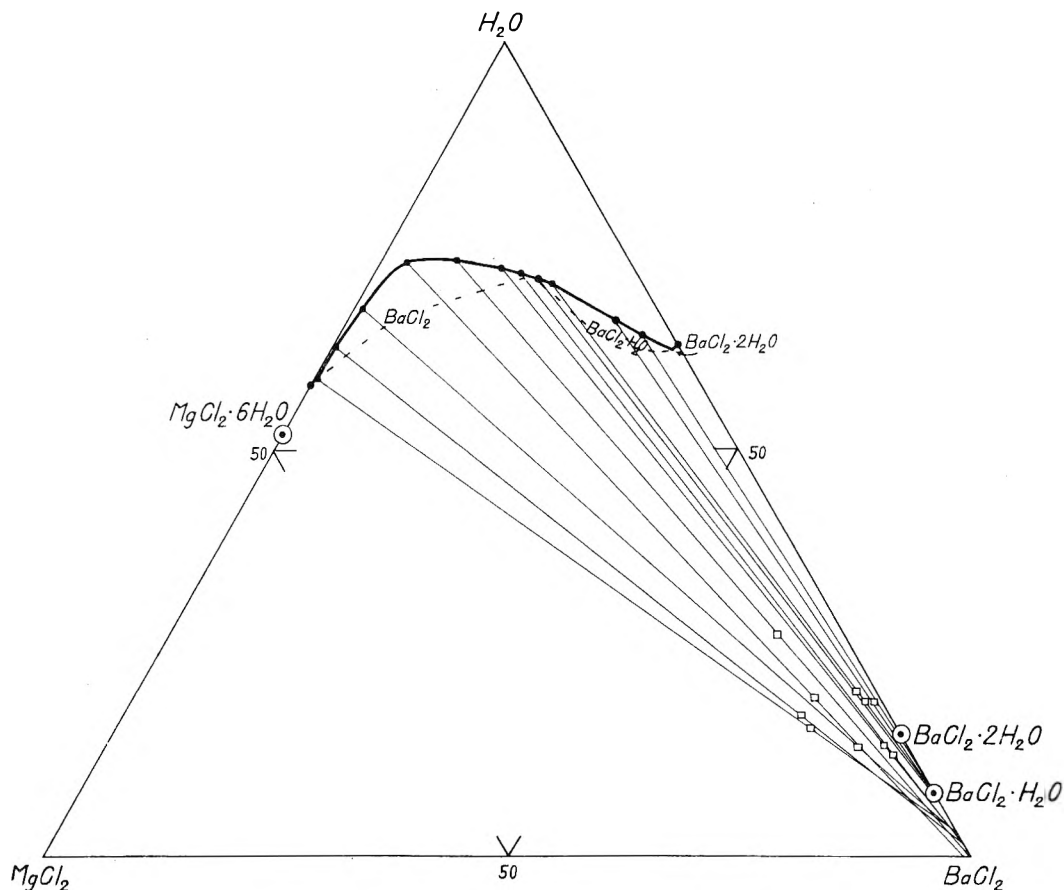
Fig. 2.—The ternary system $MgCl_2$–$BaCl_2$–H_2O: the isotherm at 100°.

more exactly than $83 \pm 3°$. The more dilute solutions of the 70° isotherm, partly given in Table I, and of the 100° isotherm in Table II, show the formation of the stable phases. In order to confirm the results, some X-ray photographs were taken in a high temperature camera. A sample of barium chloride dihydrate was ground together with 10% magnesium chloride hexahydrate under water-free mineral oil. The oil was removed by pressing the sample between filter

Fig. 3.—The ternary system $MgCl_2$–$BaCl_2$–H_2O: synopsis on the isothermally invariant equilibria.

TABLE II

THE TERNARY SYSTEM $MgCl_2$–$BaCl_2$–H_2O ISOTHERMS AT 50 AND 100°

Temp., °C.	Soln.		Wet residue		
	$MgCl_2$	$BaCl_2$	$MgCl_2$	$BaCl_2$	Phase[a]
50	37.4	...	...	...	Mg 6
	36.9	0.05	...	...	Ba 1 + Mg 6
	36.7	0.05	11.6	64.0	Ba 1
	34.1	0.15	9.1	68.4	Ba 1 X
	32.5	0.20	5.1	73.8	Ba 2 X
	26.8	0.40	3.5	75.0	Ba 2
	20.7	2.30	2.0	78.8	Ba 2
	12.2	10.60	...	...	Ba 2
	...	30.4	...	...	Ba 2
100	42.2	...	...	...	Mg 6
	40.9	0.2	9.8	74.6	Ba
	37.6	0.2	9.6	72.8	Ba
	31.5	0.9	5.1	81.3	Ba
	24.0	2.9	7.7	73.3	Ba
	18.4	8.0	7.3	65.1	Ba
	13.9	14.0	2.2	84.0	Ba
	12.7	15.7	1.7	85.8	Ba
	11.3	17.7	1.8	72.2	Ba 1 X
	9.9	20.2	2.4	78.0	Ba 1 X
	4.2	29.7	0.6	80.0	Ba 1
	2.4	33.2	0.8	81.2	Ba 1
	...	37.3	...	...	Ba 2

[a] Symbols see Table I.

paper; the sample, now consisting of very minute crystals, was packed into capillaries of Lindemann glass which were then fixed into the heating camera. The temperature of the camera could only be regulated rather approximatively, and the temperatures used for these experiments were 25–30°, 50–55° and 100–105°. The X-ray photographs showed in the first case dihydrate, in the second case mono-

hydrate and in the third case anhydrous salt of the barium chloride, in very good agreement with those photographs obtained from the corresponding pure compounds.

The main outlines of the present system are given in Fig. 3 which with some assumptions for the highest and the lowest temperatures gives a survey of the formation of the solids.

THE CRITICAL MICELLE CONCENTRATIONS IN AQUEOUS SOLUTIONS OF POTASSIUM ALKANE TRICARBOXYLATES

By Kozo Shinoda[1]

Department of Physical Chemistry, Faculty of Engineering, Yokohama National University, Minamiku, Yokohama, Japan

Received May 28, 1956

The critical micelle concentrations (CMC) in aqueous solutions of paraffin chain salts which possess three carboxyl groups at one end of their hydrocarbon chain have been determined. The CMC values are determined as 0.79 mole/l. for R_6CH-$(COOK)CH(COOK)_2$, 0.095 mole/l. for $R_{10}CH(COOK)CH(COOK)_2$ and 0.012 mole/l. for $R_{14}CH(COOK)CH(COOK)_2$ at 25°. The relation between the logarithm of the CMC of above substances and the number of carbon atoms in hydrocarbon chain is linear and the slope of the line is 0.52. From the comparison of CMC values of paraffin chain salts which possess one, two or three carboxyl groups at one end of their hydrocarbon chain, the electrical and cohesive energies per micelle forming ion have been determined. These values agree with the theoretical values.

Introduction

The critical micelle concentrations (CMC) in aqueous solution of paraffin chain salts which possess two carboxyl groups at one end of their hydrocarbon chain have been reported in the preceding paper.[2,3] As a result it has been found that (1) a homologous series of potassium alkyl malonates shows 3.5 ~ 15 times higher CMC values compared with that of corresponding fatty acid salts, (2) the plot of the logarithm of CMC *versus* the number of carbon atoms in hydrocarbon chain, m, is linear and (3) the logarithm of CMC as a function of the logarithm of the concentration of counterions is also linear and the slope of the line is just twice that of fatty acid salts. It also has been verified for the first time that the slope of the plot of log CMC *versus* m is not constant but varies with the number and kinds of polar groups concerned.

Consequently, it has become important and interesting to study the surfactants which possess three dissociable groups at one end of their hydrocarbon chain to gain further information on the mechanism of the micelle formation and on the action of surfactants.[4]

The present investigation has been undertaken to measure the CMC in aqueous solutions of a series of potassium 1,1,2-alkanetricarboxylates, R_iCH-$(COOK)CH(COOK)_2$, and to determine the electrical energy and cohesive energy at the micelle formation from the comparison of the CMC values of potassium alkane mono-, di- and tricarboxylates.

Experimental

"Nihon Yushi" purest grade fatty acids were used as starting materials. These fatty acids showed sharp and exact melting points. The α-bromo fatty acid was obtained by the bromination of fatty acid with bromine in the presence of a small amount of phosphorus trichloride, and purified by vacuum distillation. The α-bromo fatty acid ethyl ester was obtained by esterification of α-bromo fatty acid with ethyl alcohol, and purified by vacuum distillation. Alkane 1,1,2-tricarboxylic ester was synthesized by the addition of sodiomalonic ester to α-bromo fatty acid ethyl ester. Then alkane 1,1,2-tricarboxylic ester was saponified with alkali in alcohol and then acidified to alkane 1,1,2-tricarboxylic acid. The final purification of octane, dodecane and hexadecane 1,1,2-tricarboxylic acids were carried by the recrystallization from water, 1:1 acetic acid–water solution and glacial acetic acid, respectively, and their melting points were 129, 135.5 and 135°. The determination of the CMC has been performed by the initial change in color of pinacyanole in dilution process of concentrated solution.[5-7]

Results and Discussions

The CMC values obtained are 0.79 mole/l. for $R_6CH(COOK)CH(COOK)_2$, 0.095 mole/l. for R_{10}-$CH(COOK)CH(COOK)_2$ and 0.012 mole/l. for $R_{14}CH(COOK)CH(COOK)_2$ at 25°. The relation between the logarithms of the CMC of the homologous 1,1,2-alkanetricarboxylates and the number of carbon atoms in the hydrocarbon chain, m, fits the equation

$$\log \text{CMC} = -K_4 m + \text{Const.} \tag{1}$$

where K_4 is an experimental constant given as 0.52. The CMC values obtained by the interpolation are 0.28 mole/l. for $R_8CH(COOK)CH(COOK)_2$ and 0.034 mole/l. for $R_{12}CH(COOK)CH(COOK)_2$.

A linearity of the log CMC *versus* m had been noted previously for several homologous series of paraffin chain electrolytes.[8-11]

As a result of a series of potassium alkyl malonates,[2] it has been found that the slope of the log CMC *versus* m changes with the number of polar groups concerned. The present investigation of the homologous series of potassium alkane tricarboxylates also offers the evidence that the slope

(1) Department of Chemistry, University of California, Berkeley, California.

(2) K. Shinoda, This Journal, **59**, 432 (1955).

(3) The CMC values of osmotic pressure measurements by Brahama D. Sharma, *et al.*, show good agreement.

(4) The properties of the monolayer of alkane di- and tricarboxylic acids were reported in H. Hotta and T. Isemura, *Bull. Chem. Soc. Japan*, **29**, 90 (1956).

(5) M. L. Corrin and W. D. Harkins, *J. Am. Chem. Soc.*, **69**, 679 (1947).

(6) K. Shinoda, This Journal, **58**, 541 (1954).

(7) P. Mukerjee and K. J. Mysels, *J. Am. Chem. Soc.*, **77**, 2937 (1955).

(8) J. Stauff, *Z. physik. Chem.*, **A183**, 55 (1939).

(9) G. S. Hartley, *Kolloid Z.*, **88**, 22 (1939).

(10) K. Hess, W. Philippoff and H. Kiessig, *ibid.*, **88**, 40 (1939).

(11) A. B. Scott and H. V. Tartar, *J. Am. Chem. Soc.*, **65**, 692 (1943).

changes with the number and kinds of polar groups concerned.

The relation between the log CMC and the logarithm of the total concentration of counterions in aqueous solutions of potassium dodecane tricarboxylates is linear and the slope of the line is about 1.1. This slope is equal to that of potassium alkyl malonates. This seemingly indicates that one carboxyl group of alkane tricarboxylates creeps in the micelle and only two carboxyl groups are active.

The observed data fit the equation

$$\log \text{CMC} = -3K_3 \log C_s'' - K_0 m + \text{Const.} \quad (2)$$

where K_3 is the experimental constant determined as 0.37. In the case where no salt is added $C_s'' = 3\text{CMC}$ and we obtain

$$\log \text{CMC} = -K_0 m/(1 + 3K_3) + \text{const.} = -K_4 m + \text{Const.} \quad (3)$$

Substituting $3K_3 = 1.1$, $K_0 = 1.08$[2,12,13] we obtain

$$K_4 = 0.51 \quad (4)$$

The slope predicted in equation 3 agrees well with the observed slope in equation 1.

Hence, all the CMC values of paraffin chain salts which possess one,[14-16] two[2] or three dissociable groups at one end of their hydrocarbon chain are expressed in the equations

$$\log \text{CMC}_1 = -K_1 \log C_s - K_0 m + \text{Const.} \quad (5)$$
$$\log \text{CMC}_2 = -2K_2 \log C_s' - K_0 m + \text{Const.} \quad (6)$$
$$\log \text{CMC}_3 = -3K_3 \log C_s'' - K_0 m + \text{Const.} \quad (2)$$

In the case where no salt is added $C_s = \text{CMC}_1$, $C' = 2\text{CMC}_2$ and $C_s'' = 3\text{CMC}_3$.

At the micelle formation of ionic surfactants the cohesive energy change due to the aggregation of the hydrocarbon chain and the electrical energy on the micelle surface are the most important factors, and the CMC was given theoretically as a function of the hydrocarbon chain length and the concentration of counterions[17,18]

$$\log \text{CMC} = -\frac{m\omega}{kT} + K_1 \log \frac{2000\pi\sigma^2}{DNkTC_s} + \log \frac{1000}{N\nu} - 1 \quad (7)$$

Here ω is the cohesive energy decrease per methylene group passing from the bulk of the solution to the micelle, m the number of carbon atoms in hydrocarbon chain, K_1 the experimental constant, σ the surface charge density on the micelle surface, D the dielectric constant of the water, C_s the concentration of counterions, and $N\nu$ the molar free volume of paraffin chain salts in micellar state.

The first term on the right-hand side of equation 7 corresponds to the cohesive energy change, the second term to the electrical energy change and the other terms to the state change from aggregation to monodispersion per micelle forming ion.

In case of surfactants which possess two or three dissociable groups, the electrical energy per micelle

(12) J. T. Davis, *Trans. Faraday Soc.*, **48**, 1052 (1952).
(13) K. Shinoda, This Journal, **58**, 1136 (1954).
(14) M. L. Corrin and W. D. Harkins, *J. Am. Chem. Soc.*, **69**, 683 (1947).
(15) H. Lange, *Kolloid Z.*, **121**, 66 (1951).
(16) S. H. Herzfeld, This Journal, **56**, 959 (1952).
(17) K. Shinoda, *Bull. Chem. Soc. Japan*, **26**, 101 (1953).
(18) K. Shinoda, *ibid.*, **28**, 340 (1955).

forming ion at the micellization becomes twice or thrice,[2] and we obtain

$$\log \text{CMC}_i = -\frac{m\omega}{kT} + iK_i \log \frac{2000\pi\sigma^2}{DNkTC_s^i} + \log \frac{1000}{N\nu} - 1 \quad (8)$$

where i is the number of dissociable groups.

If it is assumed that the molar free volume and surface charge density[2,4] are constant, in these homologous compounds, the electrical energy at the micelle formation can be calculated from the comparison of the CMC values (under the same concentration of counterion) of these paraffin chain salts whose hydrocarbon chain lengths are the same. Then substituting these electrical energies in equation 8 and assuming $N\nu = 6$ cc., the cohesive energy at the micelle formation has been calculated.

On the other hand the electrical and cohesive energies at the micelle formation are given theoretically[17,18]

$$\text{electrical energy} = iK_ikT \log 2000\pi\sigma^2/DNkTC_s^i \quad (9)$$
$$\text{cohesive energy} = m\omega \quad (10)$$

Substituting $i = 1$, 2 or 3, $K_1 = 0.56$, $K_2 = 0.56$, $K_3 = 0.37$, $\sigma = e/45$ Å.^{2}, $D = 80.8$, $C_s^i = i\text{CMC}$[19] and $\omega = 1.08kT$, the electrical and cohesive energies at the micelle formation are calculated theoretically. These values of electrical and cohesive energies are summarized in Table I.

TABLE I

THE COMPARISON BETWEEN THE OBSERVED AND THEORETICAL VALUES OF ELECTRICAL AND COHESIVE ENERGIES AT THE MICELLE FORMATION OF POTASSIUM ALKANE MONO-, DI- AND TRICARBOXYLATES AT 25°

Substance	CMC, moles/l.	Exptl. electrical energy, kT	Theor. electrical energy, kT	Exptl. cohesive energy, kT	Theor. cohesive energy, kT
R$_7$COOK	0.4	2.6	2.5	7.6	7.6
R$_9$COOK	.1	3.4	3.3	9.8	9.7
R$_{11}$COOK	.025	4.3	4.1	12.1	11.9
R$_{13}$COOK	.006	5.1	4.9	14.3	14.0
R$_{15}$COOK	.0016	5.8	5.6	16.3	16.2
R$_{17}$COOK	.0004	6.7	6.4	18.6	18.4
R$_9$(COOK)$_2^a$	.35	4.7	4.5	9.8	9.7
R$_{11}$(COOK)$_2$	.13	5.9	5.6	12.1	11.9
R$_{13}$(COOK)$_2$	.048	7.1	6.7	14.2	14.0
R$_{15}$(COOK)$_2$	.017	8.2	7.8	16.4	16.2
R$_{17}$(COOK)$_2$	.0063	9.5	9.0	18.6	18.4
R$_{19}$(COOK)$_2$	.0023	10.6	10.1	20.8	20.5
R$_8$(COOK)$_3^b$	.79	3.4	3.4	7.7	7.6^c
R$_{10}$(COOK)$_3$	.28	4.4	4.4	9.8	9.7
R$_{12}$(COOK)$_3$	.095	5.4	5.4	11.9	11.9
R$_{14}$(COOK)$_3$	.034	6.5	6.6	14.0	14.0
R$_{16}$(COOK)$_3$	.012	7.6	7.7	16.1	16.2

^{a} R$_i$(COOK)$_2$ is the abbreviated formula of R$_{i-1}$CH(COOK)$_2$. ^{b} R$_i$(COOK)$_3$ is the abbreviated formula of R$_{i-2}$CH(COOK)CH(COOK)$_2$. ^{c} It is assumed that one carboxyl group creeps in the micelle, reduces the cohesive energy change of α-methylene group in case of tricarboxylates.

Though the accuracies of these electrical and cohesive energies are subject to the values of molar free volume, surface charge density, etc., we can conclude that Table I gives us an approximate energy relation at the micelle formation.

(19) C_s^i is the concentration of counterions and in this case $C_s^i = i\text{CMC}$.

Using equations 9 and 10, we can easily estimate the extent of electrical and cohesive energy contributions in various colloidal phenomena such as adsorption, mutual interaction of adsorbed molecules, electrical potential of ionized monolayer, surface activity of surfactants and so on.

Acknowledgment.—The author is greatly indebted to Mr. K. Houji of Daiichi Pharmaceutical

Co. Ltd. for his careful synthesis and purification of a series of alkane tricarboxylic acids. The author also wishes to express his sincere thanks to Prof. K. Kinoshita and Prof. H. Akamatsu for his advice and encouragement throughout this research. The expense of this research has been partly defrayed by aid from the Scientific Research Expenditure on "Collective study of surface activity."

FLUOROCARBON SOLUTIONS AT LOW TEMPERATURES. II. THE LIQUID MIXTURES C_2H_6–C_2F_6, C_2F_6–CHF_3, CH_2F_2–CHF_3, C_2H_6–CHF_3 AND Xe–CHF_3

By N. Thorp and R. L. Scott

Department of Chemistry, University of California, Los Angeles 24, California

Received June 4, 1956

The liquid–liquid binary systems C_2H_6–C_2F_6, C_2F_6–CHF_3, CH_2F_2–CHF_3, C_2H_6–CHF_3 and Xe–CHF_3 have been studied between 173–193°K. The vapor pressures of ethane–perfluoroethane, perfluoroethane–fluoroform, and methylene fluoride–fluoroform mixtures were studied at 176°K. The last system was found to be ideal. C_2H_6–C_2F_6 mixtures show abnormally large positive deviations from Raoult's law, similar to those found previously in other fluorocarbon–hydrocarbon pairs. Mixtures of C_2F_6 with CHF_3 also show greater positive deviations from ideality than can be explained by the regular solution-solubility parameter equations. Both ethane–fluoroform and xenon–fluoroform mixtures form two phases; the consolute temperature is about 186°K. for both systems. These results are also in disagreement with the predictions of the solubility parameter theory, and support the possibility of intermolecular hydrogen bonding in liquid CHF_3.

Introduction

The work reported in this paper is a continuation of a general research program on fluorocarbon solutions[1]; we have investigated the liquid–liquid binary systems of C_2H_6–C_2F_6, C_2F_6–CHF_3, CH_2F_2–CHF_3, C_2H_6–CHF_3 and Xe–CHF_3, between 173–193°K. In addition we have examined briefly the behavior of CH_2F_2 with C_2H_6, CF_4 and C_2F_6, and of CH_4 with CHF_3.

Experimental

Perfluoromethane, perfluoroethane, trifluoromethane (fluoroform) and difluoromethane (methylene fluoride) were kindly donated by the Jackson Laboratories of E. I. du Pont de Nemours and Co. The gases were further purified by repeated passage over activated charcoal held at solid CO_2 temperatures, followed by removal of dissolved air by pumping while alternating freezing and melting. Phillips research grade methane and ethane and Airco Xenon were used directly without further purification.

The general form of the apparatus used in these experiments was described in our first paper.[1] For the consolute temperature measurements the constant temperature bath was a mixture of liquid ethylene and propane. For the vapor pressure measurements, a constant temperature was obtained by a bath of freezing methanol. A small electrical heater was immersed in this bath, so that a mixture of solid and liquid methanol could be maintained, with the Dewar vessel immersed in liquid nitrogen. With adequate stirring of the bath, a constant temperature could be held for over one hour without the methanol freezing solid.

The operational procedure was the same as that previously described.

Results

Figures 1, 2 and 3 show the measured total vapor pressures for the C_2H_6–C_2F_6, C_2F_6–CHF_3 and CH_2F_2–CHF_3 systems. The circles are the experimental points, while the full curves are calculated from empirical equations of the form suggested by Scatchard[2]

$$P = p°_1 x_1 \exp x_2^2[\alpha + \beta(3x_1 - x_2)] + p°_2 x_2 \exp x_1^2 [\alpha - \beta(3x_2 - x_1)] \quad (1)$$

In this equation, the same as that used in our first paper, P is the total vapor pressure, $p°_1$ and $p°_2$ are the vapor pressures of the pure components,
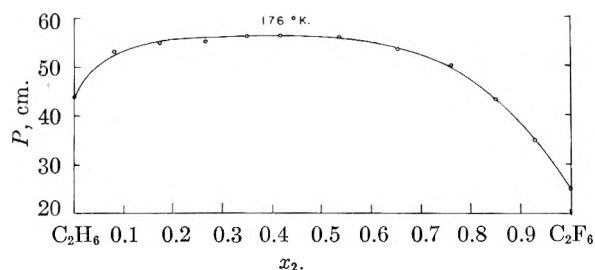

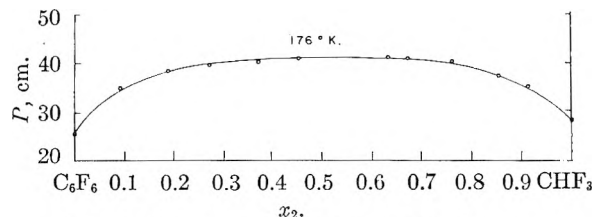Fig. 1.—Vapor pressures of C_2H_6–C_2F_6 mixtures.

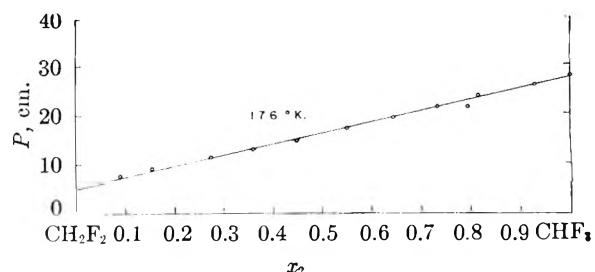Fig. 2.—Vapor pressures of C_2F_6–CHF_3 mixtures.

Fig. 3.—Vapor pressures of CH_2F_2–CHF_3 mixtures.

(1) N. Thorp and R. L. Scott, This Journal, **60**, 670 (1956).

(2) G. Scatchard, *Chem. Revs.*, **44**, 7 (1949).

x_1 and x_2 are mole fractions, and α and β are constants chosen by the method of least squares[3] to give the best fit of the experimental results. The corresponding excess free energy is of course

$$\Delta F^E = x_1 x_2 [\alpha + \beta(x_1 - x_2)] \tag{2}$$

Table I gives the best values of the constants α and β for the systems studied.

Table I

Values of the Constants α and β in Equation 1, for $C_2H_6-C_2F_6$, $C_2F_6-CHF_3$ and $CH_2F_2-CHF_3$ Systems

$$\ln \gamma_1 = [\alpha + \beta\,(3x_1 - x_2)]x_2{}^2$$
$$\ln \gamma_2 = [\alpha - \beta\,(3x_2 - x_1)]x_1{}^2$$

System	Superscript 1 denotes	α	β
$C_2H_6-C_2F_6$ at ca. $176°K$.	C_2H_6	1.82	0.35
$C_2F_6-CHF_3$ at ca. $176°K$.	C_2F_6	1.70	0.05
$CH_2F_2-CHF_3$ at ca. $176°K$.	CH_2F_2	0.0	0.0

The solubility of a component of a solution of a non-polar non-electrolyte may frequently be expressed with the aid of the simple regular solution equation.[4]

$$\Delta \bar{F}^E = (x_1 \bar{V}_1 + x_2 \bar{V}_2)(\delta_1 - \delta_2)^2 \phi_1 \phi_1 \tag{3}$$

where $\Delta \bar{F}^E$ is the molal excess free energy of mixing, x_1 and x_2 are mole fractions; ϕ_1 and ϕ_2 are volume fractions, $\bar{V}_1$ and $\bar{V}_2$ are molal volumes; and δ_1 and δ_2, the solubility parameters of the pure components, are the square roots of the energy of vaporization per ml., i.e., $(\Delta E^V/\bar{V})^{1/2}$, the subscripts referring to components 1 and 2, respectively.
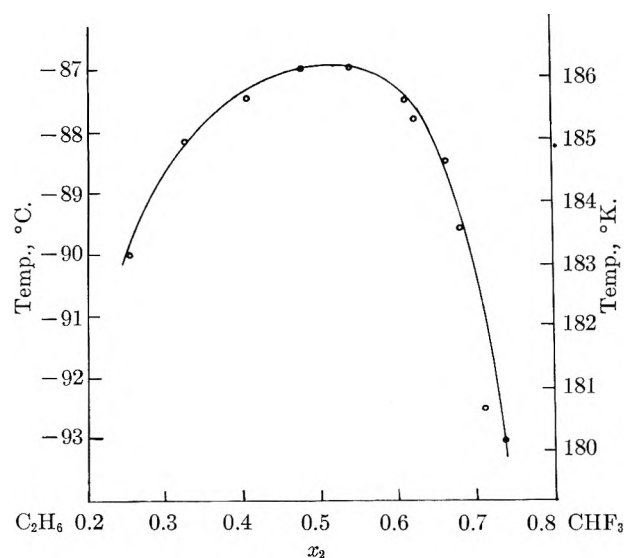

Fig. 4.—Immiscibility curve for $C_2H_6-CHF_3$.

Table II gives the "thermodynamic" solubility parameter evaluated from the heats of vaporization and molar volumes at $176°K$., estimated by methods given elsewhere.[4] The difference of these δ's is then compared with the "experimental" $(\delta_1 - \delta_2)$ difference obtained by fitting equation 2 to the experimental excess free energies of mixing at $x_1 = x_2 = 1/2$.

In the second part of Table II the experimental $(\delta_1 - \delta_2)$ differences are obtained from miscibility

(3) J. A. Barker, Austral. J. Chem., 6, 207 (1953).

(4) J. H. Hildebrand and R. L. Scott, "Solubility of Non-electrolytes," 3rd. edition, Reinhold Publ. Corp., New York, N. Y., 1950.

Table II

Calculated and Experimental $(\delta_1 - \delta_2)$ Differences

System	δ_1 at $176°K$.	δ_2 at $176°K$.	Calcd. $|\delta_1 - \delta_2|$	Exptl. $\Delta\delta$ Eq. 2	Eq. 3
$C_2H_6-C_2F_6$	7.7	6.8	0.9	3.1	...
$C_2F_6-CHF_3$	6.8	9.3	2.5	3.1	...
$CH_2F_2-CHF_3$	10.6	9.3	1.3	0.0	...
$C_2H_6-CHF_3$	7.7	9.3	1.6	...	3.9
$Xe-CHF_3$	8.0^a	9.5^a	1.5	...	4.1

^{a} Solubility parameters at $164.2°K$.

data. An approximate expression for the critical solution temperature T_c is given by regular solution theory[4]

$$4RT_c = (\bar{V}_1 + \bar{V}_2)(\delta_1 - \delta_2)^2 \tag{4}$$

Figure 4 shows the miscibility curve of $C_2H_6-CHF_3$ system. The critical solution temperature is $186.3°K$. and the critical mole fraction of CHF_3 is about 0.51 by the method of rectilinear diameters. The critical solution temperature for an approximately equimolar mixture of xenon and fluoroform was found between 185 and $186°K$. The complete liquid–liquid phase diagram of this system was not obtained due to the experimental difficulties in operating about $20°K$. above the boiling point of xenon.

Approximately equimolar mixtures of CH_2F_2 and C_2H_6, CH_2F_2 and C_2F_6, CH_2F_2 and CF_4 and CH_4 and CHF_3 have two coexistent phases between 10 and $15°K$. above the boiling point of the lowest boiling component. No consolute temperatures were obtained for these systems, because of the experimental difficulties of operating several degrees above the boiling point of one of the constituents in the mixture.

Discussion

The solubility parameters at $176°K$. for C_2H_6, C_2F_6, CHF_3 and CH_2F_2, calculated by methods described elsewhere for temperatures other than the boiling point,[4] are 7.7, 6.8, 9.3 and 10.6, respectively. This gives $(\delta_1 - \delta_2)$ differences for $C_2H_6-C_2F_6$, $C_2F_6-CHF_3$ and $CH_2F_2-CHF_3$ systems as 0.7, 2.5, 1.3 whereas the experimental values are 3.1, 3.1 and 0.0, respectively. The calculated excess free energies of mixing at $x_1 = x_2 = 1/2$ for these same systems are compared in the observed values in Table III.

Table III

Excess Free Energies of Mixing, cal./mole

at $x_1 = x_2 = 1/2$

	$C_2H_6-C_2F_6$ at about $176°K$.	$C_2F_6-CHF_3$ at about $176°K$.	$CH_2F_2-CHF_3$ about $176°K$.
Obsd.	158	147	0
Calcd. from thermodynamic δ's by eq. 2	13	93	19

The anomalous behavior of liquid–liquid binary mixtures of C_2H_6 and C_2F_6 parallels that of the CH_4-CF_4 system, and is in agreement with the discrepancies observed in other hydrocarbon–fluorocarbon pairs.[1]

The difference between the observed and calculated excess free energies of mixing for the $C_2F_6-CHF_3$ system, is about 54 calories or approximately

$0.16RT$. Discrepancies between observed and calculated excess free energies of mixing of the order of $0.10RT$ may be due to any number of causes, which are ignored in the derivation of the regular solution-solubility parameter equations. In this light, therefore, a value of $0.16RT$ for the C_2F_6–CHF_3 system is seen to be in some disagreement with theory. In our first paper[1] we suggested that the difference in physical properties of CF_4 and CHF_3 as compared to the great similarity in properties of CCl_4 and $CHCl_3$ might lie in the possibility of hydrogen bonding in CHF_3. The results for the C_2F_6–CHF_3 system would seem to level support to this point of view.

The possibility of hydrogen bonding in fluoroform is also evidenced by its behavior with ethane and xenon. With these two substances it forms two phases below a consolute temperature of about $186°K$. From equation 3 this gives an experimental $(\delta_1 - \delta_2)$ difference of 3.9 and 4.1 for C_2H_6–CHF_3 and Xe–CHF_3 mixtures, respectively. The "thermodynamic" δ difference for these systems are 1.6 and 1.5; from δ differences of this magnitude one would expect rather small deviations from ideality.

The discrepancy between the observed and calculated excess free energies of mixing for the CH_2F_2–CHF_3 is within the limits of experimental error. This result together with the high δ value for CH_2F_2 would seem to suggest hydrogen bonding in this compound also. If the hydrogen bonding between like and unlike pairs is about equivalent, then there would be no net contribution to the energy of mixing, and the solution of CHF_3 with CH_2F_2 would be nearly ideal, as it is.

If the thermodynamic δ values for the CH_2F_2–C_2H_6, CH_2F_2–C_2F_6, CH_2F_2–CF_4 and CHF_3–CH_4 systems are substituted in equation 3 consolute temperatures well above the boiling point of the lowest boiling component are expected. This is borne out by the experimental results, all these systems having two phases above the boiling point of one of the components in the mixture. On the basis of the foregoing discussion it would be expected that the consolute temperatures for CH_2F_2–C_2H_6 and CHF_3–CH_4 would be well above the calculated consolute temperatures. The systems CH_2F_2–CF_4 and CH_2F_2–C_2F_6 would probably form one phase somewhat above the calculated consolute temperatures. It is unlikely that any of these consolute temperatures could be attained without the use of high pressure apparatus.

We have no information on the volume changes occurring during mixing for these systems and little information on the ionization potential for most of these compounds studied so that we are unable to apply the corrections of Simons and Dunlap[5] or Reed.[6]

(5) J. H. Simons and R. O. Dunlap, *J. Chem. Phys.*, **18**, 335 (1950).

(6) T. M. Reed III, THIS JOURNAL, **59**, 425 (1955).

ELECTRODE POTENTIALS IN FUSED SYSTEMS. III. THE PLATINUM ELECTRODE IN SOME HALIDE MELTS[1]

By Kurt H. Stern

Department of Chemistry, University of Arkansas, Fayetteville, Arkansas

Received June 4, 1956

The galvanic cells Ag/AgCl, KCl; KCl/Pt, Ag/AgBr, KBr; KBr/Pt, and Cu/CuCl, KCl; KCl/Pt have been studied in the temperature range 800–900°. It is shown that the K^+–$K(g)$ equilibrium operates on the platinum electrode at pressures near 10^{-13} atmosphere.

Introduction

In the previous paper of this series,[2] a study of the cell Ag/AgCl, KCl/Cl_2 showed that for concentrations of AgCl less than 0.05 mole fraction the reaction Ag + KCl = AgCl + K proceeds spontaneously. It was suggested that the change of potential with time could be used for a study of reaction kinetics. Indeed, a preliminary investigation showed that over a considerable time span for a cell which was Ag/KCl/Cl_2 initially dE/dt was nearly constant, suggesting first-order kinetics.

A kinetic study of this sort requires a reference electrode. One possible objection to the chlorine

electrode used in the previous study for this purpose is that the dissolved Cl_2 in the melt may react with the metal under consideration and thus give spuriously high rates. Hence an inert metal electrode offers an attractive possibility as reference electrode, particularly if the nature of the reaction taking place on the electrode can be established. For halide melts such an electrode is platinum. Fusion of alkali halides in platinum dishes, for example, has long been standard procedure for the removal of traces of moisture in the preparation of ultra-pure salts. This can be considered evidence that chemists generally recognize the inertness of this metal in fused salts.

The present work is concerned with elucidating the electrode reaction on platinum in halide melts. Results are presented for the cells Ag/AgCl,KCl;

KCl/Pt, Ag/AgBr,KBr;KBr/Pt, and Cu/CuCl, KCl;KCl/Pt, where the semicolons represent liquid–liquid junctions between solutions of nearly the same composition. Hence liquid junction potentials are virtually negligible.

Experimental Part

Materials.—Copper and silver electrodes were made from spectroscopically pure No. 10 B. and S. gage wire. Platinum electrodes were made by braiding several strands of No. 18 wire into a small cable. All salts were Mallinckrodt Reagent Grade. Except for CuCl they are better than 99.9% pure. The assay on CuCl is 90%. KCl and KBr were dried at 110° for several days before use. AgCl and AgBr were dissolved in NH_4OH and reprecipitated with HCl and HBr, respectively. They were dried at 110° and stored in a desiccator. CuCl was used without further purification.

Experimental Methods.—Vycor cells were made by bending lengths of 25 mm. diameter tubing into U-shapes in such a way as to constrict the bend of the "U" to capillary dimensions. Cells were about 10 cm. high. While the opening between the legs of the "U," the electrode compartments, was large enough to permit electrical contact through it, it was small enough to prevent diffusion between the compartments for several hours.

The furnace was similar to the one described previously.[2] Measurements were made both under argon and in melts open to the atmosphere. No significant differences were observed. In the case of copper, oxide formed on the electrode above the melt, but the electrode remained bright in the melt, even when cells were open to the atmosphere. The temperature was measured with a chromel–alumel thermocouple whose hot junction was kept near the bottom of the furnace touching the cell. The couple was calibrated at the melting point of KCl and kept in a nickel protection tube. The temperature was constant to ±2°. Runs were carried out by heating the Vycor cells containing 15 g. of the alkali halide in each leg to the desired temperature, dissolving a quantity of AgCl, AgBr or CuCl in the proper compartment, immersing the electrodes, and measuring the potential when temperature equilibrium had again been reached. Since the cells were open to the atmosphere salt concentration in them could be varied by adding the salt through a funnel. Measurements were made as rapidly as possible to minimize diffusion between compartments. Five or six concentrations were prepared in approximately one hour. At the conclusion of a run the electrodes were withdrawn and the cooled cells examined for evidence of diffusion between the compartments, as shown by a violet color in the case of silver (after exposure to bright light) or a greenish-brown color for copper. If diffusion had occurred measurements from these cells were discarded.

In many cases analyses of the melts were carried out by separating the electrode compartments, i.e., breaking the cell at the bend of the "U," and dissolving their contents in water.

Analytical Procedure. Silver.—Silver was determined spectrophotometrically as the colloidal sulfide when present in concentrations of a few parts per million. Large quantities were precipitated as chloride.

Copper.—It was initially determined that essentially all of the copper present in the melt was in the cuprous state. This was done by dissolving the quenched melt in a solution of potassium thiocyanate. Copper(I) immediately formed the insoluble thiocyanate and copper(II) was not found to any appreciable extent in the filtrate. In subsequent analyses of the melt copper(I) was oxidized to copper(II) and determined by one of two procedures. Small quantities, of the order of a few parts per million, were determined spectrophotometrically by the diethyl dithiocarbamate method.[3] Larger quantities were determined as the sulfide.

Results and Discussion

Table I shows the results of a typical run on the cell Ag/AgCl(N_1),KCl;KCl/Pt. N_1 = mole fraction AgCl, E = measured potential, E^{02} = the standard potential, taking the standard state of Ag

to be the metal, for AgCl and KCl the pure salt, and for the (provisionally) unknown reaction on the platinum the reduced species at a to be determined concentration.

TABLE I

E.M.F.'s FOR THE CELL Ag/AgCl, KCl;KCl/Pt

$t = 875°$

N_1	E (v.)	E^{02}
0.000814	0.784	0.080
.00146	.747	.101
.00377	.680	.128
.0121	.565	.128
.0207	.517	.133
.0353	.465	.134

E^{02} values tend to constancy near 0.01 mole fraction AgCl. This is in fair agreement with the results of the previous study[2] on the cell Ag/AgCl, KCl/Cl₂ in which the reaction Ag + KCl = AgCl + K was shown to go spontaneously when the concentration of AgCl was below 0.05 mole fraction. E^{02} values for the very dilute solutions are thus thermodynamically meaningless.

In Table II are given the E^{02} values for the three cells of this study at several temperatures. Each of the E^{02} values is the result of a run such as is shown in Table I and represents the thermodynamically reversible value.

TABLE II

E^{02} VALUES FOR SEVERAL GALVANIC CELLS

(°C.)	E^{02} (volts)
	Ag/AgCl, KCl; KCl/Pt
795	0.147 ± 0.002
827	.140
862	.130
875	.131
	Ag/AgBr, KBr; KBr/Pt
760	0.303 ± 0.002
832	.276
865	.269
908	.241
	Cu/CuCl, KCl; KCl/Pt
820	0.414 ± 0.01
830	.433
840	.440
895	.418

Taking the results of the previous study[2] it seems reasonable to adopt the hypothesis that the electrode reaction on the platinum electrode is the reduction of potassium ion, i.e., $K^+ + e^- = K$, and proceed to calculate the pressure of potassium vapor at which the equilibrium operates. The method will be illustrated for the cell containing AgCl but is analogous for the other cells.

The standard potential E^{01} for the reaction Ag + KCl = AgCl + K can be calculated from recently published data on the E^0 of formation of AgCl and KCl[4] by the method outlined there. The standard state of E^{01} differs from that of E^{02} only in that for E^{01} the pressure of potassium vapor is taken as one atmosphere. Hence $E^{02} = E^{01} - RT/\mathfrak{F} \ln P_K$ and

(3) E. B. Sandell, "Colorimetric Determination of Traces of Metals," Interscience Publishers, New York, N. Y., 1944, p. 221.

(4) W. J. Homer, M. S. Molmberg and B. Rubin, J. Electrochem. Soc., 103, 8 (1956).

hence the pressure of potassium vapor operating on the platinum electrode can be calculated. For the cell involving AgBr E^{01} values were calculated from the table of thermodynamic functions prepared by the Bureau of Standards.[5]

It is instructive to compare the pressures of potassium vapor with that available from the dissociation of the potassium halide. The latter is calculated from the $E^0_{formation} = - E^0_{dissociation}$ by the equation

$$\log P_K = \frac{E^\circ_{dis} + RT/\mathfrak{F} \ln \sqrt{2}}{3/2\ RT/\mathfrak{F}}$$

In all the cells the fraction of potassium vapor on the electrode is between 0.001 and 0.1 of the dissociation pressure of the potassium halide. The results of the calculations of potassium vapor pressures are shown in Table III.

TABLE III

POTASSIUM VAPOR PRESSURES (ATM.) IN VARIOUS CELLS

t (°C.)	P_K (on Pt) $\times 10^{13}$	P_{dis} of KCl $\times 10^{11}$	P_K (on P_t)/ P_K (dis) $\times 10^{-3}$
	Ag/AgCl, KCl; KCl/Pt		
795	1.15	2.20	5.2
827	3.15	5.00	6.3
862	13.7	15.4	8.9
875	20.2	21.2	9.5
	Ag/AgBr, KBr; KBr/Pt		
760	0.279	1.0	2.8
832	7.96	6.4	1.2
865	29.0	15.5	19.0
908	373.0	50.0	75.0
	Cu/CuCl, KCl; KCl/Pt		
820	0.24	4.5	0.53
830	0.81	5.9	1.4
840	1.1	7.8	1.4
895	9.5	38.0	2.5

In general, the fraction of the total potassium vapor participating in the electrode reaction increases with rising temperature, but the results within each of the different cells show variations

(5) Circular 500, National Bureau of Standards.

within a little over one order of magnitude. This is not too surprising, considering the approximations that are made in the calculation of thermodynamic functions of substances at high temperatures. These approximations are discussed in the references cited. Thus, for example, an error of 3 kcal. in one of the ΔF^0's used would change P_K by an order of magnitude. At any rate, the results imply that between 92 and 99% of the potassium vapor available from the thermal dissociation of KCl distils into the atmosphere, the remaining 1 to 8% is adsorbed on the platinum electrode.

The increase of the dissociation pressure of the potassium halide with rising temperature parallels the rise of equilibrium vapor pressure of potassium in the reaction Ag + KCl = AgCl + K. No exact calculation of the latter is possible because the equilibrium ratio N_{AgCl}/N_{KCl} is only known within an order of magnitude. Taking this ratio as 0.01 and the activity of solid silver as one, P_K can be estimated[4] from the equilibrium constant Q. For example, at 800° $Q = 7 \times 10^{-12}$, from which $P_K = 7 \times 10^{-10}$. At 875° $Q = 7.6 \times 10^{-11}$ and $P_K = 7.6 \times 10^{-9}$, assuming no change in the equilibrium ratio of AgCl to KCl. These are equilibrium pressures attained only in closed systems. In open systems the actual pressures are much lower and the reaction is driven by the distillation of potassium, as shown previously.[2]

It seems reasonable to conclude that platinum can be used as reference electrode in fused alkali halide systems, even though the potassium pressure at which it operates is known only within an order of magnitude. Within this range its potential, whatever it is, remains constant and this is the chief requirement of a reference electrode.

At the present time no potential can be assigned to *any* half-cell reaction in molten system since there is as yet no common agreement as to a zero of potential analogous to the H+–H₂ couple in aqueous systems.

PHYSICAL PROPERTIES OF THE 17 ISOMERIC HEXENES OF THE API RESEARCH SERIES[1]

By David L. Camin and Frederick D. Rossini

Petroleum Research Laboratory, Carnegie Institute of Technology, Pittsburgh, Pennsylvania

Received July 3, 1956

For the isomeric hexenes, highly purified hydrocarbons of the API Research series, the following properties were measured: densities at 20, 25 and 30°; refractive indices at seven wave lengths at 20, 25 and 30° and boiling points and vapor pressures at 80 to 780 mm. The data on refractive indices were correlated by means of modified Cauchy and Hartmann equations, and values of the constants are given for each compound, to permit precise evaluation of the refractive index as a function of wave length. The data on vapor pressures were correlated with the Antoine equation and values of the three constants are given for each compound. Also included are calculated values of the specific dispersions, $(n_F - n_C)/d$ and $(n_G - n_D)/d$, and of heats of vaporization at 25° and the normal boiling point.

Introduction

The American Petroleum Institute Research Project 6 has so far reported data on the densities, refractive indices and boiling points and vapor pressures for 95 different API Research hydrocarbons.[2-9] In this paper are reported similar data for the 17 isomeric hexenes.

Compounds Measured

These API Research hydrocarbons were made available by the American Petroleum Institute through the API Research Project 44 at the Carnegie Institute of Technology. The samples were purified by the API Research Project 6 from material supplied by the following laboratories: *cis*-2-hexene, *trans*-2-hexene, *cis*-3-hexene, *trans*-3-hexene, 3-methyl-1-pentene, 4-methyl-1-pentene, 2-methyl-2-pentene, and 3-methyl-*trans*-2-pentene from the American Petroleum Institute Research Project 45, Ohio State University, Columbus, Ohio; 2-methyl-1-pentene, 4-methyl-*cis*-2-pentene and 4-methyl-*trans*-2-pentene from the American Petroleum Institute Research Project 6, Carnegie Institute of Technology, Pittsburgh, Pennsylvania; 3-methyl-*cis*-2-pentene, 2,3-dimethyl-1-butene and 2,3-dimethyl-2-butene from the General Motors Corporation, Detroit, Michigan; 3,3-dimethyl-1-butene from Pennsylvania State University, Hydrocarbon Laboratory, State College Pennsylvania; and 2-ethyl-1-butene from the American Petroleum Institute Research Project 6, Carnegie Institute of Technology, Pittsburgh, Pennsylvania and American Petroleum Institute Research Project, 45, Ohio State University, Columbus, Ohio.

The purification and determination of purity and freezing point of these compounds have been or will be described in other reports.[10-13] The purity of the samples measured was as follows, in mole %[10-13]: *cis*-2-hexene, 99.94 ± 0.05; *trans*-2-hexene, 99.84 ± 0.11; *cis*-3-hexene, 99.90 ± 0.08; *trans*-3-hexene, 99.95 ± 0.03; 2-methyl-1-pentene, 99.92 ± 0.07; 3-methyl-1-pentene, 99.75 ± 0.20; 4-methyl-1-pentene, 99.85 ± 0.12; 2-methyl-2-pentene, 99.96 ± 0.03; 3-methyl-*cis*-2-pentene, 99.89 ± 0.08; 3-methyl-*trans*-2-pentene, 99.89 ± 0.09; 4-methyl-*cis*-2-pentene, 99.93 ± 0.07; 4-methyl-*trans*-2-pentene, 99.92 ± 0.07; 2-ethyl-1-butene, 99.95 ± 0.04; 2,3-dimethyl-1-butene, 99.86 ± 0.13; 3,3-dimethyl-1-butene, 99.91 ± 0.06; 2,3-dimethyl-2-butene, 99.94 ± 0.05. It is believed that in each case the impurity was of such nature and present in such small amount that the properties measured were not affected beyond the indicated limits of uncertainty. The values given in the tables for the properties of 1-hexene are repeated, for convenience, from Forziati, Camin and Rossini.[6]

Table I

Values of Density for the 17 Hexenes, C_6H_{12}

Compound	Density,[a] g./ml. 20°	25°	30°	Temp. coefficient of density at 25°, g./ml. °C.
1-Hexene	0.67317	0.66848	0.66374	0.000943
cis-2-Hexene	.68720	.68252	.67776	.000944
trans-2-Hexene	.67795	.67327	.66847	.000948
cis-3-Hexene	.67990	.67522	.67052	.000938
trans-3-Hexene	.67711	.67233	.66747	.000964
2-Methyl-1-pentene	.67987	.67505	.67020	.000967
3-Methyl-1-pentene	.66745	.66287	.65793	.000952
4-Methyl-1-pentene	.66370	.65894	.65400	.000970
2-Methyl-2-pentene	.68650	.68187	.67698	.000952
3-Methyl-*cis*-2-pentene	.69761	.69302	.68814	.000947
3-Methyl-*trans*-2-pentene	.69321	.68858	.68386	.000935
4-Methyl-*cis*-2-pentene	.66918	.66441	.65941	.000977
4-Methyl-*trans*-2-pentene	.66862	.66380	.65880	.000982
2-Ethyl-1-butene	.68958	.68481	.67997	.000961
2,3-Dimethyl-1-butene	.67810	.67325	.66842	.000968
3,3-Dimethyl-1-butene	.65310	.64795	.64302	.001008
2,3-Dimethyl-2-butene	.70810	.70347	.69943	.000867

[a] For air-saturated material at 1 atm.

(1) This investigation was performed as part of the work of the American Petroleum Institute Research Project 6 in the Petroleum Research Laboratory of the Carnegie Institute of Technology, Pittsburgh, Pennsylvania.

(2) C. B. Willingham, W. J. Taylor, J. M. Pignocco and F. D. Rossini, *J. Research Natl. Bur. Standards*, **35**, 219 (1945).

(3) A. F. Forziati and F. D. Rossini, *ibid.*, **43**, 473 (1949).

(4) A. F. Forziati, W. R. Norris and F. D. Rossini, *ibid.*, **43**, 555 (1949).

(5) A. F. Forziati, *ibid.*, **44**, 373 (1950).

(6) A. F. Forziati, D. L. Camin and F. D. Rossini, *ibid.*, **45**, 406 (1950).

(7) F. D. Rossini, B. J. Mair and A. J. Streiff, "Hydrocarbons from Petroleum," Reinhold Publ. Corp., New York, N. Y., 1953.

(8) D. L. Camin, A. F. Forziati and F. D. Rossini, This Journal, **58**, 440 (1954).

(9) D. L. Camin and F. D. Rossini, *ibid.*, **59**, 1173 (1955).

(10) A. J. Streiff, J. C. Zimmerman, L. F. Soule, M. T. Butt, V. A. Sedlak, C. B. Willingham and F. D. Rossini, *J. Research Natl. Bur. Standards*, **41**, 323 (1948).

(11) A. J. Streiff, L. F. Soule, C. M. Kennedy, M. E. Janes, V. A. Sedlak, C. B. Willingham and F. D. Rossini, *ibid.*, **45**, 173 (1950).

(12) A. J. Streiff, E. T. Murphy, J. C. Zimmerman, L. F. Soule, V. A. Sedlak, C. B. Willingham and F. D. Rossini, *ibid.*, **39**, 321 (1947).

(13) Unpublished data of American Petroleum Institute Research Project 6, Carnegie Institute of Technology, Pittsburgh, Pennsylvania. Attention of Frederick D. Rossini.

TABLE II
VALUES OF REFRACTIVE INDEX FOR THE 17 HEXENES, C_6H_{12}

Refractive index
Wave length in Å.

Compound	Temp., °C.	6678.1 He$_{red}$	6562.8 H$_C$	5892.6 Na$_D$	5460.7 Spectral line Hg$_e$	5015.7 He$_{blue}$	4861.3 H$_F$	4358.3 Hg$_g$
1-Hexene	20	1.38519	1.38552	1.38788	1.38991	1.39261	1.39373	1.39837
	25	1.38235	1.38268	1.38502	1.38703	1.38971	1.39083	1.39543
	30	1.37951	1.37984	1.38216	1.38415	1.38681	1.38793	1.39249
cis-2-Hexene	20	1.39483	1.39517	1.39761	1.39972	1.40254	1.40373	1.40862
	25	1.39196	1.39230	1.39473	1.39683	1.39964	1.40082	1.40570
	30	1.38909	1.38943	1.39185	1.39394	1.39674	1.39791	1.40278
trans-2-Hexene	20	1.39083	1.39117	1.39363	1.39575	1.39857	1.39976	1.40463
	25	1.38794	1.38828	1.39073	1.39283	1.39564	1.39682	1.40167
	30	1.38505	1.38539	1.38783	1.38991	1.39271	1.39388	1.39871
cis-3-Hexene	20	1.39191	1.39226	1.39479	1.39697	1.39989	1.40110	1.40611
	25	1.38903	1.38938	1.39189	1.39405	1.39694	1.39814	1.40312
	30	1.38615	1.38650	1.38899	1.39113	1.39399	1.39518	1.40013
trans-3-Hexene	20	1.39145	1.39180	1.39429	1.39645	1.39931	1.40052	1.40546
	25	1.38854	1.38889	1.39137	1.39351	1.39636	1.39756	1.40248
	30	1.38563	1.38598	1.38845	1.39057	1.39341	1.39460	1.39950
2-Methyl-1-pentene	20	1.38923	1.38957	1.39200	1.39408	1.39688	1.39806	1.40293
	25	1.38638	1.38672	1.38912	1.39118	1.39395	1.39512	1.39994
	30	1.38353	1.38387	1.38624	1.38828	1.39102	1.39218	1.39695
3-Methyl-1-pentene	20	1.38157	1.38190	1.38422	1.38622	1.38890	1.39002	1.39467
	25	1.37870	1.37903	1.38133	1.38332	1.38598	1.38709	1.39171
	30	1.37583	1.37616	1.37844	1.38042	1.38306	1.38416	1.38875
4-Methyl-1-pentene	20	1.38003	1.38036	1.38267	1.38467	1.38735	1.38847	1.39312
	25	1.37711	1.37744	1.37974	1.38173	1.38439	1.38551	1.39013
	30	1.37419	1.37452	1.37681	1.37879	1.38143	1.38255	1.38714
2-Methyl-2-pentene	20	1.39734	1.39771	1.40030	1.40254	1.40552	1.40678	1.41195
	25	1.39444	1.39481	1.39739	1.39962	1.40259	1.40384	1.40899
	30	1.39154	1.39191	1.39448	1.39670	1.39966	1.40090	1.40603
3-Methyl-cis-2-pentene	20	1.40161	1.40197	1.40452	1.40671	1.40968	1.41093	1.41612
	25	1.39878	1.39913	1.40166	1.40384	1.40678	1.40802	1.41317
	30	1.39595	1.39629	1.39880	1.40097	1.40388	1.40511	1.41022
3-Methyl-trans-2-pentene	20	1.39870	1.39905	1.40157	1.40375	1.40668	1.40792	1.41305
	25	1.39590	1.39625	1.39876	1.40093	1.40385	1.40508	1.41019
	30	1.39310	1.39345	1.39595	1.39811	1.40102	1.40224	1.40733
4-Methyl-cis-2-pentene	20	1.38519	1.38552	1.38793	1.39000	1.39279	1.39395	1.39879
	25	1.38226	1.38259	1.38498	1.38703	1.38980	1.39096	1.39577
	30	1.37933	1.37966	1.38203	1.38406	1.38681	1.38797	1.39275
4-Methyl-trans-2-pentene	20	1.38604	1.38638	1.38878	1.39086	1.39366	1.39483	1.39971
	25	1.38311	1.38344	1.38583	1.38789	1.39067	1.39183	1.39668
	30	1.38008	1.38050	1.38288	1.38492	1.38768	1.38883	1.39365
2-Ethyl-1-butene	20	1.39394	1.39428	1.39671	1.39880	1.40162	1.40280	1.40771
	25	1.39105	1.39139	1.39380	1.39588	1.39868	1.39985	1.40473
	30	1.38816	1.38850	1.39089	1.39296	1.39574	1.39690	1.40175
2,3-Dimethyl-1-butene	20	1.38743	1.38777	1.39022	1.39231	1.39512	1.39629	1.40113
	25	1.38452	1.38486	1.38729	1.38937	1.39216	1.39332	1.39813
	30	1.38161	1.38195	1.38436	1.38643	1.38920	1.39035	1.39513
3,3-Dimethyl-1-butene	20	1.37355	1.37388	1.37620	1.37820	1.38086	1.38198	1.38657
	25	1.37051	1.37083	1.37313	1.37511	1.37775	1.37886	1.38341
	30	1.36747	1.36778	1.37006	1.37202	1.37464	1.37574	1.38025
2,3-Dimethyl-2-butene	20	1.40931	1.40968	1.41235	1.41466	1.41777	1.41909	1.42456
	25	1.40649	1.40686	1.40952	1.41182	1.41492	1.41623	1.42168
	30	1.40367	1.40404	1.40669	1.40898	1.41207	1.41337	1.41880

Measurements Made

The measurements of density were made at 20, 25 and 30°, with a density balance previously described.[14] The experimental values of density are given in Table I. Individual measurements were reproducible within 0.00003 g./ml. The accuracy of the tabulated values is estimated to be ±0.00005 to ±0.00010 g./ml.

The refractive index was measured by means of the apparatus and procedure previously described.[5]

(14) A. F. Forziati, B. J. Mair and F. D. Rossini, *J. Research Natl. Bur. Standards*, **35**, 513 (1945).

The calculations and correlations were similarly made as described previously, wherein the data obtained were correlated by means of the Hartmann equation as modified by Tilton and Gurewitz[15]

$$n_\lambda = n_\infty + C/(\lambda - \lambda^*)^{1.6} \quad (1)$$

Table II gives the values of refractive index at 7 wave lengths at 20, 25 and 30°. Table III gives the values of the constants of the modified Cauchy equation. Table IV gives the values of the constants of the modified Hartmann equation. The last columns of Tables III and IV give the root mean square values of the deviations of the observed from the calculated points. Individual measurements were reproducible within ±0.00002 to ±0.00003. The accuracy of the tabulated values is estimated to be ±0.00005 to ±0.00008.

TABLE III

VALUES OF THE CONSTANTS OF THE MODIFIED CAUCHY EQUATION FOR THE 17 HEXENES, C_6H_{12}

Compound	Constants in the eq. $\Delta n = a + b/\lambda^2$		
	$a \times 10^3$	$b \times 10^3$	$\rho \times 10^6$
1-Hexene	2.773	0.0308	4.30
cis-2-Hexene	2.834	.0171	8.73
trans-2-Hexene	2.833	.0250	4.32
cis-3-Hexene	2.798	.0371	5.31
trans-3-Hexene	2.848	.0260	5.31
2-Methyl-1-pentene	2.738	.0478	4.58
3-Methyl-1-pentene	2.800	.0304	4.89
4-Methyl-1-pentene	2.865	.0232	5.30
2-Methyl-2-pentene	2.864	.0176	5.21
3-Methyl-cis-2-pentene	2.751	.0369	4.78
3-Methyl-trans-2-pentene	2.759	.0191	5.69
4-Methyl-cis-2-pentene	2.864	.0305	2.44
4-Methyl-trans-2-pentene	2.860	.0323	2.75
2-Ethyl-1-butene	2.825	.0294	2.80
2,3-Dimethyl-1-butene	2.844	.0288	8.96
3,3-Dimethyl-1-butene	2.955	.0395	4.55
2,3-Dimethyl-2-butene	2.773	.0198	3.87

TABLE IV

VALUES OF THE CONSTANTS OF THE MODIFIED HARTMANN EQUATION FOR THE 17 HEXENES, C_6H_{12}

Compound	Constants in the eq. $n_\lambda = n_\infty + C/(\lambda - \lambda^*)^{1.6}$ at 25°			
	n_∞	C	λ^*	$\rho \times 10^6$
1-Hexene	1.37241	0.004022	0.09976	3.25
cis-2-Hexene	1.38183	.003997	.10856	1.85
trans-2-Hexene	1.37764	.004121	.10367	5.03
cis-3-Hexene	1.37845	.004235	.10345	2.73
trans-3-Hexene	1.37807	.004194	.10325	0.87
2-Methyl-1-pentene	1.37646	.003895	.11047	1.15
3-Methyl-1-pentene	1.36909	.003801	.10781	1.03
4-Methyl-1-pentene	1.36752	.003786	.10855	2.90
2-Methyl-2-pentene	1.38360	.004318	.10535	1.79
3-Methyl-cis-2-pentene	1.38843	.004001	.11561	1.71
3-Methyl-trans-2-pentene	1.38560	.003990	.11493	1.14
4-Methyl-cis-2-pentene	1.37241	.003850	.11182	3.64
4-Methyl-trans-2-pentene	1.37329	.003815	.11391	3.34
2-Ethyl-1-butene	1.38111	.003877	.11261	1.69
2,3-Dimethyl-1-butene	1.37431	.004088	.10351	2.02
3,3-Dimethyl-1-butene	1.36079	.003901	.10249	3.27
2,3-Dimethyl-2-butene	1.39565	.004165	.11772	2.20

Table V gives the values of the specific dispersions, $10^4 (n_F - n_C)/d$ and $10^4 (n_g - n_D)/d$, cal-

(15) L. W. Tilton and Helen L. Gurewitz, *Natl. Bur. Standards*, unpublished.

culated from the values of refractive index in Table II and of density in Table I.

The measurements and calculations of vapor pressures and boiling points were made as previously described[2,4,6,8] with the samples being introduced into the apparatus without contact with the air of the atmosphere.[6]

Table VI gives the experimental data on the temperature and pressures of the liquid–vapor equilibrium for the compounds measured. Using the experimental data and the method of least squares, calculations were made to yield constants for the Antoine equation for vapor pressure

$$\log_{10} P = A - B/(C + t) \quad (2)$$

Table VII gives the values of the three constants of the Antoine equation, the normal boiling point at 760 mm., the pressure coefficient of the boiling point at 760 mm. and the range of measurement in pressure and in temperature. The last column of Table VII gives the root-mean-square value of the ratios of the deviations of the observed points from the Antoine equation to the expected standard deviation. Individual measurements of boiling points were reproducible within ±0.002 to ±0.003°. The accuracy of the tabulated values of the normal boiling point is estimated to be ±0.008 to ±0.015°.

Previous Data on Physical Properties

The data reported have been obtained on compounds which appear to have a purity greater than that of any similar compounds heretofore available. A complete list of references to the literature reporting physical properties of the hexenes is given in the tables of the American Petroleum Institute Research Project 44 and need not be repeated here.[16] Within the respective limits of uncertainty, the previous data are in accord with the present values.

Calculation of Heats of Vaporization

It appeared desirable to utilize the data of the present investigation on the change of vapor pressure with temperature, in combination with reliable estimates of the difference in the molal volumes of the gas and liquid phases, to calculate values of the heats of vaporization for the 17 hexenes, at saturation pressure and at 25° and the normal boiling point.

The basic equations are[17]

$$\Delta H_v = T[V(g) - V(\text{liq})]dP/dT = T(\Delta V)dP/dT \quad (3)$$
$$z(g) = PV(g)/RT; \quad z(\text{liq}) = PV(\text{liq})/RT;$$
$$z(g) - z(\text{liq}) = \Delta z = P(\Delta V)/RT \quad (4)$$
$$\Delta H_v = 2.3026 BTP[V(g) - V(\text{liq})]/(C' + T)^2 \quad (5)$$
$$\Delta H_v = 2.3026 BTP[z(g)RT/P - V(\text{liq})]/(C' + T)^2 \quad (6)$$
$$\Delta H_v = 2.3026 BRT^2(\Delta z)/(C' + T)^2 \quad (7)$$

In the above equations, B and C' (equal to $C - 273.16$) are the second and third constants of the Antoine equation for vapor pressures; z is the compressibility factor, PV/RT, for the gas or liquid phases, as specified; ΔH_v is the molal heat of

(16) American Petroleum Institute Research Project 44. Selected values of properties of hydrocarbons and related compounds. Petroleum Research Laboratory, Carnegie Institute of Technology, Pittsburgh 13, Pennsylvania.

(17) F. D. Rossini, "Chemical Thermodynamics," John Wiley and Sons, Inc., New York, N. Y., 1950.

TABLE V

CALCULATED VALUES OF THE SPECIFIC DISPERSION FOR THE 17 HEXENES, C_6H_{12}

Temp., °C.	$10^4(n_F - n_C)/d$	$10^4(n_g - n_D)/d$	$10^4(n_F - n_C)/d$	$10^4(n_g - n_D)/d$	$10^4(n_F - n_C)/d$	$10^4(n_g - n_D)/d$
	1-Hexene		cis-2-Hexene		trans-2-Hexene	
20	121.96	155.83	124.56	160.22	126.71	162.25
25	121.92	155.73	124.83	160.73	126.84	162.49
30	121.89	155.63	125.12	161.27	127.01	162.76
	cis-3-Hexene		trans-3-Hexene		2-Methyl-1-pentene	
20	130.02	166.50	128.78	164.97	124.88	160.77
25	129.74	166.32	128.95	165.25	124.44	160.28
30	129.45	166.14	129.14	165.55	123.99	159.80
	3-Methyl-1-pentene		4-Methyl-1-pentene		2-Methyl-2-pentene	
20	121.66	156.57	122.19	157.45	132.12	169.70
25	121.59	156.59	122.47	157.68	132.43	170.12
30	121.59	156.70	122.78	157.95	132.80	170.61
	3-Methyl-cis-2-pentene		3-Methyl-trans-2-pentene		4-Methyl-cis-2-pentene	
20	128.44	166.28	127.96	165.61	125.98	162.29
25	128.28	166.08	128.23	165.99	125.98	162.40
30	128.17	165.95	128.54	166.41	126.02	162.57
	4-Methyl-trans-2-pentene		2-Ethyl-1-butene		2,3-Dimethyl-1-butene	
20	126.38	163.47	123.55	159.52	125.65	160.89
25	126.39	163.45	123.54	159.61	125.66	161.01
30	126.44	163.48	123.53	159.71	125.67	161.13
	3,3-Dimethyl-1-butene		2,3-Dimethyl-2-butene			
20	124.02	158.78	132.89	172.43		
25	123.93	158.65	133.20	172.86		
30	123.79	158.47	133.39	173.14		

TABLE VI

EXPERIMENTAL DATA ON THE TEMPERATURE AND PRESSURES OF THE LIQUID–VAPOR EQUILIBRIUM FOR THE 17 HEXENES, C_6H_{12}

t, °C.	P, mm.	t, °C.	P, mm.	t, °C.	P, mm.
1-Hexene		cis-2-Hexene		trans-2-Hexene	
64.311	780.03				
63.837	768.49	69.319	770.26	68.306	770.26
63.299	755.54	68.783	757.37	67.774	757.37
62.827	744.29	68.361	747.36	67.353	747.36
62.323	732.42	67.862	735.63	66.858	735.62
				62.084	630.30
50.914	501.03	56.395	503.02	55.387	503.03
44.763	402.82			49.124	403.35
38.993	325.27	44.086	323.78	43.165	323.78
33.399	262.04	38.522	261.17	37.574	261.17
28.762	217.44	33.505	214.15	32.621	214.15
23.720	176.15	28.149	171.64	27.324	171.64
19.950	149.61	24.760	145.84	23.547	145.84
15.890	124.85			18.989	118.69

t, °C.	P, mm.	t, °C.	P, mm.	t, °C.	P, mm.
cis-3-Hexene		trans-3-Hexene		2-Methyl-1-pentene	
66.872	770.26	67.508	770.26	62.518	769.84
66.341	757.37	66.979	757.36	61.996	757.17
65.921	747.35	66.561	747.35	61.580	747.22
65.426	735.60	66.068	735.58	61.090	735.51
60.649	630.30	61.315	630.29	56.353	630.19
53.957	503.06	54.654	503.11	49.719	502.90
47.700	403.34	48.426	403.34	43.509	403.21
41.740	323.77	42.500	323.76	37.612	323.66
36.177	261.16	36.941	261.16	32.096	261.09
31.230	214.15	32.017	214.14	27.190	214.06
25.935	171.63	26.737	171.63		

t, °C.	P, mm.	t, °C.	P, mm.	t, °C.	P, mm.
		22.158	145.84	22.980	145.83
		17.575	118.70	18.403	118.71
		13.488	98.23		
3-Methyl-1-pentene		4-Methyl-1-pentene		2-Methyl-2-pentene	
54.592	770.26	54.279	770.26	67.727	770.25
54.065	757.36	53.757	757.35	67.198	757.34
53.650	747.35	53.344	747.34	66.780	747.34
53.157	735.55	52.855	735.53	66.285	735.52
48.424	630.29	48.156	630.28	61.533	630.28
41.792	503.16	41.571	503.20	54.872	503.21
35.593	403.34	35.420	403.33	48.651	403.33
29.702	323.76	29.574	323.75	42.727	323.75
24.182	261.16	24.102	261.15	37.175	261.15
19.282	214.14	19.233	214.13	32.238	214.13
14.143	171.62	14.035	171.62	26.958	171.62
				23.187	145.82
				18.641	118.73

t, °C.	P, mm.	t, °C.	P, mm.	t, °C.	P, mm.
3-Methyl-cis-2-pentene		3-Methyl-trans-2-pentene		4-Methyl-cis-2-pentene	
70.859	770.25	68.125	770.24	56.797	770.25
70.326	757.33	67.589	757.32	56.277	757.32
69.905	747.33	67.170	747.32	55.866	747.32
69.409	735.51	66.674	735.52	55.380	735.52
64.624	630.27	61.879	630.26	50.697	630.26
57.913	503.23	55.168	503.24	44.140	503.24
51.635	403.32	48.886	403.32	38.006	403.32
45.660	323.74	42.913	323.73	32.176	323.73
40.062	261.14	37.317	261.14	26.717	261.14
35.094	214.12	32.337	214.12	21.864	214.11
29.774	171.61	27.023	171.60	16.696	171.60
25.982	145.81	23.235	145.80		
21.376	118.74	18.618	118.75		
17.243	98.14				

TABLE VI (Continued)

t, °C.	P, mm.	t, °C.	P, mm.	t, °C.	P, mm.
4-Methyl-trans-2-pentene		2-Ethyl-1-butene		2,3-Dimethyl-1-butene	
59.022	770.24	65.101	770.24	56.027	770.24
58.503	757.32	64.577	757.32	55.506	757.30
58.092	747.32	64.161	747.32	55.094	747.31
57.605	735.52	63.671	735.52	54.607	735.54
52.921	630.25	58.936	630.25	49.916	630.24
46.359	503.24	52.303	503.24	43.342	503.23
40.220	403.32	46.104	403.31	37.198	403.30
34.381	323.72	40.208	323.72	31.347	323.70
28.911	261.13	34.686	261.13	25.874	261.12
24.055	214.11	29.785	214.11	21.019	214.10
18.862	171.60	24.538	171.59	15.815	171.58
		20.803	145.80		
		16.237	118.76		
3,3-Dimethyl-1-butene		2,3-Dimethyl-2-butene			
41.649	770.24	73.628	770.23		
41.141	757.30	73.095	757.28		
40.738	747.31	72.672	747.29		
40.263	735.55	72.171	735.54		
35.676	630.24	67.354	630.22		
29.250	503.20	60.604	503.12		
23.265	403.30	54.282	403.29		
17.568	323.70	48.274	323.69		
		42.642	261.11		
		37.648	214.09		
		32.288	171.57		
		28.481	145.77		
		23.817	118.80		
		19.636	98.00		
		15.856	82.14		

vaporization at the given temperature and pressure; V is the molal volume for the gas or liquid phases, as specified. The values of the Antoine constants required for the above calculations were taken from the present investigation. For the calculation at 25°, the molal volume of the liquid phase was evaluated from the values of density determined in the present investigation and the molal volume of the gas was evaluated from the following empirical relationship provided by the American Petroleum Institute Research Project 44[18]

$$z(g) = PV(g)/RT = 1 - P(0.025 + 0.00070t_B) \quad (8)$$

where P is in atmospheres and t_B is the normal boiling point in °C. For the calculation at the normal boiling point, the difference in the molal volumes was taken from the American Petroleum Institute Research Project 44 as[18]

$$\Delta z = 0.96583 + 2.00 \times 10^{-5}T_b - 25.0 \times 10^{-8}T_b^2 \quad (9)$$

where T_b is the normal boiling point in °K.

The resulting values of the heats of vaporization are given in Table VIII for each of the 17 hexenes. The only precise values in the literature with which a comparison can be made are those of Waddington, et al.,[19] on 2,3-dimethyl-2-butene. For this compound, their data yield 7.78 and 7.08 kcal./mole at 25° and the normal boiling point, at saturation pressure, which values are to be compared with the values 7.78 and 7.07 kcal./mole, respectively, from the present investigation.

(18) Unpublished, Petroleum Research Laboratory, Carnegie Institute of Technology, Pittsburgh 13, Pennsylvania.
(19) D. W. Scott, H. L. Finke, J. P. McCullough, M. E. Gross, J. F. Messerly, R. E. Pennington and Guy Waddington, *J. Am. Chem. Soc.*, **77**, 4993 (1955).

TABLE VII

SUMMARY OF THE RESULTS OF THE CORRELATION OF THE EXPERIMENTAL DATA WITH THE ANTOINE EQUATION FOR VAPOR PRESSURE FOR THE 17 HEXENES, C_6H_{12}

Compound	Constants of the Antoine eq. $\log_{10} P = A - B/(C + t)$ or $t = B/(A - \log_{10} P) - C$ P in mm.; t in °C.			Normal b.p. at 760 mm., °C.	Pressure coefficient dt/dP at 760 mm., °C./mm.	Range of measurement Pressure, mm.	Temp., °C.	Measure of precision ρ
	A	B	C					
1-Hexene	6.86573	1152.971	225.849	63.485	0.04149	124–780	15.9–64.3	0.96
cis-2-Hexene	7.03805	1258.571	233.851	68.891	.04161	145–770	24.7–69.3	1.78
trans-2-Hexene	6.89342	1173.343	224.530	67.884	.04164	118–770	18.9–68.3	0.97
cis-3-Hexene	6.87854	1164.134	224.749	66.450	.04162	98–770	13.4–66.8	.50
trans-3-Hexene	6.91780	1180.707	225.384	67.088	.04140	118–770	18.4–67.5	.52
2-Methyl-1-pentene	6.85030	1138.516	224.704	62.113	.04129	214–770	27.1–62.5	.28
3-Methyl-1-pentene	6.75523	1086.316	226.204	54.178	.04135	171–770	14.1–54.6	1.92
4-Methyl-1-pentene	6.83529	1121.302	229.687	53.866	.04098	171–770	14.0–54.3	0.72
2-Methyl-2-pentene	6.92367	1183.837	225.514	67.308	.04139	118–770	18.6–67.7	.99
3-Methyl-cis-2-pentene	6.92634	1194.527	224.833	70.438	.04171	98–770	17.2–70.9	.63
3-Methyl-trans-2-pentene	6.91073	1186.402	226.696	67.703	.04175	118–770	18.6–68.1	.80
4-Methyl-cis-2-pentene	6.84129	1120.707	226.586	56.387	.04083	171–770	16.6–56.8	.74
4-Methyl-trans-2-pentene	6.88030	1142.874	227.143	58.612	.04083	171–770	18.8–59.0	.64
2-Ethyl-1-butene	6.99712	1218.352	231.300	64.682	.04109	118–770	16.2–65.1	2.58
2,3-Dimethyl-1-butene	6.86236	1134.675	229.367	55.617	.04090	171–770	15.8–56.0	0.66
3,3-Dimethyl-1-butene	6.67751	1010.516	224.909	41.248	.04006	323–770	17.5–41.6	0.99
2,3-Dimethyl-2-butene	6.95058	1215.428	225.443	73.205	.04193	82–770	15.8–73.6	1.21

Tᴀʙʟᴇ VIII

Cᴀʟᴄᴜʟᴀᴛᴇᴅ Vᴀʟᴜᴇꜱ ᴏꜰ ᴛʜᴇ Hᴇᴀᴛꜱ ᴏꜰ Vᴀᴘᴏʀɪᴢᴀᴛɪᴏɴ ᴏꜰ ᴛʜᴇ 17 Hᴇxᴇɴᴇꜱ, C_6H_{12}, ᴀᴛ 25° ᴀɴᴅ ᴛʜᴇ Nᴏʀᴍᴀʟ Bᴏɪʟɪɴɢ Pᴏɪɴᴛ, ᴀᴛ Sᴀᴛᴜʀᴀᴛɪᴏɴ Pʀᴇꜱꜱᴜʀᴇ

| | Heat of vaporization at satn. pressure, kcal./mole | | |
Compound	At 25°	At the normal b.p.	Normal b.p. (at 760 mm.), °C.
1-Hexene	7.32	6.76	63.485
cis-2-Hexene	7.52	6.96	68.891
trans-2-Hexene	7.54	6.91	67.884
cis-3-Hexene	7.47	6.86	66.450
trans-3-Hexene	7.54	6.92	67.088
2-Methyl-1-pentene	7.29	6.74	62.113
3-Methyl-1-pentene	6.83	6.43	54.178
4-Methyl-1-pentene	6.86	6.47	53.866
2-Methyl-2-pentene	7.55	6.93	67.308
3-Methyl-cis-2-pentene	7.67	7.00	70.438
3-Methyl-trans-2-pentene	7.49	6.89	67.703
4-Methyl-cis-2-pentene	7.04	6.59	56.387
4-Methyl-trans-2-pentene	7.16	6.68	58.612
2-Ethyl-1-butene	7.41	6.88	64.682
2,3-Dimethyl-1-butene	6.97	6.55	55.617
3,3-Dimethyl-1-butene	6.36	6.13	41.248
2,3-Dimethyl-2-butene	7.78	7.07	73.205

Discussion

When the data of the present investigation on the 17 hexenes can be combined with data on higher monoölefins, particularly those with large alkyl groups attached to the doubly bonded carbon atoms, in both the cis and trans configurations, it will be possible to produce a more satisfactory correlation of properties with molecular structure of the monoölefins than has previously been possible.[20]

(20) W. J. Taylor, J. M. Pignocco and F. D. Rossini, *J. Research Natl. Bur. Standards*, **34**, 413 (1945).

THE THERMODYNAMICS OF CHELATE FORMATION. II. A MONTE CARLO STUDY OF THE DISTRIBUTION OF CONFIGURATIONS IN SHORT CHAINS

Bʏ F. Aʟʙᴇʀᴛ Cᴏᴛᴛᴏɴ ᴀɴᴅ Fʀᴀɴᴋ E. Hᴀʀʀɪꜱ[1]

Department of Chemistry, Harvard University, Cambridge, Massachusetts

Received July 3, 1956

The distribution of end-to-end distances in short chains with fixed valence angles has been investigated by a Monte Carlo method. The results are used to make a crude estimate of the entropy changes accompanying ring closures. Estimated and measured values are compared for a system involving cyclic thia-alkanes.

I. Introduction

Experimental studies of the thermodynamic functions for closure of chelate rings have indicated that both the enthalpy and entropy changes depend upon the size of the ring being formed.[2] While the data are not all in complete agreement as to the relative importance of enthalpy and entropy contributions, it appears quite likely that the differences in entropy are not negligible. One contribution to the variation in entropy with ring size must be the differences in configurational freedom among rings of different sizes. In order to see whether this contribution could be the main source of the entropy variation, it was decided to study the configurational properties of model systems chosen so as to approximate the species under consideration.

The present study is of course not the first attempt to evaluate the configurational entropies of ring or chain molecules.[3,4] Previous theoretical considerations have proved most successful for polymer molecules, where it is ordinarily satisfactory to use limiting results which apply to long chains.[3] Applications to short chains, while in principle understood, have not been amenable to simple evaluation. Schwarzenbach[4] has provisionally suggested that the configurational entropy of a short chain be taken to be proportional to the volume which one end of the chain can reach when the other end is held fixed. However, he found that this assumption did not satisfactorily account for observed results. Also, since the quantity used by Schwarzenbach is not related in a simple manner to the number of possible configurations, a more accurate calculation would still seem to be desirable.

For the reasons outlined above, we have calculated the distribution of end-to-end distances for chains of 4, 5, 6 and 7 links, assuming a fixed tetrahedral valence angle, but otherwise permitting free rotation. The calculation was performed by examining a random sample of the configuration space (Monte Carlo method) as indicated in more detail below. As shown in the discussion which follows, the results are interpreted so as to indicate both the distribution of end-to-end distances and the configurational contribution to the entropy of ring closure. Finally, the calculated results are compared with actual systems for which sufficient experimental data are available.

II. Method of Computation

The chains whose end-to-end distances were computed were composed of an initial link 2.0 Å.

(1) Department of Chemistry, University of California, Berkeley, California.

(2) F. A. Cotton and F. E. Harris, Tʜɪꜱ Jᴏᴜʀɴᴀʟ, **59**, 1203 (1955); H. Irving, R. S. P. Williams, D. S. Ferrett and A. E. Williams, *J. Chem. Soc.*, 3494 (1954) and references therein.

(3) For a general discussion see, for example, P. J. Flory, "Principles of Polymer Chemistry," Cornell University Press, Ithaca, N. Y., 1953.

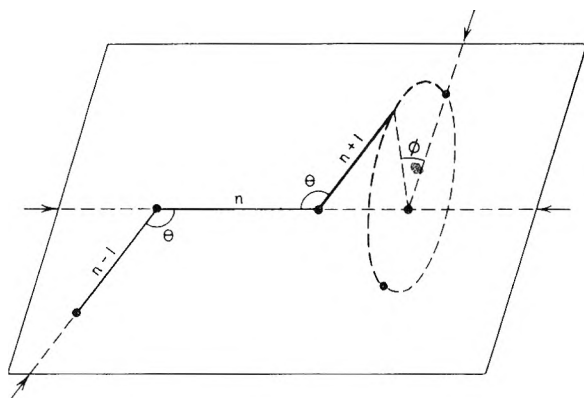(4) G. Schwarzenbach, *Helv. Chim. Acta*, **35**, 2344 (1952).

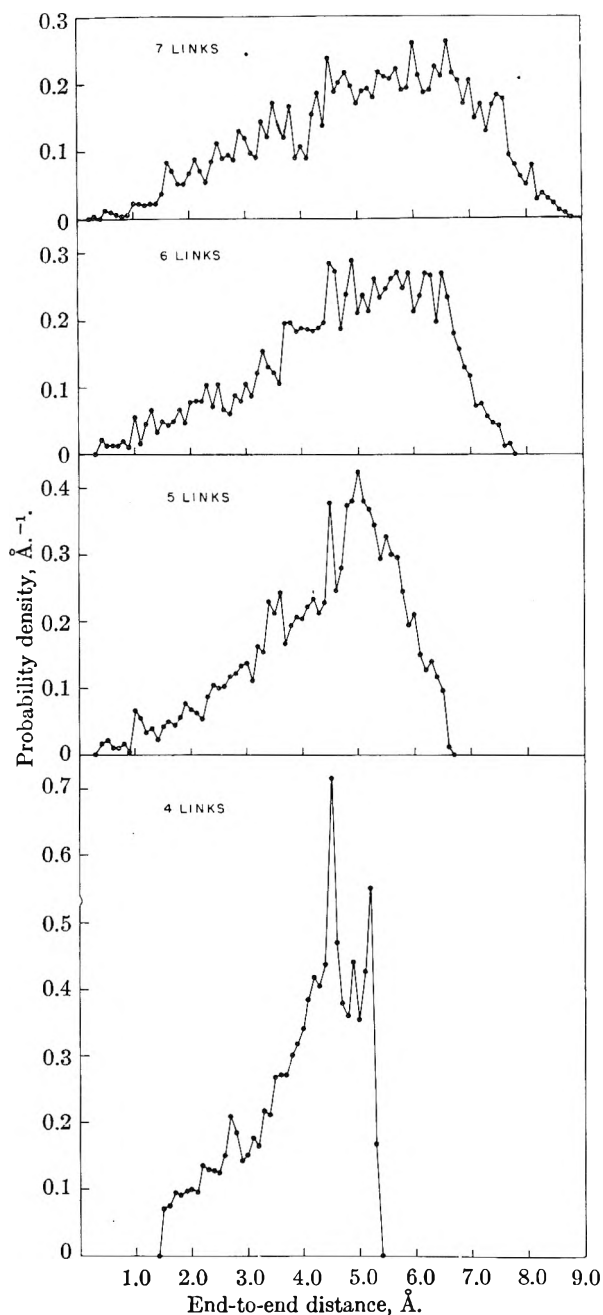Fig. 1.—Coördinate system used in the computation.

Fig. 2.—Distribution of end-to-end distances for the short chains described in the text.

long, followed by the requisite number of 1.5 Å. links. These dimensions were chosen to correspond approximately to distances found in ammine complexes. The computation was performed by constructing a large number of chains, placing each link at a random angle ϕ with respect to those preceding (but with the fixed valence angle θ), and counting the numbers of chains with end-to-end distances between limits 0.1 Å. apart. See Fig. 1 for a definition of the angles θ and ϕ. The random angle ϕ was selected with the aid of random numbers generated by a process described by Moshman.[5] A total of 3000 chains of each length was constructed using a self-checking routine on a digital computer. The computing time was approximately 2 hours. An analysis of these results indicated that substantially greater certainty in the end-to-end distributions could only be obtained with an order of magnitude greater computation time, so that the project was terminated after 3000 chains.

The probability density of end-to-end distance for each length chain was then obtained by dividing the numbers of chains at each distance by a normalizing factor. The results are shown graphically in Fig. 2.

III. Discussion

Before drawing any conclusions from the graphs of Fig. 2, let us consider the accuracy to be associated with the given probability distributions. Over the bulk of the range of end-to-end distances, enough chains were examined that it is possible to conclude that the larger of the irregular "sawteeth" are intrinsic to the problem, and are not the result of an insufficiently refined calculation. If the individual points on the curves are replaced by lines covering 75%, or even 90% confidence intervals, the irregularities are not removed with anything approaching 75%, or 90% efficiency. We therefore believe that these irregularities stem from the fact that we are considering small numbers of rigid links, and that the curves are, for the most part, accurate to about 10%. Results for 1000 chain portions of the total sample reveal that the values shown evolved in a manner which does not cause suspicion to be placed upon the operation of the computer. This is the only conclusion which can be drawn from the partial results as their consideration separately can add no statistical information to the combined results we have reported.

We shall be concerned here with the entropy involved in ring closure, which we will evaluate in terms of the probability that the two ends of a chain will be separated by a distance suitable for the ring-closing bond to be formed. It is clear that this is a rather naive way of calculating this entropy, as no consideration is thereby made of the bond angles about the atoms at the ends of the original chain, and as no allowance is made for the small, but significant differences in energy among different conformations of the chain. This latter factor is quite important as the conformations available to a closed ring may not sample uniformly those available to an open chain. Furthermore, the vibrational characteristics of the ring
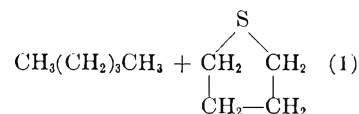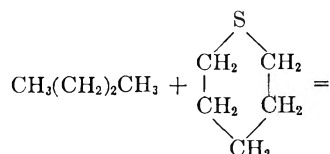
(5) J. Moshman, *J. Assoc. Computing Machinery*, **1**, 88 (1954).

and chain compounds differ in a manner not allowed for by this analysis. Nevertheless, we shall tentatively assume that the entropy of ring close can be approximated by consideration of the probability that the two ends of the chain be between certain limits. If the arbitrary limits 1.6 to 2.4 Å. be chosen, it is found that the probability of ring closure of the 4 link chain (to form a 5-membered ring) is 0.09, with the 5, 6 and 7 link chains possessing closure probabilities of 0.062, 0.065 and 0.063, respectively. While the absolute magnitudes of these figures depend upon the region in which a chain is called a ring, the relative magnitudes of these figures are almost completely unaltered if the "ring" region be extended to 1.4–2.6 Å. or more.

To check that the order of magnitude of these probabilities is reasonable, calculations can be made of the relative numbers of ring and chain configurations on lattices of various kinds. As an example, the probability of formation of a six-membered ring on a tetrahedral lattice was computed by direct enumeration, and found to be 0.049, in reasonable correspondence with our value of 0.062 quoted above. It is also of interest to compare the length distributions obtained here with those predicted by use of the Gaussian approximation so successful in describing longer chains. The distributions of Fig. 2 all show much smaller probability densities near the origin than do Gaussian chains, with maxima much nearer the extreme extension consistent with the chain construction.

It should perhaps be mentioned that an alternative method of computation could be adopted if the only objective were to deduce relative extents of ring formation. Such a method would consist of studying chains of n links, and deducing therefrom the probability density for zero end-to-end distance. This probability density would not bear a simple relation to other characteristics of an n or $n - 1$ link chain, but could be used to compute the probability of closure of an n-membered ring relative to those of other sizes.

.Finally, let us examine the correspondence between actually observed entropies of ring closure and those calculated as described in the foregoing text. Inasmuch as the data for the chelates are, as mentioned above, not completely agreed upon, and since the chelate studies are all in aqueous solution where many additional factors may require consideration, we shall compare our calculations with data on gaseous thiacyclopentane[6] and thiacyclohexane.[7] These compounds are a particularly suitable choice since their dimensions are close to those used in the calculation, which were chosen with reference to the chelates. We therefore propose to consider the equilibrium

$$CH_3(CH_2)_2CH_3 + \begin{array}{c} S \\ \diagup \quad \diagdown \\ CH_2 \quad CH_2 \\ | \qquad | \\ CH_2 \quad CH_2 \\ \diagdown \quad \diagup \\ CH_2 \end{array} =$$

This reaction has the advantage that the numbers of molecules and bonds are the same on both sides of the equation, so that the major difference should be due to the difference in ring size. Using the existing data for n-butane and n-pentane,[8] together with the data already referred to for the sulfur compounds, reaction 1 is found to have a standard entropy (gas phase, 298°K.) $\Delta S° = +6.0$ e.u.

The thermodynamic functions of 5- and 6-membered aliphatic rings have been discussed by Kilpatrick, Pitzer and Spitzer[9] and the thermodynamic data on the sulfur-containing rings were found to be satisfactorily explainable in terms of the same concepts.[6,7] The points of relevance here are two in number, both stemming from the consideration of hydrogen–hydrogen repulsions which we have thus far ignored. First, the various distinct conformations which a molecule may assume, while equi-energetic for the hydrogen-less skeleton, will no longer necessarily be of the same energy. The lower energy conformations will be more highly populated than will be the others. Secondly, the constraints introduced by ring closure may cause the potential restricting rotation to have an anomalous influence on the vibrational properties of the molecule concerned. Consideration of the first of these points leads to the conclusion that the calculated probability of closure of the 6-membered ring is too large by a factor of about 4, since of the four conformations for the hetero-ring, one is believed to be ca. 95% prevalent at room temperature.[7,9] There is but one distinct conformation for a 5-membered ring, so that no adjustment of its calculated entropy is necessary for this first reason. The second point has also already been assumed to be of importance in cyclopentane and its analog.[6,9] It was proposed that a very low frequency vibration, equivalent to the migration of a point of puckering around the ring, is caused by the hydrogenic repulsions. This would cause the entropy of the 5-membered ring to be larger than the calculated value by the order of R.

On the basis of the considerations summarized above, we would calculate the entropy change of reaction 1 as

$$\Delta S = \Delta S_c + \Delta S_1 + \Delta S_2$$

where ΔS_c is the unmodified ring closure configurational entropy, and ΔS_1 and ΔS_2 account for the corrections already mentioned. Evaluating the various terms, we find

$$\Delta S = 4.6 \log (0.09/0.062) + 4.6 \log 4 + 2 = +5.4 \text{ e.u.}$$

in fortuitously good agreement with the experimental value +6.0 e.u.

Since the calculated and observed entropies are of the same order of magnitude, we would like to

$$CH_3(CH_2)_3CH_3 + \begin{array}{c} S \\ \diagup \quad \diagdown \\ CH_2 \quad CH_2 \\ | \qquad | \\ CH_2—CH_2 \end{array} \quad (1)$$

(6) W. N. Hubbard, et al., J. Am. Chem. Soc., **74**, 6025 (1952).

(7) J. P. McCullough, et al., J. Am. Chem. Soc., **76**, 2663 (1954).

(8) National Bureau of Standards, "Selected Values of Chemical Thermodynamic Properties," Washington, D. C., 1949.

(9) J. E. Kilpatrick, K. S. Pitzer and R. Spitzer, J. Am. Chem. Soc., **69**, 2483 (1947).

suggest that this method of estimating ring-chain entropies may be useful in many cases where a complete statistical thermodynamic calculation is impractical.

NOTES

REACTION HEATS OF ORGANIC HALOGEN COMPOUNDS. VI. THE CATALYTIC HYDROGENATION OF SOME ALKYL FLUORIDES[1]

By J. R. Lacher, A. Kianpour and J. D. Park

Department of Chemistry, University of Colorado, Boulder, Colorado

Received December 12, 1955

In a previous paper[2] an isothermal constant flow calorimeter was described which operated at a temperature of about 248°. Its reliability was determined by measuring the heat of formation of HCl; we also reported the heats of hydrogenation of methyl, ethyl and vinyl chlorides. The present paper deals with the catalytic hydrogenation of methyl, ethyl, n-propyl and isopropyl fluorides. Only the last two reactions were sufficiently quantitative to permit calorimetric measurements.
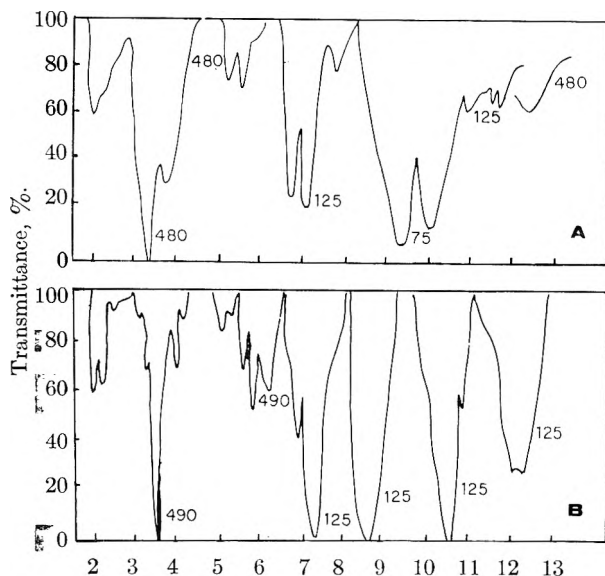
Fig. 1.—Infrared spectra of (A) normal propyl fluoride; (B) isopropyl fluoride; gas at room temp. in 10-cm. cell at indicated mm. pressure; Perkin–Elmer single beam spectrometer with sodium chloride optics.

Experimental Details.—Methyl and ethyl fluorides[3] were prepared by the reaction of the corresponding iodides with mercuric fluoride. The apparatus consisted of a one-liter copper reaction flask equipped with a copper condenser

(1) This research was supported by the A.E.C. Contract No. AT (29-1), Program A.

(2) J. R. Lacher, E. Emery, E. Bohmfalk and J. D. Park, This Journal, **60**, 492 (1956).

(3) A. L. Henne and Thomas Midgley, Jr., *J. Am. Chem. Soc.*, **58**, 884 (1936).

and an inlet for the mercuric fluoride. The methyl fluoride was purified by a simple trap to trap distillation. The ethyl fluoride was purified by distilling in a low temperature Podbielniak column. It boiled at −46° at 625 mm. Five hundred grams of n- and isopropyl fluorides were prepared using a procedure described by Grosse and Linn.[4] The compounds were carefully purified by distilling in a 100-plate Podbielniak column. The n-propyl fluoride boiled at −9.0 to −8.8° and the isopropyl at −15.6° at a pressure of 627.7 mm. mercury. The infrared spectra of the compounds in the region between 2 and 15μ are illustrated in Fig. 1. A sodium chloride prism and optics were used in this determination.

The catalyst used consisted of palladium on activated carbon. The carbon was sized so that it passed a 6 and was retained by a 20 mesh screen. It was first treated with 10% nitric acid, washed several times with distilled water, dried at 100°, and finally evacuated for 24 hours at 350° and about 1 mm. pressure. Eight grams of palladium chloride was dissolved in 50 ml. of 15% hydrochloric acid and the solution was added to 65 g. of purified activated carbon. The mixture was dried over a steam-bath and placed in a catalyst chamber. Hydrogen was passed through at a temperature of 248° to reduce the palladium chloride. After the reduction was complete, the catalyst was evacuated at 1 mm. for 24 hours.

In order to determine the effectiveness of the catalyst in bringing about the hydrogenation of the alkyl fluorides in question, the reactions were studied in a pilot plant. The flow rates of the hydrogen and organic material were set to be approximately those to be used in a calorimetric measurement. The catalyst chamber was placed in an electrically heated can for convenient though approximate temperature control. The exit gases were passed through a tube containing sodium fluoride pellets to remove hydrogen fluoride. The products were analyzed by means of infrared absorption. The strong band at 10.30μ shown by n-propyl fluoride (Fig. 1) and that at 12.25μ in isopropyl fluoride occur in regions where propane is transparent. The intensities of these peaks were measured at different pressures and used as reference for quantitative analyses.

Using a flow rate for hydrogen of 1.0×10^{-3} mole/min. and for isopropyl fluoride 0.5×10^{-3} mole/min., it was found that the reaction was quantitative at the temperatures of 235, 200 and 155°. At 110° only about 5 to 10% conversion was obtained. Using the same flow rates it was found that n-propyl fluoride was more difficult to hydrogenate. If a new and active catalyst was used, the reaction was quantitative at temperatures of 190° and above. Even though elaborate precautions were taken, the maximum conversion of methyl and ethyl fluoride to methane and ethane was 10% at 240°.

In making a calorimetric run hydrogen was used in excess. The rate of reaction was taken as being equal to the rate of formation of hydrogen fluoride. The reaction products were diverted for a known length of time to a copper collecting tower filled with Teflon chips. The absorbing solution consisted of 100 ml. of dilute sodium hydroxide. The excess hydroxide was titrated with a standard 0.05 N sulfuric acid solution. Of eight runs made on n-propyl fluoride, seven were completed without experimental difficulties and are given in Table I.

Discussion of Results.—In order to use the present results to calculate the standard heats of

(4) A. V. Grosse and C. B. Linn, *J. Org. Chem.*, **3**, 26 (1938).

<div style="text-align:center">

TABLE I

HYDROGENATION OF n-PROPYL FLUORIDE, 248°

</div>

H_2 flow, moles/min. $\times 10^4$	HF formation, moles/min. $\times 10^4$	Energy rate, cal./min.	$-\Delta H$, kcal./mole n-C_3H_7F
6.20	3.050	6.887	22.58
8.50	2.420	5.477	22.63
6.55	3.000	6.807	22.69
8.45	4.025	9.353	22.24
8.30	4.025	9.244	22.97
8.30	3.000	6.942	23.14
7.00	3.015	6.923	22.96

<div style="text-align:center">

$-\Delta H$ av. 22.88 kcal./mole

Twice the stand. dev. from the mean: $\pm 1.6\%$

</div>

Five runs were made on isopropyl fluoride and they are given in Table II.

<div style="text-align:center">

TABLE II

HYDROGENATION OF ISOPROPYL FLUORIDE, 248°

</div>

H_2 flow moles/min. $\times 10^4$	HF formation, moles/min. $\times 10^4$	Energy rate, cal./min.	$-\Delta H$, kcal./mole iso-C_3H_7F
7.00	3.215	6.692	20.85
8.00	4.52	9.563	21.16
7.30	3.50	7.419	21.19
7.45	3.50	7.445	21.27
7.45	3.013	6.346	21.06

<div style="text-align:center">

$-\Delta H$ av. 21.11 kcal./mole

Twice the stand. dev. from the mean: $\pm 0.69\%$

</div>

formation of n- and isopropyl fluoride, it is necessary to know their gaseous heat capacities in the range between 25 and 248°. The data are not available. However, it is possible to calculate the heat of isomerization of normal to isopropyl fluoride at 248°. One finds that the iso compound is more stable by 1.80 kcal./mole. The uncertainty in this value is about 2%.

THE NATURE OF THE ACTIVATED INTERMEDIATE IN THE HOMOGENEOUS CATALYTIC ACTIVATION OF HYDROGEN BY CUPRIC SALTS

By J. Halpern, E. R. Macgregor and E. Peters

Department of Mining and Metallurgy, The University of British Columbia, Vancouver, Canada

In an earlier paper,[1] a kinetic study of the Cu^{++}-catalyzed reduction of $Cr_2O_7^=$ and other substrates by H_2, was described. At low acidities, the kinetics were found to be of the form

$$-d[H_2]/dt = k[Cu^{++}][H_2] \qquad (1)$$

suggesting that an H_2 molecule reacts homogeneously with a Cu^{++} ion in the rate-determining step, leading to the formation of an "activated intermediate" which reduces $Cr_2O_7^=$ in a subsequent fast reaction.

It was reported[1] that the rate of this reaction decreased slightly as the concentration of $HClO_4$ was increased, but the limitations of the equipment which was available at that time, precluded any studies with solutions containing more than 0.1 M $HClO_4$. However, by using a titanium-lined auto-

(1) E. Peters and J. Halpern, This Journal, **59**, 793 (1955).

clave, we have since been able to extend the investigation to solutions of higher acidity. The results of this work are reported here since they throw some further light on the mechanism of the reaction and on the nature of the activated intermediate which is formed in the rate-determining step.

The procedure was the same as that employed earlier,[1] i.e., the rate of reaction of H_2 was calculated from the measured zero-order rate of reduction of $Cr_2O_7^=$ using the known stoichiometry of the reaction, i.e.

$$Cr_2O_7^= + 3H_2 + 8H^+ \longrightarrow 2Cr^{+++} + 7H_2O \qquad (1)$$
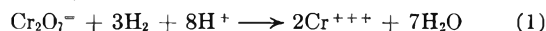
The decrease in rate as the $HClO_4$ concentration was increased is shown in Fig. 1. At 1 M $HClO_4$ the rate was only about 30% of its value at low $HClO_4$ concentrations.
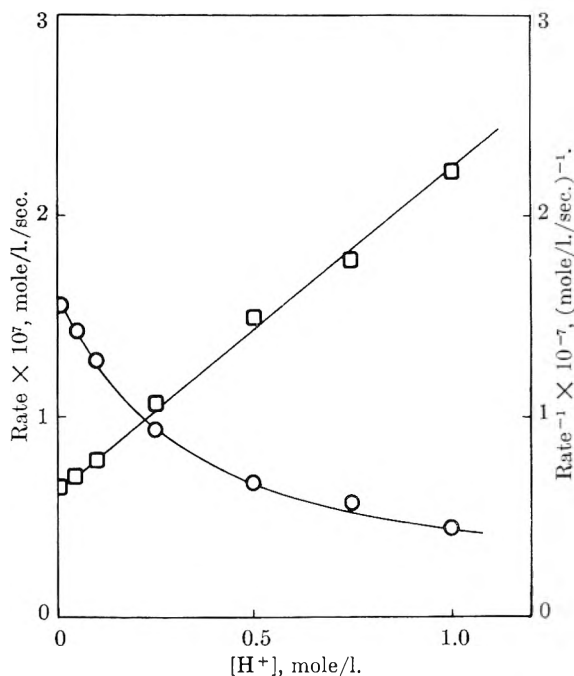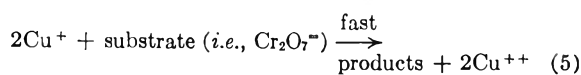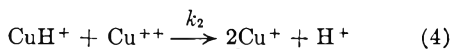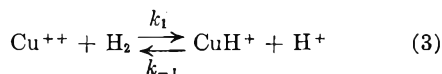

Fig. 1.—Dependence of the rate of reaction of H_2 on the H^+ concentration at 0.1 M Cu^{++}, 110°, 20 atm. H_2: O, rate *vs.* $[H^+]$; □, rate^{-1} *vs.* $[H^+]$.

An earlier suggestion[1] that this apparent decrease in rate might be due to the reduction of ClO_4^- competing with that of $Cr_2O_7^=$ appears untenable in the light of our failure to detect any Cl^- in the solutions and of our observations that the rate depends only on the concentration of H^+ and is insensitive to variations in the ClO_4^- concentration.

An alternative interpretation is that the rate-determining step, in which H_2 is converted to a reactive intermediate complex, releases an H^+ ion and that the decrease in rate is due to the fact that the reversal of this step, which regenerates H_2, competes with the subsequent reaction of this complex, i.e., with the reduction of $Cr_2O_7^=$. The zero-order dependence of the rate on the $Cr_2O_7^=$ concentration, even at high H^+ concentrations, suggests that the complex does not react directly with $Cr_2O_7^=$. The most likely alternative is that it reacts with another Cu^{++} ion, reducing it to Cu^+, which in turn reacts rapidly with $Cr_2O_7^=$. These steps are incorporated in the mechanism

$$Cu^{++} + H_2 \underset{k_{-1}}{\overset{k_1}{\rightleftarrows}} CuH^+ + H^+ \qquad (3)$$

$$CuH^+ + Cu^{++} \overset{k_2}{\longrightarrow} 2Cu^+ + H^+ \qquad (4)$$

$$2Cu^+ + \text{substrate } (i.e., Cr_2O_7^=) \overset{\text{fast}}{\longrightarrow} \text{products} + 2Cu^{++} \quad (5)$$

Application of the steady-state treatment to this sequence leads to the kinetics

$$\text{Rate} = \frac{-d[H_2]}{dt} = \frac{k_1[Cu^{++}]^2[H_2]}{[Cu^{++}] + (k_{-1}/k_2)[H^+]} \qquad (6)$$

This becomes equivalent to equation 1 at low H^+ concentrations.

At constant $[Cu^{++}]$ and $[H_2]$, as shown in Fig. 1, the experimental results conform to a reasonably good plot of rate^{-1} vs. $[H^+]$, as required by equation 6. At 110°, the values of k_1 and of the ratio (k_{-1}/k_2), obtained from the intercept and slope of this plot, are 9.5×10^{-5} l. mole^{-1} sec.$^{-1}$ and 0.26, respectively.

Equation 6 also predicts a linear relation between $[Cu^{++}]$/rate and $[Cu^{++}]^{-1}$ whose slope, given by $(k_{-1}/k_2)[H^+]/k_1[H_2]$, should increase with $[H^+]$ while the intercept remains constant. In effect, this implies a shift of the kinetic dependence on the Cu^{++} concentration from first toward second order with increasing H^+ concentration. The results in Fig. 2 showing the dependence of the rate on $[Cu^{++}]$ at 0.01 and 1.0 M HClO$_4$ are in quantitative accord with this prediction. The values of k_1 and of
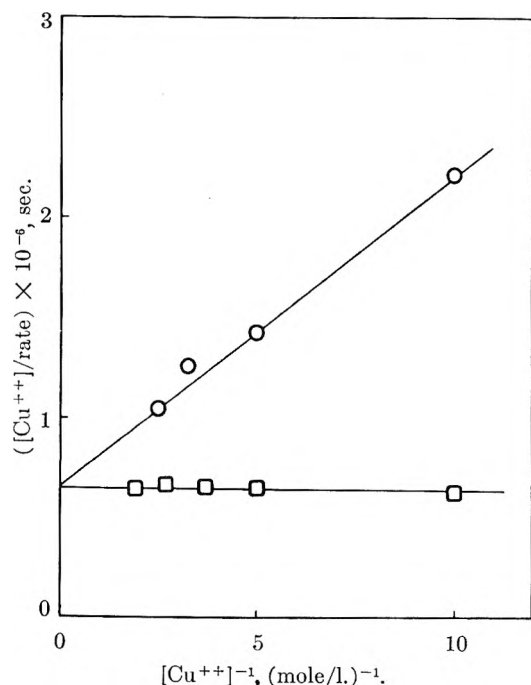

Fig. 2.—Dependence of the rate of reaction of H_2 on the concentration of Cu^{++} at 110°, 20 atm. H_2: □, 0.01 M HClO$_4$; ○, 1.0 M HClO$_4$.

(k_{-1}/k_2) obtained from these plots are 9.4×10^{-5} l. mole^{-1} sec.$^{-1}$ and 0.25, respectively. These agree well with the values estimated earlier from the dependence of the rate on $[H^+]$.

Some further evidence, as follows, may also be advanced in support of the suggestion that CuH^+ is the activated intermediate in this system.

1. The available thermochemical data suggest that formation of other intermediate species which might be considered to result from the interaction of an H_2 molecule with a Cu^{++} ion, i.e., Cu^+ or $Cu^°$, is energetically inconsistent with the observed activation energy of 26 kcal./mole for the over-all reaction. On the other hand, the formation of CuH^+ appears plausible on energetic grounds.[2]

2. A similar intermediate has previously been postulated to explain the homogeneous catalytic activation of H_2 by cuprous salts in quinoline solution.[3] In this system the kinetics demonstrate that two Cu^+ ions are involved in the rate-determining step which may be most reasonably depicted as

$$2Cu^+ + H_2 \longrightarrow 2CuH^+ \qquad (7)$$
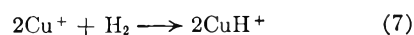
Similar considerations apply to the catalytic activation of H_2 by silver salts in aqueous solution where an analogous intermediate, AgH^+, appears probable.[2,4]

3. The promoting influence of certain anions on the catalytic activity of Cu^{++} can be explained in terms of the proposed mechanism by assigning to them the role of stabilizing the H^+ ion which is released in the initial step, i.e.

$$CuX^+ + H_2 \longrightarrow CuH^+ + HX \qquad (8)$$

Consistent with this interpretation, the catalytic activities have been observed[5] to decrease in the same order as the basicity of the anion (X), i.e., butyrate, propionate > acetate > sulfate > chloride > perchlorate.

Several examples have been reported earlier of homogeneous hydrogenation reactions in which the kinetic dependence on the catalyst concentration shifts from first to second order with a change of solvent. For example, the catalytic activation of H_2 by cuprous acetate is second-order kinetically in quinoline solution but first order in pyridine and dodecylamine.[3,6] Similarly, in silver salt-catalyzed hydrogenation reactions, the kinetic dependence on the catalyst concentration shifts from first to second order in going from pyridine to aqueous solutions.[4,6] Some insight into this phenomenon may be derived from the interpretation which has been proposed above for the Cu^{++} system, and which demonstrates how such a change in the apparent order of the reaction may occur, without a real change in the mechanism of the H_2 activation process.

(2) J. Halpern, Proc. Int. Cong. Catalysis, in press (1956).

(3) M. Calvin, J. Am. Chem. Soc., 61, 2230 (1939); S. Weller and G. A. Mills, ibid., 75, 769 (1953); M. Calvin and W. K. Wilmarth, ibid., 78, 1301 (1956).

(4) A. H. Webster and J. Halpern, THIS JOURNAL, 60, 280 (1956).

(5) E. Peters and J. Halpern, Can. J. Chem., 34, 554 (1956).

(6) L. Wright, S. Weller and G. A. Mills, THIS JOURNAL, 59, 1060 (1955).

THE HEATS OF COMBUSTION OF DYSPROSIUM AND YTTERBIUM[1]

By Elmer J. Huber, Jr., Earl L. Head and Charles E. Holley, Jr.

Contribution from the University of California, Los Alamos Scientific Laboratory, Los Alamos, New Mexico

This paper is the sixth in a series reporting measurements of the heats of formation of the rare earth oxides.[2-6] The method, involving the determination of the heat evolved from the combustion of a weighed sample of the metal in a bomb calorimeter at a known initial pressure of oxygen, has been described elsewhere.[6] The same units and conventions are used here.

Dysprosium and Ytterbium Metals.—The dysprosium and ytterbium metals were analyzed and found to have the following per cent. impurities

	C	H	N	O	Ca	Li	Y
Dy	0.0224	0.0194	0.007	0.036	0.01	0.005	
Yb	.036	.025	.004	.003	.02	.005	0.05

No other metallic impurities were detected.

Each of the metals thus contained about 0.1% impurities. If it is assumed that the non-metallic impurities are combined with dysprosium and ytterbium as the carbide, hydride, nitride and oxide, the dysprosium is 97.92 mole per cent. metal (atomic weight $Dy = 162.51$) and the ytterbium 97.23 mole per cent. metal (atomic weight $Yb = 173.04$).

An X-ray pattern of the dysprosium showed a two atom hexagonal close-packed unit cell and a calculated density of 8.534 g./cc. A pattern of the ytterbium revealed a face-centered cubic unit cell and a calculated density of 6.966 g./cc. A small amount of impurity was observed in the ytterbium which is believed to be the hydride.

Combustion of Dysprosium and Ytterbium.— Each of the metals was burned on sintered discs of the corresponding oxide in oxygen at 25 atmospheres pressure. The oxides were approximately 99.9% pure. Neither of the metals showed any increase in weight when exposed to O_2 at 25 atm. pressure for one hour. Combustion varied from 99.84 to 100.00% of completion. The average initial temperature for the dysprosium runs was 25.0° and for the ytterbium runs 25.1°. The results are listed in Table I.

The average values of 5718.9 ± 11.6 and 5251.1 ± 5.0 j./g. must be corrected for the impurities present.

Correction for Impurities.—The calculated percentage composition of the dysprosium by weight is Dy metal 98.01; DyH_2, 1.58; Dy_2O_3, 0.28; DyN, 0.088; C, 0.0224; Ca, 0.01; Li, 0.005. The carbon is probably present as DyC_2 but the heat of formation of the latter is not known and is probably small. The heat of combustion of Dy metal cor-

TABLE I

THE HEAT OF COMBUSTION OF DYSPROSIUM

Mass Dy burned, g.	Wt. Mg, mg.	Wt. Dy₂O₃, g.	J./deg., total	ΔT, °K.	Energy from Firing, j.	Dy, j./g.	Dev. from mean
2.1173₅	7.1₅	45.1	10031.6	1.2240	12.1	5710.1	9.3
1.9135₅	6.5₅	50.0	10032.9	1.1064	17.8	5707.2	12.3
2.0192	7.1	43.3	10031.2	1.1685	11.9	5712.4	6.6
1.9711	7.7	38.9	10030.0	1.1458	12.9	5727.6	9.9
2.0737₅	7.6	45.1	10031.6	1.2059	12.0	5737.2	18.1
					Av.	5718.9	10.8
					Standard dev.		5.8

THE HEAT OF COMBUSTION OF YTTERBIUM

Mass Yb burned, g.	Wt. Mg, mg.	Wt. Yb₂O₃, g.	J./deg., total	ΔT, °K.	Energy from Firing, j.	Yb, j./g.	Dev. from mean
2.0283₅	7.4	65.6	10036.3	1.0825	12.6	5260.0	8.8
2.0623	7.2	33.2	10028.2	1.0980	12.3	5247.1	4.1
2.1622	8.0	36.1	10028.9	1.1539	21.5	5250.9	0.2
2.3298	7.2	60.0	10034.9	1.2373	17.1	5245.7	5.4
2.4132	7.7	34.8	10028.6	1.2842	15.0	5251.9	0.7
					Av.	5251.1	3.8
					Standard dev.		2.5

rected[6] for impurities is 5726.4 j./g. The correction due to impurities amounts to 0.13% of the uncorrected value.[8]

The percentage composition of the ytterbium is Yb metal 97.64; YbH_2, 2.17; Yb_2O_3, 0.0246; YbN, 0.053; C, 0.036; Ca, 0.02; Li, 0.005; Y, 0.05. The corrected heat of combustion for ytterbium gives a value of 5,231.0 j./g. The correction for impurities amounts to 0.38% of the uncorrected value.

Calculation of the Uncertainty.—The uncertainty to be attached to the corrected values includes the uncertainty in the energy equivalent which is 0.04%, the uncertainty in the calorimetric measurements which is 11.6 j./g. or 0.20% for the dysprosium and is 5.0 j./g. or 0.095% for the ytterbium, and the uncertainty introduced in the correction for the impurities.[6]

The combined uncertainty is 11.9 j./g. for the dysprosium and 6.5 j./g. for the ytterbium. The values for the heats of combustion give for the reaction in the bomb a value of $\Delta E_{25.0°} = -1861.2 \pm 3.9$ kj./mole for dysprosium and $\Delta E_{25.0°} = -1810.3 \pm 2.2$ kj./mole for the ytterbium.

Composition of the Dysprosium and Ytterbium Oxides.—Each oxide formed was tan in color. An X-ray pattern of the dysprosium oxide showed it to be composed of roughly equal proportions of B and C-types of the sesquioxide. Unfortunately the energy of transition between these two forms is not known. It is probably small, however. The X-ray pattern of the ytterbium oxide showed lines

(1) This work was performed under the auspices of the A.E.C.

(2) E. J. Huber, Jr., and C. E. Holley, Jr., J. Am. Chem. Soc., 74, 5530 (1952).

(3) E. J. Huber, Jr., and C. E. Holley, Jr., ibid., 75, 3594 (1953).

(4) E. J. Huber, Jr., and C. E. Holley, Jr., ibid., 75, 5645 (1953).

(5) E. J. Huber, Jr., and C. E. Holley, Jr., ibid., 77, 1444 (1955).

(6) E. J. Huber, Jr., C. O. Matthews and C. E. Holley, Jr., ibid., 77, 6493 (1955).

(7) The specific heats of Dy_2O_3 and Yb_2O_3 are estimated to be 0.26 and 0.25 j./g./°, respectively. The specific heat of Pt is taken as 0.136 j./g./° and the specific heat of O_2 as 0.651 j./g./°. The amount of MgO formed is so small that its contribution to the energy equivalent of the calorimeter may be neglected.

(8) The heats of formation of DyH_2 and YbH_2 are estimated at −45 kcal./mole from the known values for NdH_2 and PrH_2. See R. N. R. Mulford and C. E. Holley, Jr., This Journal, 59, 1222 (1955). The heats of formation of DyN and YbN are estimated at −75 kcal./mole from the published values of LaN and CeN. See Selected Values of Chemical Thermodynamic Properties, N.B.S. Circular 500, 1952, pp. 350, 354. The heats of combustion of graphite (to CO_2), calcium (to CaO), lithium (to Li_2O_2), and yttrium (to Y_2O_3), are taken as 33,000, 16,000, 45,800 and 10,800 j./g., respectively. The heats of formation of $H_2O(g)$ and NO_2 are taken as −58 and +8 kcal./mole.

only of the C-type sesquioxide. Analysis by the method of Barthauer and Pierce[9] showed no oxygen above that necessary for the sesquioxide.

Heats of Formation of Dy_2O_3 and Yb_2O_3.— Using methods of calculation reported elsewhere[6] the heat of formation of Dy_2O_3, $\Delta H_{25°} = -1865.4 \pm 3.9$ kj./mole. In defined calories this is -445.84 ± 0.93 kcal./mole. For the heat of formation of Yb_2O_3, $\Delta H_{25°} = -1814.5 \pm 2.2$ kj./mole or -433.68 ± 0.53 kcal./mole. No literature values are available for comparison. It should probably be remarked, however, that this value for the heat of formation of Dy_2O_3 is larger in magnitude by about 10 kcal. than would be expected on the basis of the value for Yb_2O_3 (C-form) and the reported values for Gd_2O_3 (B-form) $(-433.94 \pm 0.86$ kcal./mole)[5] and Sm_2O_3 (B-form) $(-433.89 \pm 0.48$ kcal./mole).[6] The measurements were made at intervals over a two-month period along with measurements on other materials, two of the five measurements on dysprosium being made before the ytterbium measurements and the other three afterwards so that it seems unlikely that there is a calorimetric error of the necessary magnitude involved. Also, since Sm_2O_3 and Gd_2O_3 form B-type oxides and Yb_2O_3 forms the C-type oxide, the fact that Dy_2O_3 forms a mixture of B and C-types can hardly be the explanation.

Acknowledgments.— The authors wish to acknowledge the valuable assistance of D. Pavone, F. H. Ellinger, O. R. Simi and E. Van Kooten in the analytical work.

They also appreciate the courtesy of Dr. F. H. Spedding of the Ames Laboratory, A.E.C., through whom the metals and oxides were obtained.

(9) G. L. Barthauer and D. W. Pierce, *Ind. Eng. Chem.*, **18**, 479 (1946).

THE PREPARATION OF DRY ALKALI CHLORIDES FOR SOLUTES AND SOLVENTS IN CONDUCTANCE STUDIES[1]

By Henry J Gardner, Charles T. Brown and George J. Janz

Department of Chemistry, Rensselaer Polytechnic Institute, Troy, N. Y.

Received April 27, 1956

In the course of investigations on the conductance of alkali metal titanium fluorides as solutes in potassium chloride–lithium chloride eutectic melts at 350–500°, a need was felt for a criterion of purity in the preparation of dry alkali chlorides.

The importance of potassium chloride as conductance reference standard in both aqueous[2,3] and non-aqueous (fused salt)[4] measurements is well recognized. While Jones and Bradshaw[3] recommended fusion of the potassium chloride to remove last traces of water, modern practice is to effect this in a slow stream of dry argon[4,5] or nitrogen[6] to displace moisture laden air and minimize the possibility of contamination by hydrolysis. Potassium chloride, precipitated from strong hydrochloric acid, fused in this way usually contains no more than 0.001% of free alkali.[6b] For very hygroscopic material, as lithium chloride, a more rapid stream of the inert gas, and electrolysis of the molten salt at low current density to remove the hydroxides have been recommended[5] as additional pretreatments before use in high temperature electrochemical investigations.

The gain or loss in weight of the alkali chlorides as a function of temperature and time, using modern high vacuum techniques and a dry inert gas to purge the samples, would provide a ready reference for the drying of these salts for electrochemical studies. The present communication describes the results of a series of weight loss determinations designed to meet this need and to supplement the existing information concerning the dryness and purity of molten salts.[5-7]

Experimental

An all glass vacuum-transfer system constructed for work under controlled atmospheres was used in the present investigation. The lithium, sodium and potassium chlorides, Fisher reagent grade chemicals, were powdered to pass a 30 mesh A.S.T.M. sieve and used without further purification. The vials used to hold the samples (about 20 g. salt) for the measurements were a simple test-tube design made from 25 mm. Pyrex or Vycor tubing and connected to the vacuum manifold through a 14/35 ⊤ male joint. An indentation in the bottom was made to receive a calibrated chromel-alumel thermocouple for temperature measurements. A small General Electric Co. combustion furnace was used to heat these vials. Argon or nitrogen, carefully purified and dried, was used to provide the inert atmosphere. All weighings were corrected for air buoyancy.

The general procedure for measurement of the weight loss-temperature dependence was as follows. The salt was placed in a weighed dry vial to obtain the weight before drying. The sample was then evacuated to 10^{-5} mm. at room temperature or at 100°. The criterion, that the leak rate on the vacuum manifold system with the sample in be the same as that with the sample out, was taken as the indication that the sample was "dry" at that temperature. The use of a dry argon or nitrogen "flush" at the temperature of drying to hasten the removal of water vapor was also introduced. The rate of drying would normally be controlled by the rate of diffusion of the water vapor through the salt mass. It was found with 10 g. of KCl, for example, that with three dry gas "flushes," the sample would pump down to 10^{-6} mm. in 30 minutes or less, whereas without this practice a period of several hours was required to achieve dryness. To remove a sample for weighing, the manifold and vial were filled with the dry pre-purified inert gas at a pressure slightly greater than atmospheric. The vial was removed and the stopcock grease adhering to the joint wiped off with a cloth damp with carbon tetrachloride under this flow of gas. The tube was then quickly capped for weighing. The reproducibility of weighings after such treatment was ± 0.2 mg. Extended evacuation at 10^{-6} mm. did not produce any further decrease in weight. The weight loss having been achieved at the temperature in question, this procedure was repeated with the same sample at the next higher temperature, until in increments of approximately 100°, the upper limit of temperature was reached.

(2) F. Kohlrausch, L. Holborn and H. Diesselhorst, *Wied. Ann.*, **64**, 417 (1898).

(3) G. Jones and B. C. Bradshaw, *J. Am. Chem. Soc.*, **55**, 1780 (1933).

(4) E. R. Van Arsdalen and I. S. Yaffe, This Journal, **59**, 118 (1955).

(5) S. Senderoff and A. Brenner, *J. Electrochem. Soc.*, **106**, 16 (1954).

(6) (a) G. D. Pinching and R. G. Bates, *J. Research Natl. Bur. Standards*, **37**, 311 (1946). (b) Heating to fusion ensures removal of occluded hydrochloric acid from the salt precipitated in a strong solution of the acid.

(7) C. Duval, "Inorganic Thermogravimetric Analysis," Elsevier Publ. Co., Houston, Texas, 1953.

The results for the vacuum drying of the three alkali chlorides are summarized in Fig. 1. In the present vacuum system, with the inert gas flush technique, a period of some 40 hr. at 25°, and an additional period of 20 hr. at 100° were required to achieve the 10^{-6} mm. equilibrium pressure above lithium chloride (22 g.). The time was much less for the other two alkali chlorides.

The constitution of the volatile components was investigated using larger samples. Batches of 200 g. of LiCl and KCl, respectively, were heated at 500° for 12 hr. under high vacuum. The volatiles were collected at liquid nitrogen temperatures in each case, diluted with de-ionized water, and analyzed for pH and hydrochloric acid content. These results are summarized in Table I. In each case a test for chloride in the volatiles was positive.

When samples of lithium chloride and potassium chloride, respectively, were fused under air in platinum, their aqueous solutions (approximately 1 molar) were found to be 9.4 and 8.3 in pH. Samples of these two chlorides dried with slowly increasing temperatures using the high vacuum technique already discussed gave pH readings of 7.1 and 6.6, respectively, for their aqueous solutions.

TABLE I

ANALYSIS OF VOLATILE MATTER

Salt[a]	pH	Normality as an acid	Grams of acid per 100 g. salt	% Hydrolysis
LiCl	2.3	0.0175	7.87×10^{-2}	0.00914
KCl	4.5	0.000145	6.51×10^{-5}	1.33×10^{-4}

[a] 200-g. sample heated 12 hr. at 500° under high vacuum.

Discussion

The temperature dependence of the weight loss results is illustrated in Fig. 1 in terms of per cent. weight loss. The sample weights after drying at 100° for LiCl, NaCl and KCl, were 23.0744, 28.8103 and 22.3928 g., respectively, below 510° in Pyrex vials. For the measurements above 510°, in Vycor, the sample weights were 23.2713, 24.4745 and 24.3503 g., respectively, for these salts in the same order. The horizontal portions of the three curves at the higher temperatures correspond to no further measurable weight loss. The precision of the results, estimated from the vial weighing and capping technique, was less than 1% for the lithium chloride, and less than 2% for the sodium and potassium chlorides. The curves show that LiCl, NaCl and KCl can be prepared in a dry state at temperatures as low as 450, 420 and 300°, respectively, if the practices described in the present work are observed, i.e., use of high vacuum pumping in stages of gradually increasing temperatures with the criterion of a 10^{-6} mm. equilibrium pressure as a measure of dryness. The process can be hastened by the use of a dry inert gas flush at intervals to hasten the removal of water vapor. Under these conditions, hydrolysis of the salts, and, accordingly, contamination by hydroxide, is minimized.

The weight loss temperature dependence of the alkali chlorides has been investigated by Duval[7] using a continuously recording thermogravimetric balance but the results reported are qualitative rather than quantitative. Inspection of the data shows that for NaCl and KCl the results are in agreement, but for LiCl, Duval's weight loss curve shows the loss beginning at 25° with a small region of constant weight at 100°. Since bottled samples of lithium chloride contain up to 0.7% water which may be removed in vacuo at 25°, the initial decrease in weight between 25 and 100° observed by Duval is thus explained.
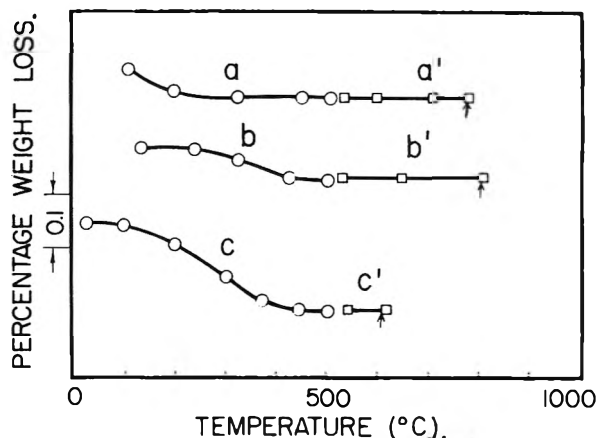

Fig. 1.—Temperature-dependence of weight loss in drying the alkali chlorides under high vacuum: KCl (curves a, a'); NaCl (curves b, b'); LiCl (curves c, c'); the results are expressed as percentages of the weight at the lowest temperature shown on each curve. The primed letters refer to the use of Vycor glass vessels, and the arrows indicate the melting points.

More recently, Laitinen, Osteryoung and Ferguson[8] have studied the preparation of lithium chloride–potassium chloride eutectic melts using a polarographic technique to investigate the state of dryness achieved under various conditions. A well-defined polarographic step at -1.0 volt with a large residual current was obtained if the mixture was fused by heating at 500° under vacuum. The current step at -1.0 volt could be nearly eliminated if dry nitrogen was bubbled through the melt for one hour followed by evacuation overnight. Melts exhibiting reproducible low residual currents (about 3 amperes) could be achieved if the fused salt was treated with hydrogen chloride gas, nitrogen, and pre-electrolysis in that order. These investigators estimated that melts thus achieved were less than 0.001 N in impurities, i.e., a very high degree of purity. It was reported that this degree of purity was sometimes nearly achieved by simple fusion under vacuum at 500°. The present results (Fig. 1) serve to emphasize the importance of a stepwise procedure in the high-vacuum drying practice, with stress on the need for pre-drying each salt separately before preparing the mixture of the eutectic composition. All possible water is not removed from lithium chloride until a temperature of at least 450° has been reached, whereas the LiCl–KCl eutectic mixture melts at 352°. The high and irreproducible residual currents in the eutectic melts observed by Laitinen, Osteryoung and Ferguson polarographically, may be attributed in part to the uncertain amounts of hydrolysis occurring due to the presence of any water during the melting of these mixtures.[9]

In the investigations in progress in this Laboratory[1] salts pre-dried by the practices described in

(8) R. A. Osteryoung, Ph.D. Thesis, University of Illinois, 1954.

(9) Present practice consists of prolonged vacuum drying of the powdered mixture at room temperature, followed by a gradual heating under vacuum during an 8-hour period up to 300°, followed by admission of HCl vapor and fusion. After using vacuum treatment and dry argon flushing, the preparation is entirely reproducible; pre-electrolysis is no longer used (H. A. Laitinen, private communication).

this communication melt smoothly *in vacuo* without ebullition of gas. Pyrex glass vessels are only slightly etched after several weeks of contact with the molten salts. This work is being extended to investigations of the thermal stabilities of the alkali metal titanium fluorides, to be described elsewhere.

THE HEAT OF FORMATION OF NITRAMIDE

By James D. Ray and Richard A. Ogg, Jr.

Department of Chemistry, Stanford University, Stanford, Cal.

Received May 4, 1956

The rapid reaction of nitramide in basic solution to form nitrous oxide and water, which was shown by Thiele and Lachmann[1] to be quantitative, was used to determine the heat of formation of nitramide.

Materials and Method.—Nitramide was prepared by the method of Thiele and Lachmann[1] as modified by Marlies and LaMer.[2] The observation of Bell and Wilson[3] that nitramide so prepared contained about 1% acidic impurity was confirmed. To eliminate this impurity the following refinements in the preparative method were carried out. It was found that if the starting material, urethan, was recrystallized three times from benzene, no such relatively non-volatile acidic material was present in the end-product nitramide. Recrystallization of the intermediate ammonium nitrourethan from methanol to remove any yellow discoloration was also necessary to ensure a pure final product. Elimination of the above two steps gave a nitramide which led to heats of decomposition in the calorimeter which were lower than for the pure compound by about a kilocalorie per mole. No high precision method for analysis of nitramide has been reported; however, Brönsted and King[4] were unable to observe any effect on the conductivity of aqueous solutions of nitramide by repeated recrystallization or by vacuum sublimation. In agreement with this observation, the heat of decomposition obtained from vacuum sublimed sample II (Table I below) is not significantly different from that of the others which were not vacuum sublimed. Tong and Olson[5] found no strong acid or basic impurity in the solution resulting from decomposition of nitramide, and were able to account for greater than 99% of the theoretically expected nitrous oxide. The purity of the nitramide samples used in the present calorimetric studies is believed to be at least 99.8%.

The calorimeter consisted of a 1 quart Dewar flask. A mercury seal on the glass paddle stirrer allowed collection of the small amount of non-dissolved nitrous oxide product in an external system. A Beckmann thermometer was used to measure the temperature. The nitramide samples were placed in small "Pyrex" thin walled bulbs which had been previously weighed. The bulbs were then evacuated to remove any water which might have formed from slow spontaneous decomposition of the sample during storage. The sample bulbs containing the nitramide were then again weighed just prior to use in the calorimeter. One-gram samples in bulbs left on the balance pan for several hours were observed to lose only 0.4 mg. per hour. Small paraffin-impregnated corks were then shoved down in the necks of the bulbs flush with the spherical surface so as to ensure complete reaction of the nitramide. The bulbs were then attached to the lower end of the stirrer. Lowering the stirrer caused the glass bulbs to shatter against the bottom of the Dewar flask to initiate the reaction.

(1) J. Thiele and A. Lachmann, *Ann.*, **288**, 267 (1893).

(2) C. A. Marlies and V. K. LaMer, *J. Am. Chem. Soc.*, **57**, 2008 (1935).

(3) R. P. Bell and G. L. Wilson, *Trans. Faraday Soc.*, **46**, 407 (1950).

(4) J. N. Brönsted and C. V. King, *J. Am. Chem. Soc.*, **49**, 193 (1927).

(5) L. K. J. Tong and A. R. Olson, *ibid.*, **63**, 3406 (1941).

Sample	I	II	III
Wt. nitramide, g.	0.7896	0.7994	0.9184
Temp. rise, °C.	0.808	0.819	0.942
Obsd. cal.	422.50	428.25	492.57
N$_2$O not dissolved, dry ml. STP	16.4	14.2	11.9
H$_2$O vaporized along with N$_2$O	0.52	0.45	0.38
Correction for N$_2$O, cal.	3.88	3.35	2.82
Correction for H$_2$O, cal.	0.25	0.21	0.18
Cor. cal./sample	426.63	431.86	495.57
ΔH, cal./mole for N$_2$O aq. prod.	−33515	−33507	−33471
		Av. −33500	

The heat capacity of the calorimeter was determined by the heat of solution of Baker and Adamson reagent grade potassium chloride. Recrystallization of the potassium chloride had no effect on its heat of solution. The heat of solution of potassium chloride was taken from Rossini, *et al.*[6] Four determinations led to a calorimeter heat capacity of 522.9 ± 1.2 cal./°C. Correction for the calorimeter temperature drift during the solution process was made by graphical evaluation of the integral in Newton's law of cooling.

0.032 *N* sodium hydroxide solution used in the calorimeter allowed the reaction to be complete in all cases in less than a minute.

Experimental Results.—Three determinations of the heat of decomposition of nitramide to form nitrous oxide (largely dissolved) and liquid water were made. The results are listed in Table I. Blank runs in a tall glass container of identical shape to the inside of the Dewar flask allowed visual observation of the course of the decomposition of nitramide. The crystals were observed to decompose without rising to the surface. The random variation in amount of nitrous oxide not absorbed by the solution was seen to depend upon the size of the few initially evolved large nitrous oxide bubbles—thus the degree of agglomeration of the nitramide sample and the specific manner in which the sample bulb shattered were determining factors. The solution of nitrous oxide resulting from the reaction was metastable with respect to further loss of nitrous oxide into the air space above the solution; however, further evolution of nitrous oxide was so slow as not to be detectable in the gas collecting buret over a period of a minute (less than 0.1 ml. per minute). Carlson[7] has made a kinetic study of the process of nitrous oxide evolution from supersaturated aqueous solutions in an apparatus similar to the calorimeter described here. This slow continuing evolution of nitrous oxide made necessary evaluation of the final temperature drift of the calorimeter on a second solution not containing nitrous oxide, but under identical conditions of temperature and stirring. The decomposition of nitramide was so rapid that the time between the initial and final temperature readings was only one minute, and the corresponding Newton's law cooling correction less than 0.001° in all cases,

(6) F. D. Rossini, D. D. Wagman, W. H. Evans, S. Levine and I. Jaffe, U. S. Bur. Standards Circ. 500 (1952).

(7) T. Carlson, *J. Chem. Phys.*, **9**, 228 (1911).

so no appreciable error was involved in this procedure.

The process of solution of a single 0.8264-g. sample of nitramide in 500 ml. of 0.001 N sulfuric acid at 24° was found to be endothermic by 3700 cal./mole.

For calculation of the heat of formation of nitramide at 24° from the elements, the following values were used. Enthalpy for the process of solution of nitrous oxide in water −5303 cal./mole (ΔC_p between 0 and 40° +35.9 cal./°C.) as derived from the solubility data of Markham and Kobe[8]; heat of formation of nitrous oxide +19490 cal./mole and of liquid water −68310 as given by Rossini, et al.[6]

The value for the heat of decomposition of nitramide (c) to form nitrous oxide gas and liquid water was calculated to be exothermic by 28200 ± 85 cal./mole. The uncertainty in this value includes that of sample purity, and that of calorimetric measurement. The heat of formation of nitramide (c) from the elements was calculated to be 20630 ± 85 cal./mole (exothermic) at 24°, that for aqueous nitramide, −16930 cal./mole. Comparison of this latter value with the heat of formation of hyponitrous acid in aqueous solution from the elements as determined by Latimer and Zimmerman,[9] and recalculated by Rossini, et al.,[6] −13700 cal./mole shows that aqueous nitramide is more stable by 3230 cal./mole than hyponitrous acid.

(8) A. E. Markham and K. A. Kobe, *J. Am. Chem. Soc.*, **63**, 449 (1941).

THE VAPOR PRESSURE OF HCl ABOVE NON-AQUEOUS SOLUTIONS

By J. J. Fritz

Department of Chemistry, The Pennsylvania State University, University Park, Pa.

The writer and Fuget[1] have recently published tables of the vapor pressures of HCl above aqueous solutions, as calculated from available cell measurements. The same methods are applicable to non-aqueous solutions. The purpose of this communication is to make available data for facilitating the calculation of vapor pressures of HCl above non-aqueous media.

In general, the vapor pressure of HCl is given by

$$\ln f_{HCl} = \frac{F}{RT}(E_g^0 - E) \tag{1}$$

where E is the voltage of the cell H_2, Pt/HCl (solvent)/AgCl, Ag, (corrected to 1 atm. pressure of hydrogen); E_g^0 is the standard potential of the cell for unit fugacity of HCl. Values of E_g^0 from 0 to 40° are given by Aston and Gittler,[2] and can be calculated readily for other temperatures. Some typical vapor pressures of HCl at 25°, so calculated, are: in water (1 m), 2.2 × 10^{-4} mm. Hg; 50 mole % ethanol-water (1 m), 1.2 × 10^{-3} mm. Hg; ethanol (1 m), 0.46 mm. Hg; methanol (0.56 m), 8 × 10^{-4} mm. Hg.

(1) J. J. Fritz and C. R. Fuget, *Ind. Eng. Chem.*, to be published.
(2) J. G. Aston and F. L. Gittler, *J. Am. Chem. Soc.*, **77**, 3173 (1955).

By use of the standard potential for hypothetical 1 molal solution (E^0) in equation 1, the standard fugacity of HCl is obtained for each system. Table I gives some representative values of the standard fugacity at 25°.

Table I

FUGACITY OF HCl IN HYPOTHETICAL 1 MOLAL STANDARD STATE AT 25°

Solvent	f^0 HCl, atm.	f^0 HCl, mm. Hg	Source of cell data
Water	4.92 × 10^{-7}	3.74 × 10^{-4}	3
Methanol	4.19 × 10^{-3}	3.18	4
Ethanol	5.06 × 10^{-2}	38.5	4
Dioxane–water[a]			
N_2 = 0.0487	1.045 × 10^{-6}	7.93 × 10^{-4}	5
N_2 = 0.1433	4.86 × 10^{-6}	3.69 × 10^{-3}	5
N_2 = 0.3231	2.34 × 10^{-4}	0.178	5
N_2 = 0.4823	1.41 × 10^{-2}	10.7	5

[a] N_2 is the mole fraction of dioxane in the solvent.

The vapor pressure of HCl is then given by

$$f_2 = a_2 f_2^0 = m^2 \gamma^2 \pm f_2^0 \tag{2}$$

where $\gamma_\pm$ is the mean in activity coefficient as ordinarily tabulated. The fugacity is a measure of the absolute activity of HCl in the solution, as contrasted to the relative activity usually tabulated.

As demonstrated in our analysis of the aqueous system,[1] the vapor pressures obtained from cell measurements are frequently more accurate than the results of direct measurements. Where measurements are available to sufficient dilution, the vapor pressure of the solvent can, of course, be calculated by means of the Duhem equation.

(3) H. S. Harned and R. W. Ehlers, *ibid.*, **54**, 1350 (1932).
(4) H. S. Harned and B. B. Owen, "Physical Chemistry of Electrolytic Solutions," Reinhold Publ. Corp., New York, N. Y., 1950, p. 336.
(5) H. S. Harned, J. O. Morrison, F. Walker, J. G. Donelson and C. Calman, *J. Am. Chem. Soc.*, **61**, 49 (1939).

NUCLEATION OF COPPER METAL FROM AQUEOUS SOLUTION

By Welby G. Courtney[1]

Chemical Construction Corporation, 525 West 43 Street, New York, N. Y.

Theories of nucleation can be divided into the classical "supersaturation" viewpoint[2] that the size of the critical nucleus varies significantly with temperature and supersaturation (*i.e.*, reagent activities), and the less widely accepted "constant number" viewpoint[3] that the critical nucleus is essentially independent of temperature and activities. In view of the vanishingly small solubility of metals in water, supersaturation would appear to be an uncertain concept when applied to the nucleation of metal particles by reduction of the metal ion from aqueous solution. However, the results of the following exploratory study of the nucleation of Cu metal from aqueous solution can

(1) Experiment Incorporated, Richmond, Virginia.
(2) M. Volmer, "Kinetik der Phasenbildung," T. Steinkopff, Dresden 1939.
(3) J. A. Christiansen and A. Nielsen, *Acta Chem. Scand.*, **5**, 103 (1949); F. R. Duke, R. J. Bever and H. Diehl, *Iowa State College J. Sci.*, **23**, 297 (1949).

be adequately interpreted by the constant number theory.

Experimentally, the nucleation of Cu metal by the disproportionation of Cu(I) was studied at $25 \pm 1°$ by noting the induction period, τ, for a Tyndall effect to appear in an unstirred aqueous solution containing initial concentrations of $0.00077-0.0015\ M$ Cu(I), $0.2-6\ M$ H$^+$, $0.02-2\ M$ NH$_4^+$ and $0.0001-0.01\ M$ Cu(II), all as the sulfates. Runs were made by pouring together with rapid shaking 2–20 ml. of [Cu(NH$_3$)$_x$]$_2$SO$_4$ and 10–100 ml. of H$_2$SO$_4$ stock solutions in a test-tube or 250-ml. erlenmeyer flask. The Cu(I) stock solution was prepared from recrystallized CuSO$_4$·5H$_2$O, excess 99.95% Cu^0 powder (-325 mesh) and NH$_3$ in 10-fold molar excess over the expected final Cu(I) concentration. Conversion to Cu(I) was practically complete in 48 hours when agitation was used. A N$_2$ atmosphere protected all solutions. The final Cu^0 product from a nucleation run was composed of 5–10 micron flocs of 0.5–1 μ polyhedral particles.

Figure 1 plots typical results showing the dependence of $1/\tau$ upon the initial Cu(I) molar concentration, c_0, at a constant $1\ M$ H$^+$ concentration.
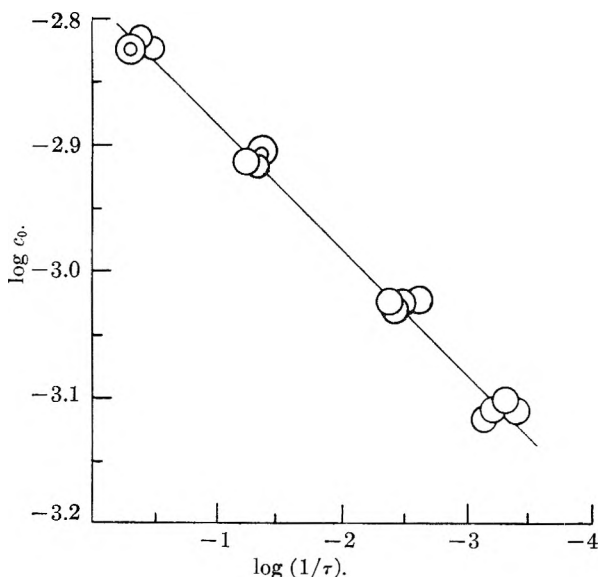
Fig. 1.—Variation of induction period (τ) with initial Cu(I) molar concentration (c_0) for constant H$^+$ ion concentration equal to $1\ M$; see equation 1. τ was measured in seconds.

A slight but uncertain effect of H$^+$ upon τ was noted, but further work on this problem had to be indefinitely postponed. τ was independent of (NH$_4$)$_2$SO$_4$ and CuSO$_4$ in the concentration ranges used here. The data at H$^+$ equal to $1\ M$ corresponded to

$$10^{-27.9} = c_0^{10} \cdot \tau \qquad (1)$$

Precision in τ appeared to be limited by subjective error only, being independent of the order of mixing of reagents, a 1000% variation in the volumes of solutions, and a 200% variation in concentrations in the stock solutions. It is therefore concluded that τ is at least partially related to nucleation kinetics.

If τ is interpreted as essentially resulting from nucleation kinetics only,[4] it can be shown theoretically, following the constant number theory, that

$$c_0 - c_\tau = Kc_\tau^p\tau \qquad (2)$$

where c_0 and c_τ are the molar concentrations of Cu(I) at times zero and τ, K is a temperature-dependent constant which includes thermodynamic and kinetic factors, and p is the total number of Cu(I) ions involved in nucleation, *i.e.*, in the rate-determining step plus any prior equilibria.

Linearity of the experimental plot of $\log(1/\tau)$ *vs.* $\log c_0$ suggests that (a) the data can be adequately interpreted by the constant number theory, and (b) $c_0 - c_\tau$ is both very small and essentially constant for the experimental metal sols. Therefore, the observed slope of 10 in Fig. 1 may be identified with p in equation 2. A possible nucleation mechanism would be the prior equilibrium formation of a cluster of four metal atoms, or

$$\overset{\text{fast}}{8\text{Cu(I)} = (\text{Cu}^0)_4 + 4\text{Cu(II)}}$$

$$\overset{\text{fast}}{(\text{Cu}^0)_4 + \text{Cu(I)} = (\text{Cu}^0)_4 \cdot \text{Cu(I)} \text{ "adsorption"}} \qquad (3)$$

$$\overset{\text{slow}}{(\text{Cu}^0)_4 \cdot \text{Cu(I)} + \text{Cu(I)} \rightarrow (\text{Cu}^0)_5 + \text{Cu(II)}}$$

$$(\text{Cu}^0)_5 \xrightarrow[\text{growth}]{\text{fast}} \text{microscopic particle}$$
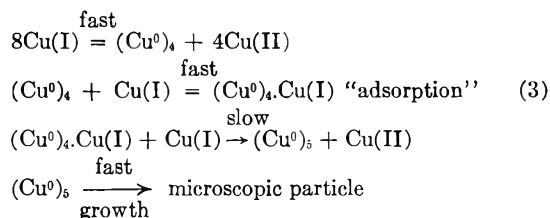
This mechanism is somewhat supported by the conclusion of Taylor, *et al.*,[5] on quantum mechanical grounds that the 5-atom Cu^0 cluster is thermodynamically the least stable of small Cu^0 clusters which are in contact with Cu^0 vapor. Thus, if the growth of Cu^0 clusters of different sizes involves similar kinetics, then in the extreme case the formation of the least stable cluster would be the rate-determining step in particle formation.

The author is pleased to acknowledge the advice of Drs. H. M. Hulburt and F. A. Schaufelberger and the assistance of Messrs. P. B. Eng and J. J. Shaw.

(4) If τ is attributed to both nucleation and growth kinetics, it can be shown, following R. A. Johnson and J. D. O'Rourke [*J. Am. Chem. Soc.*, **76**, 2124 (1954)] that the Cu^0 nucleus would involve 18 to 20 metal atoms. Such a number would seem remarkably large unless unknown trace impurities give an "organizer" mechanism where a polymeric complex of metal ions and impurity reacts to form a metal nucleus [J. Turkevitch, R. C. Stevenson and J. Hillier, *Disc. Faraday Soc.*, **11**, 55 (1951)].

(5) H. S. Taylor, H. Eyring and A. Sherman, *J. Chem. Phys.*, **1**, 68 (1933).

BROMINE PENTAFLUORIDE. FREEZING AND BOILING POINTS, HEAT OF VAPORIZATION AND VAPOR PRESSURE-TEMPERATURE RELATIONS[1]

By Max T. Rogers and John L. Speirs

Contribution from Kedzie Chemical Laboratory, Michigan State University, East Lansing, Michigan

Received May 9, 1956

As part of a program investigating the physical properties of the halogen fluorides, we have redetermined certain physical properties of bromine pentafluoride originally reported by Ruff and

Menzel.[2] Availability of more suitable materials and apparatus made it desirable to redetermine their values on material of higher purity.

Experimental

Material.—Commercial bromine pentafluoride (Harshaw Chemical Co.) containing traces of bromine and bromine trifluoride, and some hydrogen fluoride, was purified by use of methods and apparatus previously described.[3] Bromine as an impurity was easily fluorinated by pretreatment with a minimum amount of chlorine trifluoride. In the subsequent fractionation operation we found it necessary to discard as much as the first 20% of the product before the more volatile impurities, principally hydrogen fluoride, were eliminated. Fractionation was carried out at approximately 480–490 mm. pressure.

Methods.—The freezing points were determined in the previously described apparatus.[3] The freezing curve analysis was made less accurate by the preferential freezing of the material as a shell on the wall of the plastic freezing point tube. This resulted in jamming of either reciprocating or rotating stirrers after approximately 50% solidification. Usually Freon 12 was placed as a heat transfer medium in the intermediate tube separating the freezing point tube from the external acetone–Dry Ice freezing bath. Crushed Dry Ice in a Dewar flask was used as a reference temperature for thermocouple measurements. The equilibrium reference temperature was checked during measurements with a calibrated platinum resistance thermometer. Potential measurements were made as in the earlier work using both an amplifier–recorder combination and a precision potentiometer.

By use of an apparatus of improved design in which the sample was stirred by shaking[1] it was possible to carry the temperature readings to the point of about 90% solidification. The results for sample 7 of Table I were obtained in this way[1] and agree well with the other data reported here.

The vapor pressure–temperature relations were determined in the manner previously described.[3] The range of pressure covered was limited by inability to operate the apparatus much below room temperature or much above atmospheric pressure. Measurements of pressure and temperature were made at nine points approximately evenly spaced over the range of 410 to 760 mm.

Treatment of Data.—By a modification of the method of Witschonke[4] the impurity contents of eleven different samples were determined from the freezing curve. Assuming that the impurity was hydrogen fluoride and using a value of 1.76 kcal./mole for the heat of fusion (based on liquid and solid vapor pressure data of Ruff and Menzel),[2] the impurity content varied from 0.2 to 0.7 mole per cent. The results obtained for samples of different purity are shown in Table I. Although the average deviation from the mean value of the freezing point ($-60.48°$) is only $\pm0.09°$ the reported freezing point may be in error by a somewhat larger amount because of the uncertainty in judging x, the fraction of sample frozen out. It is believed that this error does not exceed 0.2–$0.3°$ since t_0 for sample 7, which was purer material prepared at a different time and studied in an apparatus[1] in which 90% of the sample could be frozen, agrees well with the other values.

The vapor pressure measurements were corrected to mm. at 0° and the simple vapor pressure equation, with suitable choice of the constants, was found adequate to express the temperature dependence without systematic error over this pressure range. The r.m.s. deviation of experimental from calculated pressures was 1.04 mm. Temperature measurements had an uncertainty believed to be no greater than $\pm0.05°$.

(1) Physical Properties of the Halogen Fluorides. IX. For previous articles of this series see M. T. Rogers, M. B. Panish and J. L. Speirs, *J. Am. Chem. Soc.*, **78**, 3288 (1956).

(2) O. Ruff and W. Menzel, *Z. anorg. allgem. Chem.*, **202**, 49 (1931).

(3) M. T. Rogers, J. L. Speirs, H. B. Thompson and M. B. Panish, *J. Am. Chem. Soc.*, **76**, 4843 (1954).

(4) C. R. Witschonke, *Anal. Chem.*, **24**, 350 (1952).

TABLE I

FREEZING POINTS OF BROMINE PENTAFLUORIDE SAMPLES

Sample	Trial	t_f,[a] °C.	t_x, °C.	m_i	t_0, °C.
1	1	−60.59	−60.75	0.015	−60.43
	2	−60.59	−60.72	0.12	−60.46
2	1	−60.59	−60.81	.020	−60.37
	2	−60.66	−60.91	.023	−60.41
3	1	−60.69	−60.81	.011	−60.57
	2	−60.62	−60.91	.027	−60.33
4	1	−60.75	−61.09	.015	−60.41
5	1	−60.88	−61.03	.032	−60.73
	2	−60.78	−61.00	.020	−60.56
6	1	−60.73	−60.94	.019	−60.52
7	1	−60.60	−60.70	.009	−60.50
Av.				.019	−60.48 ± 0.09

[a] t_f, extrapolated freezing point of original sample; t_x, temperature of one-half frozen sample; m_i, the molal concentration of impurity in the original sample; t_0, the freezing point of pure solvent calculated by the method of Witschonke.[4] The equations used are

$$t_0x = t_f - t_x(1-x)$$
$$t_0 - t_f = Km_i$$

where x is the fraction frozen out and K is the molal freezing point lowering of bromine pentafluoride (10.8).

Results

The freezing point of pure bromine pentafluoride was found to be $-60.5 \pm 0.1°$ as determined by analysis of the freezing curve on ten samples of about 99.6 mole % purity. An earlier value reported by Ruff and Menzel[2] was $-61.3°$.

The vapor pressure as a function of temperature was found to be given by the expression

$$\log p(\text{mm. at } 0°) = 7.9727 - 1598.2/T$$

with a probable error of ±1 mm. over the range from 400 to 760 mm. It is believed that this equation can be used over the entire liquid range down to the freezing point (without exceeding the stated error), as judged by the agreement with the lower range values given by Ruff and Menzel. They reported, for the range 213 to 297°K., $\log p = 8.0716 - 1627.7/T$.

Our calculated boiling point is $40.76 \pm 0.05°$. This represents only a slight extrapolation from the closest measured pressure point at 757 mm. where the difference between experimental and calculated values is $0.03°$. The value calculated by Ruff and Menzel from their equation was $40.5 \pm 0.5°$.

The value calculated for the heat of vaporization from our pressure-temperature function is 7.31 kcal./mole. The molar entropy of vaporization calculated from these data is then 23.3 e.u., a reasonable value for a non-associated liquid composed of molecules with a dipole moment[5] of 1.51 D. Iodine pentafluoride, which shows behavior more typical of associated liquids, has a Trouton constant of 26.4.[3]

(5) M. T. Rogers, R. D. Pruett, H. B. Thompson and J. L. Speirs *J. Am. Chem. Soc.*, **78**, 44 (1956).

THE CONCENTRATION DEPENDENCE OF THE DIFFUSION COEFFICIENT OF RAFFINOSE IN DILUTE AQUEOUS SOLUTION AT 25°

By Peter J. Dunlop

Contribution from the Department of Chemistry, University of Wisconsin, Madison, Wisconsin

Since the introduction of certain interferometric techniques for studying the diffusion process in liquid systems,[1-6] accurate diffusion data have been reported for both two and three-component systems. This note presents data, obtained by means of the Gouy Diffusiometer, for the trisaccharide raffinose in dilute aqueous solution. The concentration dependence of the density, specific refractive increment and the relative viscosity of this system were also measured over the same concentration range at 25° and are included.

Materials, Solutions and Experimental Procedure

Hydrated raffinose[7] was heated *in vacuo* at 80° to remove the water of crystallization. This was necessary since, in agreement with the observations of previous workers,[8] it was found that the hydrated sample did not contain exactly five water molecules of hydration.

Solutions of raffinose were prepared by weight, using as solvent doubly-distilled water which had been saturated with air. Concentrations, c, in g./100 ml. of solution were calculated from the weight percentages *in vacuo* and the measured density data. Pyrex pycnometers of 30-ml. capacity were used to measure the densities, d; the data are reproduced by the equation

$$d = 0.997075 + 0.003927c \qquad c \leqslant 5.75 \qquad (1)$$

with an average deviation of $\pm 0.0006\%$. Using a Ubbelohde type viscometer with a water flow time of 265.8 sec., relative viscosities were determined on portions of the solutions prepared for diffusion. The kinetic energy correction applied in each case was never greater than 0.15%. The data are best represented by the quadratic equation

$$\eta_{rel} = 1 + 0.02742c + 0.00076c^2 \qquad c \leqslant 5.75 \qquad (2)$$

with an average deviation of $\pm 0.04\%$.

The Gouy diffusiometer used to measure the diffusion coefficients, D, and the specific refractive increments, $\Delta n/\Delta c$, has been previously described,[9,10] as have the methods employed to obtain D, $\Delta n/\Delta c$ and the graph of the relative fringe deviations, Ω_j, *versus* the reduced fringe number $f(\zeta_j)$.[11] An average δ correction of $+6\,\mu$ was applied in all experiments and in all cases the same Tiselius cell, with a 2.5103 cm. "a" dimension, was used. All experiments were performed within $0.004°$ of 25° and the diffusion coefficients corrected to $25.00_0°$ by means of the Stokes–Einstein relation.

Results

Values of D obtained at the mean concentrations $\bar{c} = (c_1 + c_2)/2$ and concentration increments $\Delta c = (c_2 - c_1)$ are tabulated in column 5 of Table I. To

represent the experimental diffusion coefficients the method of least squares was used to obtain the expression

$$D \times 10^5 = 0.43592 - 0.00677c \qquad c \leqslant 5.0 \qquad (3)$$

with an average deviation of $\pm 0.05\%$.

TABLE I

Diffusion Coefficients of Raffinose in Water at 25°

1 $\bar{c}$, g./ 100 ml.	2 Δc,[a] g./ 100 ml.	3 j_m	4 $(\Delta n/\Delta c)$ $\times 10^6$	5 $D \times 10^5$, cm.^{2} sec.$^{-1}$
0.37958	0.75915	51.16	1466.0[b]	0.43296[b]
0.62480[c]	1.24960	84.27	1467.0	.43201
0.75004	1.50009	101.19	1467.4	.43080
1.99974	1.50028	101.14	1466.4	.42261
3.50031	1.50086	101.18	1466.5	.41231
5.00008	1.49867	100.87	1464.1	.40195

[a] Δc is the difference in concentration between the bottom solution, c_2, and the upper solution, c_1. [b] These values may be compared with those of Longsworth who, at this same concentration, obtained 1467.1×10^{-6} for $\Delta n/\Delta c$ and 0.4339×10^{-5} for D. The Rayleigh Integral Fringe method was used in his experiment. [c] The author is indebted to Mr. I. J. O'Donnell of this Laboratory for the results of this experiment.

Specific refractive increments were calculated from the relationship $\Delta n/\Delta c = (\lambda j_m/a\Delta c)$, where j_m is the total number of fringes in a Gouy experiment and λ is the wave length, 5460.7 Å., of the green mercury line in air. These values are listed in column 4 of Table I. It should be noted that the values of $\Delta n/\Delta c$ are almost constant, thus indicat-
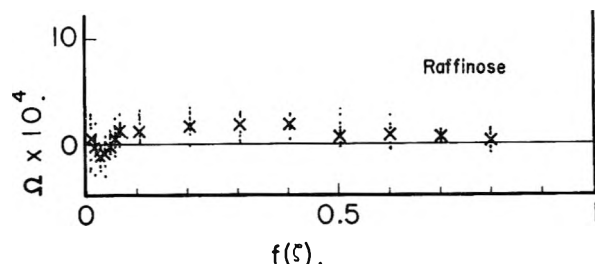

Fig. 1.—Relative fringe deviation graph for the experiment in which $\bar{c} = 5.00008$. At a given value of $f(\zeta)$ crosses indicate the average of the experimental points obtained from ten different Gouy photographs of the same boundary. Individual points are represented with dots.

ing that the refractive index of raffinose solutions is nearly a linear function of solute concentration when the latter is expressed as weight per unit volume of solution. A similar dependence of n on c has been found for sucrose.[12]

The density measurements provide a value of 0.6091 ml./g. for the partial specific volume of raffinose in the concentration range studied; this may be compared with the value of 0.6078 ml./g. previously determined by Longsworth.[13] A fringe deviation graph for raffinose is shown in Fig. 1. That the values of Ω_j are virtually zero at all values of $f(\zeta_j)$ indicates that the boundary was of Gaussian form within the error of measurement.

It is hoped that some of the data presented above will be of use in testing the experimental accuracy of a new Beams type equilibrium ultracentrifuge which is being installed in this Laboratory. From

(1) L. G. Longsworth, *J. Am. Chem. Soc.*, **69**, 2510 (1947).

(2) G. Kegeles and L. J. Gosting, *ibid.*, **69**, 2516 (1947).

(3) C. A. Coulson, J. T. Cox, A. G. Ogston and J. St. L. Philpot, *Proc. Roy. Soc. (London)*, **A192**, 382 (1948).

(4) J. St. L. Philpot and G. H. Cook, *Research*, **1**, 234 (1948).

(5) H. Svensson, *Acta Chem. Scand.*, **3**, 1170 (1949).

(6) L. G. Longsworth, *J. Am. Chem. Soc.*, **74**, 4155 (1952).

(7) Obtained from Pfanstiehl Chemical Co., Waukegan, Illinois.

(8) E. J. McDonald and B. G. Goss, Report E, 11th Session, Int. Comm. Uniform Method Sugar Analysis, Paris, 1954.

(9) L. J. Gosting, E. M. Hanson, G. Kegeles and M. S. Morris, *Rev. Sci. Instruments*, **20**, 209 (1949).

(10) P. J. Dunlop and L. J. Gosting, *J. Am. Chem. Soc.*, **75**, 5073 (1953).

(11) D. F. Akeley and L. J. Gosting, *ibid.*, **75**, 5685 (1953).

(12) L. J. Gosting and M. S. Morris, *J. Am. Chem. Soc.*, **71**, 1998 (1949).

(13) L. G. Longsworth, *ibid.*, **75**, 5705 (1953).

experiments with such a centrifuge it should be possible to measure molecular weights[14] if the necessary activity data are available, or, for substances of known molecular weight, one may obtain ratios of activity coefficients[15] at two different concentrations.

Acknowledgments.—It is a pleasure to thank Professors J. W. Williams and L. J. Gosting for their criticism of this manuscript. Financial support to make this investigation possible was supplied by the U. S. Public Health Service (G-4196-C). Grateful acknowledgment is hereby recorded.

(14) J. W. Beams, H. M. Dixon, III, A. Robeson and N. Snidow, This Journal, **59**, 915 (1955).

(15) J. S. Johnson, K. T. Kraus and T. F. Young, J. Am. Chem. Soc., **76**, 6 (1954).

THE PHOTOSENSITIZED OXIDATION OF CARBON MONOXIDE ON CUPROUS OXIDE[1]

By William M. Ritchey and Jack G. Calvert[2]

The McPherson Chemical Laboratory, The Ohio State University, Columbus, Ohio

Photosensitization of the oxidation of CO on Cu_2O has been observed in this work. Significant evidence has been obtained for the importance of electron-reactant interaction at the Cu_2O surface in a rate-determining step of the reaction. The composition, surface area and electrical properties of the catalyst samples used in the study are summarized in Table I. The photochemical rate data for varied reactant pressures and the different catalyst samples are shown in Table II. Comparison of reaction rates in consecutive runs at a given light intensity (within a pair of horizontal lines in Table II) is necessary to avoid the complications of arc aging and possible catalyst structural changes which may result from prolonged reactions.

Table I

Composition, Surface Area and Electrical Properties of the Cu_2O Samples

Sample	Element added	Atomic ratio, impurity/Cu, p.p.m.	Surface area, m.²/g.	Voltage drop, v./400 ma./in.² area
a	"none"[a]	0	0.0329[b]	0.66
b	sulfur	158	.0334	.52
c	sulfur	871	.0345	.32
d	antimony	207	.0323	.63
e	antimony	1041	.0270	.58
f	Bakers, C.P.	...	.826	...

[a] Less than 10 p.p.m. total impurity of Se and Fe and probably <2 p.p.m. of Fe according to activation analysis made at Oak Ridge. [b] Calculated from the smoothed curve of surface area vs. composition using the data of samples b, c, d and e. The measured value (0.038 m.²/g.) for "pure" Cu_2O is considered less reliable because of experimental difficulties which we encountered in this determination.

(1) Taken from the thesis of W. M. Ritchey submitted in partial fulfillment of the requirements for the Ph.D. degree, The Ohio State University, 1955. Presented in part before the Division of Physical and Inorganic Chemistry, 129th Meeting of the American Chemical Society, Dallas, Texas, 1956.

(2) Author to whom communications should be addressed.

Table II

Photochemical Rates of CO Oxidation at 25° with Various Reactant Pressures and S- and Sb-Doped Cu_2O Samples

Run	Cu_2O sample	Irrad. time, hr.	P_{O_2}, mm.	P_{CO}, mm.	R_{CO_2}, mm./6 hr.
1	d	6.00	162.5	80.8	0.504
2	d	6.00	200.3	42.2	.546
3	d	0.00[a]	164.1	39.5	.001
4	d	6.00	160.2	40.8	.504
5	d	6.07	319.3	83.5	.589
8	d	6.00	80.6	20.1	.542
9	e	6.00	79.9	19.4	.400
10	e	6.00	80.7	19.7	.424
11	b	6.00	79.7	21.0	.432
12	c	6.00	80.1	20.2	.332
16	a	6.00	80.2	19.7	.365
17	d	6.00	80.3	19.8	.313
18	d	5.00	79.9	21.0	.339
19	d	6.07	80.5	19.2	.321
20	d	2.00	78.7	20.3	.267
21	e	6.05	80.2	20.0	.252
22	b	6.00	80.0	20.4	.294
23	c	6.00	79.6	20.7	.260
24	d	6.00	80.1	19.0	.336
25	d	6.00	80.0	81.1	.264
30	d	4.00	81.1	20.8	.186
31[b]	d	4.00	79.8	21.7	.025

[a] Dark run; time that the reactants were in contact with the Cu_2O was the same as in the 6 hr. photochemical runs. [b] A glass filter was added in this run. It removed 89% of the ultraviolet light $\lambda < 4100$ Å. and passed 75% of the visible light.

Several features of the reaction are discernible from these data. (1) The absorption of light of $\lambda < 4100$ Å. by Cu_2O at 25° photosensitizes the reaction, $2CO + O_2 \rightarrow 2CO_2$, with an estimated average $\Phi_{CO_2} \cong 4 \times 10^{-4}$ at high light intensities (1.7×10^{18} q./sec., $2500 < \lambda < 4100$ Å.). For a given catalyst and light intensity the rate of CO_2 formation is reproducible and independent of the exposure time for small percentage conversions (compare runs 17, 18, 19, 20 and 24). (2) The variation of rate with reactant pressure (runs 1, 2, 4, 5 and 24, 25) is described satisfactorily by the rate law, $R_{CO_2} = k_1 P_{O_2}/(1 + k_2 P_{O_2} + k_3 P_{CO})$. This is the form expected theoretically if the primary process I

$$Cu^+ \text{ (in } Cu_2O) + h\nu \longrightarrow Cu^{++} \text{ (in } Cu_2O) + e^- \text{ (conduction band in } Cu_2O) \quad \text{(I)}$$
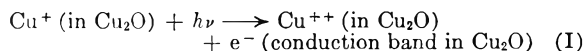
is followed by a reaction sequence such as that suggested by Garner and co-workers[3] in explanation of the thermal catalysis, or certain alternative reactions involving the interaction of electrons and reactants at the surface of the catalyst. (3) There is a striking correlation between the photochemical rates/surface area (symbolized as R_i for the ith Cu_2O sample) and the electrical data (E_i) for the different Cu_2O samples. In Fig. 1, R_i for each sample is shown as a function of catalyst composi-

(3) (a) W. E. Garner, T. J. Gray and F. S. Stone, Disc. Faraday Soc., **8**, 246 (1950); (b) T. J. Gray and S. D. Savage, ibid., **8**, 250 (1950); (c) F. S. Stone and P. F. Tiley, ibid., **8**, 254 (1950); (d) W. E. Garner, F. S. Stone and P. F. Tiley, Proc. Roy. Soc. (London), **A211**, 472 (1952); (e) R. Derry, W. E. Garner and T. J. Gray, J. chim. phys., **51**, 670 (1954).

tion by the solid curves; the upper curve (Photochemical I) is derived from the sequence of runs 8–12 at the highest intensity, and the lower curve (photochemical II) from runs 16, 17, 18, 19, 21, 22 and 23, at an undetermined lower intensity (about 100 hr. arc operation time separated the two sequences). For the various ratios, $R_i/R_a \cong E_i/E_a$; R_i/R_a for series I, R_i/R_a for series II, and E_i/E_a, respectively, are: Cu_2O sample (d), 0.95, 0.93, 0.95; sample (e), 0.86, 0.84, 0.88; sample (b),
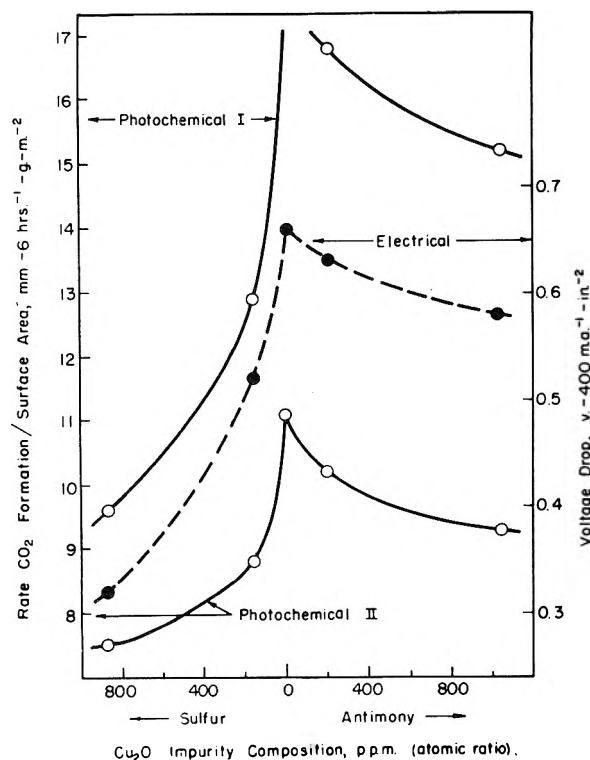
Fig. 1.—The effect of S and Sb concentration in Cu_2O on the rate of the photochemical CO_2 formation (solid curves) and on the electrical properties of the samples (dotted curve): in the photochemical runs, P_{O2} about 80 mm.; P_{CO} about 20 mm.; the absorbed flux was essentially constant in the series I at about 2×10^{18} q./sec. ($\lambda < 4100$ Å.), and in series II it was constant at some lower undetermined value; the voltage drop in Cu_2O was measured at a constant sample thickness, for a current density of 400 ma./in.^{2}

0.73, 0.79, 0.79; sample (c), 0.54, 0.68, 0.48. (R_a for series I was obtained by extrapolation of the data in Fig. 1.) Presumably the higher the conductivity of the Cu_2O sample (or the lower the E_i) the lower will be the amount of charge unbalance which the crystal can maintain at the steady state; the lower population of electrons at the surface results in a lower photochemical rate, R_i. A quantitative treatment of the data in terms of the Garner or other mechanisms is unwarranted at the present stage of this research. Additional studies of this reaction and gaseous reactions photosensitized at other solid surfaces (PbO, Fe_2O_3, etc.) are planned. From these it may be possible to evaluate the contribution to smog-forming reactions of oxidations photosensitized on the surface of particulate matter suspended in the atmosphere.

Experimental

Apparatus.—The apparatus was an all-glass, high vacuum system suitable for both surface area determinations and catalytic studies. The surface area equipment was of conventional design.[4] The catalytic reaction system consisted of a thin rectangular quartz reaction cell ($200 \times 20 \times 6$ mm.), a solenoid-operated circulating pump (pumping rate, 60 cc./min.), a bulb of 400-cc. volume to facilitate the mixing of the reactants and to minimize the build-up of products, and a freeze-out U-tube. The Cu_2O catalyst was irradiated with ultraviolet and visible light from a type A Hanovia lamp operated with 3.00 amp. a.c. at 155 v. A quartz cell, 1 cm. thick, filled with distilled water was placed between the arc and the reaction cell to absorb infrared radiation. The geometry of the arc mounting, the filter cell, and the Cu_2O sample was the same in runs of a given sequence.

Materials.—Research grade tank gases, N_2, He, CO and O_2 were purified by the conventional procedures. The Cu_2O samples were prepared from high purity Cu obtained from American Smelting and Refining Company which was further purified by zone refining. The S and Sb were added to portions of the Cu, and the mixture homogenized by melting in graphite boats under an atmosphere of A by induction heating. Upon cooling, the samples were cold rolled to a 1 in. width and 0.040 in. thickness. The strips were cleaned electrolytically in an alkaline bath and were then oxidized at 900° for 1 hr. in an O_2-enriched dry air atmosphere. The samples were annealed at 600° for 20 min. and then allowed to cool to room temperature. The Cu_2O layer was about 0.010 in. thick in all samples, sufficient to absorb practically completely light with $\lambda < 4000$ Å. Bars of these materials ($7.5 \times 0.63 \times 0.040$ in.) were used in the catalytic studies. The powdered samples for surface area determinations were prepared from the bars which were quenched in $N_2(1)$ to loosen the oxide layer; the Cu_2O was then scraped from the Cu with a razor blade.

Procedure.—The surface areas were determined by the standard B.E.T. procedure.[4] The surface areas of samples a–e are smaller by a factor of 24 to 30 than that of the Bakers C.P. powder f, reflecting the small number of grain boundaries and other imperfections in these samples. In the catalytic studies, first O_2 and then CO were introduced into the reaction system, thoroughly mixed, and equilibrated with the Cu_2O sample by operating the magnetic pump for 1 hr. prior to irradiation. Following the exposure (usually 6 hr.) at $25 \pm 2°$ the product CO_2 was condensed at $N_2(1)$ temperature in the U-tube by circulating the CO–O_2–CO_2 mixture for a period of 45 min.; the unreacted CO and O_2 were pumped off. The CO_2 was then distilled into a small calibrated vessel (6.20 cc.) and the pressure measured with a Hg manometer and a cathetometer. All the rates are given in mm. of CO_2 pressure (at 25° in the volume of the system, 506 cc.) per 6 hr. of irradiation. The rate of the thermal reaction was negligible in this study (compare runs 3 and 4). The possibility that light absorption may have caused significant heating of the oxide during the photochemical runs with an attendant increase in the thermal reaction can be eliminated.

Electrical Measurements.—Voltage measurements were made on circular samples (about 0.63 in. in diameter) of Cu_2O on Cu. The Cu samples were cut from the bars of the compositions shown in Table I and oxidized on one side to a uniform thickness. Contact between electrodes and the Cu_2O and Cu surfaces was established at constant pressure (40 lb./in.^{2}) with a hydraulic press. The Cu_2O layer was connected to the positive, the Cu base to the negative pole, causing the current to flow across the Cu_2O–Cu boundary in the direction of low resistance. The voltage necessary to cause a current of 400 ma./in.^{2} was determined repeatedly with each sample, and the averages are recorded in Table I.

(4) W. E. Barr and V. J. Auhorn, "Scientific Glass Blowing," Instrument Publishing Company, Pittsburgh, Pa., 1949.

and E. I. du Pont de Nemours and Company for a Grant-in-Aid which W. M. R. received during the course of this work.
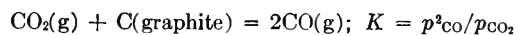
NOTE ON THE PRODUCER GAS EQUILIBRIUM AND THE ENTROPY OF GRAPHITE

By John Chipman

Department of Metallurgy, Massachusetts Institute of Technology, Cambridge, Massachusetts

Received May 24, 1956

The producer gas reaction and its equilibrium constant

$$CO_2(g) + C(graphite) = 2CO(g); \quad K = p^2_{CO}/p_{CO_2}$$

have been subject to a number of investigations since the classic study of Boudard.[1] Of the direct determinations of the equilibrium constant the ones which appear to have been done with greatest care are those of Rhead and Wheeler,[2,3] Jellinek and Diethelm,[4] and Dent and Cobb.[5] These and certain indirect studies were reviewed by Chipman[6] in 1932 to obtain an equation representing the average experimental results shown as line A in Fig. 1. The position of the line was determined in large measure by the 1911 results of Rhead and Wheeler, an unfortunate choice since there is reason to believe that their 1910 data are the more dependable. The experimental results in the range 800–1000° are plotted. Below 800 the reaction is so slow that attainment of equilibrium is doubtful; above 1000 the concentration of CO_2 is below the range of accurate analysis. Results of earlier studies including those of Boudard are omitted. They were reviewed by Jellinek and Diethelm and on the average agree with line A.

The first calculation of the equilibrium from spectroscopic data was made by Gordon[7] from his own analysis of CO_2, that Clayton and Giauque[8] for CO and the heat of combustion of graphite by Roth and Naeser.[9] His results fell slightly above line B of Fig. 1 which represents the present best values for K based upon revised spectroscopic calculations[10,11] and the newer heat of combustion of graphite.[12] Gordon called attention to the discrepancy and suggested that it could be explained by a zero-point entropy of graphite of about 0.5 e.u. The purpose of this study is to re-examine the data to determine whether a real discrepancy exists and whether the experiments actually indicate a finite zero-point entropy for graphite.

(1) O. Boudard, *Ann. chim. phys.*, **24**, 1 (1901).

(2) T. F. E. Rhead and R. V. Wheeler, *J. Chem. Soc.*, 2178 (1910).

(3) T. F. E. Rhead and R. V. Wheeler, *ibid.*, 1140 (1911).

(4) K. Jellinek and A. Diethelm, *Z. anorg. allgem. Chem.*, **124**, 203 (1922).

(5) F. J. Dent and J. W. Cobb, *J. Chem. Soc.*, 1903 (1929).

(6) J. Chipman, *Ind. Eng. Chem.*, **24**, 1013 (1932).

(7) A. R. Gordon, *J. Chem. Phys.*, **1**, 308 (1933).

(8) J. O. Clayton and W. F. Giauque, *J. Am. Chem. Soc.*, **54**, 2610 (1932).

(9) W. A. Roth and W. Naeser, *Z. Elektrochem.*, **31**, 461 (1925).

(10) Selected values of Chemical Thermodynamic Properties, U. S. Bureau of Standards, 1947–49.

(11) H. W. Wooley, *J. Research Natl. Bur. Standards*, **52**, 289 (1954).

(12) E. J. Prosen, R. S. Jessup and F. D. Rossini, *ibid.*, **33**, 447 (1944).
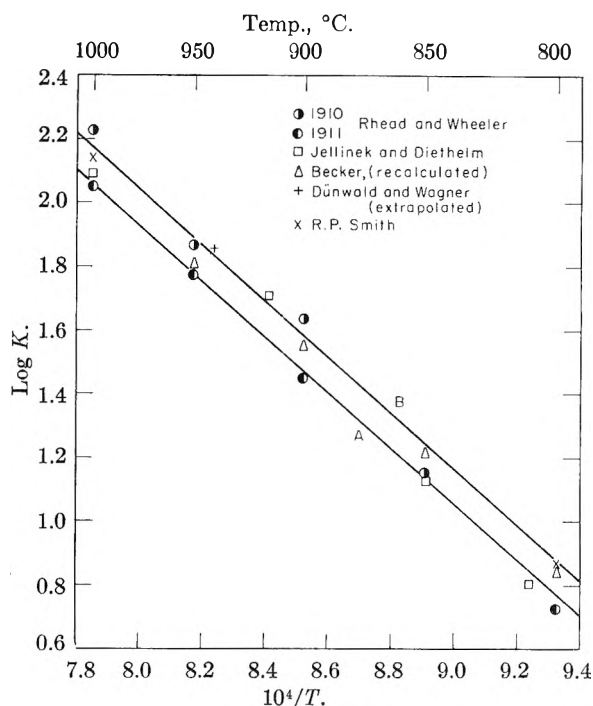
Fig. 1.—The equilibrium constant $K = p^2_{CO}/p_{CO_2}$: line A, average of older direct determinations; line B, from calorimetric and spectroscopic data.

Direct Determinations.—Principal sources of error include non-uniformity of temperature and inaccuracies in its measurement, and limitations in accuracy of gas analysis. Thermal diffusion if present would yield a too-low value of K but this is not an obvious source of error in any of the investigations. Deposition of carbon from the effluent gas sample would likewise lower K; but most of the investigators prevented this by rapid cooling. Incomplete graphitization of charcoal or coke leads to a higher value of K as shown clearly by Dent and Cobb. They found however that after prolonged out-gassing at 900° these materials give the same equilibrium constant as graphite at 800° and their K at this temperature confirmed the 1911 value of Rhead and Wheeler.

In the 1910 series of Rhead and Wheeler the thermocouple was embedded in the carbon specimen whereas in the 1911 series it was outside the reaction vessel in contact with the furnace tube. They pointed out that in this second series the carbon surface may have been at lower temperature than measured; in the earlier series they thought it might have been a little higher. If the 1911 temperatures were in error by 20° this would account for the deviation. The furnace used in this study was too short to provide a satisfactory zone of constant temperature. The thermocouple measured the temperature at the hottest point and it seems altogether possible that parts of the reaction bulb were more than 20° lower in temperature. The 1910 data contained no source of such large error and, with the exception of the lowest temperature, the agreement with the spectroscopic calculations is fair.

The data of Jellinek and Diethelm scatter about equally between the lines. Their lowest point at

810, like that of Dent and Cobb at 800, would require correction by 20° to conform with line B. There is nothing in the description of either experimental apparatus which would lead one to suspect so large an error.

Indirect Studies.—Becker[13] measured the total pressure in a system containing SrO, SrCO₃ and graphite, and found the same result using graphitized cast iron and ceylon graphite. His calculation of the equilibrium constant depended upon an extrapolation of the carbonate dissociation pressures obtained by Jones and Becker.[14] The original unsatisfactory extrapolation was improved upon by Chipman[15] who obtained an equation applicable in the range 650–1100°. Becker's results at 800–950° recalculated with the aid of this extrapolation are included in Fig. 1 where they lie between the two lines. It may be remarked that this method is free from some of the errors of others, including thermal diffusion and that it ought to find wider use in studies involving carbon and carbides.
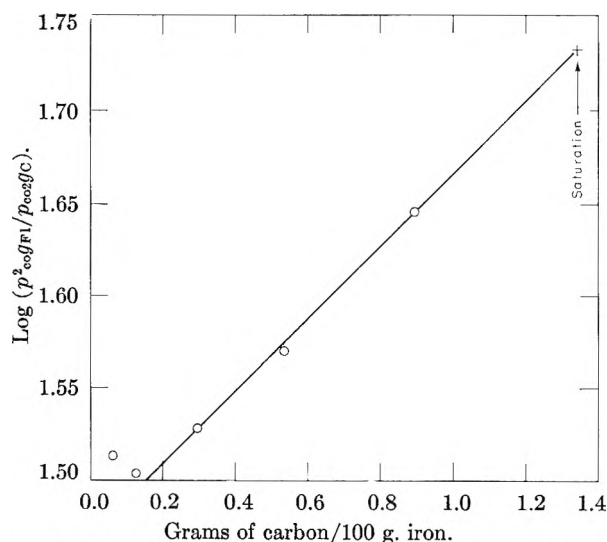
Fig. 2.—Equilibrium: C (in Fe) + CO₂ = 2CO at 940°; data of Dünwald and Wagner.

The equilibrium of CO–CO₂ mixtures with solid solutions of carbon in iron has been studied by a number of investigators. Among the earlier investigations the highest precision has been attained in the work of Becker mentioned above and in that of Dunwald and Wagner.[16] Of the latter results, only the series at 940° extends to high enough carbon concentration to permit extrapolation to graphite saturation. A plot of these data is shown in Fig. 2. Here the logarithm of the quotient $p^2_{CO}g_{Fe}/p_{CO2}g_{C}$ in which g_{Fe}/g_{C} is the weight ratio of iron to carbon in the solution, is plotted against concentration. It is known from the work of Smith[17] that the form of curve is a straight line. Linear extrapolation to 1.32% car-

(13) M. L. Becker, *J. Iron Steel Inst.*, **121**, 337 (1930).
(14) E. O. Jones and M. L. Becker, *J. Chem. Soc.*, 2669 (1927).
(15) J. Chipman, *Trans. Faraday Soc.*, **29**, 1266 (1933).
(16) H. Dunwald and C. Wagner, *Z. anorg. allgem. Chem.*, **199**, 321 (1931).
(17) R. P. Smith, *J. Am. Chem. Soc.*, **68**, 1163 (1946).

bon, the graphite solubility found by Gurry[18] leads to $p^2_{CO}/p_{CO2} = 72$ with an uncertainty of about ±5. It is seen in Fig. 1 that this result agrees very well with line B.

Similar studies of Fe–C alloys by Smith have been carried up to concentrations approaching saturation and in these the error of extrapolation is negligible. Values thus obtained at 800 and at 1000° were 7.28 and 137.2. In connection with these experiments Smith also carried out direct determinations. He suspended pieces of graphite in the gas mixture and determined the rate of loss or gain in weight. The point of zero weight gain established values of K at 800 and 1000° of 7.33 and 138.6. The direct and indirect results agree so closely that they are not distinguished in Fig. 1. These are the most accurate of all the experimental points; they reduce the discrepancy between experimental and calculated results to about one-fifth of its former magnitude.

Conclusions.—The principal data which led to line A suffered from ununiformity of temperature and errors in its measurement. The more reliable data are slightly below line B which is based upon calorimetric and spectroscopic data. The remaining discrepancies may be ascribed to minor errors of calorimetry or equilibrium measurements. Until the latter have been further improved in precision, it is unnecessary to postulate a zero-point entropy of graphite and the best values for the producer gas equilibrium are those represented in the Bureau of Standards tabulations.

(18) R. W. Gurry, *Trans. Am. Inst. Mining Met. Engrs.*, **150**, 147 (1942).

THE ELECTRODE POTENTIAL OF THE OsO₂–OsO₄ COUPLE[1]

By G. H. CARTLEDGE

Contribution from the Chemistry Division, Oak Ridge National Laboratory, Oak Ridge, Tennessee

In connection with a study of the passivation of iron by osmium(VIII) oxide[2] it was observed that the metal is quickly raised to a remarkably stable noble potential. The passivation was so effective that it appeared likely that the metal was functioning essentially as an indicator electrode for an oxidation–reduction couple between the osmium(VIII) oxide and its reduction product on the iron. So far as could be found, there is no value in the literature for the normal potential of the couple OsO₂(c) + 2H₂O → OsO₄ (aq) + 4H⁺ + 4e⁻. Latimer[3] has estimated the free energy of formation of osmium dioxide as −50 kcal. mole⁻¹, the estimate having been made from data on the disproportionation of the dioxide into metal and tetroxide. This leads to a calculated electrode potential of about −1.0 v. for the couple indicated above. The potential observed with the iron electrode was so close to the value calculated from this

(2) The results of this study will be presented in a forthcoming paper.
(3) W. M. Latimer, "Oxidation Potentials," Prentice-Hall, Inc., Second Ed., New York, N. Y., 1952, p. 232.

normal potential for the conditions of the experiment as to indicate that it should be possible to measure the electrode potential accurately.

In agreement with Moraht and Wischin,[4] it was found easy to deposit some form of osmium dioxide electrolytically from an alkaline solution of osmium(VIII) oxide. Electrodes were prepared by coating platinum gauze, foil and wire in a solution of osmium(VIII) oxide at a pH of 9.6, with a minimum current density of 4 ma. per sq. cm. on the wire and foil, until a blue-black or black film was present. Certain electrodes were prepared in an acid medium, but more uniform deposits were obtained from the alkaline solution. The electrodes came to steady potentials within one hour, as a rule, but most of the data were derived from electrodes that had been aged in the osmium solution for several hours or overnight. Only freshly prepared solutions were used for the measurements themselves.

The osmium solution was prepared by dissolving crystalline osmium(VIII) oxide in distilled water to make a stock solution containing 1 g. per 100 ml. (0.039 f). This stock solution was then diluted to concentrations as low as 5 × 10^{-3} f. To give the solution adequate conductivity, a supporting electrolyte was used. In different series of experiments this was either 1 or 2 × 10^{-3} f potassium sulfate, 10^{-2} f potassium chloride, 5 × 10^{-2} f phthalate or 10^{-2} f phosphate buffer. In certain experiments the osmium dioxide electrode was contained in a cell with a bridge leading through a closed stopcock to a beaker containing the supporting electrolyte only; a calibrated saturated calomel electrode dipped into this beaker. In other cases both the electrodes dipped into the osmium solution. The same results were obtained from both types of cell. The electromotive force was measured by a vibrating-reed electrometer and Brown recorder at laboratory temperature of 24.5°.

The first measurements were made in a potassium sulfate solution such as had been used in the experiments with iron electrodes. The acidity of the solution was adjusted by addition of sulfuric acid or sodium hydroxide to give pH values ranging from 0.5 to 9.65. When the observed e.m.f.'s were plotted against pH, it was observed that a slope of 0.059 was obtained in the pH range of 3.5 to 6.5. When the pH value fell below 3.5, the electrodes continued to respond rapidly and fairly reproducibly to changes in acidity, but the slope of the curve dropped considerably below the value corresponding to the electrode reaction as written. When the pH exceeded 6.5, a complicating reaction set in, involving dissolution of the dioxide with formation of osmium (VI) compounds. It was quite evident that over the intermediate range of acidities the slope corresponded to the value appropriate to the electrode reaction given above. The quick response of the potentials to changes in acidity made it apparent that the system reacts reproducibly and reversibly under these conditions.

The measurements in chloride and phthalate solutions gave electromotive forces that were a few millivolts less than those in the sulfate solutions. In these solutions there was a slight reduction of the osmium(VIII) oxide, which was manifested by a very small loose precipitate of osmium dioxide and a slight rise in the pH value. The freshly precipitated dioxide apparently increased the activity of the reduced component at the electrode sufficiently to lower the e.m.f. The effect was more noticeable at the higher acidities. From the plotted results it appeared that the chloride measurements would agree with those obtained in sulfate solutions if the pH value could be raised to 7. An experiment in a phosphate buffer at pH 7.08 showed, however, that the complicating reaction was already in effect at this acidity. The phosphate data agreed closely with the sulfate results in two experiments at pH's of 5.51 and 6.26. For these reasons, only the sulfate and phosphate data are used in the calculations.

The calculation of an $E°$ value was based upon the assumption of an activity coefficient of unity for the neutral

osmium(VIII) oxide. The acidities were measured by a Beckman Model G pH meter. The measuring instruments were calibrated against a Rubicon Precision Potentiometer. The electrolyte was stirred gently during the measurements. Table I gives the data obtained in sulfate and phosphate systems in the intermediate range of acidities and the $E°$ values calculated therefrom. The calculation to the hydrogen standard was based upon the value −0.242 v. for the saturated calomel electrode, including any liquid-junction potential.[5]

TABLE I
ELECTRODE POTENTIAL, OsO_2–OsO_4(AQ.), 24.5°

[OsO$_4$ (aq.)], f	pH	E.m.f.,[a] volt	$E°$, calcd., v.
0.039	4.03	+0.459	−0.961
.039	4.70	+ .422	− .963
.039	4.77	+ .421	− .965
.039	4.92	+ .413	− .967
.039	6.30	+ .327	− .963
.039	6.38	+ .322	− .965
.039	6.50	+ .315	− .963
.010	4.38	+ .431	− .963
.005	3.59	+ .476	− .964
.005	4.04	+ .454	− .969
.005	4.66	+ .421	− .966
.010[b]	5.51	+ .368	− .966
.010[b]	6.26	+ .321	− .963

Av. −0.964 ± 0.002 volt

[a] The e.m.f. has the sign of the osmium electrode. [b] Phosphate system; all others in sulfate solutions.

An attempt was made to identify the form of the osmium dioxide deposit by the electron diffraction of stripped films.[6] According to the literature,[7] the black, precipitated oxide exists as a dihydrate. This should perhaps be written as $Os(OH)_4$, since, according to Latimer,[8] entropies for such compounds may be estimated better if they are treated as metal hydroxides, rather than as oxide hydrates. When films of varying thickness were deposited electrolytically on platinum foil and stripped, only broad lines characteristic of amorphous material could be detected by electron diffraction. It will be assumed for calculation, therefore, that the free energy value directly measured refers to $Os(OH)_4$ (ppt) and presumably amorphous.

An anhydrous, brown form of osmium dioxide may be obtained by fusion of the hexachloroösmium(VI) complex with sodium carbonate.[7] An attempt was therefore made to determine whether the electromotive force could be measured in a cell in which solid dioxide was merely suspended in an osmium(VIII) oxide solution in a supporting electrolyte. The cell had a platinum wire sealed through the bottom of a tube of such size that a Beckman saturated calomel electrode neatly closed the open end. The cell was then filled with the suspension. When the black, precipitated form of dioxide was used in a 0.02 f phosphate buffer at pH 6.04, the cell attained a steady potential in less than 30 min., the calomel half-cell having been removed once to permit agitation of the solution. The calculated $E°$ values for two such experiments were −0.965 and −0.961 v., in close agreement with the value derived from Table I.

Since this type of half-cell was thus shown to be feasible, an attempt was made to use the anhydrous oxide in it. For its preparation, some of the precipitated dihydrate was placed in a porcelain crucible with a mixture of sodium carbonate and sodium chloride (to inhibit escape of osmium (VIII) oxide). The mixture was heated to fusion and held there for about 10 minutes. When the mass was extracted with boiling water the brown osmium dioxide remained. This was thoroughly washed, finally with dilute sulfuric acid, and then suspended in a sulfate solution of osmium (VIII) oxide. It was found, however, that in spite of the

(4) H. Moraht and C. Wischin, Z. anorg. Chem., 3, 153 (1893).

(5) W. M. Latimer, ref. 3, p. 177.

(6) The author is indebted to Mr. T. E. Wilmarth of the Analytical Chemistry Division of this Laboratory for making the examination.

(7) Gmelin's "Handbuch der anorganischen Chemie," Verlag Chemie, Berlin, 1939, System-Number 66, pp. 26 ff.

(8) W. M. Latimer, ref. 3, p. 364.

washing alkali was still being leached from the oxide to such an extent that reliable measurements could not be made.

The oxide was therefore suspended in a 0.02 f phosphate buffer at a pH of about 6 and magnetically stirred in a closed flask for an hour. After repeated centrifugal washing the solid was suspended in 0.010 f osmium(VIII) oxide in 0.02 f phosphate buffer and returned to the cell. Although alkali was still being released slowly, the e.m.f. was much more stable than before and the apparent $E°$ value was not very different from that measured with the black oxide. The oxide was then left for 40 hours in the buffered solution after which it was still brown. It was again centrifuged and washed and returned to the cell in fresh phosphate-osmium(VIII) solution, with a glass-encased magnet for continuous stirring. The pH value now remained essentially constant, but the electrode approached equilibrium much less rapidly than it did when the more reactive precipitated oxide was used. An apparently stable potential at pH 6.06 indicated an $E°$ value of -0.952 v., but when the pH value was lowered the electrode responded sluggishly and after 1.8 hours indicated an $E°$ value of only -0.921 v. It is therefore evident that the brown oxide is too impure and unreactive to give accurate results. It appears, however, that the two couples do not differ very much in their potentials.

While it would have been preferable to exclude oxygen from the cells, this would have been difficult because of the volatility of the tetroxide. By passing a stream of purified nitrogen through the bridged cell for ten minutes it was demonstrated that the presence of air appeared not to affect the measurements appreciably. The e.m.f. did not change by as much as 1 mv., whereas in similar measurements with technetium dioxide[9] the e.m.f. shifted quickly when air and nitrogen were interchanged in the cell. It is apparent that the establishment of the equilibrium between the two osmium oxides is sufficiently rapid to render the oxygen effect negligible.

On the assumption that the normal potential obtained in Table I is the true thermodynamic value, the free energy of formation of the black hydrated osmium(IV) oxide may be calculated. For this purpose, the free energy of formation of $OsO_4(aq)$ was taken from Latimer[3] to be -68.59 kcal. mole^{-1}. This leads to a value of -157.5 kcal. mole^{-1} for $\Delta F_f°$ for the formation of $Os(OH)_4$ (ppt). If the method of Latimer[10] for estimating the entropy of solid compounds is followed, the entropy of the black hydroxide is found to be $ca.$ 25 e.u. This value, with the $\Delta F_f°$ calculated above, gives $\Delta H_f° = -200$ kcal. mole^{-1}.

It is not possible to give an accurate set of thermodynamic values for the brown oxide from the present measurements. If it is assumed that the correct $E°$ value for the half-cell $OsO_2(c) + 2H_2O(l) \rightleftarrows OsO_4(aq) + 4H^+ + 4e^-$ is -0.952 v., as derived from the apparently stable e.m.f. at a pH of 6.06, then the $\Delta F_f°$ of $OsO_2(c)$ is -43.0 kcal. mole^{-1} and the estimated $\Delta H_f°$ is -54.9 kcal. mole^{-1}. These values would correspond to a $\Delta H°$ of hydration of the brown oxide by liquid water of -8.9 kcal. mole^{-1}, due chiefly to the change in entropy.

According to the free-energy values obtained, the dioxides are stable at room temperature with respect to the disproportionation into metal and tetroxide, but the $\Delta H°$ for the process is also posi-

tive, so that at some elevated temperature the observed reaction is to be expected.

ACIDS AND BASES. X. CONDUCTANCES OF ANTIMONY TRIBROMIDE AND STANNOUS CHLORIDE IN DIMETHYLFORMAMIDE ON ADDITION OF PIPERIDINE[1]

By W. F. Luder and Leonard S. Hamilton

Contribution from the Department of Chemistry, Northeastern University, Boston, Mass.

In the preceding paper of this series[2] conductance curves for the behavior of several bases and non-hydrogen acids in thionyl chloride were interpreted according to the electronic theory of acids and bases.[3] Thionyl chloride is a rather strong acid.[4] Therefore, it seemed desirable to conduct a similar investigation in a more basic solvent such as dimethylformamide. But with dimethylformamide several difficulties were encountered that have not been met with by other workers using other solvents, and this solvent has been abandoned. However, some of the results throw light on the electronic theory of acids and bases, and are reported here.

These results indicate that antimony tribromide and stannous chloride in dimethylformamide act as secondary acids toward piperidine.

Experimental

Materials.—C.P. antimony tribromide and stannous chloride were dried several days over phosphorus pentoxide in a vacuum desiccator. Piperidine was dried over calcium hydride, and fractionally distilled just prior to use. Dimethylformamide was dried over potassium hydroxide and calcium oxide, decanted and fractionated; its specific conductance was negligible (between 1×10^{-7} and 3×10^{-7} mho) compared with the rather high conductance of the solutions.

Apparatus.—The apparatus employed in the conductance measurements was similar to that described in the preceding paper.[2] The cell constant was 2.513. An oil thermostat maintained the temperature at $25 \pm 0.01°$.

The experiments with indicators were carried out in a three-neck 250-ml. flask containing a magnetic stirrer, and connected to a source of dry nitrogen so that carbon dioxide and moisture were kept out of contact with the solvent and reactants.

Procedure.—Conductance measurements were made as described in the preceding paper,[2] except that weighing tubes instead of fragile bulbs were used for the acids.

The indicator experiments were carried out in the apparatus mentioned above by adding a few drops of a saturated solution of the appropriate indicator (Table I) in dimethylformamide to the acid solution, then slowly adding the basic solution until the basic color of the indicator was observed.

To check the weight measurements the piperidine solutions were standardized with maleic acid, which was much more satisfactory than the benzoic acid first tried. With neutral red as the indicator maleic acid has one equivalent per mole in dimethylformamide, as in water.[5]

Results

Although many more check measurements were

(1) Abstracted from a thesis submitted by Leonard S. Hamilton to the faculty of Northeastern University in partial fulfillment of the requirements for the M.S. degree, June, 1954.

(2) L. E. D. Pease, Jr., and W. F. Luder, *J. Am. Chem. Soc.*, **75**, 5195 (1953).

(3) W. F. Luder and S. Zuffanti, "The Electronic Theory of Acids and Bases," John Wiley and Sons, Inc., New York, N. Y., 1946.

(4) R. A. Hubbard, Jr., and W. F. Luder, *ibid.*, **73**, 1327 (1951).

(5) H. M. E. Cardwell, J. D. Dunitz and L. E. Orgel, *J. Chem. Soc.*, 3740 (1953).

(9) G. H. Cartledge and Wm. T. Smith, Jr., This Journal, **59**, 1111 (1955).

(10) W. M. Latimer, ref. 3, pp. 359 ff.

made, typical results from the conductance runs are shown in Fig. 1, and from the indicator experiments in Table I.
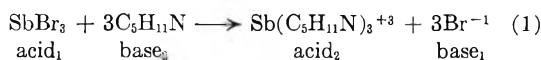
In the upper curve of Fig. 1, the conductance rises rapidly as the base piperidine is added to the acid antimony tribromide, until a maximum is reached near a ratio of three moles of base to one of acid. However, because a white precipitate was observed just before this maximum was reached, its significance was doubtful. Also, runs at higher concentrations exhibited a shift of the maximum to the left. Therefore, the addition of base to acid was tried using several indicators. With neutral red (the one that gave the sharpest endpoint) the color changed at a three-to-one ratio (Table I). The presence of the precipitate did not interfere with the color-change.

TABLE I

REACTIONS OF ANTIMONY TRIBROMIDE AND STANNOUS CHLORIDE WITH PIPERIDINE IN THE PRESENCE OF INDICATORS

Acid, A,	Base, B	Vol. A, ml.	Vol. B, ml.	$\dfrac{\text{Moles B}}{\text{Moles A}}$
0.2919 M SbBr$_3$	0.0999 M	20.57	20.00	3.005
(neutral red)	C$_5$H$_{11}$N	20.55	20.00	3.002
		20.60	20.00	3.009
0.02662 M SnCl$_2$	0.05340 M	42.66	21.10	1.007
(brom cresol	C$_5$H$_{11}$N	43.30	21.60	1.004
green)		44.72	22.45	0.993

The rapid rise in conductance, and the three-to-one ratio, may be interpreted, by means of the following equation, as the displacement of one base by another

$$\text{SbBr}_3 + 3\text{C}_5\text{H}_{11}\text{N} \longrightarrow \text{Sb}(\text{C}_5\text{H}_{11}\text{N})_3{}^{+3} + 3\text{Br}^{-1} \quad (1)$$
acid$_1$ base$_2$ acid$_2$ base$_1$

The conductance rises rapidly because of the production of ions as shown in the equation; it begins to fall when the solubility limit is reached and the further addition of piperidine decreases the solubility of the product. The indicator changes from its acid color to its basic color at the three-to-one ratio because piperidine is no longer being used up in the reaction.

The interpretation of the lower curve of Fig. 1 is similar to that of the upper one, except that a white precipitate forms sooner.[3] Again, therefore, the addition of base to acid was carried out in the presence of several indicators. With brom cresol green the color changed at a one-to-one ratio of acid to base (Table I).

The rapid rise in conductance, and the one-to-one ratio, may be interpreted, by means of the following equation, as the displacement of one base by another

(6) To find out whether all the precautions to exclude water and carbon dioxide were necessary, several conductance runs were made as follows. Using dried and purified materials, but without the other precautions, such as filling the cell with pure nitrogen, both curves run at the same concentrations as those of Fig. 1 gave slightly lower values of conductance. However, the shapes of the curves were the same, and precipitates were still obtained. Somewhat surprised that the conductances were lower, we repeated the runs using solvent directly from the bottle, without purification. In these runs the conductances were much lower (less than 60% of the highest values at the same concentrations), the shapes of the curves were entirely different, and no precipitates were formed. Thus the importance of the precautions was established.
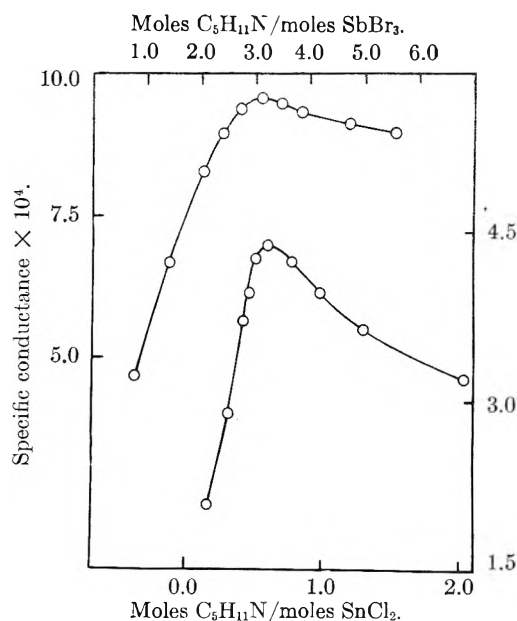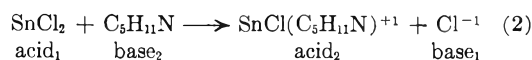

Fig. 1.—Upper curve (scales at top and left): conductance of 0.01221 M antimony tribromide in dimethylformamide upon addition of 0.4461 M piperidine; lower curve (scales at bottom and right): conductance of 0.01218 M stannous chloride in dimethylformamide upon addition of 0.1914 M piperidine.

$$\text{SnCl}_2 + \text{C}_5\text{H}_{11}\text{N} \longrightarrow \text{SnCl}(\text{C}_5\text{H}_{11}\text{N})^{+1} + \text{Cl}^{-1} \quad (2)$$
acid$_1$ base$_2$ acid$_2$ base$_1$

Because no theoretical reason exists for supposing that the displacement of chloride ion by piperidine should stop at a one-to-one ratio, the fact that it seems to do so in this experiment may indicate that stannous chloride is a weaker acid than antimony tribromide.

According to the accepted electronic formulas of antimony tribromide and stannous chloride

$$\text{Br—Sb—Br and Cl—Sn—Cl}$$
$$|$$
$$\text{Br}$$
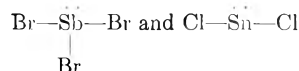
one would expect neither to show much tendency to act as a primary acid. However, according to the evidence here presented as summarized in equations 1 and 2 both can act as secondary acids[3] toward piperidine.

The displacement of halide ion by piperidine in these reactions is analogous to a Brönsted reaction, as represented by eq. 3, in which hydrogen chloride acts as a secondary acid.

$$\text{HCl} + \text{C}_5\text{H}_{11}\text{N} \longrightarrow \text{C}_5\text{H}_{11}\text{NH}^{+1} + \text{Cl}^{-1} \quad (3)$$
acid$_1$ base$_2$ acid$_2$ base$_1$

ESTIMATE OF THE SIZE AND SHAPE OF THE O$_2{}^-$ ION

By P. Smith

Chemistry Department, Purdue University, Lafayette, Indiana

The recent discovery[1,2] of the salts of the hypo-

(1) G. P. Nikol'skiĭ, L. I. Kazarnovskaya, Z. A. Bagdasar'yan and I. A. Kazarnovskiĭ, Doklady Akad. Nauk S.S.S.R., 72, 713 (1950).

(2) I. A. Kazarnovskiĭ, G. P. Nikol'skiĭ and T. A. Abletsova ibid., 64, 69 (1949); G. P. Nikol'skiĭ, Z. A. Bagdasar'yan and I. A. Kazarnovskiĭ, ibid., 77, 69 (1951); T. P. Whaley and J. Kleinberg, J. Am. Chem. Soc., 73, 79 (1951).

thetical HO_3 free radical has interesting implications. Firstly, it supports the idea that the parent HO_3 radical may exist. Secondly, it provides a source of structural information on a 19-valence electron molecule, the O_3^- ion.

The likelihood that the HO_3 radical and related species may occur as intermediates in several chemical processes has received little attention so far.[3] Reactions involved in the breakdown of aqueous hydrogen peroxide are possible examples. These are frequently not fully understood so far in terms of more conventional intermediates. For example, the recent, unconfirmed claim[4] for the participation of HOOOOH in the photolysis of aqueous hydrogen peroxide typifies our ignorance of this superficially simple reaction. It is worth noting that the apparent production[5] of the $NH_2NHNH-NH_2$ reaction intermediate during the decomposition of hydrazine seems to support this claim.

Apart from the case of ClO_2, data on the size and shape of 19-valence electron molecules are seemingly lacking. X-Ray powder photographic examination of solid potassium ozonide, 92.3% KO_3, was first claimed to prove that the O_3^- ion is linear and the KO_3 lattice arrangement is essentially the same as that of KN_3. This led to calculated values for the lattice energy of solid KO_3 and the electron affinity of ozone. The detailed X-ray data have now been published.[6] They seem somewhat questionable because of the admitted impurity of the potassium ozonide specimen. In order to explain one of the revealed discrepancies between the patterns of KO_3 and KN_3 it was suggested that the O_3^- ion may be bent, unlike the N_3^- ion[7] which is linear. With the help of recent structural data it is possible to estimate the size and shape of the O_3^- ion in agreement with this idea.

Consideration of the monotonous sequence of molecules NO_2^+, NO_2, NO_2^- and $NO_2^=$ suggests,[8] by extrapolation, that the hypothetical ion $NO_2^=$ is symmetrical and bent, θ (< O-N-O) = 108 ± 4° and r (N-O) = 1.30 ± 0.05 Å., in agreement with expectation.[9] The structure of O_3 is now securely established,[10] $\theta = 116.8 ± 0.5°$ and $r = 1.278 ± 0.002$ Å., not surprisingly close to that of

NO_2^- which, although less well known, probably has $\theta = 115 ± 4°$ and $r = 1.24 ± 0.03$ Å.[11,12] By extrapolation similar to that above it may be deduced that for O_3^-, $\theta = 110 ± 5°$ and $r = 1.34 ± 0.05$ Å.

For the above extrapolation the following data were used: NO_2^+, $\theta = 180.0°$, $r = 1.154 ± 0.01$ Å.[13]; NO_2, $\theta = 134.07 ± 0.25°$, $r = 1.188 ± 0.004$ Å.[14]; NO_2^-, $\theta = 115.7 ± 3°$, $r = 1.233 ± 0.04$ Å.[11] and $\theta = 114.2 ± 4°$, $r = 1.247 ± 0.035$ Å.[12] One recent value for NO_2^+, $r = 1.06$ Å., was not used because it is derived from uncertain data.[15] Plots of physical property against number of valence electrons were employed.

The above result may be compared against the recent, carefully redetermined θ value for ClO_2[16] of 116.5 ± 2.5°. This figure has been criticized as being a few degrees too high.[9] However, it does seem to fit into the admittedly uncertain trend of θ change in the sequence NO_2^- and O_3^- extrapolated to include the hypothetical FO_2, and the θ increase in the sequence O_3 to SO_2[9] assumed to hold for FO_2 and ClO_2.

The θ value estimate for O_3^- suggests that KO_3 may not have the tetragonal potassium bifluoride lattice of KN_3.[7] This view is supported by comparing the powder photograph of monoclinic KNO_2[17] with that of KO_3. There is a correspondence between most of the comparable spacings, those of KO_3 being fairly uniformly about 5–10% bigger than those of KNO_2. This might be expected because the O_3^- ion is slightly larger than the NO_2^- ion. In view of the impurities in the KO_3 specimen and the possible inaccuracies in the data for KNO_2, which are rather old, detailed conclusions are hardly worth attempting at present.

The possibility that KO_3 has the pseudo-NaCl type lattice of KNO_2 and not the pseudo-CsCl type lattice of KN_3 suggests that the electron affinity of ozone may not be 66.5 kcal. mole^{-1} as claimed.[1,18] Of course, it is doubtful whether the crystal energy calculations involved in this estimate, relating as they do to a structure made up of polyatomic ions,[19] merit calling attention to this uncertainty.

(3) W. C. Bray, *J. Am. Chem. Soc.*, **60**, 82 (1938); P. Smith, *Chemistry and Industry*, 1299 (1954); W. C. Schumb, C. N. Satterfield and R. L. Wentworth, "Hydrogen Peroxide," Reinhold Publ. Corp., New York, N. Y., 1955, Chapter 6.

(4) A. P. Purmal, *Zhur. Fiz. Khim.*, **29**, 744, 846 (1955).

(5) W. C. E. Higginson and D. Sutton, *J. Chem. Soc.*, 1402 (1955); F. O. Rice and F. Scherber, *J. Am. Chem. Soc.*, **77**, 291 (1955).

(6) G. S. Zhdanov and Z. V. Zvonkova, *Zhur. Fiz. Khim.*, **25**, 100 (1951).

(7) S. B. Hendricks and L. Pauling, *J. Am. Chem. Soc.*, **47**, 2904 (1925); L. K. Frevel, *ibid.*, **58**, 779 (1936); *Z. Krist.*, **94A**, 197 (1936).

(8) P. Gray and A. D. Yoffe, *Quart. Rev.*, **9**, 362 (1955).

(9) A. D. Walsh, "Progress in Stereochemistry," Vol. I, Butterworths Scientific Publications, London, 1954, p. 1.

(10) R. H. Hughes, *J. Chem. Phys.*, **24**, 131 (1956).

(11) G. B. Carpenter, *Acta Cryst.*, **5**, 132 (1952).

(12) M. R. Truter, *ibid.*, **7**, 73 (1954).

(13) E. Grison, K. Eriks and J. L. de Vries, *ibid.*, **3**, 290 (1950).

(14) G. E. Moore, *J. Opt. Soc. Amer.*, **43**, 1045 (1953).

(15) K. Eriks and C. H. MacGillavry, *Acta Cryst.*, **7**, 430 (1954).

(16) J. D. Dunitz and K. Hedberg, *J. Am. Chem. Soc.*, **72**, 3108 (1950).

(17) G. E. Ziegler, *Z. Krist.*, **94A**, 491 (1936); I. D. Hanawalt, H. W. Rinn and L. K. Frevel, *Ind. Eng. Chem., Anal. Ed.*, **10**, 457 (1938).

(18) H. O. Pritchard, *Chem. Revs.*, **9**, 362 (1953).

(19) D. H. Templeton, *J. Chem. Phys.*, **23**, 1826 (1955).

TWO CURRENT TITLES
in the
Advances In Chemistry Series

No. 10 LITERATURE RESOURCES FOR CHEMI-CAL PROCESS INDUSTRIES

Discusses various information sources with 13 articles on market research, 7 on resins and plastics, 6 on textile chemistry, 10 on the food industry, 10 on petroleum, and 13 on general topics, plus 34 pages of index.

582 pages—paper bound—$6.50 per copy

No. 11 NATURAL PLANT HYDROCOLLOIDS

Reviews materials usually used as protective colloids or "stabilizers" such as Calcium Pectinates, Agar, Gum Arabic, Gum Karaya, Tragacanth, Locust Bean Gum, Alginates and Red Seaweed Extracts.

103 pages—paper bound—$2.50 per copy

also available: No. 4, Searching The Chemical Literature, $2.00 . . . No. 5, Progress In Petroleum Technology, $3.00 . . . No. 6, Azeotropic Data, $4.00 . . . No. 7, Agricultural Applications of Petroleum Products, $1.50 . . . No. 8, Chemical Nomenclature, $2.50 . . . and No. 9, Fire Retardent Paints, $2.50.

order from: Special Publications Department

American Chemical Society

1155 Sixteenth Street, N.W.

Washington 6, D. C.